UNIVERSITY OF LEEDS

Optimal Stopping for Actuarial Use: A Study on Unemployment Insurance Schemes

Jason Susanna Anquandah

University of Leeds

School of Mathematics

Submitted in accordance with the requirements for the degree of

Doctor of Philosophy

November, 2020

This thesis is dedicated to someone.

Intellectual Property Statement

The candidate confirms that the work submitted is her own and that appropriate credit has been given where reference has been made to the work of others.

This copy has been supplied on the understanding that it is copyright material and that no quotation from the thesis may be published without proper acknowledgement.

The right of Jason Susanna Anquandah to be identified as Author of this work has been asserted by her in accordance with the Copyright, Designs and Patents Act 1988.

Acknowledgements

I would like to take this opportunity to first and foremost thank God Almighty for giving me the strength, wisdom, knowledge, ability, blessings and opportunity to undertake this research study.

My unalloyed appreciation goes to my supervisors, Dr Tiziano De Angelis, Dr Elena Issoglio and Dr Leonid Bogachev, for the endless hours they invested, not only to enhance my mathematical knowledge, particularly in stochastic theory, but also to help me develop my own way of reasoning and thinking. They have mentored me and tirelessly guided me through every step of this doctoral journey. Their encouragement, support and words of hope in the course of this study are highly appreciated. I thank my examiners, Dr. Alet Roux and Prof. Charles Taylor, for their useful feedback and contribution.

I gratefully appreciate the support from University of Leeds for the Leeds Anniversary Scholarship (LARS) and their contribution to the realization of this report by awarding me the scholarship to undertake doctoral studies. I would like to thank the academic and administrative staff from the School of Mathematics of the University of Leeds for their useful feedback, comments and administrative support. I am grateful to my fellow Ph.D. student from the University of Kent, Frank Donkor, for his invaluable contribution towards the fulfillment of this thesis. To all other staff from the Cluver group, I register my appreciations.

A special thank you to my parents, James and Josephine Anquandah. There are no words to describe how grateful I am for your endless love, prayers, encouragement and support. Dr Ps Obed Obeng-Addae, thank you for your guidance. I would like to thank Dr Fiifi Manful for encouraging and inspiring me to pursue this degree and for being my muse, editor, proofreader, and support. Loving thanks to Jeffrey Anquandah, Dr and Dr Garr, Mr and Mrs Alagbe, Mr and Mrs Antwi, Dr Osa Noi-Sanar, Mrs Amakwah, Awo, Celestina, Emmanuella and Coded. To all my family and friends who have constantly been by my side, you will always have a special place in my heart.

Abstract

Managing unemployment is one of the key issues in social policies. Unemployment insurance schemes are designed not only to cushion against the severe blow to finance and morale caused by the loss of job but also to encourage the unemployed to seek new jobs more proactively due to the continuous reduction of benefit payments. This thesis is concerned with the entry time into unemployment insurance schemes. First, a simple model of unemployment insurance is proposed with a focus on optimality of the individual's entry into the scheme. The corresponding optimal stopping problem is solved, and its similarity and differences with the perpetual American call option are discussed. Beyond a purely financial point of view, we argue that in the actuarial context the optimal decisions should take into account other possible preferences through a suitable utility function. Some examples in this direction are worked out. Second, we expand the UI model by making the parameters time dependent. This causes obvious complications to the model and gives rise to an optimal stopping problem which involves the computation of a time dependent boundary. An exact computational formula for this time dependent optimal boundary is unknown. Nevertheless, some numerical approaches are proposed to approximate the optimal boundary. Third, we focus on the analysis and modelling the labour force data from the Office for National Statistics (ONS) in UK. The labour force data is used because it consistently captures in details the estimates of the number of individuals employed, unemployed and inactive in UK, which are key features needed to compute the unemployment and reemployment rates in our UI scheme. Additionally, aside the aforementioned key features, the data also details the movement of individuals between employment, unemployment, and inactivity. Hence enabling us to understand and interpret the changes in the level of the labour market per quarter. To make our UI model more realistic, we explore a variety of multi-state models and lake models using the data and give highlights of the approaches and the results. Finally, we summarise the results and indicate a few directives that can be further explored.

Contents

List of Figures

List of Tables

Abbreviations

ILO	International labour organization
UI	Unemployment insurance
eNPV	Expected net present value
ODE	Ordinary differential equation
SDE	Stochastic differential equation
PDE	Partial differential equation
ONS	Office for national statistics
LFS	Labour force survey
MJP	Markov jump process
KDE	Kolmogorov differential equation
DA	Diagonal adjustment
LST	Labour force state transition
RMSE	Root mean square error
R^2	Coefficient of determination
AD	Anderson-Darling test statistic
CDF	Cumulative distribution function
AIC	Akaike information criterion
BIC	Bayesian information criterion
E	Employment
U	Unemployment
I	Inactivity
B	Entry
D	Exit
N	Total labour force
$\bar{N}$	Total population
MLE	Maximum likelihood estimates

Common Symbols

t	Time
X_t	Dynamics of individual's wage
τ	Entry time
τ_0	Time of unemployment
τ_1	Time of reemployment
$h(\cdot)$	Benefit schedule
λ_0	Unemployment transition rate
λ_1	Reemployment transition rate
λ_2	Mortality rate
P	Premium
r	Risk-free rate
s_0	Grace period for job search
δ	Benefit falling rate
x	Initial wage
C	Continuation region
S	Stopping region
L	Infinitesimal generator
$\%\Delta$	Percentage change
P	Probability
E	Expectation
$\mathbf{\Lambda}$	Generator matrix
$\boldsymbol{P}$	Probability matrix
$\sum$	Sum
$\prod$	Product
μ	Exit rate
β	Entry rate

Chapter 1

Introduction

1.1 Unemployment

There are several definitions for unemployment across different disciplines. However, one of the most known definitions of unemployment is "all persons above a certain age without paid work or self-employment, who at the time of assessment were available for work either in paid employment or in self-employment, and who at the specified time of assessment had taken specific steps to seek employment or self-employment" by [62]. Based on this definition, International Labour Organization (ILO) summarized the definition of unemployment as without work, currently available for work and seeking work in [81].

There are several classifications of unemployment. Some are broad (individuals willing to work but are not searching due to circumstances such as injury and lost hope in finding employment) and narrow (individuals willing to work and are enthusiastically searching for jobs). Long-term (individuals out of a job for more than 27 weeks) and short term (individuals out of a job for less than 27 weeks) are other classifications. Furthermore, there are several types of unemployment which are somewhat associated to each other. Some are structural unemployment (when wage earner skills no longer fit the job market), cyclical unemployment (a fall in economic activity and business cycle) and frictional unemployment (when individuals are briefly moving between occupations). For simplicity in our subsequent computations, the analysis of unemployment is argued when an individual becomes unemployed voluntarily as well as involuntarily.

All types of unemployment vary depending on causal factors associated to economic,

political, social and individual aspects in a society. In our work, we consider the causes of unemployment that are beyond a person's control such as wage, inflation rate, unemployment rate and re-employment rates. Unemployment also has several perilous consequences. In the society, unemployment leads to issues such as poverty, corruption, delinquency and a reduction in the socio-economic growth and development [98]. Furthermore, the physical and emotional wellbeing of the affected individuals is negatively affected causing conditions such as depression, shame, and resentment [98]. These effects keep mounting so fast that regularly reviewed sustainable strategies for affected societies and individuals have been suggested and implemented to reduce unemployment. However, to determine the level of success of these strategies, one must be able to measure unemployment.

Unemployment is measured to ascertain the rates and dynamics of the labour market. Due to diverse definitions of unemployment and sources of data, the computation of the unemployment rate often differs. Knowing how to compute the unemployment rate helps to improve the efficiency and effectiveness of an economy to utilize its work force, increase the productivity of the labour market and most importantly reduce unemployment. In this thesis, there are four rates of measurement for unemployment; the unemployment transition rates, the unemployment probability rates, the percentage rates of change and the rates which show the proportion of the individuals in each state to the total labour force. Further details on these rates are provided as the computations unfold.

Thus, effectual strategies and policies to reduce the rate of unemployment rate such as creating more jobs, education, training, employment subsidies and unemployment insurance (UI) will help maintain the socio-economic stability in the society.

1.2 Motivation for the study

According to the literature, unemployment insurance (UI) scheme is a policy that can solve the challenge of unemployment in both short-term and long-term [6], [93, §2]. UI schemes are designed not only to cushion against the severe blow to finance and morale caused by the loss of jobs but also to encourage the unemployed to seek new jobs more pro-actively due to the continuous reduction of benefit payments.

UI provides protection for unemployed individuals without negatively affecting the economy by addressing some major economic issues. For instance, firstly, according to

[54] UI solves the issue of decreasing labour input rate in the economy because it serves as an incentive that motivates unemployed workers to pursue more productive job offers to increase their productivity and inspire companies to create these offers. Secondly, UI ensures economic stability during economic recessions by providing unemployment benefits to jobless individuals when there are insufficient jobs [78]. Thirdly, during economic recessions, UI reduces the workforce drop-out rate by making it easier to exit from unemployment than exit the workforce altogether [1]. Fourthly, UI may also lead to better quality of job match between employees and employers because unemployed workers receive financial assistance and support during the unemployment spell until they find the best jobs that fit their skills. Based on the raised arguments, the purpose of our study is to reduce unemployment rates by investigating UI schemes. Specifically, we consider an individual's optimal entry time into such a UI scheme.

1.3 Risk and Insurance

Assessing the risk in financial industries often aims at finding optimal choices in decision making. In the insurance sector, optimality considerations are crucial primarily for the insurers, who have to address monetary issues (such as how to price the insurance policy so as not to run at a loss but also to keep the product competitive) and time issues (e.g., when to release the product to the market). Less studied but also important are optimal decisions on behalf of the insured individuals, related to monetary issues (e.g., how profitable is taking up an insurance policy and the right portion of wealth to invest), consumption decisions (e.g., whether to maximise or optimise own consumption), or time-related decisions (such as when it is best to enter or exit an insurance scheme). In the insurance literature, there has been much interest towards using optimality considerations, including optimal stopping problems. From the standpoint of the insurer seeking to maximise their expected returns, the optimal stopping time may be interpreted as the time to suspend the current trading if the situation is unfavourable, and to recalculate premiums (see, e.g., [72, 75, 96] and further references therein). Insurance research has also focused on optimality from the individual's perspective. One important direction relevant to the UI context was the investigation of the job seeking processes, especially when returning from the unemployed status [17, 88, 133]. This was complemented by a more general research exploring ways to optimise and improve the efficacy of the UI systems (also in terms of reducing government expenditure),

using incentives such as a decreasing benefit throughout the unemployment spell, in conjunction with sanctions and workfare (see [52, 60, 65, 77, 79], to cite but a few). A related strand of research is the study of optimal retirement strategies in the presence of involuntary unemployment risks and borrowing constraints [27, 35, 55, 70, 124].

To the best of our knowledge, optimal stopping problems in the UI context (such as the optimal entry to / exit from a UI policy) have not received sufficient research attention. This issue is important, because knowing the optimal entry strategies is likely to enhance the motivation for individuals to join the UI scheme, thus ensuring better societal benefits through the UI policies (see analysis and discussion in [112]). Knowledge of the optimal entry time for insured individuals, which has impact on the amount and duration of benefits to be claimed, will also help the insurers (both state and private) to optimise their financial practices (see a discussion in [80]). Thus, our present work attempts to fill in the gap by addressing the question of the optimal timing to join the UI scheme.

1.4 Scope of thesis

In this thesis we focus on the particular type of products related to *unemployment insurance (UI)*, whereby an employed individual is covered against the risk of involuntary unemployment (e.g., due to redundancy). Various UI systems are designed to help cushion against the severe blow to finance (as well as morale) caused by the loss of jobs and to encourage unemployed workers to find a new job as early as possible in view of the continued reduction of benefits. The protection is normally provided in the form of regular financial benefits (usually tax free) payable after the insured individual becomes unemployed and until a new job is found, but often only up to a certain maximum duration and with payments gradually decreasing over time. Many countries have UI schemes in place [64, 76], often run and funded by the governments, with contributions from employers and workers, but also by private insurance companies [56]. For example, the governmental UI systems administered in France and Belgium in the 1990s provided benefits decreasing with time according to a certain schedule; the amount of the benefit was determined by the age of the worker, their final wage/salary, the number of qualifying years in employment, family circumstances, etc.

In this work we introduce and analyse UI models focusing on the optimal time for the individual to join the scheme. Before setting out the model formally, let us describe

the situation in general terms. Consider an individual currently at work but who is concerned about a possible loss of job, which may be a genuine potential threat due to the fluidity of the job market and the level of demand in the particular employment sector. To mitigate this risk, the employer or the social services has an unemployment insurance scheme in place, available to this person (perhaps after a certain qualifying period at work), which upon payment of a one-off entry premium would guarantee to the insured a certain benefit payment proportional to their final wage and determined by a specified declining benefit schedule, until a new job is found (see Fig. 1). The mode of paying the premium is a fixed lump sum or total amount before the unemployment insurance coverage begins.

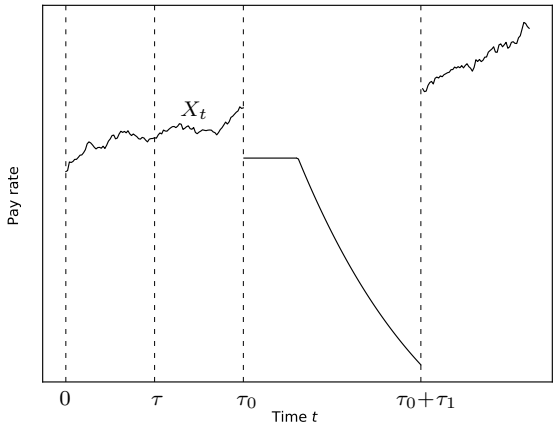

FIGURE 1: A time chart of the unemployment insurance scheme. The horizontal axis shows (continuous) time; the vertical axis indicates the pay rate (i.e., income receivable per unit time). The origin $t = 0$ indicates the start of employment. Two pieces of a random path X_t depict the dynamics of the individual's wage whilst in employment. The individual joins the UI scheme at entry time τ (by paying a premium P). When the current job ends (at time $\tau_0 > \tau$), a benefit proportional to the final wage X_{τ_0} is payable according to a predefined schedule (e.g., see Example 2.2.1), until a new job is found after the unemployment spell of duration τ_1.

The decision the individual is facing is *when* (rather than *if*) to join the scheme. What are the considerations being taken into account when contemplating such a decision? On the one hand, delaying the entry may be a good idea in view of the monetary

inflation over time — since the entry premium is fixed, its actual value is decreasing with time. Also, it may be reasonably expected that the wage is likely to grow with time (e.g., due to inflation but also as a reward for improved skills and experience), which may have a potential to increase the total future benefit (which depends on the final wage). Last but not least, some savings may be needed before paying the entry premium becomes financially affordable. On the other hand, delaying the decision to join the insurance scheme is risky, as the individual remains unprotected against loss of job, with its associated impact on finance and morale.

Thus, there is a scope for optimizing the decision about the entry time — probably not too early but also not too late. Apparently, such a decision should be based on the information available to date, which of course includes the inflation rate and also the unemployment and redeployment rates, all of which should, in principle, be available through the published statistical data. Another crucial input for the decision-making is the individual's wage as a function of time. We prefer to have the situation where this is modelled as a random process, the values of which may go up as well as down. This is the reason why we do not consider salaries (which are in practice piecewise constant and unlikely to decrease), and instead we are talking about *wages*, which are more responsive to supply and demand and are also subject to "real-wage" adjustments (e.g., through the consumer price index, CPI). Besides, loss of job is more likely in wage-based employments due to the fluidity of the job market. For simplicity, we model the wage dynamics using a diffusion process called *geometric Brownian motion* (GBM). The arguments for using GBM to model wages are as follows. Firstly, the GBM process only assumes positive values, just like wages. Secondly, the GBM process shows the same kind of uncertainty in its paths as we see in some real wages for very low income and high income earners. Finally, computations with GBM processes are relatively easier because the assumption of the volatility and drift can be adjusted in an attempt to make the wage fixed which is the case for some workers. [1]

[1] For technical convenience, we choose to work with continuous-time models, but our ideas can also be adapted to discrete time (which may be somewhat more natural, since the wage process is observed by the individual on a weekly time scale).

1.5 UI scheme models

In this thesis, we study two UI scheme models in Chapter 2 and Chapter 3 and here a brief review of the results is presented. The first case is the time-independent model which allows for an explicit solution whereas the second case is the time-dependent model which allows for an analytical characterization of the solution but with no explicit formula for the optimal strategy.

Time-independent model

For the time-independent case in Chapter 2, the optimization problem for our model aims to maximise the expected net present value (for an individual) of the UI scheme by choosing an optimal entry time τ^* to the contract. We will show that this problem can be solved exactly by using the well-developed *optimal stopping theory* [107, 109, 121]. It turns out that the answer is provided by the *hitting time* of a suitable threshold b^*, that is, the first time τ_{b^*} when the wage process X_t will reach this level. Since the value of b^* is not known in advance, this leads to solving a *free-boundary problem* for the differential operator (generator) associated with the diffusion process (X_t). In fact, we first conjecture the aforementioned structure of the solution and find the value b^*, and then verify that this is indeed the true solution to the optimal stopping problem.

It is interesting to point out that our optimal stopping problem and its solution have a lot in common with (but are not identical to) the well-known American call option in financial mathematics, where the option holder has the right to exercise it at any time (i.e., to buy a certain stock at an agreed price), and the problem is to determine the best time to do that, aiming to maximise the expected financial gain. However, unlike the American call option setting based on purely financial objectives, the optimal stopping solution obtained in our UI model is not entirely satisfactory from the individual's point of view, because the (optimal) waiting time τ_{b^*} may be infinite with positive probability (at least for some values of the parameters), and even if it is finite with probability one, the expected waiting time may be very long.

Motivated by this observation, we argue that certain elements of *utility* should be added to the analysis, aiming to quantify the individual's "impatience" as a measure of purpose and satisfaction. We suggest a few simple ideas of how utility might be accommodated in the UI optimal stopping framework. Despite the simplicity of such examples, in most cases they lead to much harder optimal stopping problems. Not

attempting to solve these problems in full generality, we confine ourselves to exploring suboptimal solutions in the class of hitting times, which nonetheless provide useful insight into possible effects of inclusion of utility into the optimal stopping context.

The general concept of utility in economics was strongly advocated in the classical book by von Neumann and Morgenstern [99], whose aim was in particular to overcome the idealistic assumption of a strictly rational behaviour of market agents.[1] These ideas were quickly adopted in insurance, dating back to Borch [16] and soon becoming part of the insurance mainstream, culminating in the Expected Utility Theory (see a recent book by Kaas et al. [73]) routinely used as a standard tool to price insurance products. In particular, examples of use of utility in the UI analysis are ubiquitous (see, e.g., [1, 7, 52, 60, 64, 65, 77, 79, 80]). There have also been efforts to combine optimal stopping and utility [26, 27, 61, 75, 96, 133]. However, all such examples were limited to using utility functions to re-calculate wealth, while other important objectives and preferences such as the desire to buy the policy or to reduce the waiting times have not been considered as yet, as far as we can tell.

Time-dependent model

We study the time-dependent problem in Chapter 3 which is an extension of the model in Chapter 2. In particular, we are interested in finding the optimal stopping rule that maximises the expected payoff for an unemployed individual under the UI scheme. We formulate the stopping problem based on the assumption that risk-free rate, unemployment rate and reemployment rate are time-dependent. We also prove that the optimal stopping time for our problem is the first time the wage process exceeds a time-dependent optimal boundary $b(t)$, which is non-negative, continuous, either non-decreasing or non-increasing and bounded. Prior to this, we prove the continuity of the value function. We further find the regularity for the value function and derive an integral equation that uniquely characterises the optimal boundary. Finally, we numerically solve the integral equation and provide plots of the optimal boundary.

[1] Impact of individualistic (not always rational) perception in economics and financial markets is the subject of the modern behavioural economics (see, e.g., a recent monograph [38]).

1.6 Analysis and modelling of labour force data

For simplicity, the time until the current employment ends τ_0 and the unemployment spell of duration τ_1 are assumed to have exponential distribution due to the Markovian nature of transition from employment to unemployment and back. These times τ_0 and τ_1 have parameters $\lambda_0(t)$ and $\lambda_1(t)$ respectively. In Chapter 2, the parameters are constants (i.e. $\lambda_0(t) = \lambda_0$ and $\lambda_1(t) = \lambda_1$) and time-varying (i.e. $\lambda_0(t)$ and $\lambda_1(t)$)in Chapter 3.

One direction to make our UI scheme models more realistic is to include real labour force data. In that case, labour force data modelling is a crucial part of this work. Due to accessibility, we explore a variety of models using the labour force dataset from the Office for National Statistics (ONS) in the United Kingdom (UK) [101]. The labour force data contains estimates of variables related to the labour market [135, 134, 71, 102, 114]. Specifically, information on the number of individuals employed, unemployed and inactive and their corresponding rates in the UK per quarter, which are key features needed to compute the unemployment and reemployment rates in our UI scheme is captured in the underlying data. Additionally, the data gives details of the number of individuals that transition between employment, unemployment and inactivity hence enabling us to understand and interpret the changes in the level of the labour market per quarter.

In Chapter 4, we give a brief overview of the dataset using descriptive statistics and visualization. Following this, we use a two-state, a four-state and a five-state model collectively known as labour force state transition (LST) models to investigate the movement between employment, unemployment and inactivity. The LST models are used as decision models because they can be used to simulate labour market' transitions across various states over time. Thus, we run time-step (t-step) simulations using the LST models. We further explore some lake models (two-state and three-state) for the labour force market and run simulations for them as well. The performance and accuracy of the LST and lake modelling techniques are obtained by comparing our simulations to the actual data. Additionally, we fit distributions to data in order to choose the best candidate probability distribution for future work suggestions.

1.7 Optimal stopping theory

Here, we give a brief summary of optimal stopping theory. Optimal stopping theory is one of the most developed areas of contemporary stochastic calculus. The objective of optimal stopping problems is to determine when an underlying stochastic process should be stopped in relation to taking a decision. These decisions are made to optimise the value of certain functionals, to maximise gain functions or minimise loss and cost functions. Optimal stopping has been applied in different disciplines for instance economics [18], engineering [129], physics [37], mathematical finance [137].

Optimal stopping theory is known to have originated around the 1940's from the sequential analysis of statistical observations with a theory of the sequential probability ratio test from Wald in [132] and has developed extensively till date. Based on Wald's initial development, Snell in [123] introduced the generalization of sequential analysis to problems of pure stopping without the use of statistical structures. Sequentially, Snell gave a different approach to solving optimal stopping problems by the characterization of the value function as the smallest super-martingale dominating a stochastic process which is known as the Snell envelope [107].

The equation for the value function was introduced by [5]. This was further developed by Bellman in [12] as the simplest equation of dynamic programming. This finding resulted from the dynamic programming principle of backward induction and also denoted as the Wald-Bellman equation. Dvoretzky in [44] introduced sequential testing problems for continuous-time processes using the discrete time results from [132, 5, 107].

An additional feature of optimal stopping theory is the reduction of an optimal stopping problem to a free boundary problem from mathematical analysis in [136, 20, 84, 117, 9] to solve problems in sequential analysis, optimal stopping, and optimal stochastic control. In [58], a link between free boundary problems for differential operators and optimal stopping problems for Markov processes is identified.

Dynkin [45] then highlighted that on the occasion when the succession of random variables is Markovian, the super martingale characterization of the value function of the optimal stopping problem is superharmonic. Dynkin did a detailed analysis of the discrete time case and identified that similar findings are derived in the continuous time case. Subsequently in the 60's and 70's outcomes of general theory of optimal stopping for discrete time and continuous time in both martingale and Markovian

approaches were explored. Some references such as [58, 118, 122, 125, 116, 50, 127, 47, 97] covered continuous time cases. Shiryaev in [119] also gives a comprehensive overview of the general theory of optimal stopping for the discrete and continuous time Markovian cases. The martingale approach for optimal stopping problems for discrete time stochastic processes is presented in [28].

Accordingly, we see that there are two approaches considered when solving an optimal stopping problem: martingale approach and the Markovian approach. The formulated problem and the probabilistic evolution of the stochastic process helps to determine which approach to use. A modern and detailed overview of the optimal stopping theory and the two approaches used to solve optimal stopping problems for several stochastic models is given in [107] along with several examples.

This thesis deals with the application of optimal stopping theory to UI and the development of the methodology to solve a time-independent and a time-dependent optimal stopping problem. In the time-independent problem, the value function can be explicitly computed by means of a free boundary formulation and the principle of smooth fit [130], that requires certain regularity of the value function. The free boundary technique is an approach based on the solution of a suitable differential equation in a domain with an unknown boundary, the so called free boundary. The smooth-fit principle leads to additional boundary conditions which provide equations that can be used in a verification argument. The latter is used to prove that the solution of the free-boundary problem is indeed the value function of the optimal stopping problem and the free boundary turns out to be the optimal stopping boundary.

It is interesting to point out that in our time independent case, the value function is found explicitly along with a constant optimal stopping threshold. When the parameters of the model are made time-dependent, obvious complications to the model are caused. More specifically, the inclusion of time-dependent functions leads to the alteration the value function to a time-dependent optimal stopping problem. This is often more challenging to solve than the previous case as the free-boundary problem for the value function is in the form of a partial differential equation (PDE) of parabolic type. The optimal boundary in this case is a function of time and an exact computational formula is not known. Nevertheless, some numerical approach done in [8, 33] is proposed to approximate the optimal boundary.

1.8 A brief introduction to mathematical tools

In this section, we will give a brief outline of some major theorems in stochastic analysis and calculus that will be used throughout this work. We assume that the reader has some general knowledge on probability theory, stochastic processes and statistics. These tools are intended to accompany the thesis, and in places are a bit brief. This section is a compilation of materials from [107, 109, 104, 43] and more details can generally be found there.

1.8.1 The martingale approach

We address the continuous time setting. Generally, the concepts in continuous time are similar to the concepts in the discrete time case. Let $G = (G_t)_{t\geq 0}$ (gains process) be a stochastic process defined on a filtered probability space $(\Omega, \mathcal{F}, (\mathcal{F}_t)_{t\geq 0}, \mathrm{P})$. Here G stands for gain, so the process is to be thought of as what we gain if we stop now. Also, G is adapted to the filtration $(\mathcal{F}_t)_{t\geq 0}$, and $\mathcal{F}_t$ is interpreted as all the information we have after observing G up to time t. Optimal stopping theory is concerned with finding a stopping time such that G above is optimised in some sense.

Definition 1.8.1. A random variable $\tau : \Omega \to [0, \infty]$ which is a random time, is called a stopping time if, $\{\tau \leq t\} \coloneqq \{\omega \in \Omega : \tau(\omega) \leq t\} \in \mathcal{F}_t$ for all $t \geq 0$ and $\mathrm{P}(\tau < \infty) = 1$.

Consequently, the general optimal stopping problem will be of the form:

$$V_t = \sup_{t\leq\tau\leq T} \mathrm{E}[G_\tau|\mathcal{F}_t] \tag{1.8.1}$$

where τ is a stopping time and T takes either a finite or infinite form. In order to obtain the theorem about the problem's solution, some assumptions are made about G. In the general treatment of the theory it is assumed that the process G is right continuous and left-continuous over stopping times. This means that $\mathrm{P}\left(\lim_{n\to\infty} G_{\tau_n} = G_\tau\right) = 1$ if $\tau_n \uparrow \tau$ as $n \to \infty$ where τ_n is a sequence of stopping times. This is a weaker condition than left-continuity. Here, we assume for simplicity that G is continuous which is what we need in this thesis. Further extensions can be found in [107].

An integrability condition is also needed:

$$\mathrm{E}\left(\sup_{0\leq t\leq T} |G_t|\right) < \infty. \tag{1.8.2}$$

The problem (1.8.1) is solved for both the uses of finite and infinite time horizon T. In this case, the supremum is taken over the stopping times $\tau < \infty$. Consequently, the concept of essential supremum is introduced (see [107] p.6-7) as follows.

Lemma 1.8.1. *Let $\{Z_\alpha : \alpha \in I\}$ be a family of random variables defined on $(\Omega, \mathcal{F}, (\mathcal{F}_t)_{t\geq 0}, \mathrm{P})$ where the index set I can be arbitrary. Then there exists a countable subset J of I such that the random variable $Z^* : \Omega \to \overline{\mathbb{R}}$ defined by*

$$Z^* = \sup_{\alpha \in J} Z_\alpha \tag{1.8.3}$$

satisfies the following two properties:

(i) $\mathrm{P}(Z_\alpha \leq Z^*) = 1$ *for each* $\alpha \in I$

(ii) If $\bar{Z} : \Omega \to \overline{\mathbb{R}}$ *is another variable satisfying* (1.8.3) *in place of* Z^* *then* $\mathrm{P}(Z^* \leq \bar{Z}) = 1$.

The random variable Z^* above is called the essential supremum of $\{Z_\alpha : \alpha \in I\}$ relative to P and is denoted by $Z^* = \operatorname{ess\,sup}_{\alpha \in I} Z_\alpha$. It is determined uniquely up to a P-null set by the two properties above. The concept of essential supremum is needed because V_t must be $\mathcal{F}_t - measurable$ and this is not gained if we don't use essential supremum in (1.8.1).

Now back to our problem, consider the process $V = (V_t)_{t\geq 0}$ defined by

$$V_t = \operatorname*{ess\,sup}_{\tau \geq t} \mathrm{E}(G_\tau | \mathcal{F}_t) \tag{1.8.4}$$

and known as "Snell envelope" of G. Let us also introduce the stopping time

$$\tau_t = \inf\{s \geq t : V_s = G_s\}, \tag{1.8.5}$$

which will be used in the theorem below.

The main result about the existence of an optimal stopping time in the martingale framework is as follows:

Theorem 1.8.2. *Consider the optimal stopping problem* (1.8.1) *and assume that* (1.8.2) *holds. Assume furthermore that $P(\tau < \infty) = 1$ where $t \geq 0$. Then for all $t \geq 0$ we have:*

$$V_t \geq \mathrm{E}(G_\tau | \mathcal{F}_t) \text{ for all } \tau \in \mathcal{M}_t \text{ and } V_t = \mathrm{E}(G_{\tau_t} | \mathcal{F}_t) \tag{1.8.6}$$

where $\mathcal{M}_t$ denotes the family of all stopping times τ satisfying $\tau \geq t$ (being also smaller than or equal to T when the latter is finite). Moreover, if $t \geq 0$ is given and fixed, then

we have that the stopping time τ_t is optimal in (1.8.1). If τ^* is an optimal stopping time in (1.8.1) then $\mathrm{P}(\tau_t \leq \tau^*) = 1$. The process $(V_s)_{s\geq t}$ is the smallest right-continuous supermartingale which dominates $(G_s)_{s\geq t}$. The stopped process $(V_{s\wedge\tau_t})_{s\geq t}$ is a right-continuous martingale. If $\mathrm{P}(\tau_t = \infty) > 0$ then, with probability 1, there is no optimal stopping time in (1.8.1).

The proof of this theorem is long, and can be found in [107, §1, Section II, p.29]. Let us now give an overview of the other approach.

1.8.2 The Markovian approach

In the martingale approach, we can consider very general gain processes $(G_t)_{t\geq 0}$. Here we restrict the attention to Markov processes. Consider a strong Markov process $X = (X_t)_{t\geq 0}$ defined on a filtered probability space $(\Omega, \mathcal{F}, (\mathcal{F}_t)_{t\geq 0}, \mathrm{P}_x)$ taking values in $(\mathbb{R}^d, \mathcal{B}(\mathbb{R}^d))$ where $\mathcal{B}(\mathbb{R}^d)$ is the Borel σ-algebra on $\mathbb{R}^d$. Furthermore, assume that $\mathrm{P}_x(X_0 = x) = 1$ and that the sample paths of X are continuous and that $(\mathcal{F}_t)_{t\geq 0}$ is right-continuous. Introducing an integrability condition, we consider a measurable function G on $\mathbb{R}^d$, with values in $\mathbb{R}$, that satisfies

$$\mathrm{E}\left(\sup_{0\leq t\leq T} |G(X_t)|\right) < \infty. \tag{1.8.7}$$

where $G(X_t) = 0$ if $T = \infty$. Subsequently, the optimal stopping problem of interest is given by

$$V(x) = \sup_{0\leq\tau\leq T} \mathrm{E}_x G(X_\tau). \tag{1.8.8}$$

Note that $x \in \mathbb{R}^d$ and the supremum is taken over all stopping times τ with respect to $(\mathcal{F}_t)_{t\geq 0}$. Different aspects of the problem are tackled. First is to obtain the aforementioned supremum through the finding of the optimal stopping time τ^*. Secondly, $\mathbb{R}^d$ can be split into two regions: the continuation region (C) where it is optimal to continue and the stopping region $S = \mathbb{R}^d \backslash C$ where it is optimal to stop. Another part of solving the problem is finding the C and S.

A few definitions to compute the results are given below. First we want to understand what it means for a function to be superharmonic.

Definition 1.8.2. A measurable function $F : \mathbb{R}^d \to \mathbb{R}$ is said to be superharmonic if

$$\mathrm{E}_x F(X_\sigma) \leq F(x) \tag{1.8.9}$$

for all stopping times σ and all $x \in \mathbb{R}^d$.

Next we look at the concept of semi-continuity.

Definition 1.8.3. An extended real-valued function F is called lower semi-continuous (lsc) at the point y if

$$F(y) \neq -\infty \text{ and } F(y) \leq \liminf_{x \to y} F(x). \tag{1.8.10}$$

It is called upper semi-continuous (usc) at the point y if

$$F(y) \neq +\infty \text{ and } F(y) \geq \limsup_{x \to y} F(x). \tag{1.8.11}$$

We can say that if it is upper (lower) semi continuous at all points then F is upper (lower) semi-continuous.

The perpetual case for (1.8.8) is when $T = \infty$. In that case the continuation region is given as

$$C = \{x \in \mathbb{R}^d : V(x) > G(x)\} \tag{1.8.12}$$

and the stopping region as

$$S = \{x \in \mathbb{R}^d : V(x) = G(x)\}. \tag{1.8.13}$$

The first entry time of X into S is also denoted by

$$\tau_S = \inf\{t \geq 0 : X_t \in S\} \tag{1.8.14}$$

Based on the definitions of C and S, it is natural to say that

$$V(x) > G(x) \iff \sup_{\tau \geq 0} \mathrm{E}_x G(X_\tau) > G(x) \tag{1.8.15}$$

This means that it is not optimal to stop when $\mathrm{E}_x G(X_\tau) > G(x)$ for $\tau \in [0, \infty]$. Alternatively, it is optimal to stop if

$$V(x) = G(x) \iff \sup_{\tau \geq 0} \mathrm{E}_x G(X_\tau) = G(x). \tag{1.8.16}$$

That is to say when we set $\tau = 0$ then no greater value can be achieved. Using the assumption that V is lsc and G is usc then τ_S is a stopping time with respect to $(\mathcal{F}_t)_{t \geq 0}$. Next, in the Markovian framework, the main theorem about optimal stopping times is given by:

Theorem 1.8.3. *Assuming that (1.8.7) holds, lets consider the perpetual case of problem (1.8.8). Additionally, assume that there exists a smallest superharmonic function $\hat{V}$ which dominates the gain function G on $\mathbb{R}^d$. Also assume that $\hat{V}$ is lsc and G is usc. Then $\hat{V} = V$ and τ_S defined in (1.8.14) is optimal in (1.8.8), if $\mathrm{P}_x(\tau_S < \infty) = 1$ for all $x \in \mathbb{R}^d$. There is also no optimal stopping time in (1.8.8) P_x-a.s., if $\mathrm{P}_x(\tau_S < \infty) < 1$ for some $x \in \mathbb{R}^d$.*

Under the same assumptions as above the theorem holds also for the case of a finite horizon ($T < \infty$) in which case we take $t \in [0, T]$ in the definition of τ_s in (1.8.14). The above theorem hence states that finding a $\hat{V}$ as described is equivalent to solving our initial problem (1.8.8). As we briefly discuss next, this goal can be achieved by free boundary techniques and more details are displayed in [107].

1.8.3 Reduction to free-boundary problem

A differential equation which is defined in some domain by means of an unknown boundary is called free-boundary problem. In our set-up, the boundary may take the form of a function, for instance of a time parameter t, or it may be a constant. Peskir [107] indicates that computing the arbitrage free price of the perpetual American put option leads to a free-boundary problem with a constant boundary b. Solving this problem results to solving the equation itself and finding the unknown boundary. This type of problems is seen in different disciplines. However, in this thesis, we are interested in financial applications. Indeed, our main task later on will be to solve a problem which requires a reduction of an optimal stopping problem to a free-boundary problem. This subsection will serve as a brief introduction to this technique. We retain the notation and settings from the previous section. Based on this, we consider a strong Markov process $X = (X_t)_{t \geq 0}$, which is continuous and takes values in $\mathbb{R}^d$. Additionally, we take a sufficiently regular, measurable function $G : \mathbb{R}^d \to \mathbb{R}$ as given, and consider the optimal stopping problem

$$V(x) = \sup_{\tau} \mathrm{E}_x \left[G(X_\tau) \right]. \tag{1.8.17}$$

Now the stopping times are taken with respect to the filtration generated by X, and $\mathrm{P}_x(X_0 = x) = 1$ for $x \in \mathbb{R}^d$. We have already seen that finding the smallest superharmonic function $\hat{V} : \mathbb{R}^d \to \mathbb{R}$ which dominates the gain function G on $\mathbb{R}^d$ is equivalent to solving such a problem. As mentioned earlier, we split $\mathbb{R}^d$ into the stopping set $S = \{\hat{V} = G\}$, and the continuation set $C = \{\hat{V} > G\}$. The first entry of X into S is

optimal for (1.8.17), and we denote this by

$$\tau_S = \inf\{t \geq 0 : X_t \in S\} \tag{1.8.18}$$

We then formulate the free-boundary problem: $\hat{V}$ and C should solve

$$L_X \hat{V} \leq 0 \qquad (\hat{V}, \text{minimal}), \tag{1.8.19}$$

$$\hat{V} \geq G \qquad (\hat{V} > G \text{ on } C \ \& \ \hat{V} = G \text{ on } S) \tag{1.8.20}$$

$$L_X \hat{V} = 0 \qquad (\text{ on } C). \tag{1.8.21}$$

where L_X is the infinitesimal generator of X. As mentioned in the beginning of this section, both $\hat{V}$ and C are unknown in the above system, and both are to be determined. Under the conditions of Theorem 1.8.3 (see [107] for the details), it is possible to identify $\hat{V}$, with V as in (1.8.17). It follows that we are able to write

$$V(x) = \mathrm{E}_x \left[G(X_{\tau_S}) \right] \tag{1.8.22}$$

where τ_S is defined by (1.8.18). In summary, it can be seen that V solves the Dirichlet problem given by

$$L_X V(x) = 0, \qquad x \in C \tag{1.8.23}$$

$$V(x) = G(x), \quad x \in S \tag{1.8.24}$$

where ∂C is the optimal boundary. The function G and the optimal boundary ∂C have to fulfill some conditions for the above discussion to be valid (again consult [107] for the details). We assume that G is smooth in a neighborhood of ∂C. Also, we assume that X starting at ∂C enters C immediately, which gives rise to the so-called smooth fit condition

$$\frac{\partial V}{\partial x} = \frac{\partial G}{\partial x}, \quad x \in \partial C. \tag{1.8.25}$$

In our thesis, we seek to obtain the right version of the Dirichlet problem for our payoff functions. Certain necessary conditions are assumed when deriving these analogue problems. Note that for our time-independent UI problem, the above method is used. On the other hand, for our UI time-dependent problem, the approach is as follows.

The equation (1.8.23) becomes more complicated as the PDE becomes parabolic with a term $\frac{\partial}{\partial t}$ and usually cannot be solved explicitly. Consequently, finding a candidate function to which a verification procedure is to be applied is often impossible in

this case. One can attempt to characterise V and C (i.e. S) using the free-boundary problem attained above. A more polished method is to derive V in terms of ∂C and find a nonlinear equation for ∂C.

To demonstrate the time-dependent method, let us consider the optimal stopping problem

$$V(t,x) = \sup_{\tau} \mathrm{E}_{t,x} G(t+\tau, X_{t+\tau}) \tag{1.8.26}$$

where the supremum is taken over all stopping times τ of X and $(t,x) \in \mathbb{R}_+ \times \mathbb{R}$. Also, $\mathrm{E}_{t,x}$ denotes the expectation with respect to the distribution of the process $Z_t = (t, X_t)$ for $t \geq 0$ given the initial value $X_t = x$. It follows that (1.8.23), (1.8.24) and (1.8.25) become

$$V_t + L_X V = 0 \text{ in } C, \tag{1.8.27}$$

$$V|_S = G|_S, \tag{1.8.28}$$

$$\left.\frac{\partial V}{\partial x}\right|_{\partial C} = \left.\frac{\partial G}{\partial x}\right|_{\partial C}, \quad \text{(smooth fit)} \ . \tag{1.8.29}$$

As stated earlier this is a brief overview of materials from [107, 109]. Thus, the question of existence and uniqueness of the solution to the free-boundary problem will be studied in subsequent chapters.

1.9 Contributions

The main objective of this thesis is to determine the optimal time for an individual to join the UI scheme. A novel feature of this project is the incorporation of optimal stopping techniques for a dynamic adjustment of the UI policy terms. Optimal stopping is utilised to model and evaluate UI schemes, involving both internal and external covariates that are likely to impact the decision of an individual to enter the scheme. The internal covariates are the wage dynamics, the concept of utility and the premium paid by the individual; and the external covariates are inflation, unemployment, employment, mortality and the benefit paid based on the terms of the policy from the insurance company.

Another important feature is checking the sensitivity of the UI scheme models to variation in the parameters as well as testing how they work over time. These tests are complemented with numerical illustrations using the programming languages Python

and R. To this end, we give insight into the economic implications of the changes in parameters and how the variations affect the individual's decision to enter the scheme.

In addition to the models, the research gives valuable insight into the dynamics of the labour market and how it is affected by shock waves such as the financial recession and COVID-19 shock wave. We further fit models based on the Markov assumption on the time of unemployment and reemployment when formulating our UI scheme and assess the performance of the Markov models against the actual data. Furthermore we explore distributions that best fit the labour force data. This labour force analysis is an important element and a stepping stone to modify the UI scheme models making them more realistic and aid individuals make the best decisions on the optimal time to enter UI schemes.

Our UI models, and more generally the research methods developed in this thesis, are a strong potential to find important applications in actuarial science beyond the specific context of unemployment. A portfolio of sustainable insurance products could be developed to offer competitive benefits based on the possible states of the policy holder (such as 'unemployed/employed', 'dead', 'marriage', 'education',etc).

1.10 Summary of chapters

In Chapter 2, a simple model of unemployment insurance is proposed with a focus on optimality of the individual's entry into the scheme. The corresponding optimal stopping problem is solved, and its similarity and differences with the perpetual American call option are discussed. Beyond a purely financial point of view, we argue that in the actuarial context the optimal decisions should take into account other possible preferences through a suitable utility function.

In Chapter 3, we formulate a problem which is an extension of the simple model, to include time dependent unemployment, reemployment and inflation rates. We implement several tools that will serve as a framework for solving the new model. Before outlining the main steps of the solution, we give a detailed formulation of the problem and examine its properties in order to determine sufficient assumptions for its solution. We justify our results with an analytical approach but we don't derive an explicit solution. Instead we use a numerical method to evaluate the optimal stopping boundary numerically.

In Chapter 4, we analyse and model the United Kingdom labour force data. The

initial part of the chapter is devoted to understanding how the data is generated and the structure of the dataset. This is followed by multistate modelling and lake modelling of the labour market. We run time-step (t-step) simulations using the models and assess the performance and accuracy of the modelling techniques by comparing our simulations to the actual data. Additionally, we fit distributions to data in conjunction with some diagnostic justifications to choose the best fitting models for future work suggestions.

Finally Chapter 5 summarises our findings and concludes with suggestions for future research on the UI scheme models and its application in the economy. The appendix provides some technical definitions and tables discussed in the thesis. It also contains the Python and R codes of some critical computations in the thesis that were implemented.

Chapter 2

Optimal Stopping in a Simple Model of Unemployment Insurance

In this chapter following [4], we present an explicit solution to the optimal stopping problem in a simple model of unemployment insurance. The method of proof is based on the transformation of the optimal stopping problem for the underlying geometric Brownian motion to an appropriate free-boundary problem. The free-boundary problem is solved and the subsequent martingale verification. We also address some statistical issues and numerical illustrations as well as introduce the concept of utility to formulate an optimal stopping problem.

2.1 The model of unemployment insurance

Let us describe our model in more detail. Suppose that time $t \geq 0$ is continuous and is measured (in the units of weeks) starting from the beginning of the individual's employment We assume without loss of generality that the unemployment insurance policy is available immediately (although in practice, a qualifying period at work would normally be required for eligibility). Let $X_t > 0$ denote the individual's wage (i.e., payment per week, paid in arrears) as a function of time $t \geq 0$, such that $X_0 = x$. We treat $X = (X_t,\, t \geq 0)$ as a random process defined on a filtered probability space $(\Omega, \mathcal{F}, (\mathcal{F}_t), \mathrm{P})$, where Ω is a suitable sample space (e.g., consisting of all possible paths

of (X_t)), the filtration $(\mathcal{F}_t)$ is an increasing sequence of σ-algebras $\mathcal{F}_t \subset \mathcal{F}$, and P is a probability measure on the measurable space $(\Omega, \mathcal{F})$ which determines the distribution of various random inputs in the model, including (X_t). It is assumed that the process (X_t) is adapted to the filtration $(\mathcal{F}_t)$, that is, X_t is $\mathcal{F}_t$-measurable for each $t \geq 0$. Intuitively, $\mathcal{F}_t$ is interpreted as the full information available up to time t, and measurability of X_t with respect to $\mathcal{F}_t$ means that this information includes knowledge of the values of the process X_t.

Furthermore, remembering that X_t is positive valued, we use for it a simple model of *geometric Brownian motion* driven by the stochastic differential equation

$$\frac{\mathrm{d}X_t}{X_t} = \mu\,\mathrm{d}t + \sigma\,\mathrm{d}B_t, \qquad X_0 = x, \tag{2.1.1}$$

where B_t is a standard Brownian motion (i.e., with mean zero, $\mathrm{E}(B_t) = 0$, and variance $\mathrm{Var}(B_t) = t$, and with continuous sample paths), and $\mu \in \mathbb{R}$ and $\sigma > 0$ are the drift and volatility rates, respectively. The equation (2.1.1) is well known to have the explicit solution (see, e.g., [121, Ch. III, §3a, p. 237])

$$X_t = x \exp\{(\mu - \tfrac{1}{2}\sigma^2)\,t + \sigma B_t\} \quad (t \geq 0). \tag{2.1.2}$$

Note that

$$\mathrm{E}_x(X_t) = x\,\mathrm{e}^{\mu t}, \qquad \mathrm{Var}_x(X_t) = x^2\mathrm{e}^{2\mu t}(\mathrm{e}^{\sigma^2 t} - 1), \tag{2.1.3}$$

where E_x and Var_x denote expectation and variance with respect to the distribution of X_t given the initial value $X_0 = x$.

Let us now specify the unemployment insurance scheme. An individual who is currently employed may join the scheme by paying a fixed one-off premium $P > 0$ at the point of entry. If and when the current employment ends (say, at time instant τ_0), the benefit proportional to the final wage X_{τ_0} is payable according to the *benefit schedule* $h(s)$; that is, the payout at time $t \geq \tau_0$ is given by $X_{\tau_0} h(t - \tau_0)$. However, the payment stops when a new job is found after the unemployment spell of duration τ_1. For simplicity, we assume that both τ_0 and τ_1 have *exponential distribution* (with parameters λ_0 and λ_1, respectively); as mentioned in the Introduction, this guarantees the Markovian nature of the corresponding transitions. These random times are also assumed to be statistically independent of the process (X_t).

Possible transitions in the state space of our insurance model are shown in Fig. 2, where symbols "0" and "1" encode the states of being employed and unemployed,

respectively, whereas suffixes "+" and "–" indicate whether insurance is in place or not. Note that all transitions, except from 0– to 0+ (which is subject to optimal control based of observations over the wage process (X_t)), occur in a Markovian fashion; that is, the holding times are exponentially distributed (with parameters λ_0 if in states 0– and 0+, or λ_1 if in states 1– and 1+).

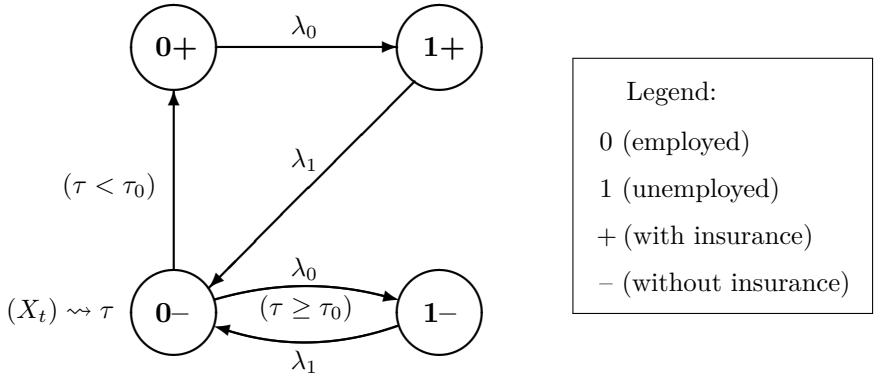

FIGURE 2: Schematic diagram of possible transitions in the unemployment insurance scheme. Here, τ_0 and τ_1 are the (exponential) holding times in states 0 and 1, with parameters λ_0 and λ_1, respectively, whereas τ is the entry time (i.e., from state 0– to state 0+), which is subject to optimal control based on observations over the wage process (X_t).

The individual's decision about a suitable time to join the scheme is based on the information available to date. In our model, this information encoded in the filtration $(\mathcal{F}_t)$ is provided by ongoing observations over the wage process (X_t). Thus, *admissible strategies* for choosing τ must be *adapted* to the filtration $(\mathcal{F}_t)$; namely, at any time instant $t \geq 0$ it should be possible to determine whether τ has occurred or not yet, given all the information in $\mathcal{F}_t$. In mathematical terms, this means that τ is a *stopping time*, whereby for any $t \geq 0$ the event $\{\tau > t\}$ belongs to the σ-algebra $\mathcal{F}_t$ (see, e.g., [138, Ch. 1, §3, p. 25]).

Remark 2.1.1. In general, a stopping time τ is allowed to take values in $[0, \infty]$ including ∞, in which case waiting continues indefinitely and the decision to join the scheme is never taken. In practice, it is desirable that the stopping time τ be finite almost surely (a.s.) (i.e., $\mathrm{P}_x(\tau < \infty) = 1$), but this may not always be the case (see Section 2.4.1).

2.2 Setting the optimal stopping problem

As was explained informally in the Introduction, there is a scope for optimizing the choice of the entry time τ, where optimality is measured by maximizing the expected financial gain from the scheme. Our next goal is to obtain an expression for the expected gain under the contract. First of all, conditional on the final wage X_{τ_0}, the expected future benefit to be received under this insurance contract is given by

$$X_{\tau_0}\,\mathrm{E}\left(\int_0^{\tau_1} \mathrm{e}^{-rs}\,h(s)\,\mathrm{d}s\right) = \beta X_{\tau_0}, \tag{2.2.1}$$

where r is the *inflation rate* and

$$\beta := \int_0^{\infty} \lambda_1\,\mathrm{e}^{-\lambda_1 t} H(t)\,\mathrm{d}t, \qquad H(t) := \int_0^t \mathrm{e}^{-rs}\,h(s)\,\mathrm{d}s. \tag{2.2.2}$$

Note that the expectation in formula (2.2.1) is taken with respect to the (exponential) random waiting time τ_1 (with parameter λ_1), and that the expression inside the integrand involves discounting to the beginning of unemployment at time τ_0.

Example 2.2.1. A specific example of the benefit schedule $h(s)$ may be as follows,

$$h(s) = \begin{cases} h_0, & 0 \le s \le s_0, \\ h_0\,\mathrm{e}^{-\delta(s-s_0)}, & s \ge s_0, \end{cases} \tag{2.2.3}$$

where $0 < h_0 \le 1$, $0 \le s_0 \le \infty$ and $\delta > 0$. Thus, the insured receives a certain fraction of their final wage (i.e., $h_0 X_{\tau_0}$) for a grace period s_0, after which the benefit is falling down exponentially with rate δ. This example is motivated by the declining unemployment compensation system in France [76].[1] Having specified the schedule function, all calculations can be done explicitly. In particular, the constant β in (2.2.1) is calculated from (2.2.2) as

$$\beta = \frac{h_0\bigl(1-\mathrm{e}^{-(r+\lambda_1)s_0}\bigr)}{r+\lambda_1} + \frac{h_0\,\mathrm{e}^{-(r+\lambda_1+\delta)s_0}}{r+\lambda_1+\delta}.$$

[1] More specifically, according to the French UI system back in the 1990s (see [76, p. 8]), a worker aged 50 or more, with eight months of insurable employment in the last twelve months, was entitled to full benefits equal to 57.4% of the final wage payable for the first eight months, thereafter declining by 15% every four months; however, the payments continued for no longer than 21 months overall. This leads to choosing the following numerical values in (2.2.3): $h_0 = 0.574$, $s_0 = 8\,(52/12) \doteq 34.7$ (weeks) and $\delta = -(3/52)\ln(1-0.15) \doteq 0.0094 = 0.94\%$ (per week). The restriction of the benefit term by $21\,(52/12) = 91$ weeks can be taken into account in our model by adjusting the parameter λ_1 from the condition $\mathrm{E}(\tau_1) = 91$, giving $\lambda_1 \doteq 0.0110$. A more conservative choice is to use a tail probability condition, for example, $\mathrm{P}(\tau_1 > 91) = 0.10$, yielding $\lambda_1 = -\ln(0.10)/91 \doteq 0.0253$ (with $\mathrm{E}(\tau_1) \doteq 39.5$).

In the extreme cases $s_0 = 0$ or $s_0 = \infty$, this expression simplifies to

$$\beta = \begin{cases} \dfrac{h_0}{\lambda_1}\left(1 - \dfrac{r+\delta}{r+\lambda_1+\delta}\right), & s_0 = 0, \\ \dfrac{h_0}{\lambda_1}\left(1 - \dfrac{r}{r+\lambda_1}\right), & s_0 = \infty. \end{cases}$$

Here, the first factor has a clear meaning as the product of pay per week (h_0) and the mean duration of the benefit payment ($\mathrm{E}(\tau_1) = 1/\lambda_1$), whereas the second factor takes into account the discounting at rates r and δ.

Returning to the general case, if the contract is entered immediately (subject to the payment of premium P), then the net expected benefit discounted to the entry time $t = 0$ is given by the *gain function*

$$g(x) := \mathrm{E}_x(\mathrm{e}^{-r\tau_0}\beta X_{\tau_0}) - P, \tag{2.2.4}$$

where $x = X_0$ is the starting wage and the symbol E_x now indicates expectation with respect to both τ_0 and X_{τ_0}. Recall that the random time τ_0 is independent of the process (X_t) and has the exponential distribution with parameter λ_0. Using the total expectation formula (see, e.g., [120, §II.7.4, Definition 3, p. 214, and Property G*, p. 216]) and substituting the expression (2.1.3), the expectation in (2.2.4) is computed as follows,

$$\begin{aligned} \mathrm{E}_x(\mathrm{e}^{-r\tau_0}X_{\tau_0}) &= \mathrm{E}_x\left[\mathrm{e}^{-r\tau_0}\,\mathrm{E}_x(X_{\tau_0}\,|\,\tau_0)\right] \\ &= \mathrm{E}_x\left[\mathrm{e}^{-r\tau_0}(x\,\mathrm{e}^{\mu\tau_0})\right] = x\int_0^\infty \mathrm{e}^{(\mu-r)t}\,\lambda_0\,\mathrm{e}^{-\lambda_0 t}\,\mathrm{d}t \\ &= \frac{\lambda_0\,x}{r+\lambda_0-\mu}. \end{aligned} \tag{2.2.5}$$

Thus, substituting (2.2.5) into (2.2.4) and denoting

$$\tilde{r} := r + \lambda_0, \qquad \beta_1 := \frac{\beta\lambda_0}{\tilde{r}-\mu}, \tag{2.2.6}$$

the gain function is represented explicitly as

$$g(x) = \beta_1 x - P. \tag{2.2.7}$$

Of course, the computation in (2.2.5) is only meaningful as long as

$$\mu < r + \lambda_0 = \tilde{r}. \tag{2.2.8}$$

Assumption 2.2.1. In what follows, we always assume that the condition (2.2.8) is satisfied.

Remark 2.2.1. In real life applications, the wage growth rate μ is rather small (but may be either positive or negative). It is unlikely to exceed the inflation rate r, but even if it does, then it is hardly possible economically that it is greater than the combined inflation–unemployment rate $\tilde{r} = r + \lambda_0$. Thus, the condition (2.2.8) is absolutely realistic.

To generalize the expression (2.2.7), consider a delayed entry time $\tau > 0$ (tacitly assuming that $\tau < \infty$). Discounting first to the entry time τ when the deduction of the premium P is activated, and then further down to the initial time moment $t = 0$, yields the *expected net present value* of the total gain as a function of the initial wage x,

$$\mathrm{eNPV}(x;\tau) := \mathrm{E}_x\big[\mathrm{e}^{-r\tau}\big(\mathrm{e}^{-r(\tau_0-\tau)}\beta X_{\tau_0} - P\big)\,\mathbb{1}_{\{\tau<\tau_0\}}\big], \tag{2.2.9}$$

where the expectation on the right now also includes averaging with respect to τ, which is a functional of the path (X_t). Note that the indicator function under the expectation specifies that the entry time τ must occur prior to τ_0, for otherwise there will be no gain.

Remark 2.2.2. The notation (2.2.9) emphasizes that the expected net present value depends on the specific entry time τ. As was intuitively explained in the Introduction, there is a scope for optimizing the choice of τ, where optimality is measured by *maximizing* $\mathrm{eNPV}(x;\tau)$.

Formula (2.2.9) indicates that the decision time τ has a finite (random) expiry date τ_0 (using the terminology of financial options). However, the expectation in (2.2.9) involves averaging with respect to τ_0. Moreover, taking advantage of exponential distribution of τ_0, the expression (2.2.9) can be rewritten without any expiry date (i.e., as a *perpetual option*).

Lemma 2.2.1. *The expected net present value defined by formula* (2.2.9) *can be expressed in the form*

$$\mathrm{eNPV}(x;\tau) = \mathrm{E}_x\big[\mathrm{e}^{-\tilde{r}\tau}g(X_\tau)\,\mathbb{1}_{\{\tau<\infty\}}\big], \tag{2.2.10}$$

where the function $g(\cdot)$ is defined in (2.2.4) *and $\tilde{r} = r + \lambda_0$ (see* (2.2.6)).

Proof. Since the distribution of τ_0 is exponential, the excess time $\tilde{\tau}_0 := \tau_0 - \tau$ conditioned on $\{\tau < \tau_0\}$ is again exponentially distributed (with the same parameter λ_0)

and independent of τ. Hence, conditioning on τ (restricted to the event $\{\tau < \infty\}$) and using the total expectation formula as before [120, §II.7, Property G*, p. 216]), together with the (strong) Markov property of the process (X_t), we get from (2.2.9)

$$\begin{aligned}\mathrm{eNPV}(x;\tau) &= \mathrm{E}_x\big(\mathrm{E}_x\big[\mathrm{e}^{-r\tau}\big(\mathrm{e}^{-r(\tau_0-\tau)}\beta X_{\tau_0} - P\big)\mathbb{1}_{\{\tau_0>\tau\}}\big|\tau\big]\big)\\ &= \mathrm{E}_x\Big(\mathrm{e}^{-r\tau}\,\mathrm{E}_x\big[(\mathrm{e}^{-r\tilde{\tau}_0}\beta X_{\tau+\tilde{\tau}_0} - P)\big|\tau\big]\cdot\mathrm{E}_x\big[\mathbb{1}_{\{\tau_0>\tau\}}\big|\tau\big]\Big)\\ &= \mathrm{E}_x\Big(\mathrm{e}^{-r\tau}\,\mathrm{E}_{X_\tau}\big[(\mathrm{e}^{-r\tilde{\tau}_0}\beta \widetilde{X}_{\tilde{\tau}_0} - P)\big]\cdot\mathrm{P}_x(\tau_0>\tau|\tau)\Big),\end{aligned} \tag{2.2.11}$$

where $\widetilde{X}_t := X_{\tau+t}$ $(t \geq 0)$ is a shifted wage process starting at $\widetilde{X}_0 = X_\tau$. Substituting $\mathrm{P}_x(\tau_0 > \tau|\tau) = \mathrm{e}^{-\lambda_0\tau}$ and recalling notation (2.2.4), formula (2.2.11) is reduced to (2.2.10). □

Finally, without loss we can remove the indicator from the expression (2.2.10) by defining the value of the random variable under expectation to be zero on the event $\{\tau = \infty\}$. This definition is consistent with the limit at infinity. Indeed, observe using (2.1.2) and (2.2.5) that

$$\begin{aligned}\mathrm{e}^{-\tilde{r}t}g(X_t) &= \mathrm{e}^{-\tilde{r}t}\left(\beta_1 x\,\mathrm{e}^{(\mu-\sigma^2/2)t+\sigma B_t} - P\right)\\ &= \beta_1 x\exp\left\{-t\big(\tilde{r}-\mu+\tfrac{1}{2}\sigma^2+\sigma\,t^{-1}B_t\big)\right\} - P\,\mathrm{e}^{-\tilde{r}t}.\end{aligned} \tag{2.2.12}$$

Due to the condition (2.2.8), $\tilde{r} - \mu + \frac{1}{2}\sigma^2 > \frac{1}{2}\sigma^2 > 0$. In addition, by the (strong) law of large numbers for the Brownian motion (see, e.g., [42, Exercise 6.4, p. 265] or [121, Ch. III, §3b, p. 246]),

$$\lim_{t\to\infty} t^{-1}B_t = 0 \quad (\mathrm{P}\text{-a.s.}).$$

Thus, the limit of (2.2.12) as $t \to \infty$ is zero (P_x-a.s.). Hence, the event $\{\tau = \infty\}$ does not contribute to the expectation (2.2.10), so that, substituting (2.2.5), we get

$$\mathrm{eNPV}(x;\tau) = \mathrm{E}_x\big[\mathrm{e}^{-\tilde{r}\tau}g(X_\tau)\big]. \tag{2.2.13}$$

To summarize, identification of the optimal entry time $\tau = \tau^*$, in the sense of maximizing the expected net present value $\mathrm{eNPV}(x;\tau)$ as a function of strategy τ (see (2.2.13)), is reduced to solving the following *optimal stopping problem*,

$$v(x) = \sup_\tau \mathrm{E}_x\big[\mathrm{e}^{-\tilde{r}\tau}g(X_\tau)\big], \tag{2.2.14}$$

where the function $g(x)$ is given by (2.2.7) and the supremum is taken over the class of all admissible stopping times τ (i.e., adapted to the filtration $(\mathcal{F}_t)$). The supremum $v(x)$ in (2.2.14) is called the *value function* of the optimal stopping problem.

2.2.1 Allowing for mortality

The simple model of unemployment insurance set out in Section 2.1 can be easily extended to include mortality. Following [91, pp. 399–401], suppose that the individual who contemplates taking out the unemployment insurance policy may die (say, at a random time τ_2 from zero), independently of employment-related events and subject to a constant force of mortality λ_2. That is to say, given that the individual is alive at current age $t \geq 0$, the residual lifetime $\tau_2 - t$ is an independent random variable exponentially distributed with parameter λ_2,

$$\mathrm{P}\left(\tau_2 - t > s \,|\, \tau_2 > t\right) = \mathrm{e}^{-\lambda_2 s} \quad (s \geq 0).$$

The necessary modifications to the unemployment insurance model of Section 2.2 start by adjusting the formula for the expected future benefit (see (2.2.1)). Assuming that death does not occur prior to the time τ_0 of losing the job (i.e., $\tau_2 > \tau_0$, so that $\tilde{\tau}_2 := \tau_2 - \tau_0$ is exponentially distributed with parameter λ_2), the benefit payments cease at $\tau_1 \wedge \tilde{\tau}_2$ (i.e., when a new job is found or at death, whichever occurs first). Since τ_1 and $\tilde{\tau}_2$ are independent and both have exponential distributions, the random variable $\tau_1 \wedge \tilde{\tau}_2$ has the exponential distribution with parameter $\lambda_1 + \lambda_2$. Hence, the constant β from (2.2.2) is now written as

$$\beta = \int_0^\infty (\lambda_1 + \lambda_2)\, \mathrm{e}^{-(\lambda_1+\lambda_2)\, t}\, H(t)\, \mathrm{d}t.$$

Next, we need to take into account the effect of death in service, that is, if $\tau_2 \leq \tau_0$. To be specific, it is reasonable to assume that the lump sum to be paid by the employer in this case is proportional to the final wage, say $a^\dagger X_{\tau_2}$. Then, separating the cases where death occurs after or prior to loss of job, it is easy to see that the definition (2.2.4) of the gain function (i.e., net expected benefit discounted to the policy entry time) takes the form

$$g(x) = \mathrm{E}_x\big(\mathrm{e}^{-r\tau_0}\, \beta\, X_{\tau_0}\, \mathbb{1}_{\{\tau_0 < \tau_2\}}\big) + \mathrm{E}_x\big(\mathrm{e}^{-r\tau_0}\, a^\dagger X_{\tau_2}\, \mathbb{1}_{\{\tau_2 \leq \tau_0\}}\big) - P. \tag{2.2.15}$$

The first expectation in (2.2.15) is computed using conditioning on τ_0 and the total

expectation formula (cf. (2.2.5)),

$$\begin{aligned}\mathrm{E}_x(\mathrm{e}^{-r\tau_0}\,X_{\tau_0}\,\mathbb{1}_{\{\tau_0<\tau_2\}}) &= \mathrm{E}_x[\mathrm{e}^{-r\tau_0}\,\mathrm{E}_x(X_{\tau_0}\,\mathbb{1}_{\{\tau_0<\tau_2\}}\,|\,\tau_0)]\\ &= \mathrm{E}_x[\mathrm{e}^{-r\tau_0}\,\mathrm{E}_x(X_{\tau_0}\,|\,\tau_0)\cdot\mathrm{P}_x(\tau_2>\tau_0\,|\,\tau_0)]\\ &= \mathrm{E}_x(\mathrm{e}^{-r\tau_0}\,x\,\mathrm{e}^{\mu\tau_0}\,\mathrm{e}^{-\lambda_2\tau_0}) = x\int_0^\infty \mathrm{e}^{(\mu-r-\lambda_2)t}\,\lambda_0\,\mathrm{e}^{-\lambda_0 t}\,\mathrm{d}t\\ &= \frac{\lambda_0\,x}{r+\lambda_0+\lambda_2-\mu},\end{aligned}\tag{2.2.16}$$

where in the second line we used conditional independence of X_{τ_0} and τ_2 given τ_0. Similarly, by conditioning on τ_2 the second expectation in (2.2.15) is represented as

$$\begin{aligned}\mathrm{E}_x(\mathrm{e}^{-r\tau_0}\,X_{\tau_2}\,\mathbb{1}_{\{\tau_2\le\tau_0\}}) &= \mathrm{E}_x[X_{\tau_2}\,\mathrm{E}_x(\mathrm{e}^{-r\tau_0}\,\mathbb{1}_{\{\tau_0\ge\tau_2\}}\,|\,\tau_2)]\\ &= \mathrm{E}_x\Big[X_{\tau_2}\int_{\tau_2}^\infty \mathrm{e}^{-rt}\,\lambda_0\,\mathrm{e}^{-\lambda_0 t}\,\mathrm{d}t\Big]\\ &= \frac{\lambda_0}{r+\lambda_0}\,\mathrm{E}_x(X_{\tau_2}\,\mathrm{e}^{-(r+\lambda_0)\tau_2}).\end{aligned}\tag{2.2.17}$$

Again conditioning on τ_2, the last expectation is computed as follows,

$$\begin{aligned}\mathrm{E}_x(X_{\tau_2}\,\mathrm{e}^{-(r+\lambda_0)\tau_2}) &= \mathrm{E}_x[\mathrm{e}^{-(r+\lambda_0)\tau_2}\,\mathrm{E}_x(X_{\tau_2}\,|\,\tau_2)]\\ &= \mathrm{E}_x(\mathrm{e}^{-(r+\lambda_0)\tau_2}\,x\,\mathrm{e}^{\mu\tau_2})\\ &= x\int_0^\infty \mathrm{e}^{-(r+\lambda_0-\mu)t}\lambda_2\,\mathrm{e}^{-\lambda_2 t}\,\mathrm{d}t\\ &= \frac{\lambda_2\,x}{r+\lambda_0+\lambda_2-\mu}.\end{aligned}\tag{2.2.18}$$

Finally, substituting the expressions (2.2.16), (2.2.17) and (2.2.18) into the definition (2.2.15), we obtain explicitly

$$g(x) = \frac{\lambda_0\,x}{r+\lambda_0+\lambda_2-\mu}\left(\beta+\frac{\lambda_2\,a^\dagger}{r+\lambda_0}\right)-P.$$

This expression has the same form as (2.2.7) but with the parameters $\tilde{r}$ and β_1 redefined as follows (cf. (2.2.6)),

$$\tilde{r} := r+\lambda_0+\lambda_2, \qquad \beta_1 := \frac{\lambda_0}{\tilde{r}-\mu}\left(\beta+\frac{\lambda_2\,a^\dagger}{r+\lambda_0}\right).$$

In addition, the inequality (2.2.8) of Assumption 2.2.1 is updated accordingly. Subject to this reparameterization, all subsequent calculations leading to the optimal stopping problem (2.2.14) remain unchanged.

For the sake of clarity and in order not to distract the reader by unnecessary technicalities, in the rest of the paper we adhere to the original version of the model (i.e., with no mortality, $\lambda_2 = 0$); however, see the discussion at the end of Section 2.6.4 indicating an important regularizing role of mortality, helping to avoid undesirable inconsistencies of the model at small unemployment rates λ_0.

2.2.2 A priori properties of the value function

The next lemma shows that the optimal stopping problem (2.2.14) is well posed.

Lemma 2.2.2. *The value function $x \mapsto v(x)$ of the optimal stopping problem (2.2.14) has the following properties:*

(i) $v(0) = 0$ *and, moreover,* $v(x) \geq 0$ *for all* $x \geq 0$;

(ii) $v(x) < \infty$ *for all* $x \geq 0$.

Proof. (i) If $x = 0$ then, due to (2.1.2), $X_t \equiv 0$ (P_0-a.s.) and the stopping problem (2.2.14) is reduced to

$$v(0) = \sup_{\tau} \mathrm{E}_0(-P\,\mathrm{e}^{-\tilde{r}\tau}),$$

which has the obvious solution $\tau = \infty$ (P_0-a.s.), with the corresponding supremum value $v(0) = 0$. Furthermore, by considering $\tau = \infty$ (P_x-a.s.) it readily follows from (2.2.14) that $v(x) \geq 0$ for all $x \geq 0$.

(ii) Recalling that $\mu < \tilde{r}$ (see Assumption 2.2.1), observe that the process $\mathrm{e}^{-\tilde{r}t}X_t$ is a *supermartingale*; indeed, for $0 \leq s \leq t$ we have, using (2.1.2) and (2.1.3),

$$\begin{aligned}
\mathrm{E}_x\big[\mathrm{e}^{-\tilde{r}t}X_t \,|\, \mathcal{F}_s\big] &= \mathrm{e}^{-\tilde{r}t}X_s\,\mathrm{E}\big[\mathrm{e}^{\sigma(B_t-B_s)+(\mu-\frac{1}{2}\sigma^2)(t-s)}\big] \\
&= \mathrm{e}^{-\tilde{r}t}X_s\,\mathrm{e}^{\mu(t-s)} \\
&\leq \mathrm{e}^{-\tilde{r}s}X_s \quad (\mathrm{P}_x\text{-a.s.}).
\end{aligned}$$

In particular,

$$\mathrm{E}_x(\mathrm{e}^{-\tilde{r}t}X_t) \leq \mathrm{E}_x(X_0) = x.$$

Hence, by Doob's optional sampling theorem for non-negative, right-continuous supermartingales (see, e.g., [138, Theorem 8.18, pp. 140–141]), for any stopping time τ we have

$$\mathrm{E}_x(\mathrm{e}^{-\tilde{r}\tau}X_\tau) \leq \mathrm{E}_x(X_0) = x,$$

and it follows that the supremum in (2.2.14) is finite. □

2.2.3 The optimal stopping rule

For the wage process (X_t), consider the *hitting time* τ_b of a threshold $b \in \mathbb{R}$, defined by

$$\tau_b := \inf\{t \geq 0 \colon X_t \geq b\} \in [0, \infty].$$

(As usual, we make a convention that $\inf \varnothing = \infty$.) Clearly, τ_b is a stopping time, that is, $\{\tau \leq t\} \in \mathcal{F}_t$ for all $t \geq 0$. Since the process X_t has a.s.-continuous sample paths, on the event $\{\tau_b < \infty\}$ we have $X_{\tau_b} = b$ (P_x-a.s.). As we will show, the optimal strategy for the optimal stopping problem (2.2.14) is to wait until the random process X_t hits a certain threshold b^* (see Fig. 3). More precisely, the solution to (2.2.14) is provided by the following stopping rule,

$$\tau^* = \begin{cases} \tau_{b^*} & \text{if } x \in [0, b^*], \\ 0 & \text{if } x \in [b^*, \infty). \end{cases} \tag{2.2.19}$$

That is to say, if $x \geq b^*$ then one must stop and buy the policy immediately, or else wait until the hitting time $\tau_{b^*} \geq 0$ occurs and buy the policy then. (Of course, these two rules coincide when $x = b^*$.) However, if it happens so that $\tau_{b^*} = \infty$, then, according to the above rule, one must wait indefinitely and, therefore, never buy the policy.

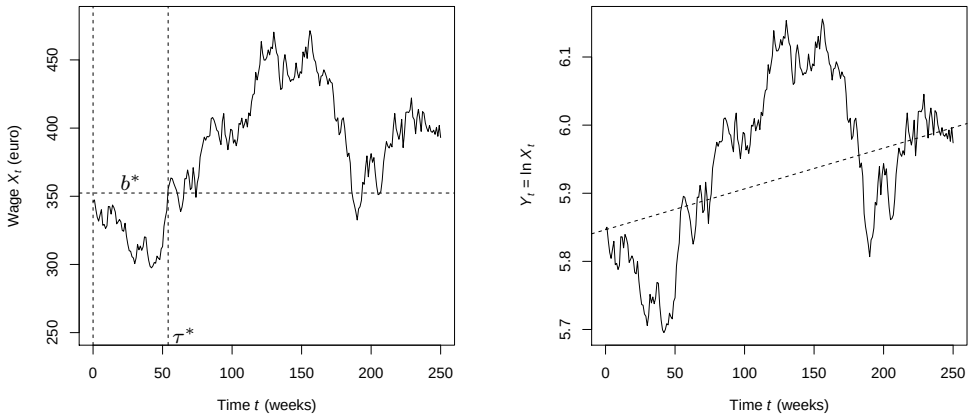

FIGURE 3: Simulated wage process X_t (left) and $Y_t = \ln X_t$ (right) according to the geometric Brownian motion model (2.1.2), with $X_0 = 346$ (euros) and parameters $\mu = 0.0004$ and $\sigma = 0.02$ (see Example 2.5.2). The dashed horizontal line on the left plot indicates the optimal threshold $b^* \doteq 352.37$ (euros) first attained in this simulation at $\tau^* = 54$ (weeks). The dashed line on the right plot shows the estimated drift of the log-transformed data (see Section 2.5.2).

The specific value of the critical threshold b^* is given by

$$b^* = \frac{Pq_*}{\beta_1(q_* - 1)}, \tag{2.2.20}$$

where

$$q_* = \frac{1}{\sigma^2}\left(-(\mu - \tfrac{1}{2}\sigma^2) + \sqrt{(\mu - \tfrac{1}{2}\sigma^2)^2 + 2\tilde{r}\sigma^2}\right). \tag{2.2.21}$$

It is straightforward to check, using condition (2.2.8), that $q_* > 1$ (see also Section 2.3.2). Finally, the corresponding value function (2.2.14) is specified as

$$v(x) = \begin{cases} (\beta_1 b^* - P)\left(\dfrac{x}{b^*}\right)^{q_*}, & x \in [0, b^*], \\ \beta_1 x - P, & x \in [b^*, \infty). \end{cases} \tag{2.2.22}$$

Equivalently, substituting the expression (2.2.20), formula (2.2.22) is explicitly rewritten as

$$v(x) = \begin{cases} \dfrac{P}{q_* - 1}\left(\dfrac{\beta_1(q_* - 1)x}{Pq_*}\right)^{q_*}, & 0 \le x \le \dfrac{Pq_*}{\beta_1(q_* - 1)}, \\ \beta_1 x - P, & x \ge \dfrac{Pq_*}{\beta_1(q_* - 1)}. \end{cases} \tag{2.2.23}$$

In particular, the function $x \mapsto v(x)$ is strictly increasing for $x \ge 0$, with $v(0) = 0$ (cf. Lemma 2.2.2).

These results will be proved in Section 2.3.

2.2.4 Deterministic case

For orientation, it is useful to consider the simple baseline case $\sigma = 0$, where the random process X_t (see (2.1.2)) degenerates to the deterministic function

$$X_t = x\,\mathrm{e}^{\mu t} \quad (t \ge 0).$$

Hence, any stopping time τ is non-random, say $\tau = t$, and the optimal stopping problem (2.2.14) is reduced to

$$v(x) = \sup_{t \ge 0}[\mathrm{e}^{-\tilde{r}t}(\beta_1 x\,\mathrm{e}^{\mu t} - P)]. \tag{2.2.24}$$

The problem (2.2.24) is easily solved, with the maximizer t^* given by

$$t^* = \inf\{t \ge 0 \colon x\mathrm{e}^{\mu t} \ge b_0^*\} \in [0, \infty], \tag{2.2.25}$$

where

$$b_0^* = \begin{cases} \dfrac{P\tilde{r}}{\beta_1(\tilde{r}-\mu)}, & \mu > 0, \\ \dfrac{P}{\beta_1}, & \mu \le 0. \end{cases} \tag{2.2.26}$$

The expression (2.2.26) is consistent with the general formula (2.2.20), noting that, in the limit as $\sigma \downarrow 0$, the quantity (2.2.21) is reduced to (cf. (2.2.8))

$$q_* = \begin{cases} \dfrac{\tilde{r}}{\mu} > 1, & \mu > 0, \\ \infty, & \mu \le 0. \end{cases}$$

With this convention, it is easy to check that the value function (2.2.24) is given by the general formula (2.2.22). In particular, if $\mu \le 0$ and $x < b_0^*$ then, according to (2.2.25), $t^* = \infty$ and from (2.2.24) we get $v(x) = 0$; indeed, the function $t \mapsto x\mathrm{e}^{\mu t}$ is non-increasing, so it never attains the required threshold $b_0^* > x$. In contrast, if $x \ge b_0^*$ then by (2.2.25) $t^* = 0$ (for any μ), and (2.2.24) readily yields $v(x) = \beta_1 x - P$.

2.3 Solving the optimal stopping problem

The optimal stopping problem (2.2.14) involves two tasks: (i) evaluating the value function $v(x)$, and (ii) identifying the maximizer $\tau = \tau^*$. A standard approach is to try and *guess* the solution and then to *verify* that it is correct.

2.3.1 Guessing the solution

Let us look more closely at the nature of the value function $v(x)$ that we are trying to identify. Observe that by picking $\tau = 0$ in (2.2.14) yields the lower estimate

$$v(x) \ge g(x). \tag{2.3.1}$$

Clearly, if $v(x) > g(x)$ then we have not yet achieved the maximum payoff available, so we should continue to wait. On the other hand, if $v(x) = g(x)$ then the maximum has been attained and we should stop. This motivates the definition of the two regions, C (*continuation*) and S (*stopping*),

$$C := \{x \ge 0 \colon v(x) > g(x)\}, \qquad S := \{x \ge 0 \colon v(x) \le g(x)\}.$$

By virtue of the Markov property of the process X_t, the same argument can be propagated to any time $t \ge 0$, provided that stopping has not yet occurred. Namely,

if $X_t = x'$ (and $\tau \geq t$) then the problem (2.2.14) is updated with the new (residual) stopping time $\tau' = \tau - t$ and with the initial value x replaced by x'.

Thus, it is natural to expect that the optimal strategy prescribes to continue as long as the current wage value X_t belongs to the region C (i.e., $v(X_t) > g(X_t)$), but to stop when X_t first enters the region S (i.e., $v(X_t) \leq g(X_t)$). That is to say, the optimal stopping time should be given by[1]

$$\tau^* = \inf\{t \geq 0 \colon X_t \in S\} = \inf\{t \geq 0 \colon v(X_t) \leq g(X_t)\} \in [0, \infty]. \tag{2.3.2}$$

To clarify the plausible structure of the stopping set S, recall (see the proof of Lemma 2.2.2(i)) that a zero value of the stopping problem (2.2.14) is achieved by simply using the strategy $\tau \equiv \infty$, that is, by never joining the scheme. Thus, if the initial wage $X_0 = x$ is small (e.g., such that $g(x) = \beta_1 x - P < 0$) then, in order to secure a positive payoff, we should wait for a sufficiently high wage X_t. This suggests that the stopping rule (2.3.2) is reduced to the first hitting time for a certain set on the plane $\{(t, x) \colon t \geq 0,\, x \geq 0\}$. Furthermore, noting that the definition (2.3.2) is time homogeneous, in that it does not change in the course of time t, we also hypothesize the simplest situation whereby the regions C and S are determined by a constant threshold $y = b^* > 0$,

$$C = [0, b^*), \qquad S = [b^*, \infty). \tag{2.3.3}$$

In other words, the conjectural hitting boundary does not depend on time.

Hence, we are led to the reduced optimal stopping problem over the subclass of hitting times,

$$u(x) = \sup_{b \geq 0} \mathrm{E}_x \left[\mathrm{e}^{-\tilde{r}\tau_b} g(X_{\tau_b}) \right]. \tag{2.3.4}$$

In particular, formula (2.3.2) specializes to

$$\tau_{b^*} = \inf\{t \geq 0 \colon X_t \geq b^*\} = \inf\{t \geq 0 \colon u(X_t) \leq g(X_t)\} \in [0, \infty]. \tag{2.3.5}$$

Our first task is to identify the value function $u(x)$ in (2.3.4) and the corresponding maximizer $b = b^*$ by solving the corresponding free-boundary problem (Section 2.3.2). After that, we will have to show that this solution is optimal in the general class of stopping times, that is, $u(x) = v(x)$ for all $x \geq 0$ (Section 2.3.3).

[1] This conclusion is in accord with the general optimal stopping theory [107, §II.2.2].

2.3.2 Free-boundary problem

According to general theory of optimal stopping (see, e.g., [107, Ch. IV]), in the continuation region $C = [0, b)$ (see (2.3.3)) the value function $u(x)$ from (2.3.4) must be *harmonic* with respect to the underlying process $\widetilde{X}_t$ generated by X_t. More precisely, due to the discounting exponential factor in the optimal stopping problem (2.3.4), the process $\widetilde{X}_t$ is obtained from X_t by independent *killing* (or discounting) with rate $\tilde{r}$ (see [107, §§ 5.4, 6.3]). Thus, if b is a suitable threshold and τ_b is the corresponding hitting time, then for any $x \geq 0$ the following condition must hold,

$$\mathrm{E}_x[\mathrm{e}^{-\tilde{r}(\tau_b \wedge t)} u(X_{\tau_b \wedge t})] = u(x) \quad (t \geq 0). \tag{2.3.6}$$

Note that the geometric Brownian motion X_t determined by the stochastic differential equation (2.1.1) is a diffusion process with the infinitesimal generator

$$L := \mu x \frac{\mathrm{d}}{\mathrm{d}x} + \tfrac{1}{2}\sigma^2 x^2 \frac{\mathrm{d}^2}{\mathrm{d}x^2} \quad (x > 0). \tag{2.3.7}$$

The generator of the killed process $\widetilde{X}_t$ is then given by (see [107, § 6.3, p. 127])

$$\tilde{L} = L - \tilde{r}I, \tag{2.3.8}$$

where I is the identity operator. Then the harmonicity condition (2.3.6) can be reduced to the differential equation $\tilde{L}u = 0$, that is, $Lu - \tilde{r}u = 0$ (see (2.3.8)).

On the boundary $x = b$ of the set $C = [0, b)$, due to the stopping rule (2.3.5) we have $u(b) = g(b)$. Moreover, according to the *smooth fit principle* (see [107, § 9.1]), we must also satisfy the condition $u'(b) = g'(b)$. Finally, in view of the equality $v(0) = 0$ (see Lemma 2.2.2(i)), we add a Dirichlet boundary condition at zero, $u(0+) = \lim_{x \downarrow 0} u(x) = 0$. Thus, we arrive at the following *free-boundary problem*,

$$\begin{cases} Lu(x) - \tilde{r}u(x) = 0, & x \in (0, b), \\ u(b) = g(b), \\ u'(b) = g'(b), \\ u(0+) = 0, \end{cases} \tag{2.3.9}$$

where both $b > 0$ and $u(x)$ are unknown.

Substituting (2.2.7) and (2.3.7), the problem (2.3.9) is rewritten explicitly as

$$\begin{cases} \mu x\, u'(x) + \frac{1}{2}\sigma^2 x^2 u''(x) - \tilde{r}u(x) = 0, \quad x \in (0,b), \\ u(b) = \beta_1 b - P, \\ u'(b) = \beta_1, \\ u(0+) = 0. \end{cases} \tag{2.3.10}$$

Let us look for a solution of (2.3.10) in the form $u(x) = x^q$ $(x > 0)$, with a suitable parameter $q \in \mathbb{R}$. Then the differential equation in (2.3.10) yields

$$\tfrac{1}{2}\sigma^2 q(q-1) + \mu q - \tilde{r} = 0. \tag{2.3.11}$$

This quadratic equation has two distinct roots,

$$q_{1,2} = \frac{1}{\sigma^2}\left(-(\mu - \tfrac{1}{2}\sigma^2) \pm \sqrt{(\mu - \tfrac{1}{2}\sigma^2)^2 + 2\tilde{r}\sigma^2}\right),$$

where $q_2 < 0 < q_1 = q_*$ (see (2.2.21)). Also note that, due to the condition (2.2.8), the left-hand side of (2.3.11) is negative at $q = 1$, therefore $q_1 > 1$. Thus, the general solution of the differential equation (2.3.10) is given by

$$u(x) = Ax^{q_1} + Bx^{q_2}, \quad x \in (0,b), \tag{2.3.12}$$

with arbitrary constants A and B. But since $q_2 < 0$, the condition $u(0+) = 0$ implies that $B = 0$. Hence, (2.3.12) is reduced to $u(x) = Ax^{q_1} \equiv Ax^{q_*}$ $(0 < x < b)$. Furthermore, the boundary conditions in (2.3.10) yield

$$\begin{cases} Ab^{q_*} = \beta_1 b - P, \\ Aq_* b^{q_*-1} = \beta_1, \end{cases}$$

whence we find

$$A = \frac{\beta_1 b - P}{b^{q_*}}, \qquad b = \frac{Pq_*}{\beta_1(q_* - 1)}. \tag{2.3.13}$$

Thus, the required solution to (2.3.10) is given by

$$u(x) = \begin{cases} (\beta_1 b - P)\left(\dfrac{x}{b}\right)^{q_*}, & x \in [0,b], \\ \beta_1 x - P, & x \in [b,\infty) \end{cases} \tag{2.3.14}$$

where the threshold b is defined in (2.3.13) and $q_* > 1$ is the positive root of the equation (2.3.11), given explicitly by formula (2.2.21).

2.3.3 Verification of the found solution

Using (2.3.13) and (2.3.14), it is easy to see that

$$\begin{aligned} u(x) &= g(x), \quad x \in [b, \infty), \\ u(x) &> g(x), \quad x \in [0, b), \end{aligned} \tag{2.3.15}$$

in accord with the heuristics outlined in Section 2.3.1 (see (2.3.3)). However, there is no need to check that the function $u(x)$ defined in (2.3.14) solves the reduced optimal stopping problem (2.3.4), because we can prove directly that $u(x)$ provides the solution to the original optimal stopping problem (2.2.14), that is, $u(x) = v(x)$ for all $x \geq 0$.

Remark 2.3.1. Since $u(0) = 0$ by formula (2.3.14), and $v(0) = 0$ according to Lemma 2.2.2(i), in what follows it suffices to assume that $x > 0$.

The proof of the claim above (commonly referred to as *verification theorem*) consists of two parts.

(i) Let us first show that $u(x) \geq v(x)$ $(x > 0)$. If the map $x \mapsto u(x)$ was a C^2-function (i.e., with continuous second derivative), then the classical *Itô formula* (see, e.g., [104, Theorem 4.1.2, p. 44]) applied to $\mathrm{e}^{-\tilde{r}t}u(X_t)$ would yield, on account of (2.1.1) and (2.3.7),

$$\mathrm{e}^{-\tilde{r}t}u(X_t) = u(x) + \int_0^t \mathrm{e}^{-\tilde{r}s}\big(Lu(X_s) - \tilde{r}u(X_s)\big)\,\mathrm{d}s + M_t \quad (\mathrm{P}_x\text{-a.s.}), \tag{2.3.16}$$

where

$$M_t := \int_0^t \mathrm{e}^{-\tilde{r}s}u'(X_s)\,\sigma X_s\,\mathrm{d}B_s \quad (t \geq 0). \tag{2.3.17}$$

However, for the function $u(x)$ given by (2.3.14), its C^2-smoothness breaks down at the point $x = b$, where it is only C^1. But $u(x)$ is strictly convex on $(0, b)$ (i.e., $u''(x) > 0$) and linear on (b, ∞), and we can define the action $Lu(x)$ at $x = b$ by using the one-sided second derivative, say,

$$u''(b-) = Pq_*b^{-2}. \tag{2.3.18}$$

In this situation, a generalization of the Itô formula holds, known as the *Itô–Meyer formula* (see [121, Ch. VIII, §2a, p. 757]), which ensures that the representation (2.3.16) is still valid.

Recall that by construction (see the differential equation in (2.3.9)), we have

$$Lu(x) - \tilde{r}u(x) = 0, \quad x \in (0, b). \tag{2.3.19}$$

Moreover, it is easy to check using (2.3.18) that the equality (2.3.19) also extends to $x = b$. On the other hand, on account of the condition (2.2.8) and the definition of b in (2.3.13), for $x > b$ we get

$$\begin{aligned} Lu(x) - \tilde{r}u(x) &= \mu\beta_1 x - \tilde{r}(\beta_1 x - P) \\ &= \beta_1 x(\mu - \tilde{r}) + \tilde{r}P \\ &< \beta_1 b(\mu - \tilde{r}) + \tilde{r}P \\ &= \frac{P(\mu q_* - \tilde{r})}{q_* - 1} < 0, \end{aligned} \tag{2.3.20}$$

because, due to the equation (2.3.11) and the inequality $q_* > 1$,

$$\mu q_* - \tilde{r} = -\tfrac{1}{2}\sigma^2 q_*(q_* - 1) < 0.$$

Thus, combining (2.3.19) and (2.3.20) we obtain

$$Lu(x) - \tilde{r}u(x) \le 0 \quad (x > 0). \tag{2.3.21}$$

Substituting the inequality (2.3.21) into formula (2.3.16), we conclude that, for any $x > 0$ and all $t \ge 0$,

$$u(x) + M_t \ge \mathrm{e}^{-\tilde{r}t} u(X_t) \quad (\mathrm{P}_x\text{-a.s.}). \tag{2.3.22}$$

According to formula (2.3.17), (M_t) is a continuous local martingale (see, e.g., [121, Ch. II, §1c, p.101]). Let (τ_n) be a localizing sequence of bounded stopping times, so that $\tau_n \uparrow \infty$ (P_x-a.s.) and the stopped process $(M_{\tau_n \wedge t})$ is a martingale, for each $n \in \mathbb{N}$.

Now, let τ be an arbitrary stopping time of (X_t). From (2.3.22) we get

$$\begin{aligned} u(x) + M_{\tau_n \wedge \tau} &\ge \mathrm{e}^{-\tilde{r}(\tau_n \wedge \tau)} u(X_{\tau_n \wedge \tau}) \\ &\ge \mathrm{e}^{-\tilde{r}(\tau_n \wedge \tau)} g(X_{\tau_n \wedge \tau}) \quad (\mathrm{P}_x\text{-a.s.}), \end{aligned} \tag{2.3.23}$$

using that $u(x) \ge g(x)$ for all $x \ge 0$ (see (2.3.15)). Taking expectation on both sides of the inequality (2.3.23) gives

$$u(x) \ge \mathrm{E}_x[\mathrm{e}^{-\tilde{r}(\tau_n \wedge \tau)} g(X_{\tau_n \wedge \tau})], \tag{2.3.24}$$

since by Doob's optional sampling theorem (see, e.g., [138, Theorem 8.10, p. 131])

$$\mathrm{E}_x[M_{\tau_n \wedge \tau}] = \mathrm{E}_x[M_0] = 0.$$

By Fatou's lemma (see, e.g., [120, §II.6, Theorem 2(a), p. 187]), from (2.3.24) it follows

$$u(x) \geq \mathrm{E}_x\big[\liminf_{n\to\infty} \mathrm{e}^{-\tilde{r}(\tau_n\wedge\tau)}\, g(X_{\tau_n\wedge\tau})\big] = \mathrm{E}_x\big[\mathrm{e}^{-\tilde{r}\tau}\, g(X_\tau)\big]. \tag{2.3.25}$$

Finally, taking in (2.3.25) the supremum over all stopping times τ, we obtain

$$u(x) \geq \sup_\tau \mathrm{E}_x\big[\mathrm{e}^{-\tilde{r}\tau}\, g(X_\tau)\big] = v(x) \quad (x > 0),$$

as claimed.

(ii) Let us now prove the opposite inequality, $u(x) \leq v(x)$ $(x > 0)$. According to (2.3.1) and (2.3.15), we readily have $u(x) = g(x) \leq v(x)$ for $x \in [b, +\infty)$. Next, fix $x \in (0, b)$ and consider the representation (2.3.16) with t replaced by $\tau_n \wedge \tau_b$, where (τ_n) is the localizing sequence of stopping times for (M_t) as before. Then, by virtue of the identity (2.3.19) (which, as has been explained, is also true for $x = b$), it follows that

$$u(x) + M_{\tau_n\wedge\tau} = \mathrm{e}^{-\tilde{r}(\tau_n\wedge\tau_b)}\, u(X_{\tau_n\wedge\tau_b}) \quad (\mathrm{P}_x\text{-a.s.}). \tag{2.3.26}$$

Similarly as above, taking expectation on both sides of the equality (2.3.26) and again applying Doob's optional sampling theorem to the martingale $(M_{\tau_n\wedge t})$, we obtain

$$u(x) = \mathrm{E}_x\big[\mathrm{e}^{-\tilde{r}(\tau_n\wedge\tau_b)}\, u(X_{\tau_n\wedge\tau_b})\big]. \tag{2.3.27}$$

Note that, for $0 < x < b$, we have $0 \leq u(x) \leq u(b)$ and $0 \leq X_{\tau_n\wedge\tau_b} \leq b$ (P_x-a.s.), hence

$$0 \leq \mathrm{e}^{-\tilde{r}(\tau_n\wedge\tau_b)}\, u(X_{\tau_n\wedge\tau_b}) \leq u(b) \quad (\mathrm{P}_x\text{-a.s.}).$$

Using that $\tau_n \uparrow \infty$, observe that, P_x-a.s.,

$$\begin{aligned}\lim_{n\to\infty} \mathrm{e}^{-\tilde{r}(\tau_n\wedge\tau_b)}\, u(X_{\tau_n\wedge\tau_b}) &= \mathrm{e}^{-\tilde{r}\tau_b}\, u(X_{\tau_b})\, \mathbb{1}_{\{\tau_b<\infty\}} + \lim_{n\to\infty} \mathrm{e}^{-\tilde{r}\tau_n}\, u(X_{\tau_n})\, \mathbb{1}_{\{\tau_b=\infty\}} \\ &= \mathrm{e}^{-\tilde{r}\tau_b}\, u(b)\, \mathbb{1}_{\{\tau_b<\infty\}},\end{aligned} \tag{2.3.28}$$

because $X_{\tau_b} = b$ on the event $\{\tau < \infty\}$, while $0 \leq u(X_{\tau_n}) \leq u(b)$ on the event $\{\tau = \infty\}$. Hence, letting $n \to \infty$ in (2.3.27) and using the dominated convergence

theorem (see, e.g., [120, §II.6, Theorem 3, p. 187]), we get, on account of (2.3.28),

$$\begin{aligned} u(x) &= \mathrm{E}_x\bigl[\mathrm{e}^{-\tilde{r}\tau_b}\,u(b)\,\mathbb{1}_{\{\tau_b<\infty\}}\bigr] \\ &= \mathrm{E}_x\bigl[\mathrm{e}^{-\tilde{r}\tau_b}\,g(b)\,\mathbb{1}_{\{\tau_b<\infty\}}\bigr] \\ &= \mathrm{E}_x\bigl[\mathrm{e}^{-\tilde{r}\tau_b}\,g(X_{\tau_b})\,\mathbb{1}_{\{\tau_b<\infty\}}\bigr] \\ &\le v(x), \end{aligned}$$

according to (2.2.14). That is, we have proved that $u(x) \le v(x)$ for all $0 < x < b$, as required.

Thus, the proof of the verification theorem is complete.

2.4 Elementary solution of the reduced problem

2.4.1 Distribution of the hitting time

In view of the formula (2.1.2), the hitting problem for the process X_t is reduced to that for the Brownian motion with drift,

$$\tau_b := \inf\{t \ge 0\colon X_t = b\} \equiv \inf\{t \ge 0\colon B_t + \tilde{\mu}t = \tilde{b}\}, \tag{2.4.1}$$

where

$$\tilde{\mu} = \frac{\mu - \frac{1}{2}\sigma^2}{\sigma}, \qquad \tilde{b} = \frac{1}{\sigma}\ln\frac{b}{x}. \tag{2.4.2}$$

Suppose that $x \le b$, so that $\tilde{b} \ge 0$. The explicit expression for the Laplace transform of the hitting time (2.4.1) is well known (see, e.g., [42, Exercises 6.29 and 6.31, p. 268] or [49, Proposition 3.3.5, p. 61]).

Proposition 2.4.1. *For $x \le b$ and any $\theta > 0$, set*

$$\Phi_{x,b}(\theta) := \mathrm{E}_x(\mathrm{e}^{-\theta\tau_b}) \equiv \mathrm{E}_x(\mathrm{e}^{-\theta\tau_b}\,\mathbb{1}_{\{\tau_b<\infty\}}). \tag{2.4.3}$$

Then

$$\Phi_{x,b}(\theta) = \exp\biggl\{-\tilde{b}\,\Bigl(\sqrt{\tilde{\mu}^2 + 2\theta} - \tilde{\mu}\Bigr)\biggr\}, \quad \theta > 0, \tag{2.4.4}$$

where $\tilde{\mu}$ and $\tilde{b}$ are defined in (2.4.2).

Substituting the expressions (2.4.2), the formula (2.4.4) is rewritten as

$$\Phi_{x,b}(\theta) = \Bigl(\frac{x}{b}\Bigr)^{q_1(\theta)}, \quad \theta > 0, \tag{2.4.5}$$

where $q_1(\theta)$ is given by (cf. (2.2.21))

$$q_1(\theta) = \frac{1}{\sigma^2}\left(-(\mu - \tfrac{1}{2}\sigma^2) + \sqrt{(\mu - \tfrac{1}{2}\sigma^2)^2 + 2\theta\sigma^2}\right). \tag{2.4.6}$$

As usual, it is straightforward to extract from the Laplace transform (2.4.3) some explicit information about the distribution of the hitting time τ_b. First, by the monotone convergence theorem (see, e.g., [120, §II.6, Theorem 1(a), p. 186] we have

$$\lim_{\theta \downarrow 0} \Phi_{x,b}(\theta) = \mathrm{E}_x(\mathbb{1}_{\{\tau_b < \infty\}}) = \mathrm{P}_x(\tau_b < \infty).$$

Hence, noting from (2.4.6) that

$$q_1(0) = \begin{cases} 0 & \text{if } \mu - \frac{1}{2}\sigma^2 \geq 0, \\ 1 - \dfrac{2\mu}{\sigma^2} & \text{if } \mu - \frac{1}{2}\sigma^2 < 0, \end{cases} \tag{2.4.7}$$

we obtain

$$\mathrm{P}_x(\tau_b < \infty) = \left(\frac{x}{b}\right)^{q_1(0)} = \begin{cases} 1, & \mu - \frac{1}{2}\sigma^2 \geq 0, \\ \left(\dfrac{x}{b}\right)^{1-2\mu/\sigma^2}, & \mu - \frac{1}{2}\sigma^2 < 0. \end{cases} \tag{2.4.8}$$

Remark 2.4.1. The result (2.4.8) shows that hitting the critical threshold $b = b^*$, as required by the stopping rule, is only certain when the wage growth rate is large enough, $\mu \geq \frac{1}{2}\sigma^2$. Thus, the "dangerous" case is when $\mu < \frac{1}{2}\sigma^2$, whereby relying only on the optimal stopping recipe may not be practical. This observation may serve as a germ of the idea to connect the optimality problem in the insurance context with the notion of *utility* (cf. the discussion in Section 2.7.1 below).

Via the Laplace transform $\Phi_{x,b}(\theta)$, we can also obtain the mean hitting time $\mathrm{E}_x(\tau_b)$ in the case $\mu \geq \frac{1}{2}\sigma^2$, where $\tau_b < \infty$ (P_x-a.s.). Namely, again using the monotone convergence theorem we have

$$\lim_{\theta \downarrow 0} \frac{\partial \Phi_{x,b}(\theta)}{\partial \theta} = -\lim_{\theta \downarrow 0} \mathrm{E}_x(\tau_b \, \mathrm{e}^{-\theta\tau_b}) = -\mathrm{E}_x(\tau_b).$$

Hence, differentiating formula (2.4.5) at $\theta = 0$ and noting from (2.4.6) that $q_1(0) = 0$ (cf. (2.4.7)) and

$$q_1'(0) = \begin{cases} \infty, & \mu = \frac{1}{2}\sigma^2, \\ \dfrac{1}{\mu - \frac{1}{2}\sigma^2}, & \mu > \frac{1}{2}\sigma^2, \end{cases}$$

we get

$$\mathrm{E}_x(\tau_b) = -\ln\left(\frac{x}{b}\right)\left(\frac{x}{b}\right)^{q_1(0)} q_1'(0) = \begin{cases} \infty, & \mu = \frac{1}{2}\sigma^2, \\ \dfrac{\ln(b/x)}{\mu - \frac{1}{2}\sigma^2}, & \mu > \frac{1}{2}\sigma^2. \end{cases} \tag{2.4.9}$$

2.4.2 Alternative derivation

An alternative (and more direct) method to derive the formulas (2.4.8) and (2.4.9) is based on general theory of Markov processes by solving the suitable boundary value problems (see, e.g., [104, §9]). Namely, the hitting probability $\pi(x) := \mathrm{P}_x(\tau_b < \infty)$ as a function of $x > 0$ satisfies the Dirichlet problem [104, §9.2]

$$\begin{cases} L\pi(x) = 0 \quad (0 < x < b), \\ \pi(b) = 1. \end{cases} \tag{2.4.10}$$

The differential equation in (2.4.10) reads

$$\tfrac{1}{2}\sigma^2 x^2 \pi''(x) + \mu x \pi'(x) = 0 \quad (0 < x < b),$$

which is easily solved to give

$$\pi(x) = c_1 x^{1-2\mu/\sigma^2} + c_2.$$

If $1 - 2\mu/\sigma^2 < 0$ (i.e., $\mu - \frac{1}{2}\sigma^2 > 0$) then $c_1 = 0$ (since $\pi(x)$ is bounded), and due to the boundary condition $\pi(b) = 1$ it follows that $c_2 = 1$ and $\pi(x) \equiv 1$. A similar argument shows that $\pi(x) \equiv 1$ in the case $1 - 2\mu/\sigma^2 = 0$. Finally, if $1 - 2\mu/\sigma^2 > 0$ then, noting that $\pi(0) = 0$, we conclude that $c_2 = 0$ and, due to the boundary condition, $c_1 = b^{-1+2\mu/\sigma^2}$. Thus, formula (2.4.8) is proved.

Similarly, the mean hitting time $m(x) := \mathrm{E}_x(\tau_b)$ (with $\mu - \frac{1}{2}\sigma^2 > 0$) satisfies the Poisson problem [104, §9.3]

$$\begin{cases} Lm(x) = -1 \quad (0 < x < b), \\ m(b) = 0. \end{cases} \tag{2.4.11}$$

As usual, to solve the problem (2.4.11), it is convenient to approximate it with a two-sided boundary problem by adding an auxiliary Neumann (reflection) condition at $\varepsilon > 0$,

$$\begin{cases} Lm_\varepsilon(x) = -1 \quad (\varepsilon < x < b), \\ m_\varepsilon(b) = 0, \\ m_\varepsilon'(\varepsilon) = 0, \end{cases} \tag{2.4.12}$$

and then taking the limit of $m_\varepsilon(x)$ as $\varepsilon \downarrow 0$. This procedure will produce the correct solution $m(x)$ since $\lim_{\varepsilon\downarrow 0} \mathrm{P}_x(\tau_\varepsilon < \infty) = \mathrm{P}_x(\tau_0 < \infty) = 0$ (for any $x > 0$).

A particular solution to the inhomogeneous differential equation

$$\tfrac{1}{2}\sigma^2 x^2 m_\varepsilon''(x) + \mu x m_\varepsilon'(x) = -1 \quad (\varepsilon < x < b)$$

can be sought in the form $m_0(x) = c_0 \ln x$, which gives $c_0 = -1/(\mu - \frac{1}{2}\sigma^2)$. Thus, the general solution of (2.4.12) can be expressed as

$$m_\varepsilon(x) = -\frac{\ln x}{\mu - \frac{1}{2}\sigma^2} + c_1 x^{1-2\mu/\sigma^2} + c_2. \tag{2.4.13}$$

Now, using the boundary conditions in (2.4.12) it is straightforward to check that

$$\lim_{\varepsilon\downarrow 0} c_1 = 0, \qquad \lim_{\varepsilon\downarrow 0} c_2 = \frac{\ln b}{\mu - \frac{1}{2}\sigma^2}.$$

Hence, from (2.4.13) we get

$$m(x) = \lim_{\varepsilon\downarrow 0} m_\varepsilon(x) = \frac{\ln(b/x)}{\mu - \frac{1}{2}\sigma^2},$$

which retrieves the result (2.4.9).

Remark 2.4.2. The same method applied to the killed process $\widetilde{X}_t$ with generator $\tilde{L} = L - \tilde{r}I$ (see (2.3.8)) provides a neat interpretation of the value function $u(x)$ as given by (2.3.14). Namely, rewrite the expectation in (2.3.4) (i.e., $\mathrm{eNPV}(x;\tau_b)$) in the form $\tilde{\mathrm{E}}_x[g(\widetilde{X}_{\tau_b})]$, where $\tilde{\mathrm{E}}_x$ denotes expectation with respect to the killed process $(\widetilde{X}_t)$, and note that, for $b \geq 0$,

$$\tilde{\mathrm{E}}_x[g(\widetilde{X}_{\tau_b})] = \begin{cases} g(b)\,\tilde{\mathrm{P}}_x(\tau_b < \infty), & x \in [0, b], \\ g(x), & x \in [b, \infty). \end{cases}$$

In turn, the hitting probability $\tilde{\pi}(x) := \tilde{\mathrm{P}}_x(\tau_b < \infty)$ can be easily found by solving the corresponding Dirichlet problem (cf. (2.4.10)),

$$\begin{cases} \tilde{L}\tilde{\pi}(x) = 0 \quad (0 < x < b), \\ \tilde{\pi}(b) = 1. \end{cases}$$

Indeed, repeating the calculations in Section 2.3.2, it is straightforward to get $\tilde{\pi}(x) = (x/b)^{q^*}$.

2.4.3 Direct maximization

Using the results of the previous sections, we can easily solve the optimal stopping problem (2.2.14), at least in the subclass of hitting times $\tau = \tau_b$ (see (2.3.4)),

$$u(x) = \sup_{b\geq 0} \mathrm{eNPV}(x;\tau_b) = \sup_{b\geq 0} \mathrm{E}_x\big[\mathrm{e}^{-\tilde{r}\tau_b}(\beta_1 X_{\tau_b} - P)\big]. \tag{2.4.14}$$

Observe that if $x \geq b$ then $\tau_b = 0$ and $X_{\tau_b} = x$ (P_x-a.s.), so that $\mathrm{eNPV}(x;\tau_b) \equiv \beta_1 x - P$ for all $b \in [0, x]$. Let now $b \in [x, \infty)$. As already noted, on the event $\{\tau_b < \infty\}$ we have $X_{\tau_b} = b$ (P_x-a.s.), hence, according to (2.2.14) and (2.4.5),

$$\mathrm{eNPV}(x;\tau_b) = (\beta_1 b - P)\,\mathrm{E}_x\big(\mathrm{e}^{-\tilde{r}\tau_b}\big) = (\beta_1 b - P)\left(\frac{x}{b}\right)^{q_*} \quad (b \geq x), \tag{2.4.15}$$

where $q_* = q_1(\theta)|_{\theta=\tilde{r}}$ (cf. (2.2.21) and (2.4.6)). It is straightforward to find the maximizer for the function (2.4.15). Indeed, the condition $(\partial/\partial b)\,\mathrm{eNPV}(x;\tau_b) \geq 0$, equivalent to

$$\beta_1 b^{-q_*} - q_*(\beta_1 b - P)\,b^{-q_*-1} \geq 0,$$

holds for all $b \in [0, b^*]$, where

$$b^* = \frac{P q_*}{\beta_1(q_* - 1)}, \tag{2.4.16}$$

which is the same optimal threshold as before (cf. (2.2.20)). Thus, the supremum of $\mathrm{eNPV}(x;\tau_b)$ over $b \geq x$ is attained at $b = b^*$ if $x \leq b^*$ or at $b = x$ if $x \geq b^*$.

The corresponding value function $u(x)$ is then calculated as (cf. (2.2.22))

$$u(x) = \begin{cases} (\beta_1 b^* - P)\left(\dfrac{x}{b^*}\right)^{q_*}, & x \in [0, b^*], \\ \beta_1 x - P, & x \in [b^*, \infty). \end{cases} \tag{2.4.17}$$

Finally, substituting (2.4.16) into (2.4.17), we obtain explicitly (cf. (2.2.23))

$$u(x) = \begin{cases} \dfrac{P}{q_* - 1}\left(\dfrac{\beta_1(q_* - 1)x}{P q_*}\right)^{q_*}, & 0 \leq x \leq \dfrac{P q_*}{\beta_1(q_* - 1)}, \\ \beta_1 x - P, & x \geq \dfrac{P q_*}{\beta_1(q_* - 1)}. \end{cases} \tag{2.4.18}$$

2.5 Statistical issues and numerical illustration

2.5.1 Specifying the model parameters

From the practical point of view, in order to exercise the stopping rule (2.2.19) the individual concerned needs to be able to compute the critical threshold b^* expressed in

(2.2.20), for which the knowledge is required about β_1 (defined in (2.2.6)) and therefore about the parameters r, λ_0, μ and β (see (2.2.2)); furthermore, to evaluate the quantity q_* defined in (2.2.21), one needs to estimate $\mu - \frac{1}{2}\sigma^2$ and σ^2 itself. Specifically:

- The loss-of-job rate λ_0 can be extracted from the publicly available data about the mean length at work, which is theoretically given by $\mathrm{E}(\tau_0) = 1/\lambda_0$.
- Likewise, the inflation rate r is also in the public domain.
- To specify the wage growth rate μ, a simple approach is just to set $\mu = r$ as a crude version of a "tracking" rule. However, it may be possible that the individual's wage growth rate μ is, to some extent, stipulated by the job contract — for example, that it must not exceed the inflation rate r by more than 1% per annum (applicable, e.g., to civil servants) or, by contrast, that it must be no less than r minus 0.5% per annum (more realistic in the private sector). In practical terms, this would often mean that the actual growth rate μ is kept on the lowest predefined level.
- More generally, the wage growth rate μ can be estimated by observing the wage process X_t. This can be implemented by first using regression analysis on $Y_t = \ln X_t$ and estimating the regression line slope $\mu - \frac{1}{2}\sigma^2$ (see (2.1.2)). In addition, the volatility σ^2 can be estimated by using a suitable quadratic functional of the sample path Y_t.
- Finally, knowing the benefit schedule (which should be available through the insurance policy's terms and conditions), it is in principle possible to calculate, or at least estimate the value β.

To summarize, certain estimation procedures need to be carried out along with the on-line observation of the sample path (X_t). More details (most of which are quite standard) are provided in the next two subsections.

2.5.2 Estimating the drift and volatility

Denote for short $a := \mu - \frac{1}{2}\sigma^2$. According to the geometric Brownian motion model (2.1.2), we have

$$Y_t := \ln X_t = \ln x + \sigma B_t + at, \qquad Y_0 = \ln x.$$

Suppose the process X_t is observed over the time interval $t \in [0, T]$ on a discrete-time grid $t_i = iT/n$ $(i = 0, \ldots, n)$, and consider the consecutive increments

$$Z_i := Y_{t_i} - Y_{t_{i-1}} = \sigma(B_{t_i} - B_{t_{i-1}}) + a\,(t_i - t_{i-1}) \quad (i = 1, \ldots, n). \tag{2.5.1}$$

Note that the increments of the Brownian motion in (2.5.1) are mutually independent and have normal distribution with zero mean and variance $t_i - t_{i-1} = T/n$, respectively. Therefore, (Z_i) is an independent random sample with normal marginal distributions,

$$Z_i \sim \mathcal{N}\left(\frac{aT}{n}, \frac{\sigma^2 T}{n}\right) \quad (i = 1, \dots, n).$$

Then, it is standard to estimate the parameters via the sample mean and sample variance,

$$\hat{a}_n := \frac{n}{T} \cdot \bar{Z} = \frac{Z_1 + \cdots + Z_n}{T} = \frac{Y_T - Y_0}{T}, \tag{2.5.2}$$

$$\hat{\sigma}_n^2 := \frac{n}{T} \cdot \frac{1}{n-1} \sum_{i=1}^{n} (Z_i - \bar{Z})^2. \tag{2.5.3}$$

These estimators are unbiased,

$$\mathrm{E}(\hat{a}_n) = a = \mu - \tfrac{1}{2}\sigma^2, \qquad \mathrm{E}(\hat{\sigma}_n^2) = \sigma^2,$$

with mean square errors

$$\mathrm{Var}(\hat{a}_n) = \frac{\sigma^2}{T}, \qquad \mathrm{Var}(\hat{\sigma}_n^2) = \frac{2\sigma^4}{n-1}.$$

In turn, the parameter μ is estimated by

$$\hat{\mu}_n = \hat{a}_n + \tfrac{1}{2}\hat{\sigma}_n^2,$$

with mean $\mathrm{E}(\hat{\mu}_n) = \mathrm{E}(\hat{a}_n) + \frac{1}{2}\mathrm{E}(\hat{\sigma}_n^2) = a + \frac{1}{2}\sigma^2 = \mu$ and mean square error

$$\mathrm{Var}(\hat{\mu}_n) = \mathrm{Var}(\hat{a}_n) + \tfrac{1}{4}\mathrm{Var}(\hat{\sigma}_n^2) = \frac{\sigma^2}{T} + \frac{\sigma^4}{2(n-1)}$$

(due to independence of the estimators $\hat{a}_n$ and $\hat{\sigma}_n^2$).

Note that the estimator $\hat{a}_n$ in (2.5.2) only employs the last observed value, Y_T; in particular, its mean square error is not sensitive to the grid size $\Delta t_i = T/n$, and only tends to zero with increasing observational horizon, $T \to \infty$. This makes the estimation of the drift parameter a difficult in the sense that very long observations over Y_t are required to achieve an acceptable precision (see, e.g., [46, Example 2.1, p. 3]). For instance, let $\mu = 0.004$ and $\sigma = 0.02$ (per week), then $a = 0.0038$; if $T = 25$ (weeks) then the 95%-confidence bounds for a are given by $\hat{a} \pm 1.96\,\sigma/\sqrt{T} = \hat{a} \pm 0.00784$, so the margin of error is about twice as big as the value of a itself. To reduce it, say to $0.5a$, one needs $T \approx 425$ (weeks), which exemplifies slow convergence.

In contrast, the mean square error of the estimator $\hat{\sigma}_n^2$ in (2.5.3) tends to zero as $n \to \infty$, with T fixed. Thus, estimation of the parameter σ^2 can be made asymptotically precise.

A numerical example illustrating the estimation of μ and σ^2 using simulated data will be given at the end of Section 2.5.4. A brief discussion of practical choices of μ, based on sensitivity analysis, is provided at the end of Section 2.6.3.

2.5.3 Hypothesis testing

In view of the drawback in the general solution of the optimal stopping problem in that the stopping time τ_{b^*} may be infinite, that is, $\mathrm{P}_x(\tau_{b^*} = \infty) > 0$ (which occurs when $a = \mu - \frac{1}{2}\sigma^2 < 0$, see Section 2.4.1), a reasonable pragmatic approach to decision making in our model may be based on testing the null hypothesis $H_0 \colon a \geq 0$ versus the alternative $H_1 \colon a < 0$ (at some intuitively acceptable significance level, e.g. $\alpha = 0.05$). Namely, as long as H_0 remains tenable, one keeps waiting for the hitting time τ_{b^*} to occur, but once H_0 has been rejected, it is reasonable to terminate waiting and buy the policy immediately.

The corresponding test is specified as follows. Again, suppose that the process Y_t is observed on a discrete time grid $t_i = iT/n$, and set $Z_i = Y_{t_i} - Y_{t_{i-1}}$ $(i = 1, \ldots, n)$. Let $z(\alpha)$ be the upper α-quantile of the standard normal distribution $\mathcal{N}(0,1)$, that is, $1 - \Phi(z(\alpha)) = \alpha$, where $\Phi(x) = \frac{1}{\sqrt{2\pi}} \int_{-\infty}^{x} \mathrm{e}^{-u^2/2}\, \mathrm{d}u$. Then the null hypothesis $H_0 \colon a \geq 0$ is to be rejected at significance level α whenever

$$Z_1 + \cdots + Z_n \leq \inf_{a \geq 0} \left\{ aT - z(\alpha)\, \sigma \sqrt{T} \right\},$$

that is,

$$Y_T - Y_0 \leq -z(\alpha)\, \sigma \sqrt{T}. \tag{2.5.4}$$

This test is uniformly most powerful among all tests with probability of error of type I not exceeding α, that is, $\mathrm{P}(\text{reject } H_0 \,|\, H_0 \text{ true}) \leq \alpha$.

The normal test (2.5.4) assumes that the variance σ^2 is known. As mentioned before, this presents no real restriction if the process Y_t is observable continuously (i.e., if the grid (t_i) can be refined indefinitely). If this is not the case (e.g., because the wage process can only be observed on the weekly basis) then the test (2.5.4) is replaced by the t-test,

$$Y_T - Y_0 \leq -t_{n-1}(\alpha)\, \hat{\sigma}\, \sqrt{T},$$

where $\hat{\sigma}^2$ is the sample variance (see (2.5.3)) and $t_{n-1}(\alpha)$ is the upper α-quantile of the t-distribution with $n-1$ degrees of freedom.

In practice, the hypothesis testing is carried out sequentially (e.g., weekly) as the observational horizon T increases. The advantage of this approach is that the resulting stopping time is finite with probability one (i.e., P_x-a.s.); indeed, it is the minimum between the optimal stopping time τ_{b^*} (which is finite P_x-a.s. under the null hypothesis $H_0\colon a \geq 0$) and the first time of rejecting H_0 (which is finite P_x-a.s. if H_0 is false).

2.5.4 Numerical examples

To be specific, we use euro as the monetary unit. First of all, the value of the constant β, which encapsulates information about the benefit schedule as well as the rate λ_1 of finding new job (see (2.2.2)), is chosen to be

$$\beta = 30.$$

Thus, the overall expected benefit payable over the lifetime of the policy (and projected to the beginning of unemployment) is taken to be equal to 30 weekly wages; that is, if the final wage is 400 (euro per week) then the total to be received is

$$400.00 \times 30 = 12\,000.00 \text{ (euro)}.$$

Further, we set

$$\lambda_0 = 0.01, \qquad r = 0.0004.$$

This means that the expected time until loss of job is $1/\lambda_0 = 100$ (weeks), that is, about 1 year and 11 months, whereas the annual inflation rate is

$$\mathrm{e}^{(365/7)\cdot 0.0004} - 1 = 0.02107617 \approx 2.11\%,$$

which is quite realistic.

Next, we need to specify the premium P and the parameters of the wage process X_t, First, choose the initial value $x = X_0$ as

$$x = 346.00 \text{ (euro)}.$$

This is motivated by the French labour legislation, whereby the current minimum pay rate is set as 9.88 euro per hour [131], with a 35-hour workweek [48, 59], giving

$$9.88 \times 35 = 345.80 \text{ (euro per week)}.$$

As for the premium, it is set at the value

$$P = 9\,000.00 \text{ (euro)},$$

which equates to about 26 minimum weekly wages (i.e., income over about half a year). For simplicity, we also choose

$$\mu = r = 0.0004, \tag{2.5.5}$$

so that the wage growth rate is the same as inflation r (in reality, it could be slightly less). Then from (2.2.6), using (2.5.5), we get

$$\beta_1 = \frac{\lambda_0 \beta}{\tilde{r} - \mu} = \beta = 30.$$

For the volatility σ, we will illustrate two opposite cases, $\mu < \frac{1}{2}\sigma^2$ and $\mu > \frac{1}{2}\sigma^2$.

Example 2.5.1. Set $\sigma = 0.04$, then $\mu - \frac{1}{2}\sigma^2 = -0.0004 < 0$. From (2.2.21) we calculate $q_* = 3.864208$, then (2.3.13) yields

$$b^* = 404.7410 = 404.74 \text{ (euro)}.$$

Using (2.4.8), the hitting probability is calculated as

$$\mathrm{P}_x(\tau_{b^*} < \infty) = 0.9245906.$$

Finally, using (2.3.14), we obtain the value of this contract,

$$v(346) = 1\,714.2780 = 1\,714.28 \text{ (euro)}.$$

Example 2.5.2. Now, set $\sigma = 0.02$, then $\mu - \frac{1}{2}\sigma^2 = 0.0002 > 0$. Furthermore, using (2.2.21) we calculate $q_* = 6.728416$, and from (2.3.13)

$$b^* = 352.3705 = 352.37 \text{ (euro)}.$$

Hence, using (2.4.9), the expected hitting time is found to be

$$\mathrm{E}(\tau_{b^*}) = 91.22197 = 91.2 \text{ (weeks)}.$$

Finally, according to formula (2.2.22), the value of this contract is calculated as

$$v(346) = 1\,389.6190 = 1\,389.62 \text{ (euro)}.$$

In the simulation of the process X_t shown in Fig. 3, the drift $a = \mu - \frac{1}{2}\sigma^2$ is estimated using formula (2.5.2) as $\hat{a} \doteq 0.0005994$. Estimation of the variance σ^2 according to formula (2.5.3) (on a weekly time grid) gives $\hat{\sigma}^2 \doteq 0.0003723$, while the true value is $\sigma^2 = 0.0004$. Hence, the parameter μ is estimated by $\hat{\mu} \doteq 0.0007855$; recall that the true value is $\mu = 0.0004$. We then substitute these estimates into the values for simulation in Example 2.5.1 and Example 2.5.2.

Example 2.5.3. Here $\hat{\mu} - \frac{1}{2}\,\hat{\sigma}^2 = 0.0006 > 0$. From (2.2.21) we calculate $q_* = 6.170339$, then (2.3.13) yields

$$b^* = 358.0233 = 358.02 \text{ (euro)}.$$

Hence, using (2.4.9), the expected hitting time is computed as

$$\mathrm{E}(\tau_{b^*}) = 56.99377 = 56.99 \text{ (weeks)}.$$

Finally, using (2.3.14), the value of this contract is given as,

$$v(346) = 1\,409.891 = 1\,409.89 \text{ (euro)}.$$

The values of b^* and v when the estimates are plugged in Example 2.5.3 are close to the true values in Example 2.5.2. It is interesting to point out that the expected hitting time ($\mathrm{E}(\tau_{b^*})$) in Example 2.5.2 is greater than Example 2.5.3 because $\hat{\mu}$ is higher making it more likely to reach the boundary faster.

2.6 Parametric dependencies

In this section, we aim to explore the parametric dependencies of the solution of our insurance problem, that is, of the optimal threshold b^* given by (2.2.20) and the value function $v = v(x)$ given by (2.2.22). In particular, it is helpful to analyse different asymptotic regimes as well as (the sign of) appropriate partial derivatives, so as to ascertain the direction of changes under small perturbations and to understand their economic meaning. This is a key ingredient of sensitivity analysis and of the so-called *comparative statics* [90, Section VII].

In what follows, we confine ourselves to a discussion of the two most important exogenous parameters — the wage drift μ and the unemployment rate λ_0. The constraint (2.2.8) implies that the range of the parameters μ and λ_0 is specified as follows,

$$-\infty < \mu < \tilde{r} = r + \lambda_0, \qquad 0 \vee (\mu - r) < \lambda_0 < \infty.$$

Remark 2.6.1. The next two technical subsections are elementary but rather tedious, and the reader wishing to grasp the results quickly may just inspect the plots in Figs. 4 and 5.

2.6.1 Monotonicity

By virtue of the quadratic equation (2.3.11), the formula (2.2.20) can be conveniently rewritten as

$$b^* = \frac{P(\frac{1}{2}\sigma^2 q_* + \tilde{r})}{\beta\lambda_0}. \tag{2.6.1}$$

First, fix λ_0 and consider the function $\mu \mapsto b^*$. Differentiating the equation (2.3.11) and then again using (2.3.11) to eliminate μ, we obtain

$$\frac{\partial q_*}{\partial \mu} = -\frac{q_*}{\frac{1}{2}\sigma^2(2q_* - 1) + \mu} = -\frac{q_*^2}{\frac{1}{2}\sigma^2 q_*^2 + \tilde{r}} < 0. \tag{2.6.2}$$

Hence, using (2.6.1) and (2.6.2),

$$\frac{\mathrm{d}b^*}{\mathrm{d}\mu} = \frac{\partial b^*}{\partial \mu} + \frac{\partial b^*}{\partial q_*}\cdot\frac{\partial q_*}{\partial \mu} = -\frac{P(\frac{1}{2}\sigma^2 q_*^2)}{\beta\lambda_0(\frac{1}{2}\sigma^2 q_*^2 + \tilde{r})} < 0, \tag{2.6.3}$$

and, therefore, b^* is a decreasing function of μ (see Fig. 4(a)).

Similarly, the equation (2.3.11) yields

$$\frac{\partial q_*}{\partial \lambda_0} = \frac{1}{\frac{1}{2}\sigma^2(2q_* - 1) + \mu} = \frac{q_*}{\frac{1}{2}\sigma^2 q_*^2 + r + \lambda_0} > 0. \tag{2.6.4}$$

From (2.6.1) and (2.6.4), after some rearrangements we obtain

$$\begin{aligned}\frac{\mathrm{d}b^*}{\mathrm{d}\lambda_0} &= \frac{\partial b^*}{\partial \lambda_0} + \frac{\partial b^*}{\partial q_*}\cdot\frac{\partial q_*}{\partial \lambda_0} \\ &= -\frac{P(\frac{1}{2}\sigma^2 q_* + r)}{\beta\lambda_0^2} + \frac{P(\frac{1}{2}\sigma^2 q_*)}{\beta\lambda_0(\frac{1}{2}\sigma^2 q_*^2 + r + \lambda_0)} \\ &= -\frac{P\left[(\frac{1}{2}\sigma^2 q_* + r)(\frac{1}{2}\sigma^2 q_*^2 + r) + \lambda_0 r\right]}{\beta\lambda_0^2(\frac{1}{2}\sigma^2 q_*^2 + r + \lambda_0)} < 0,\end{aligned} \tag{2.6.5}$$

and it follows that the function $\lambda_0 \mapsto b^*$ is decreasing (see Fig. 4(b)).

Let us now turn to the value function $v = v(x)$. First, consider v as a function of μ, thus keeping λ_0 fixed. Using the expression (2.2.20), we can rewrite the first line of the formula (2.2.22) (i.e., for $x \le b^*$) as

$$v = \frac{P}{q_* - 1}\left(\frac{x}{b^*}\right)^{q_*}. \tag{2.6.6}$$

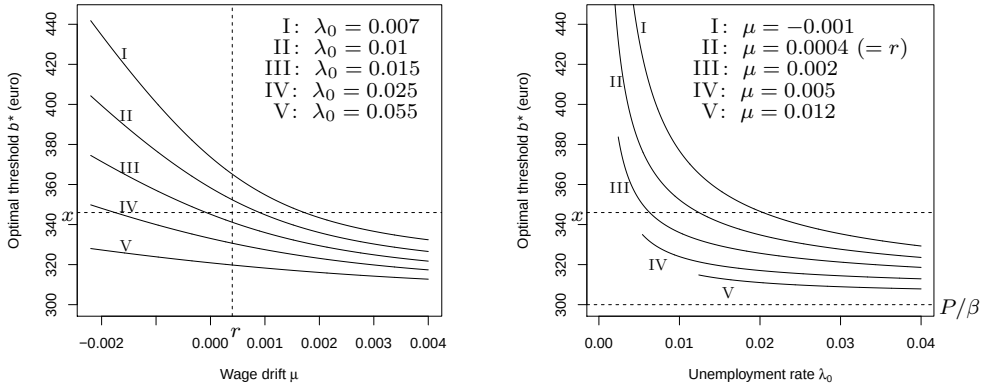

(a) $\mu \mapsto b^*$ (b) $\lambda_0 \mapsto b^*$

FIGURE 4: Graphs illustrating parametric dependencies of the optimal threshold (2.2.20): (a) on the wage drift $\mu < \tilde{r}$ and (b) on the unemployment rate $\lambda_0 > 0 \vee (\mu - r)$, for selected values of λ_0 and μ, respectively. The values of other model parameters used throughout are as in Example 2.5.2: $r = 0.0004$, $P = 9\,000$, $\beta = 30$, and $\sigma = 0.02$. The dashed horizontal line in both plots indicates the initial wage $x = 346$. The dashed vertical line in (a) indicates $\mu = r$. The lower dashed horizontal line in (b) shows the asymptote $P/\beta = 300$ (see (2.6.19)).

Differentiating (2.6.6), we get

$$\frac{\partial v}{\partial q_*} = -\frac{P}{(q_* - 1)^2} \left(\frac{x}{b^*}\right)^{q_*} \left(1 + (q_* - 1) \ln\left(\frac{b^*}{x}\right)\right) < 0, \tag{2.6.7}$$

$$\frac{\partial v}{\partial b^*} = -\frac{P q_*}{(q_* - 1)\, b^*} \left(\frac{x}{b^*}\right)^{q_*} < 0. \tag{2.6.8}$$

Hence, on account of the inequalities (2.6.2), (2.6.4), (2.6.7) and (2.6.8),

$$\frac{\mathrm{d}v}{\mathrm{d}\mu} = \frac{\partial v}{\partial \mu} + \frac{\partial v}{\partial q_*} \cdot \frac{\partial q_*}{\partial \mu} + \frac{\partial v}{\partial b^*} \cdot \frac{\mathrm{d}b^*}{\mathrm{d}\mu} > 0. \tag{2.6.9}$$

If $x \geq b^*$, then from the second line of (2.2.22) we readily obtain

$$\frac{\mathrm{d}v}{\mathrm{d}\mu} = \frac{\beta \lambda_0 x}{(\tilde{r} - \mu)^2} > 0. \tag{2.6.10}$$

Thus, in all cases $\mathrm{d}v/\mathrm{d}\mu > 0$, which implies that the function $\mu \mapsto v$ is increasing (see Fig. 5(a)).

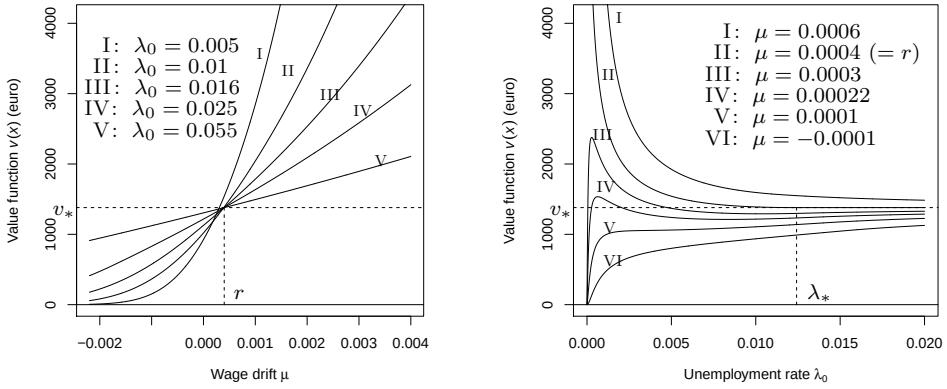

(a) $\mu \mapsto v(x)$ (b) $\lambda_0 \mapsto v(x)$

FIGURE 5: Graphs illustrating parametric dependencies of the value function (2.2.22): (a) on the wage drift $\mu < \tilde{r}$ and (b) on the unemployment rate $\lambda_0 > 0 \vee (\mu - r)$, for selected values of λ_0 and μ, respectively. The values of other model parameters used throughout are as in Example 2.5.2: $r = 0.0004$, $P = 9\,000$, $\beta = 30$, $\sigma = 0.02$, and $x = 346$. The dashed horizontal lines in both plots correspond to the value $v_* := \beta x - P = 1380$. The dashed vertical line in (a) indicates $\mu = r$; in this case, shown as curve II in plot (b), $v(x) \equiv v_*$ for all $\lambda_0 \geq \lambda_* \doteq 0.012420$ (see (2.6.12)). That is why curves III, IV and V in plot (a) all intersect at $\mu = r$.

Finally, fix μ and consider the function $\lambda_0 \mapsto v$. If $x \geq b^*$ then v is given by the second line of (2.2.22), that is,

$$v = \frac{\beta \lambda_0 x}{\lambda_0 + r - \mu} - P. \tag{2.6.11}$$

In particular, if $\mu = r$ then (2.6.11) is reduced to $v \equiv v_* := \beta x - P$. From (2.6.11) it follows that

$$\frac{\mathrm{d}v}{\mathrm{d}\lambda_0} = \frac{\beta x(r-\mu)}{(\lambda_0 + r - \mu)^2} \begin{cases} < 0, & \mu > r, \\ = 0, & \mu = r, \\ > 0, & \mu < r. \end{cases}$$

Due to monotonicity of the function $\lambda_0 \mapsto b^*$ (see (2.6.5)), v is given by (2.6.11) as long as $\lambda_0 \geq \lambda_*$, for some critical value $\lambda_* \equiv \lambda_*(\mu) \leq \infty$. It will be shown below (see (2.6.19)) that $\lim_{\lambda_0 \to \infty} b_* = P/\beta$, so $\lambda_* < \infty$ if and only $x > P/\beta$. Clearly, λ_* is

determined by the condition $b^* = x$ (see (2.2.20)) together with the equation (2.3.11). In the special case $\mu = r$ (assuming that $x > P/\beta$), these equations can be solved to yield

$$\lambda_* = \frac{P}{\beta x}\left(\frac{\frac{1}{2}\sigma^2\beta x}{\beta x - P} + r\right). \tag{2.6.12}$$

In particular, in Example 2.5.2 this gives $\lambda_* \doteq 0.012420$. From the consideration above, it also follows that if $x > P/\beta$ then (see (2.6.11))

$$\lim_{\lambda_0\to\infty} v = v_* = \beta x - P. \tag{2.6.13}$$

In the case $x \le b^*$, we use formula (2.6.6). Similarly to (2.6.9),

$$\frac{\mathrm{d}v}{\mathrm{d}\lambda_0} = \frac{\partial v}{\partial \lambda_0} + \frac{\partial v}{\partial q_*}\cdot\frac{\partial q_*}{\partial \lambda_0} + \frac{\partial v}{\partial b^*}\cdot\frac{\mathrm{d}b^*}{\mathrm{d}\lambda_0}. \tag{2.6.14}$$

Substituting the expressions (2.6.2), (2.6.4), (2.6.7) and (2.6.8) into (2.6.14), cancelling immaterial factors and recalling formula (2.6.1), the condition $\mathrm{d}v/\mathrm{d}\lambda_0 < 0$ is reduced to

$$\left(\frac{1}{2}\sigma^2 q_* + r\right)\left(\frac{1}{2}\sigma^2 q_*^2 + r\right) + \lambda_0 r < \left(\frac{1}{q_* - 1} + \ln\left(\frac{b^*}{x}\right)\right)\left(\frac{1}{2}\sigma^2 q_*^2 + r + \lambda_0\right). \tag{2.6.15}$$

It can be proved that if $\mu \ge r$ then the inequality (2.6.15) holds for all $\lambda_0 < \lambda_*$, but the analysis becomes difficult for $\mu < r$. Numerical plots (see Fig. 5(b)) suggest that in the latter case the function $\lambda_0 \mapsto v$ may be non-monotonic, with the derivative $\mathrm{d}v/\mathrm{d}\lambda_0$ possibly vanishing in up to two points, provided that $r - \varepsilon < \mu < r$ with $\varepsilon > 0$ small enough. To be more specific, the plots in Fig. 5(b) illustrate the case $x > P/\beta$, with the common asymptote (2.6.13). For $x \le P/\beta$, the plots look similar (not shown here) but with $\lim_{\lambda_0\to\infty} v = 0$ (see (2.6.22) below), so the derivative $\mathrm{d}v/\mathrm{d}\lambda_0$ may vanish in at most one point.

2.6.2 Limiting values

Let us investigate the functions b^* and v in the limits (i) $\mu \to -\infty$ or $\mu \uparrow \tilde{r}$, and (ii) $\lambda_0 \to \infty$ or $\lambda_0 \downarrow 0$ ($\mu < r$), $\lambda_0 \downarrow \mu - r$ ($\mu \ge r$). Start by observing, using equation (2.3.11), that

$$\lim_{\mu\to-\infty} q_* = \infty, \qquad \lim_{\mu\uparrow\tilde{r}} q_* = 1, \tag{2.6.16}$$

and moreover,

$$q_* - 1 \sim \frac{\tilde{r} - \mu}{\frac{1}{2}\sigma^2 + \tilde{r}} \qquad (\mu \uparrow \tilde{r}). \tag{2.6.17}$$

Similarly, $\lim_{\lambda_0\to\infty} q_* = \infty$; on the other hand, if $\mu < r$ then $\lim_{\lambda_0\downarrow 0} q_* = q_*|_{\lambda_0=0} > 1$, while if $\mu \geq r$ then

$$q_* - 1 \sim \frac{\lambda_0 - (\mu - r)}{\frac{1}{2}\sigma^2 + \mu} \qquad (\lambda_0 \downarrow \mu - r). \tag{2.6.18}$$

Hence, from (2.6.1) and (2.6.16) it readily follows that $b^* \to \infty$ $(\mu \to -\infty)$ and

$$b^* \to \frac{P(\frac{1}{2}\sigma^2 + \tilde{r})}{\beta\lambda_0} \qquad (\mu \uparrow \tilde{r}).$$

Also, using that $q_* \to \infty$ $(\lambda_0 \to \infty)$, from (2.2.20) we get

$$b^* \to \frac{P}{\beta} \qquad (\lambda_0 \to \infty). \tag{2.6.19}$$

In the opposite limit, if $\mu > r$ then, according to (2.6.1) and (2.6.18),

$$b^* \to \frac{P(\frac{1}{2}\sigma^2 + \mu)}{\beta(\mu - r)} \qquad (\lambda_0 \downarrow \mu - r), \tag{2.6.20}$$

while if $\mu \leq r$ then $\lim_{\lambda_0\downarrow 0} b^* = \infty$; in particular, for $\mu = r$

$$b^* \sim \frac{P(\frac{1}{2}\sigma^2 + r)}{\beta\lambda_0} \qquad (\lambda_0 \downarrow 0). \tag{2.6.21}$$

For the value function $v = v(x)$, from formula (2.6.6) we get, using (2.6.16) and (2.6.17),

$$\lim_{\mu\to-\infty} v = 0, \qquad \lim_{\mu\uparrow\tilde{r}} v = \infty.$$

Furthermore, according to (2.6.13), if $x > P/\beta$ then $v \to v_* = \beta x - P$ as $\lambda_0 \to \infty$. In the opposite case, due to monotonicity of b^* (see (2.6.5)) and the limit (2.6.19) we have $b^* > P/\beta \geq x$, so using formula (2.6.6) and recalling that $q_* \to \infty$, we get

$$v \leq \frac{P}{q_* - 1} \to 0 \qquad (\lambda_0 \to \infty). \tag{2.6.22}$$

Now, consider the limit of v as λ_0 approaches the lower edge of its range. If $\mu < r$ then (2.6.6) implies that $\lim_{\lambda\downarrow 0} v = 0$, since $b^* \to \infty$ and $q_* \to q_*|_{\lambda_0=0} > 1$. If $\mu = r$ then, using (2.6.18) and (2.6.21) (with $\mu = r$), we obtain

$$v \sim \beta x \lambda_0^{q_*-1} = \beta x \exp\{(q_* - 1)\ln\lambda_0\} \to \beta x \qquad (\lambda_0 \downarrow 0). \tag{2.6.23}$$

Finally, if $\mu > r$ then from (2.6.6) it readily follows, according to (2.6.18) and (2.6.20),

$$v \sim \frac{\beta x(\mu - r)}{\lambda - (\mu - r)} \to \infty \qquad (\lambda_0 \downarrow \mu - r). \tag{2.6.24}$$

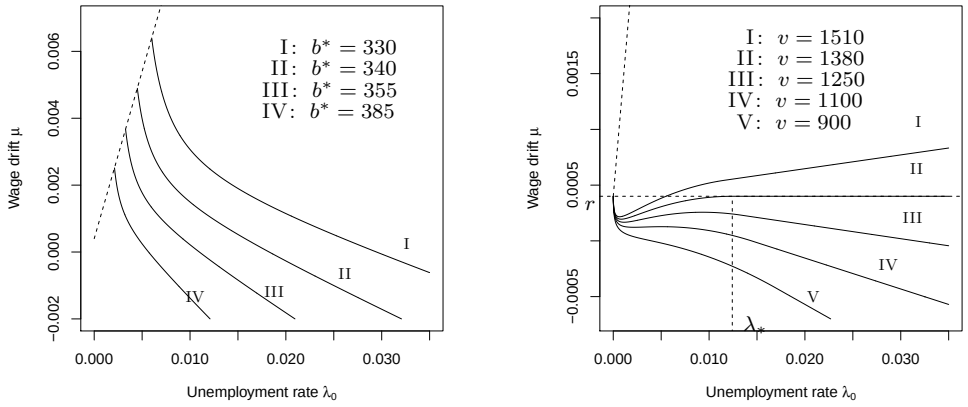

(a) Isolines of b^*

(b) Isolines of $v = v(x)$

FIGURE 6: Isolines (level curves) of the optimal stopping problem solution on the (λ_0, μ)-plane: (a) $b^*(\lambda_0, \mu) = \text{const}$ (optimal threshold (2.2.20)); (b) $v(\lambda_0, \mu) = \text{const}$ (value function (2.2.22)). The values of other parameters used throughout are as in Example 2.5.2: $r = 0.0004$, $P = 9\,000$, $\beta = 30$, $\sigma = 0.02$, and $x = 346$. The slanted dashed lines in both plots show the boundary $\mu = \lambda_0 + r$ (see (2.2.8)). In plot (b), the horizontal dashed line indicates $\mu = r$ and the vertical dashed line shows $\lambda_* \doteq 0.012420$ (cf. Fig. 5(b)).

2.6.3 Comparative statics and sensitivity analysis

The goal of comparative statics is to understand how varying values of exogenous parameters affect a target function of interest. For instance, consider the optimal threshold b^* as a function of both unemployment rate λ_0 and wage drift μ. Rather then fixing one of these parameters and then plotting b^* against the remaining parameter (as was done in Figs. 4(a) and 4(b)), it is useful to plot a family of comparative statics plots showing the *isolines* (or *level curves*) for different values (levels) of the function, that is, $b^*(\lambda_0, \mu) = \text{const}$ (see Fig. 6(a)). As may be expected from Figs. 4(a) and 4(b), the plots of the function $\lambda_0 = \lambda_0(\mu)$ (determined implicitly by the level condition) behave as monotone decreasing graphs. Analogous plots for the value function are presented in Fig. 6(b); the plots become non-monotonic for v large enough. If λ_0 is fixed then the value v grows with μ, in agreement with (2.6.9) and (2.6.10). Similarly, if $\mu > r$

is fixed then v decreases with λ_0, converging to the limit $v_* = \beta x - P$ as $\lambda_0 \to \infty$ (see (2.6.13)), represented by curve II in Fig. 5(b). If $v > v_*$ then there are up to two different values of λ_0 (and common μ) producing the same value v, while for v smaller than but close enough to v_*, the number of such roots may increase to three (see the discussion in Section 2.6.4).

Let us also comment on the sensitivity of our numerical examples presented in Section 2.5.4. The question here is, how much the output values (say, the optimal threshold b^* and the value v) would change under a small variation of one of the background parameters. In the linear approximation, the change factor is given by the corresponding partial derivative. As in the previous sections, we address the sensitivity with regard to the wage drift μ (around the set value $\mu = 0.0004$) and the unemployment rate λ_0 (around $\lambda_0 = 0.01$). Other model parameters are fixed as in Section 2.5.4, that is, $r = 0.0004$, $P = 9\,000$, $\beta = 30$, and $x = 346$. As for the volatility parameter σ, it is set to be $\sigma = 0.04$ as in Example 2.5.1 or $\sigma = 0.02$ as in Example 2.5.2. The required partial derivatives of b^* and v can be computed using the formulas derived in Section 2.6.1; the results are presented in Table 2.1(a).

Numerical values in Table 2.1(a) may seem quite big, but they should be offset by small background values of the parameters, $\mu = 0.0004$ and $\lambda_0 = 0.01$. If we increase them by a small amount, say by 1%, then the absolute increments would be

$$\Delta\mu = 0.0004/100 = 4 \cdot 10^{-6}, \qquad \Delta\lambda_0 = 0.01/100 = 10^{-4}.$$

Hence, using Table 2.1(a), we obtain the corresponding approximate increments of the target functions b^* and v (see Table 2.1(b)), which look more palatable. One interesting observation is that the value v reacts about 5 times stronger to the change of the unemployment rate λ_0 when the volatility σ gets 2 times bigger (from $\sigma = 0.02$ in Example 2.5.2 to $\sigma = 0.04$ in Example 2.5.1); in contrast, the change of v in response to an increase of the wage drift is much less pronounced. This highlights the primary significance of the unemployment rate, which is of course only natural.

Sensitivity analysis with regard to the wage drift μ is also useful in the light of the difficulty in estimation of μ from the data, mentioned in Section 2.5.2. The results in Table 2.1(b) suggest that a reasonably small error in selecting μ has only a minor effect on the identification of the optimal threshold b^* and the value v; for instance, overestimating it by 1% will decrease b^* by just 0.01 euro, while the value v will be up by about 0.60 euro. Thus, an individual using a moderately inflated value of their

(a) Derivatives

Derivative	Example 2.5.1	Example 2.5.2
$\mathrm{d}b^*/\mathrm{d}\mu$	$-16\,037.57$	$-13\,962.43$
$\mathrm{d}v/\mathrm{d}\mu$	$842\,062.30$	$993\,991.20$
$\mathrm{d}b^*/\mathrm{d}\lambda_0$	$-6\,323.813$	$-3\,161.906$
$\mathrm{d}v/\mathrm{d}\lambda_0$	$-46\,485.530$	$-8\,768.435$

(b) Increments (euro)

Increment	Example 2.5.1	Example 2.5.2
$\Delta b^*\ (\mu)$	-0.06415	-0.05585
$\Delta v\ \ (\mu)$	3.36825	3.97597
$\Delta b^*\ (\lambda_0)$	-0.63238	-0.31619
$\Delta v\ \ (\lambda_0)$	-4.64855	-0.87684

TABLE 2.1: Sensitivity check of numerical results for the functions b^* and v in Examples 2.5.1 and 2.5.2: (a) parametric derivatives; (b) increments in response to a 1%-change in the background parameters.

wage rate would take a slightly over-optimistic view about the timing of joining the insurance scheme and its expected benefit. On the other hand, a risk-averse individual may take a more conservative view and prefer to underestimate their wage drift μ, which will raise the threshold b^* resulting in a longer waiting time. For the insurance company though, it may be reasonable to try and avoid underestimation of the wage drift of potential customers, so as to reduce the risk of overpaying the benefits.

2.6.4 Economic interpretation

Monotonic decay of the optimal threshold b^* with an increase of the unemployment rate λ_0 (see (2.6.5) and Fig. 4(b)) has a clear economic appeal: a bigger unemployment rate λ_0 means a higher risk of losing the job, which demands a lower target threshold b^* in order to expedite joining the insurance scheme. The economic rationale for the

monotonicity of b^* as a function of μ (see (2.6.3) and Fig. 4(a)) is different — a bigger wage drift μ makes it more likely to reach a higher final wage X_{τ_0} by the time of loss of job, so lowering the threshold b^* adds incentive to an earlier entry.

Monotonic growth of the value v as a function of the wage drift μ (see (2.6.9), (2.6.10), and Fig. 5(a)) is also meaningful — indeed, when the wage drift μ gets bigger, there is more potential to reach a higher final wage X_{τ_0} by the time of loss of job, which increases the expected benefit β_1 (see (2.2.6)) and, therefore, the value $v = v(x)$ of the insurance policy.

The behaviour of the value function $v = v(x)$ in response to a varying unemployment rate λ_0 is more interesting, as indicated by the plots in Fig. 5(b). In the case $\mu < r$, it is satisfactory to see that the value v, vanishing in the limit as $\lambda_0 \downarrow 0$, starts growing with λ_0, thus reflecting a good efficiency of the insurance policy against an increasing risk of unemployment. On the other side of the policy, this may present a growing risk for the insurance company which will have to finance an increasing number of claims. But with the unemployment rate λ_0 getting ever bigger, the value v should stay bounded, so must converge to a limit as $\lambda_0 \to \infty$, given by $v_* = \beta x - P$ if $x > P/\beta$ (see (2.6.13)) or $v_* = 0$ otherwise (see (2.6.22)). In particular, Fig. 5(b) shows that, for a certain range of μ, the value v achieves its maximum at some λ_0. However, the graphs also reveal that if μ keeps increasing then the value plots may have a more complicated non-monotonic behaviour, which is harder to interpret economically.

On the other hand, as is evident from Fig. 5(b), in the case $\mu \geq r$ our model produces a counter-intuitive increase of the value v as λ_0 approaches the left edge of its range — it is hard to believe that the value may grow as the risk of unemployment falls. Moreover, as was computed in (2.6.24), for $\mu > r$ the corresponding limit of v is infinite! But perhaps the most striking example emerges in the borderline case $\mu = r$, whereby formally setting $\lambda_0 = 0$ we would get, according to (2.6.21), that the threshold b^* is infinite (unlike the case $\mu > r$, see (2.6.21)), so that the wage process (X_t) never reaches it; therefore, we never buy the insurance policy (understandably so, as there is no risk of losing the job), and nonetheless its value is positive in this limit (see (2.6.13)). The explanation of this paradox lies in the way how the optimal stopping is exercised for small $\lambda_0 > 0$: here, the threshold b^* is high and there is only a very small probability that it is ever reached; before this happens, we stay idle, but if and when the threshold is hit then the expected payoff is rather big, which contributes enough to the expected

net present value to keep it positive in the limit $\lambda_0 \downarrow 0$ (see (2.6.23)).

Thus, the artefacts in our model as indicated above are caused by not putting any constraint on the waiting times. This can be rectified, for example, by introducing *mortality*, as was sketched in Section 2.2.1; in particular, such a regularization should restore a zero limit of v at the lower edge of λ_0.

2.7 Including utility considerations

2.7.1 Perpetual American call option

Our model (and its solution) resembles that of the optimal stopping problem for the *(perpetual) American call option* (see a detailed discussion in [121, Ch. VIII, §2a]). More specifically, the holder of a call option may exercise the right to buy an asset (e.g., one unit of stock) at any time for a pre-determined strike price K, where the decision is based on observations over the random process of stock prices (S_t), assumed to follow a geometric Brownian motion model. The term *perpetual* is used to indicate that there is no expiration date, so the right to buy extends indefinitely.

The optimal time instant $\tau = \tau^*$ to buy, bearing in mind a purely financial target of maximizing the profit $S_\tau - K$, is the solution of the following optimal stopping problem,

$$V(x) = \sup_\tau \mathrm{E}_x(\mathrm{e}^{-r\tau}(S_\tau - K)^+), \tag{2.7.1}$$

where S_t is a geometric Brownian motion with parameters $\mu < r$ and $\sigma > 0$, the supremum is taken over all stopping times τ adapted to the filtration associated with (S_t). The positive truncation $(\cdot)^+$ corresponds to the constraint that the option holder is not in a position to buy at the price K higher than the current spot price S_t. The solution to (2.7.1) is well known (see, e.g., [121, Ch. VIII, §2a]) to be given by the hitting time $\tau^* = \tau_{b^*}$, with the optimal threshold

$$b^* = \frac{Kq^*}{q^* - 1},$$

where q^* is given by formula (2.2.21) but with $\tilde{r} = r + \lambda_0$ replaced by r. The corresponding value function is given by

$$V(x) = \begin{cases} (b^* - K)\left(\dfrac{x}{b^*}\right)^{q_*}, & x \in [0, b^*], \\ x - K, & x \in [b^*, \infty). \end{cases}$$

Observe that our optimal stopping problem (2.2.14) can be rewritten as

$$v(x) = \beta_1 \sup_{\tau} \mathrm{E}_x\big[\mathrm{e}^{-\tilde{r}\tau}(X_\tau - \tilde{K})\big], \qquad \tilde{K} := P/\beta_1, \tag{2.7.2}$$

which makes it look very similar to the perpetual American call option problem (2.7.1). However, there are several important differences. Firstly, unlike the gain function in the American call option problem (2.7.1), no truncation is applied in (2.7.2), because the financial gain is not the sole priority in this context and therefore the individual is prepared to tolerate negative values of $\beta_1 X_\tau - P$ (despite the fact that, under the optimal strategy, the value function $v(x)$ is always non-negative, see Lemma 2.2.2(i) and formula (2.2.22)).[1] In addition, as was mentioned in Remark 2.4.1 and in Section 2.5.3, the hitting time τ_{b^*} may be infinite with a positive probability (i.e., when $\mu < \frac{1}{2}\sigma^2$), which may be deemed impractical in the insurance context, but is considered to be acceptable for exercising the American call option. This simple observation helps to realize the fundamental conceptual difference between the two problems; indeed, the insurance optimal stopping does not focus only on the financial gain, but also places an ultimate priority on acquiring an insurance cover *per se*. Hence, a more realistic formulation of the optimal stopping problem in the UI model should involve a certain *utility*, which specifies the individual's weighted preferences for satisfaction — for example, impatience against waiting for too long before joining the UI scheme.

2.7.2 Heuristic optimal stopping models with utility

Here, we present a few informal thoughts about the possible inclusion of utility in the optimality analysis. As already mentioned, in the case $\mu < \frac{1}{2}\sigma^2$ the probability of hitting the critical threshold b^* is less than 1, so there is a probability that the individual will never join the insurance scheme if the optimal stopping rule is strictly followed. This is of course not desirable, as the individual puts high priority on getting insured at some point in time (hopefully, prior to loss of job).

One simple way to take these additional requirements into account is to extend the

[1] The equivalence of the problems (2.7.1) and (2.7.2), which we have established directly, is not a coincidence: it is known [130, Proposition 3.1, p. 185] that, under mild assumptions, the solution of the general optimal stopping problem $v(x) = \sup_\tau \mathrm{E}_x\big(\mathrm{e}^{-r\tau} g(X_\tau)\big)$ does not change with the positive truncation of $g(\cdot)$.

optimal stopping problem (2.2.14) as follows:

$$\begin{aligned} v^{\dagger}(x) &= \sup_{\tau} [\kappa \, \mathrm{P}_x(\tau < \infty) + \mathrm{eNPV}(x;\tau)] \\ &= \sup_{\tau} \mathrm{E}_x [\kappa \, \mathbb{1}_{\{\tau<\infty\}} + \mathrm{e}^{-\tilde{r}\tau} g(X_\tau)], \end{aligned} \tag{2.7.3}$$

where the supremum is again taken over all stopping times τ adapted to the process (X_t), and the coefficient $\kappa \geq 0$ is a predefined weight representing the individual's personal attitude (preference) towards the two contributing terms. If $\mathrm{P}_x(\tau < \infty) = 1$ then the first term in (2.7.3) is reduced to a constant (κ), leading to a pure optimal stopping problem as before; however, if $\mathrm{P}_x(\tau < \infty) < 1$ then the first term enhances the role of candidate stopping times τ that are less likely to be infinite.

The problem (2.7.3) can be rewritten in a more standard form by pulling out the common discounting factor under expectation,

$$v^{\dagger}(x) = \sup_{\tau} \mathrm{E}_x [\mathrm{e}^{-\tilde{r}\tau} G(\tau, X_\tau)], \tag{2.7.4}$$

with

$$G(t,x) := \kappa \, \mathrm{e}^{\tilde{r}t} + g(x), \quad (t,x) \in [0,\infty] \times [0,\infty). \tag{2.7.5}$$

Unfortunately, the optimal stopping problem (2.7.4) is not amenable to an exact solution as before, because the gain function (2.7.5) depends also on the time variable (see [107, Ch. IV]). In this case, the problem (2.7.4) may again be reduced to a suitable (but more complex) free-boundary problem, but the hitting boundary (of a certain set on the (t,x)-plane) is no longer a straight line.

More generally, our optimal stopping problem can be modified by replacing the indicator in (2.7.3) with the expression $\mathrm{e}^{-\rho\tau}$ ($\rho > 0$),

$$v^{\dagger}(x) = \sup_{\tau} \mathrm{E}_x [\kappa \, \mathrm{e}^{-\rho\tau} + \mathrm{e}^{-\tilde{r}\tau} g(X_\tau)], \tag{2.7.6}$$

which retains the flavour of progressively penalizing larger values of τ, including $\tau = \infty$. Here, the gain function (2.7.5) takes the form

$$G(t,x) = \kappa \, \mathrm{e}^{(\tilde{r}-\rho)t} + g(x).$$

In particular, by choosing $\rho = \tilde{r}$ the problem (2.7.6) is transformed into

$$v^{\dagger} = \sup_{\tau} \mathrm{E}_x [\mathrm{e}^{-\tilde{r}\tau} (\beta_1 X_\tau + \kappa - P)],$$

which is the same problem as (2.2.14) but with the premium P replaced by $P - \kappa$.

Another, more drastic approach to amending the standard optimal stopping problem (2.2.14) stems from the observation that even if $\tau < \infty$ (P_x-a.s.), it may take long to wait for τ to happen — for instance, if $\mathrm{E}_x(\tau) = \infty$. In other words, it is reasonable to take into account the expected value of τ, leading to the combined optimal stopping problem

$$v^\dagger(x) = \sup_\tau \big[\kappa\,\mathrm{P}_x(\tau < \infty) + \kappa\exp\{-\mathrm{E}_x(\tau)\} + \mathrm{eNPV}(x;\tau)\big]. \tag{2.7.7}$$

If $\mathrm{P}_x(\tau < \infty) < 1$ then $\mathrm{E}_x(\tau) = \infty$ and the problem (2.7.7) is reduced to (2.7.3), whereas if $\mathrm{P}_x(\tau < \infty) = 1$ then, effectively, only the term with the expectation remains in (2.7.7). However, a disadvantage of the formulation (2.7.7) is that it cannot be expressed in the form (2.7.4). Trying to amend this would take us back to the version (2.7.6).

It is interesting to look at how the value function depends on the preference parameter κ. The next property is intuitively obvious.

Proposition 2.7.1. *For each $x > 0$, the value function $v^\dagger(x)$ of the optimal stopping problem (2.7.6) is a strictly increasing function of κ. The same is true for the problem (2.7.7).*

Proof. We use the notation $v^\dagger(x;\kappa)$ to indicate the dependence of the value function on the parameter κ. For $\kappa_1 < \kappa_2$ and any stopping time $\tau \not\equiv \infty$, we have

$$\mathrm{E}_x\big[\kappa_1\,\mathrm{e}^{-\rho\tau} + \mathrm{e}^{-\tilde{r}\tau}g(X_\tau)\big] < \mathrm{E}_x\big[\kappa_2\,\mathrm{e}^{-\rho\tau} + \mathrm{e}^{-\tilde{r}\tau}g(X_\tau)\big] \le v^\dagger(x;\kappa_2). \tag{2.7.8}$$

Suppose that τ_* is a maximizer for the optimal stopping problem (2.7.6) with $\kappa = \kappa_1$. Then, according to (2.7.8),

$$v^\dagger(x;\kappa_1) = \mathrm{E}_x\big[\kappa_1\,\mathrm{e}^{-\rho\tau_*} + \mathrm{e}^{-\tilde{r}\tau_*}g(X_{\tau_*})\big] < v^\dagger(x;\kappa_2),$$

that is, $v^\dagger(x;\kappa_1) < v^\dagger(x;\kappa_2)$ as claimed. Similar arguments apply to the problem (2.7.7). □

2.7.3 Sub-optimal solutions

As already mentioned, the optimal stopping problems outlined in Section 2.6.2 are difficult to solve in full generality. To gain some insight about the qualitative effects of the added utility-type terms, it may be reasonable to restrict our attention to solutions

in the subclass of hitting times τ_b. Despite such solutions will only be suboptimal, the advantage is that the reduced problems can be solved using that all the ingredients are available explicitly (see Section 2.4.1).

For example, the original problem (2.7.3) is replaced by

$$u^\dagger(x) = \sup_{b\geq 0}\big[\kappa\,\mathrm{P}_x(\tau_b < \infty) + \mathrm{eNPV}(x;\tau_b)\big]. \tag{2.7.9}$$

Similarly as in Section 2.4.3, we only need to maximize the functional in (2.7.9) over $b \geq x$. Indeed, if $b \leq x$ then $\tau_b = 0$ (P_x-a.s.) and, according to (2.2.4) and (2.2.13),

$$\sup_{b\leq x}\big[\kappa\,\mathrm{P}_x(\tau_b < \infty) + \mathrm{eNPV}(x;\tau_b)\big] = \kappa + \mathrm{eNPV}(x;0) = \kappa + \beta_1 x - P,$$

whereas

$$\begin{aligned}\sup_{b\geq x}\big[\kappa\,\mathrm{P}_x(\tau_b < \infty) + \mathrm{eNPV}(x;\tau_b)\big] &\geq \big[\kappa\,\mathrm{P}_x(\tau_b < \infty) + \mathrm{eNPV}(x;\tau_b)\big]\big|_{b=x}\\ &= \kappa + \beta_1 x - P.\end{aligned}$$

Assume that $\mu - \frac{1}{2}\sigma^2 < 0$ (for otherwise $\mathrm{P}_x(\tau_b < \infty) = 1$, thus leading to the same optimal stopping problem as before). Then, according to (2.4.8), the probability $\mathrm{P}_x(\tau_b < \infty)$ becomes a strictly decreasing function of $b \in [x, \infty)$, and so the maximum in (2.7.9) is achieved by a different stopping strategy, with a lower optimal threshold $b^\dagger$. More precisely, by virtue of formulas (2.4.8) and (2.4.15), the problem (2.7.9) is explicitly rewritten as

$$u^\dagger(x) = \sup_{b\geq x}\left[\kappa\left(\frac{x}{b}\right)^{1-2\mu/\sigma^2} + (\beta_1 b - P)\left(\frac{x}{b}\right)^{q_*}\right], \tag{2.7.10}$$

where $q_* > 1$ is defined in (2.2.21). Differentiating with respect to b, it is easy to check that the maximizer for the problem (2.7.10) is given by

$$b^\dagger = \min\left\{b \geq x\colon\ a\kappa\left(\frac{b}{x}\right)^{q_*-a} + (q_* - 1)\beta_1 b \geq P q_*\right\},$$

where $a := 1 - 2\mu/\sigma^2 < 1 < q_*$.

The following (slightly artificial) version of the utility keeps the spirit of (2.7.9) but is amenable to the exact analysis:

$$u^\dagger(x) = \sup_{b\geq 0}\Big[\kappa\big\{\mathrm{P}_x(\tau_b < \infty)\big\}^{q_*/(1-2\mu/\sigma^2)} + \mathrm{eNPV}(x;\tau_b)\Big]. \tag{2.7.11}$$

Indeed, using the same substitutions (2.4.8) and (2.4.15) as before, (2.7.11) is reduced to (cf. (2.7.10))

$$u^\dagger(x) = \sup_{b\geq x}\Big[(\beta_1 b + \kappa - P)\Big(\frac{x}{b}\Big)^{q_*}\Big], \tag{2.7.12}$$

which is the same problem as (2.4.14) but with P replaced by $P-\kappa$ (cf. (2.4.15)). Therefore, from (2.4.16) we immediately obtain the maximizer

$$b^\dagger = \frac{(P-\kappa)q_*}{\beta_1(q_*-1)} = b^* - \frac{\kappa q_*}{\beta_1(q_*-1)} \leq b^*. \tag{2.7.13}$$

This is a strictly decreasing (linear) function of κ; in particular, $b^\dagger = b^*$ if $\kappa = 0$ and $b^\dagger = 0$ if $\kappa = P$. The corresponding value function is given by (cf. (2.4.17))

$$u^\dagger(x) = \begin{cases} (\beta_1 b^\dagger + \kappa - P)\left(\dfrac{x}{b^\dagger}\right)^{q_*}, & x\in[0,b^\dagger], \\ \beta_1 x + \kappa - P, & x\in[b^\dagger,\infty), \end{cases} \tag{2.7.14}$$

or more explicitly (cf. (2.4.18))

$$u^\dagger(x) = \begin{cases} \dfrac{P-\kappa}{q_*-1}\left(\dfrac{\beta_1(q_*-1)x}{(P-\kappa)q_*}\right)^{q_*}, & 0\leq x\leq \dfrac{(P-\kappa)q_*}{\beta_1(q_*-1)}, \\ \beta_1 x + \kappa - P, & x\geq \dfrac{(P-\kappa)q_*}{\beta_1(q_*-1)}. \end{cases} \tag{2.7.15}$$

If x is fixed then the problem value $u^\dagger$, as a function of κ, is given by the first or the second line in (2.7.15) according as $\kappa\in[0,\kappa^\dagger]$ or $\kappa\in[\kappa^\dagger,\infty)$, respectively, where

$$\kappa^\dagger := P - \frac{\beta_1(q_*-1)x}{q_*}. \tag{2.7.16}$$

The dependence of $b^\dagger$ and $u^\dagger(x)$ upon the utility parameter $\kappa\in[0,P]$ is illustrated in Fig. 7, while Fig. 8 demonstrates the functional dependence of the hitting probability $\mathrm{P}_x(\tau_b<\infty)$ and the mean hitting time $\mathrm{E}_x(\tau_b)$ upon the variable threshold $b\geq 0$, along with the corresponding plots of the expected net present value $\mathrm{eNPV}(x;\tau_b)$.

Remark 2.7.1. Note that $u^\dagger(x)$ is a strictly increasing function of $\kappa\in[0,P]$, in accord with Proposition 2.7.1. In particular, $u^\dagger(x)$ coincides with the original value function $u(x)$ given by (2.4.18), but with the premium P replaced by $P-\kappa$. This can be interpreted as the individual's consent to convert additional satisfaction, gained by virtue of pursuing the optimal stopping problem (2.7.11) instead of (2.2.14), into a higher premium, $P^\dagger = P+\kappa$. Such an effect is characteristic of the use of risk-averse utility functions under the Expected Utility Theory [73] (see also a discussion below in Section 2.6.4).

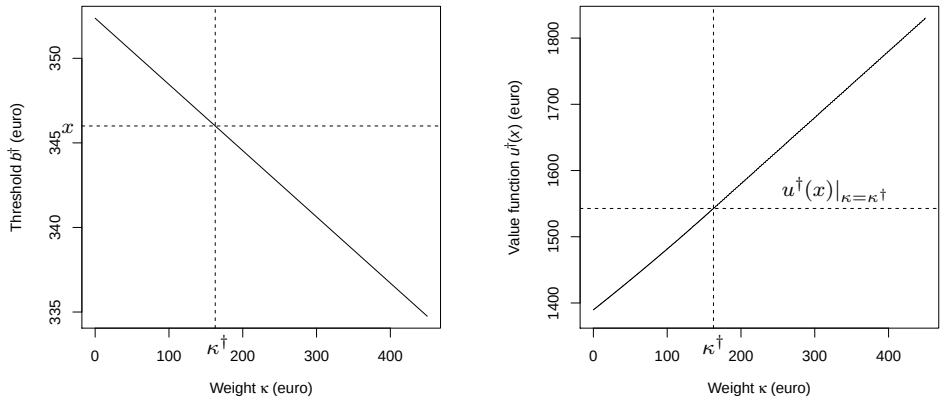

(a) $\kappa \mapsto b^\dagger$ (b) $\kappa \mapsto u^\dagger(x)$

FIGURE 7: Functional dependence on the preference weight κ in the reduced optimal stopping problem (2.7.11): (a) the optimal threshold $b^\dagger$ (see (2.7.13)); (b) the value function $u^\dagger(x)$ (see (2.7.15)). Numerical values of the parameters used are as in Example 2.5.2: $r = \mu = 0.0004$, $P = 9\,000$, $\beta = 30$, $\sigma = 0.02$, and $x = 346$. In particular, if $\kappa = 0$ then $b^\dagger$ coincides with $b^* \doteq 352.3705$ and $u^\dagger(x)$ coincides with $v(x) \doteq 1389.6190$. The dashed vertical lines on both plots indicate the value $\kappa^\dagger \doteq 162.7108$ (see (2.7.16)) separating different regimes for $u^\dagger(x)$ according to (2.7.15). When $\kappa = \kappa^\dagger$, we have $b^\dagger = x = 346$, shown as a dashed horizontal line in plot (a); the corresponding value function is given by $u^\dagger(x) = \beta_1 x + \kappa^\dagger - P \doteq 1542.7110$ (see (2.7.14)), shown as a dashed horizontal line in plot (b). Note that the graph of $u^\dagger(x)$ in plot (b) looks almost linear for $\kappa \in [0, \kappa^\dagger]$, because the ratio κ/P is quite small, $0 \le \kappa/P \le \kappa^\dagger/P \doteq 0.01808$; the slope here is approximately $v(x)(q_* - 1)/P \doteq 0.88448$, as compared to slope 1 of the linear graph for $\kappa \ge \kappa^\dagger$.

In the case $\mu > \frac{1}{2}\sigma^2$, instead of (2.7.7) we may consider the simplified problem

$$u^\dagger(x) = \sup_{b \ge 0} \big[\kappa \exp\{-\mathrm{E}_x(\tau_b)\} + \mathrm{eNPV}(x; \tau_b)\big]. \tag{2.7.17}$$

Upon the substitution of formulas (2.4.9) and (2.4.15), it is rewritten in the form (cf. (2.7.10))

$$u^\dagger(x) = \sup_{b \ge x} \left[\kappa \, \frac{\ln(b/x)}{\mu - \frac{1}{2}\sigma^2} + (\beta_1 b - P) \left(\frac{x}{b}\right)^{q_*}\right]. \tag{2.7.18}$$

Again, the maximization problem (2.7.18) can be solved (at least, numerically). For

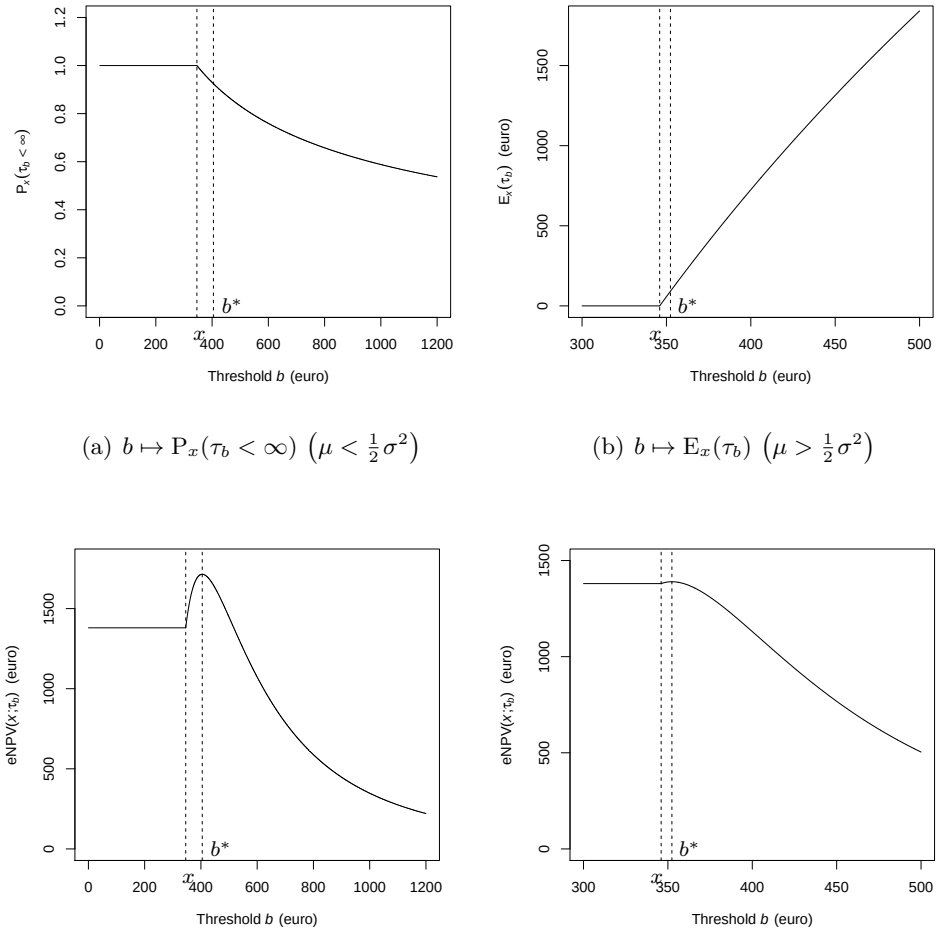

(a) $b \mapsto \mathrm{P}_x(\tau_b < \infty)$ $\left(\mu < \frac{1}{2}\sigma^2\right)$

(b) $b \mapsto \mathrm{E}_x(\tau_b)$ $\left(\mu > \frac{1}{2}\sigma^2\right)$

(c) $b \mapsto \mathrm{eNPV}(x;\tau_b)$ $\left(\mu < \frac{1}{2}\sigma^2\right)$

(d) $b \mapsto \mathrm{eNPV}(x;\tau_b)$ $\left(\mu > \frac{1}{2}\sigma^2\right)$

FIGURE 8: Theoretical graphs for functionals of the hitting time τ_b versus threshold $b \geq 0$. *Upper row:* (a) the hitting probability $\mathrm{P}_x(\tau_b < \infty)$ (see (2.4.8)); (b) the mean hitting time $\mathrm{E}_x(\tau_b)$ (see (2.4.9)). *Bottom row:* the expected net present value $\mathrm{eNPV}(x;\tau_b)$ (see (2.4.15)) with $\mu < \frac{1}{2}\sigma^2$ (c) or $\mu > \frac{1}{2}\sigma^2$ (d). The values of parameters used throughout are as in Section 2.5.4: $x = 346$, $P = 9\,000$, $\beta_1 = 30$, $\mu = 0.0004$, and $\sigma = 0.04$ (left) or $\sigma = 0.02$ (right). The dashed vertical lines on each plot indicate x and the optimal threshold b^*, respectively; specifically, $b^* \doteq 404.7410$ on the left (see Example 2.5.1) and $b^* \doteq 352.3705$ on the right (see Example 2.5.2).

an analytic solution, it is convenient to modify the problem (2.7.17) as follows,

$$u^\dagger(x) = \sup_{b \geq 0} \left[\kappa \exp\left(-\frac{q_*}{\mu - \frac{1}{2}\sigma^2} \mathrm{E}_x(\tau_b) \right) + \mathrm{eNPV}(x;\tau_b) \right].$$

Similarly to (2.7.18), this leads to the maximization problem that coincides with (2.7.12) and, therefore, has the same solution (2.7.13) and (2.7.14) (or, equivalently, (2.7.15)).

2.7.4 Connections to Expected Utility Theory

The considerations above can be linked to the standard Expected Utility Theory [73]. In the usual setting, it is assumed that an individual uses (perhaps, subconsciously) a certain utility $U(w)$, as a function of financial wealth w, to assess losses, gains and the resulting satisfaction. Generically, given the current wealth w and some random future loss Y, the expected loss (measured via utility $U(\cdot)$) may be expressed as $\mathrm{E}\big[U(w-Y)\big]$. The individual is inclined to pay a premium P and buy the insurance policy as long as the expected utility without insurance is no more than $U(w-P)$,

$$\mathrm{E}\big[U(w-Y)\big] \le U(w-P). \tag{2.7.19}$$

The balance condition

$$\mathrm{E}\big[U(w-Y)\big] = U(w-P) \tag{2.7.20}$$

determines the maximum premium $P_{\max}$ the customer is prepared to pay (in fact, at this point it makes no difference whether to buy the insurance or not).

In the baseline case with $U(w) \equiv w$, the conditions (2.7.19) and (2.7.20) are reduced to

$$P \le P_{\max} = \mathrm{E}(Y). \tag{2.7.21}$$

However, choosing a different utility function may well change this threshold. For instance, if the random loss Y has exponential distribution with parameter $\theta = 0.001$, then according to (2.7.21) we have $P_{\max} = \mathrm{E}(Y) = 1/\theta = 1\,000$. In contrast, let the utility function be chosen as $U(w) = 1 - \exp\big(-\frac{1}{2}\theta w\big)$. Here, the utility is between 0 and 1 if the wealth w is positive, but it becomes increasingly negative for a negative wealth; that is, strong weight is placed against negative wealth, which may be characteristic of a risk-averse individual. In this case, it is easy to check that

$$P_{\max} = \frac{2\ln 2}{\theta} = 1\,386.294 > 1\,000.$$

Thus, the individual is happy to pay more than before to protect themselves from the perceived risk of significant losses. That is to say, an additional amount of satisfaction is convertible into an extra premium.

In our case, if the UI was to be entered immediately, at time $t = 0$, then the value of this decision would be $\mathrm{eNPV}(x; 0) = \beta_1 x - P$ (see (2.2.5) and (2.2.13)). Clearly, in order for this to be non-negative, the premium P must satisfy the condition

$$P \leq P_{\max} = \beta_1 x.$$

For instance, in the setting of the numerical example in Section 2.5.4, we get $P_{\max} = 30 \times 346 = 10\,380$, while the set premium is $P = 9\,000$.

Similarly, if the decision was taken at a stopping time τ, then, conditional on the wage X_τ, the maximum premium payable would be given by $P_{\max} = \beta_1 X_\tau$. Thus, the value of $P_{\max}$ goes up or down together with the current wage. However, in our setting the entry time is not decided in advance, being subject to the stopping rule based on observations over (X_t). As a result, the value function $v(x)$ $(x > 0)$ of the optimal stopping problem is always positive for any premium P, no matter how high (see formula (2.2.23)). Apparently, this is manufactured by selecting the threshold b^* high enough, which guarantees that, in the (rare) event of hitting it, the mean value of this strategy will be positive.

This may not be satisfactory from the standpoint of the Expected Utility Theory; however, there is no contradiction, because in its standard version this theory does not allow for an optional stopping. Adding utility terms to the gain function in the spirit of Sections 2.6.2 and 2.6.3 helps to amend the situation (see Remark 2.7.1), but the maximum premium payable still remains indeterminate.

The explanation of this paradox lies in the simple fact that the gain function in the optimal stopping problems considered so far does not include any losses. A simple way to account for such losses is to include *consumption* in the model. Namely, suppose for simplicity that the consumption rate c is constant; for instance, the net present value of consumption over time interval $[0, t]$ is given by

$$\int_0^t \mathrm{e}^{-rs} c \, \mathrm{d}s = \frac{c(1 - \mathrm{e}^{-rt})}{r}.$$

It is natural to assume that the wage X_t is sufficient to finance the consumption, so that $\mathrm{E}_x(X_t) = x\,\mathrm{e}^{\mu t} \geq c$ for all $t \geq 0$ (see (2.1.3)). In turn, for this to hold it suffices to assume that $X_0 = x \geq c$ and $\mu \geq 0$. Hence, we need to take into account consumption only over the unemployment spell $[\tau_0, \tau_0 + \tau_1]$, where the wage is replaced by the UI

benefit. The expected net present value of this consumption is given by

$$\gamma := \mathrm{E}\left(\mathrm{e}^{-r\tau_0}\int_0^{\tau_1}\mathrm{e}^{-rs}c\,\mathrm{d}s\right) = \mathrm{E}(\mathrm{e}^{-r\tau_0})\cdot\mathrm{E}\left(\frac{c(1-\mathrm{e}^{-r\tau_1})}{r}\right)$$
$$= \frac{\lambda_0 c}{(r+\lambda_0)(r+*\lambda_1)},$$

using independence of τ_0 and τ_1 and their exponential distributions (with parameters λ_0 and λ_1, respectively). Thus, our basic optimal stopping problem (2.2.14) is modified to

$$v^{\ddagger}(x) = \sup_{\tau}\mathrm{E}_x\left[\mathrm{e}^{-\tilde{r}\tau}g(X_\tau) - \gamma\right],$$

which has the same solution as before (see Section 2.2.3) but with the new value function $v^{\ddagger}(x) = v(x) - \gamma$, that is (cf. (2.2.22)),

$$v^{\ddagger}(x) = \begin{cases} (\beta_1 b^* - P)\left(\dfrac{x}{b^*}\right)^{q_*} - \gamma, & x \in [0, b^*], \\ \beta_1 x - P - \gamma, & x \in [b^*, \infty). \end{cases}$$

Now, the inequality $v^{\ddagger}(x) \geq 0$ can be easily solved for P to yield

$$P \leq P^{\ddagger}_{\max} := \begin{cases} \beta_1 b^* - \gamma\left(\dfrac{b^*}{x}\right)^{q_*}, & x \in [0, b^*], \\ \beta_1 x - \gamma, & x \in [b^*, \infty). \end{cases} \tag{2.7.22}$$

Note that $P^{\ddagger}_{\max}$ in (2.7.22) is a decreasing function of γ, but an increasing function of x. Thus, as could be expected, the maximum affordable premium gets lower with the increase of consumption, but becomes higher with the increase of the wage.

Remark 2.7.2. Of course, consumption can also be incorporated into the optimal stopping models involving utility (see Sections 2.6.2 and 2.6.3), but we omit technical details.

Chapter 3

Optimal Stopping in a Time-Dependent Model of Unemployment Insurance

In the previous chapter we adapted a guess-and-verify approach for solving an optimal stopping problem in a simple model of unemployment insurance. This chapter aims to formalize time inhomogeneous optimal stopping problem using the concepts in Chapter 1 and Chapter 2. For subsequent analysis, we need to prove a number of properties of the value function. In addition, we show the existence of an optimal boundary which is monotonic and continuous as a function of time. In that case, we will prove that the boundary is bounded, derive an integral equation that uniquely determines its shape and we use the latter to obtain a numerical estimate of the true boundary.

3.1 The model of unemployment insurance

Having discussed into details how to construct the UI model in Chapter 2, this section addresses similar arguments in the formulation of the problem. For a precise formulation of the problem, let us consider a filtered probability space $(\Omega, \mathcal{F}, \mathbb{F} = (\mathcal{F}_t)_{t\geqslant 0}, \mathrm{P})$ carrying a standard one-dimensional Brownian motion $B = (B_t)_{t\geq 0}$. Let us define the individual's wage process $X = (X_s)_{s\geq 0}$ by

$$\mathrm{d}X_s = \mu(s)X_s^{t,x}\mathrm{d}s + \sigma(s)X_s^{t,x}\mathrm{d}B_s \tag{3.1.1}$$

which solves the stochastic differential equation

$$X_s^{t,x} = X_t \exp\left(\int_t^s \sigma(u)\mathrm{d}B_u + \int_t^s \left(\mu(u) - \frac{\sigma^2(u)}{2}\right)\mathrm{d}u\right) \tag{3.1.2}$$

where $X_s^{t,x}$ is the wage of the individual at time s with the initial condition $X_t = x$ at time t. Also, $\mu(\cdot)$ and $\sigma(\cdot)$ are continuous and denote the drift and volatility rates, respectively. We further consider the problem of determining the payoff an individual under the scheme will receive when unemployment occurs given certain conditions. More precisely, the individual can enter the scheme at stopping time τ. Furthermore, we assume that the time of unemployment τ_0 and re-employment τ_1 follow an exponential distribution with time dependent parameters such that

$$\mathrm{P}_{t,x}(\tau_0 > t+s|\tau_0 > t) = \mathrm{e}^{-\int_0^s \lambda_0(t+u)\mathrm{d}u}, \qquad \mathrm{P}_{t,x}(\tau_1 > \tau_0 + s|\tau_0) = \mathrm{e}^{-\int_{\tau_0}^{\tau_0+s} \lambda_1(t+u)\mathrm{d}u}. \tag{3.1.3}$$

Then, the optimal payoff received by the insured when unemployment occurs is given by the value of an optimal stopping problem, which we are going to introduce in the next sections.

3.2 Setting the optimal stopping problem

In this section, we are interested in modeling the benefit to an employed individual who is under the unemployment insurance cover when unemployment occurs. To begin with, we calculate the expected future benefit to be received under this insurance contract which is given by

$$f(t+\tau_0, X_{t+\tau_0}^{t,x}) = X_{t+\tau_0}^{t,x}\,\mathrm{E}\left(\int_{t+\tau_0}^{t+\tau_1} \mathrm{e}^{-\int_{t+\tau_0}^s r(u)\mathrm{d}u} h(s)\,\mathrm{d}s \middle| \tau_0, X_{t+\tau_0}^{t,x}\right) = \beta(t+\tau_0)X_{t+\tau_0}^{t,x}, \tag{3.2.1}$$

where $r(u)$ is the risk-free rate and

$$\beta(t+\tau_0) := \int_{t+\tau_0}^{\infty} \mathrm{e}^{-\int_{t+\tau_0}^s \lambda_1(u)\mathrm{d}u} H(t)\,\mathrm{d}t, \qquad H(t) := \mathrm{e}^{-\int_{t+\tau_0}^s r(u)\mathrm{d}u} h(s). \tag{3.2.2}$$

Note for the expectation in formula (3.2.1) the expression inside integration involves discounting to the beginning of unemployment at time $t+\tau_0$.

Example 3.2.1. A specific example of the benefit schedule $h(s)$ may be as follows,

$$h(s) = \begin{cases} h_0, & t+\tau_0 \le s \le t+s_0+\tau_0, \\ h_0\,\mathrm{e}^{-\int_{t+s_0+\tau_0}^s \delta(u)\mathrm{d}u}, & s \ge t+s_0+\tau_0, \end{cases} \tag{3.2.3}$$

where $0 < h_0 \leq 1$ and $\delta(t) > 0$. Thus, the insured receives a certain fraction of their final wage (i.e., $h_0 X_{t+\tau_0}$) for a grace period $0 \leq s_0 \leq \infty$, after which the benefit is falling down exponentially with rate $\delta(t)$. This example is motivated by the declining unemployment compensation system in France [76].[1]

Let us consider the following assumption because the nature of the wage dynamics in (3.1.1) presents a further numerical challenge when solving the optimal stopping problem.

Assumption 3.2.1. Let us assume that $\mu(t) = \mu$ and $\sigma(t) = \sigma > 0$ so that (3.1.2) can be written as (2.1.2). For further computations, we also assume that λ_0 and $\beta \in C^1(\mathbb{R}_+)$ and $\delta(u) = \delta > 0$.

Having specified the schedule function, $\beta(t+\tau_0)$ in (3.2.1) is calculated from (3.2.2) as

$$\beta\left(t+\tau_0\right) = h_0\Bigg(\int_{t+\tau_0}^{t+\tau_0+s_0} \mathrm{e}^{-\int_{t+\tau_0}^{s}(r(u)+\lambda_1(u))\mathrm{d}u}\mathrm{d}s + \int_{t+\tau_0+s_0}^{\infty} \mathrm{e}^{-\int_{t+\tau_0}^{s}(r(u)+\lambda_1(u))\mathrm{d}u}\mathrm{e}^{-\int_{t+s_0+\tau_0}^{s}\delta\mathrm{d}u}\mathrm{d}s\Bigg). \quad (3.2.4)$$

Then, at $\tau_0 = 0$ (3.2.1) is written as

$$f(t, X_t^{t,x}) = X_t^{t,x}\beta(t). \quad (3.2.5)$$

where

$$\beta(t) = h_0\left(\int_{t}^{t+s_0} \mathrm{e}^{-\int_{t}^{s}(r(u)+\lambda_1(u))\mathrm{d}u}\mathrm{d}s + \int_{t+s_0}^{\infty} \mathrm{e}^{-\int_{t}^{s}(r(u)+\lambda_1(u))\mathrm{d}u}\mathrm{e}^{-\int_{t+s_0}^{s}\delta\mathrm{d}u}\mathrm{d}s\right). \quad (3.2.6)$$

Returning to the general case, if the contract is entered immediately (subject to the payment of premium P), then the expected benefit discounted to the entry time t is given by the *gain function*

$$g(t,x) := \mathrm{E}_{t,x}\left(\mathrm{e}^{-\int_{t}^{t+\tau_0} r(u)\mathrm{d}u}\beta\left(t+\tau_0\right)X_{t+\tau_0}\right) - P, \quad (3.2.7)$$

where x is the starting wage and the symbol $\mathrm{E}_{t,x}$ now indicates expectation conditional on $X_t = x$. Recall that the random time τ_0 is independent of the process (X_t) and has

[1] More specifically, according to the French UI system back in the 1990s (see [76, p. 8])

exponential distribution with parameter $\lambda_0(t)$. The expectation in (3.2.7) is computed as follows,

$$\begin{aligned}
&\mathrm{E}_{t,x}\left(\mathrm{e}^{-\int_t^{t+\tau_0} r(u)\mathrm{d}u}\beta(t+\tau_0)X_{t+\tau_0}\right)\\
&\quad=\mathrm{E}_{t,x}\left(\mathrm{E}_{t,x}\left(\mathrm{e}^{-\int_t^{t+\tau_0} r(u)\mathrm{d}u}\beta(t+\tau_0)X_{t+\tau_0}|\mathcal{F}_\infty^X\right)\right)\\
&\quad=\mathrm{E}_{t,x}\left(\int_0^\infty \mathrm{e}^{-\int_t^{t+s} r(u)\mathrm{d}u}\beta(t+s)\lambda_0(t+s)X_{t+s}\mathrm{e}^{-\int_t^{t+s}\lambda_0(u)\mathrm{d}u}\mathrm{d}s\right). \qquad (3.2.8)
\end{aligned}$$

We apply Fubini's theorem (see A.1.1) to derive

$$\begin{aligned}
&\mathrm{E}_{t,x}\left(\mathrm{e}^{-\int_t^{t+\tau_0} r(u)\mathrm{d}u}\beta(t+\tau_0)X_{t+\tau_0}\right)\\
&\qquad=\int_0^\infty \mathrm{e}^{-\int_t^{t+s}(r(u)+\lambda_0(u))\mathrm{d}u}\beta(t+s)\lambda_0(t+s)\mathrm{E}_{t,x}\left(X_{t+s}\right)\mathrm{d}s \qquad (3.2.9)
\end{aligned}$$

Using explicit formula in (3.1.2) for $\mathrm{E}_{t,x}\left(X_{t+s}\right)$ we obtain

$$\begin{aligned}
&\mathrm{E}_{t,x}\left(\mathrm{e}^{-\int_t^{t+\tau_0} r(u)\mathrm{d}u}\beta(t+\tau_0)X_{t+\tau_0}\right)\\
&\qquad=\int_0^\infty \mathrm{e}^{-\int_t^{t+s}(r(u)+\lambda_0(u)-\mu)\mathrm{d}u}x\beta(t+s)\lambda_0(t+s)\mathrm{d}s\\
&\qquad=\int_t^\infty \mathrm{e}^{-\int_t^{s}(r(u)+\lambda_0(u)-\mu)\mathrm{d}u}x\beta(s)\lambda_0(s)\mathrm{d}s\\
&\qquad=x\beta_1(t) \qquad (3.2.10)
\end{aligned}$$

where

$$\beta_1(t):=\int_t^\infty \mathrm{e}^{-\int_t^s(\tilde{r}(u)-\mu)\mathrm{d}u}\beta(s)\lambda_0(s)\mathrm{d}s. \qquad (3.2.11)$$

Thus, substituting (3.2.10) into (3.2.7) and denoting

$$\tilde{r}(u):=r(u)+\lambda_0(u), \qquad (3.2.12)$$

the gain function is represented explicitly as

$$g(t,x)=\tilde{g}(t,x)-P=x\beta_1(t)-P. \qquad (3.2.13)$$

Of course, the computation in (3.2.10) is only meaningful as long as

$$\limsup_{s\to\infty}\frac{M(s)}{\tilde{R}(s)}<1 \qquad (3.2.14)$$

where $M(t)=\int_t^s \mu\mathrm{d}u$ and $\tilde{R}(u)=\int_t^s \tilde{r}(u)\mathrm{d}u$.

Assumption 3.2.2. In what follows, we always assume that the condition (3.2.14) is satisfied and $\tilde{r}(u) > r(u) > 0$. In that case, we further assume that $\tilde{r}(u) \geq \mu$ for all u.

Remark 3.2.1. In real life applications, the wage growth rate μ is rather small (but may be either positive or negative). It is unlikely to exceed the inflation rate $r(u)$, but even if it does, then it is hardly possible economically that it is greater than the combined inflation–unemployment rate $\tilde{r}(u) = r(u) + \lambda_0(u)$. Thus, the condition (3.2.14) is absolutely realistic.

The *expected net present value (eNPV)* of the total gain as a function of the initial wage x, using the expression (3.2.13), is given by

$$\mathrm{eNPV}(t, x; t+\tau) := \mathrm{E}_{t,x}\left[\mathrm{e}^{-\int_t^{t+\tau} r(u)\mathrm{d}u}\left(\mathrm{e}^{-\int_{t+\tau}^{t+\tau_0}\tilde{r}(u)\mathrm{d}u}\beta\,(t+\tau_0)\,X_{t+\tau_0} - P\right)\mathbb{1}_{\{\tau<\tau_0\}}\right], \tag{3.2.15}$$

where τ is the entry time an individual joins the UI scheme and a stopping time of $(\mathcal{F}_t)_{t\geq 0}$. The expectation on the right now also includes averaging with respect to $t+\tau$, which is a functional of the path (X_t). Note that the indicator function under the expectation specifies that the entry time $t+\tau$ must occur prior to $t+\tau_0$, for otherwise there will be no gain.

Lemma 3.2.1. *The expected net present value defined by formula* (3.2.15) *can be expressed in the form*

$$\mathrm{eNPV}(t, x; t+\tau) = \mathrm{E}_{t,x}\left[\mathrm{e}^{-\int_t^{t+\tau}\tilde{r}(u)\mathrm{d}u} g(t+\tau, X_{t+\tau})\right], \tag{3.2.16}$$

where the function $g(\cdot)$ is defined in (3.2.7) *and $\tilde{r}(u) = r(u) + \lambda_0(u)$ (see* (3.2.11)*).*

Proof. Since the distribution of τ_0 is exponential, (and hence memoryless), the excess time $\tilde{\tau}_0 := \tau_0 - \tau$ conditioned on $\{\tau < \tau_0\}$ is again exponentially distributed. Thus, from [120, §II.7, Property G*, p. 216]) it is possible to say that conditioning on $(t+\tau, X_{t+\tau})$, together with the (strong) Markov property of the process (X_t), we get from (3.2.15) that

$$
\begin{aligned}
&\mathrm{eNPV}(x;t+\tau)\\
=&\mathrm{E}_{t,x}\Bigg[\mathrm{E}_{t,x}\Bigg(\mathrm{e}^{-\int_t^{t+\tau} r(u)\mathrm{d}u}\Big(\mathrm{e}^{-\int_{t+\tau}^{t+\tau+\tilde{\tau}_0} r(u)\mathrm{d}u}\beta(t+\tau+\tilde{\tau}_0)X_{t+\tau+\tilde{\tau}_0}-P\Big)\\
&\qquad\cdot\mathbb{1}_{\{\tau_0>\tau\}}\Big|\,t+\tau,X_{t+\tau}\Bigg)\Bigg]\\
=&\mathrm{E}_{t,x}\Bigg[\mathrm{e}^{-\int_t^{t+\tau} r(u)\mathrm{d}u}\mathrm{E}_{t,x}\Bigg(\mathrm{e}^{-\int_{t+\tau}^{t+\tau+\tilde{\tau}_0} r(u)\mathrm{d}u}\beta(t+\tau+\tilde{\tau}_0)X_{t+\tau+\tilde{\tau}_0}-P\Big|\,t+\tau,X_{t+\tau}\Bigg)\\
&\qquad\cdot\mathrm{E}_{t,x}\Big(\mathbb{1}_{\{\tau_0>\tau\}}\big|\,t+\tau,X_{t+\tau}\Big)\Bigg].
\end{aligned}
\tag{3.2.17}
$$

Equation (3.2.17) can further be written as

$$
\begin{aligned}
&\mathrm{eNPV}(x;t+\tau)\\
=&\mathrm{E}_{t,x}\Bigg[\mathrm{e}^{-\int_t^{t+\tau} r(u)\mathrm{d}u}\mathrm{E}_{t+\tau,X_{t+\tau}}\Bigg(\mathrm{e}^{-\int_0^{\tilde{\tau}_0} r(u)\mathrm{d}u}\beta(\tilde{\tau}_0)\widetilde{X}_{\tilde{\tau}_0}-P\Bigg)\\
&\qquad\cdot\mathrm{P}_{t,x}\Bigg(\tau_0>\tau\Big|\,t+\tau\Bigg)\Bigg].
\end{aligned}
\tag{3.2.18}
$$

By virtue of the strong Markov property (see [107] for detailed explanation), we translate to the present wage dynamics such that $\widetilde{X}_t := X_{\tau+t}$ $(t \geq 0)$ is a shifted wage process starting at $\widetilde{X}_0 = X_\tau$. Substituting $\mathrm{P}_x(\tau_0 > \tau | t+\tau) = \mathrm{e}^{-\int_t^{t+\tau}\lambda_0(u)\mathrm{d}u}$ and (3.2.7), formula (3.2.18) is reduced to (3.2.16). □

3.2.1 The optimal stopping problem

To summarize, the identification of the optimal entry time $\tau = \tau^*$, in the sense of maximizing the expected net present value $\mathrm{eNPV}(x;t+\tau)$ as a function of the strategy τ (see (3.2.16)), is reduced to solving the following *optimal stopping problem*,

$$
v(t,x) = \sup_{\tau}\mathrm{E}_{t,x}\big[\mathrm{e}^{-\int_t^{t+\tau}\tilde{r}(u)\mathrm{d}u}g(t+\tau,X_{t+\tau})\big],
\tag{3.2.19}
$$

where the function $g(t,x)$ is given by (3.2.13) and the supremum is taken over the class of all $(\mathcal{F}_t)_{t\geq 0}$ stopping times τ. The supremum $v(t,x)$ in (3.2.19) is called the *value function* of the optimal stopping problem.

3.2.2 Free-boundary problem

Next, based on the shift property of Brownian motion and thanks to Assumption 3.2.1 also we notice that $\mathrm{Law}(X_\cdot^x) = \mathrm{Law}(X_{t+\cdot}^{t,x})$. Let us look more closely at the nature of the value function $v(t,x)$ that we are trying to identify. Observe that by picking $\tau = 0$ in (3.2.19) yields the lower estimate

$$v(t,x) \geq g(t,x). \tag{3.2.20}$$

Clearly, if $v(t,x) > g(t,x)$ then we have not yet achieved the maximum payoff available, so we should continue to wait. On the other hand, if $v(t,x) = g(t,x)$ then the maximum has been attained and we should stop. This motivates the definition of the two regions, C (*continuation*) and S (*stopping*),

$$C := \{(t,x) \in \mathbb{R}_+ \times \mathbb{R}_+ \colon v(t,x) > g(t,x)\}, \quad S := \{(t,x) \in \mathbb{R}_+ \times \mathbb{R}_+ \colon v(t,x) = g(t,x)\}. \tag{3.2.21}$$

From the general optimal stopping theory in [107, §II.2.2], the smallest optimal stopping time is

$$\tau^* = \inf\{s \in [0,\infty) \colon (t+s, X_{t+s}) \in S\}. \tag{3.2.22}$$

The key part of our work is to find the shape of the set S.

Recall (see the proof of Lemma 3.3.1(i)) that a zero value of the stopping problem (3.2.19) is achieved by simply using the strategy $\tau \equiv \infty$, that is, by never joining the scheme. Thus, if the initial wage $X_t = x$ is small (e.g., such that $g(t,x) = \beta_1(t)x - P < 0$) then, in order to secure a positive payoff, we should wait for a sufficiently high wage X_t. This suggests that the stopping rule (3.2.22) is reduced to the first hitting time for a certain set in $\mathbb{R}_+ \times \mathbb{R}_+$. Furthermore, we expect the simplest situation whereby the regions C and S are determined by a *threshold function* $b(t)$,

$$C := \{(t,x) \in \mathbb{R} \times \mathbb{R} \colon x \in [0, b(t))\}, \quad S := \{(t,x) \in \mathbb{R} \times \mathbb{R} \colon x \in [b(t), \infty)\}. \tag{3.2.23}$$

In other words, the conjectural hitting boundary that determines the stopping rule depends on time. This conjecture will be fully demonstrated in the next section.

Remark 3.2.2. The geometric Brownian motion determined by the stochastic differential equation (3.1.1) is a diffusion process with the infinitesimal generator

$$L := \mu x \frac{\mathrm{d}}{\mathrm{d}x} + \frac{1}{2}\sigma^2 x^2 \frac{\mathrm{d}^2}{\mathrm{d}x^2}. \tag{3.2.24}$$

On the boundary $x = b(t)$ of the set C, due to the stopping rule (3.2.22) we have $v(t,x) = g(t,x)$. Moreover, we must satisfy the *smooth fit principle* (see [107, §9.1]). In view of this, the standard Markovian arguments (see, e.g., [107, Ch. III]) indicate that the value function from (3.1.1) should solve the following free-boundary problem:

$$\begin{cases} (\partial_t + L - \tilde{r}(t))\, v(t,x) = 0, & \text{in } C, \\ v(t,x) = g(t,x) = \beta_1(t)x - P, & x = b(t), \\ v_x(t,x) = g_x(t,x) = \beta_1(t), & x = b(t), \\ v_t(t,x) = g_t(t,x) = \partial_t\beta_1(t)x, & x = b(t), \end{cases} \tag{3.2.25}$$

where $v_x(t,x) = \partial_x v(t,x)$, $v_t(t,x) = \partial_t v(t,x)$, $g_x(t,x) = \partial_x g(t,x)$ and $g_t(t,x) = \partial_t g(t,x)$. We will now proceed to rigorously prove that (3.2.25) indeed holds.

Lemma 3.2.2. *Let $\tilde{g}(t,x) \coloneqq x\beta_1(t)$. We have*

$$\left(L - \tilde{r}(t) + \frac{\mathrm{d}}{\mathrm{d}t}\right)\tilde{g}(t,x) = -\lambda_0(t)x\beta(t) = -\lambda_0(t)f(t,x) \tag{3.2.26}$$

Proof. Note that $\tilde{g}(t,x) \coloneqq x\beta_1(t) := \int_t^\infty \mathrm{e}^{-\int_t^s(\tilde{r}(u)-\mu)\mathrm{d}u}\beta(s)\lambda_0(s)\mathrm{d}s$ from (3.2.10) and (3.2.13). To prove (3.2.26), we first notice

$$\begin{aligned} L\tilde{g}(t,x) &= \mu x\frac{\mathrm{d}}{\mathrm{d}x}\tilde{g}(t,x) + \frac{1}{2}\sigma^2x^2\frac{\mathrm{d}^2}{\mathrm{d}x^2}\tilde{g}(t,x) \\ &= \mu x\left(\int_t^\infty \mathrm{e}^{-\int_t^s(\tilde{r}(u)-\mu+\lambda_0(u))\mathrm{d}u}\beta(s)\lambda_0(s)\mathrm{d}s\right). \end{aligned} \tag{3.2.27}$$

We also apply Leibniz integral rule to derive

$$\begin{aligned} \frac{\mathrm{d}}{\mathrm{d}t}\tilde{g}(t,x) = \left(\tilde{r}(u) - \mu + \lambda_0(u)\right)\int_t^\infty \mathrm{e}^{-\int_t^s(\tilde{r}(u)-\mu+\lambda_0(u))\mathrm{d}u}\beta(s)\lambda_0(s)\mathrm{d}s \\ - x\beta(t)\lambda_0(t). \end{aligned} \tag{3.2.28}$$

We then combine (3.2.27) and (3.2.28) along with (3.2.11) to obtain (3.2.26). □

Making use of the above argument, the optimal stopping problem in (3.2.19) is presented in another way in order to examine the scope of the optimal stopping problem in a clearer manner.

Lemma 3.2.3. *The optimal stopping problem (3.2.19) can be rewritten as*

$$v(t,x) := \sup_\tau \mathrm{E}_{t,x}\left(\int_t^{t+\tau} \mathrm{e}^{-\int_t^s \tilde{r}(u)\mathrm{d}u}\left(\tilde{r}(s)P - \lambda_0(s)f(s,X_s)\mathrm{d}s\right)\right) + \tilde{g}(t,x) - P \tag{3.2.29}$$

Proof. We apply Itô formula to $\tilde{g}(t+\tau, X_{t+\tau}) - P$ and take expectation to derive

$$\begin{aligned}
&\mathrm{E}_{t,x}\left(\mathrm{e}^{-\int_t^s \tilde{r}(u)\mathrm{d}u}\left(\tilde{g}(t+\tau, X_{t+\tau}) - P\right)\right) \\
&\quad = \mathrm{E}_{t,x}\left(\int_t^{t+\tau} \mathrm{e}^{-\int_t^s \tilde{r}(u)\mathrm{d}u}\left(L - \tilde{r}(s) + \frac{\mathrm{d}}{\mathrm{d}s}\right)\tilde{g}(s, X_s)\mathrm{d}s\right) \\
&\qquad\qquad + \mathrm{E}_{t,x}\left(\int_t^{t+\tau} \mathrm{e}^{-\int_t^s \tilde{r}(u)\mathrm{d}u}\tilde{r}(s)P\mathrm{d}s\right) + \tilde{g}(t,x) - P \\
&\quad = \tilde{g}(t,x) - P + \mathrm{E}_{t,x}\left(\int_t^{t+\tau} \mathrm{e}^{-\int_t^s \tilde{r}(u)\mathrm{d}u}\Big(-\lambda_0 f(s, X_s)\tilde{r}(s)P\Big)\mathrm{d}s\right) \\
&\qquad\qquad + \mathrm{E}_{t,x}\left(\int_t^{t+\tau} \mathrm{e}^{-\int_t^s \tilde{r}(u)\mathrm{d}u}\tilde{r}(s)P\mathrm{d}s\right). \qquad (3.2.30)
\end{aligned}$$

From (3.2.26), it is observed that $\left(L - \tilde{r}(s) + \frac{\mathrm{d}}{\mathrm{d}s}\right)\tilde{g}(s, X_s) = -\lambda_0 f(s, X_s)$. The supremum is taken over the class of all admissible τ on (3.2.30) to derive (3.2.29). □

In order to determine the structure of the optimal stopping time (i.e. the shape of the sets C and D) we will first examine basic properties of the value function.

3.3 Properties of the value function

In this section, we prove sufficiently many properties of the value function to enable us to prove the existence of an optimal boundary and that the optimal time to enter the UI scheme is when an individual's wage hits the boundary.

3.3.1 A priori properties of the value function $v(t,x)$

The next lemma shows that the optimal stopping problem given in (3.2.19) is well posed.

Lemma 3.3.1. *The value function $(t,x) \mapsto v(t,x)$ of the optimal stopping problem (3.1.1) has the following properties: for all $t \in [0,T]$, then*

(i) *$v(t,0) = 0$ and, moreover, $v(t,x) \geq 0$ for all $x \geq 0$;*

(ii) *$v(t,x) < \infty$ for all $x \geq 0$.*

Proof. (i) Based on assumption 3.2.1 where $r(t) \geq r_0 > 0$, we fix t and let $X_t \equiv 0$ ($\mathrm{P}_{t,0}$-a.s.) and the stopping problem (3.1.1) is reduced to

$$v(t,0) = \sup_\tau \mathrm{E}_{t,0}\big[-P\,\mathrm{e}^{-\int_t^{t+\tau}\tilde{r}(u)\mathrm{d}u}\big] = -P \inf_\tau \mathrm{E}_{t,0}\big[\mathrm{e}^{-\int_t^{t+\tau}\tilde{r}(u)\mathrm{d}u}\big] = 0, \qquad (3.3.1)$$

which has the obvious solution $\tau = \infty$ ($\mathrm{P}_{t,0}$-a.s.), with the corresponding supremum value $v(t,0) = 0$. Furthermore, by considering $\tau = \infty$ ($\mathrm{P}_{t,x}$-a.s.) it readily follows from (3.1.1) that $v(t,x) \geq 0$ for all $x \geq 0$ for fixed t.

(ii) Recalling that

$$\begin{aligned} v(t,x) &= \sup_{\tau} \mathrm{E}\left(\mathrm{e}^{-\int_0^\tau \tilde{r}(t+s)\mathrm{d}s} g\left(t+\tau, X_\tau^x\right)\right) \\ &= \sup_{\tau} \mathrm{E}\left(\mathrm{e}^{-\int_0^\tau \tilde{r}(t+s)\mathrm{d}s} \left(\beta_1(t+\tau)X_\tau^x - P\right)\right). \end{aligned} \tag{3.3.2}$$

From (3.2.11), it can be seen that $t \to \beta_1(t+\tau)$ is decreasing so that $\beta_1(t+\tau) \leq \beta_1(t)$ then

$$\begin{aligned} v(t,x) &\leq \sup_{\tau} \mathrm{E}\left(\mathrm{e}^{-\int_0^\tau \tilde{r}(t+s)\mathrm{d}s} \beta_1(t+\tau)X_\tau^x\right) \\ &\leq \sup_{\tau} \mathrm{E}\left(\mathrm{e}^{-\int_0^\tau \tilde{r}(t+s)\mathrm{d}s} \beta_1(t)X_\tau^x\right). \end{aligned} \tag{3.3.3}$$

From Assumption 3.2.2 it follows that the process $\mathrm{e}^{-\int_t^{t+s} \tilde{r}(u)\mathrm{d}u} X_{t+s}$ is a supermartingale for $s \in (0,\infty)$ based on Assumption 3.2.2. Also, using assumption 3.2.1 and (3.1.2) we have that

$$\begin{aligned} \mathrm{E}\left[\mathrm{e}^{-\int_t^{t+s} \tilde{r}(u)\mathrm{d}u} X_{t+s} \,\middle|\, \mathcal{F}_t\right] &= \mathrm{e}^{-\int_t^{t+s} \tilde{r}(u)\mathrm{d}u} x \mathrm{E}\left[\mathrm{e}^{\sigma(B_{t+s}-B_t)+(\mu-\frac{1}{2}\sigma^2)s} \middle| \mathcal{F}_t\right] \\ &= x\mathrm{e}^{-\int_t^{t+u} \tilde{r}(u)\mathrm{d}u+\mu s} \mathrm{E}\left[\mathrm{e}^{\sigma(B_{t+s}-B_t)-\frac{1}{2}\sigma^2 s} \middle| \mathcal{F}_t\right] \\ &\leq x. \end{aligned} \tag{3.3.4}$$

In particular,

$$\mathrm{E}\left[\mathrm{e}^{-\int_t^{t+s} \tilde{r}(u)\mathrm{d}u} X_{t+s}\right] \leq \mathrm{E}(X_t) = x.$$

Hence, by Doob's optional sampling theorem (see, e.g., [138, Theorem 6.1(a), p. 87, and Theorem 8.10, p. 131]), for any stopping time τ and all $n \in \mathbb{N}$, we have

$$\mathrm{E}\left[\mathrm{e}^{-\int_t^{(t+\tau)\wedge(t+n)} \tilde{r}(u)\mathrm{d}u} X_{(t+\tau)\wedge(t+n)}\right] \leq \mathrm{E}(X_t) = x.$$

Furthermore, noting that

$$\lim_{n\to\infty} \mathrm{e}^{-\int_t^{(t+\tau)\wedge(t+n)} \tilde{r}(u)\mathrm{d}u} X_{(t+\tau)\wedge(t+n)} = \mathrm{e}^{-\int_t^{t+\tau} \tilde{r}(u)\mathrm{d}u} X_{t+\tau} \quad (\mathrm{P}_x\text{-a.s.}),$$

by Fatou's lemma (see, e.g., [120, §II.6, Theorem 2(a), p. 187]) we conclude that

$$\mathrm{E}\left[\mathrm{e}^{-\int_t^{t+\tau} \tilde{r}(u)\mathrm{d}u} X_{t+\tau}\right] \leq x,$$

and it readily follows that the supremum in (3.2.19) is finite. □

3.3.2 Time monotonicity of the value function

Next, we prove time monotonicity of the value function relative to the stopping payoff. This property addresses the time dependence of the value function and the results will later be used to study the time dependence of the optimal boundary.

$$u(t,x) \coloneqq v(t,x) - g(t,x) = \sup_{\tau} \mathrm{E}\left(\int_t^{t+\tau} \mathrm{e}^{-\int_t^s \tilde{r}(u)\mathrm{d}u} \left(\tilde{r}(s)P - \lambda_0(s) f(s, X_s)\mathrm{d}s \right) \right). \tag{3.3.5}$$

It turns out that the following steps are helpful in deriving assumptions to make certain conclusions more elegant.

Proposition 3.3.2. (i) *If $t \mapsto \tilde{r}(t)$ is increasing and $t \mapsto \lambda_0(t)\beta(t)$ is decreasing, then $t \mapsto u(t,x)$ is increasing.*

(ii) *If $t \mapsto \tilde{r}(t)$ is decreasing and $t \mapsto \lambda_0(t)\beta(t)$ is increasing, then $t \mapsto u(t,x)$ is decreasing.*

Proof. (i) Fix $t_1 < t_2$ and pick $\tau_* = \tau_*(t_1,x) = \tau_1$ as the optimal time for $u(t_1,x)$. We know from assumption 3.2.1 that $X^{t,x}_{t+s} = X_s$ due to $\mu(t) = \mu$ and $\sigma(t) = \sigma$. Then τ_1 is suboptimal for $u(t_2,x)$ and we get

$$\begin{aligned} &u(t_1,x) - u(t_2,x) \\ &\quad \le \mathrm{E}\left(\int_0^{\tau_1} \mathrm{e}^{-\int_0^s \tilde{r}(t_1+u)\mathrm{d}u} \left(\tilde{r}(t_1+s)P - \lambda_0(t_1+s) f(t_1+s, X^{t_1,x}_{t_1+s})\mathrm{d}s \right) \right) \\ &\qquad - \mathrm{E}\left(\int_0^{\tau_1} \mathrm{e}^{-\int_0^s \tilde{r}(t_2+u)\mathrm{d}u} \left(\tilde{r}(t_2+s)P - \lambda_0(t_2+s) f(t_2+s, X^{t_2,x}_{t_2+s})\mathrm{d}s \right) \right). \end{aligned} \tag{3.3.6}$$

Note that $\int_0^{\tau_1} \mathrm{e}^{-\int_0^s \tilde{r}(t_1+u)\mathrm{d}u} \tilde{r}(t_1+s)\mathrm{d}s = 1 - \mathrm{e}^{-\int_0^{\tau_1} \tilde{r}(t_1+u)\mathrm{d}u}$, so that (3.3.6) can be written as

$$\begin{aligned} u(t_1,x) - u(t_2,x) \le \mathrm{E}&\left(P \left(\mathrm{e}^{-\int_0^{\tau_1} \tilde{r}(t_2+u)\mathrm{d}u} - \mathrm{e}^{-\int_0^{\tau_1} \tilde{r}(t_1+u)\mathrm{d}u} \right) \right) \\ &+ \mathrm{E}\left(\int_0^{\tau_1} \mathrm{e}^{-\int_0^s \tilde{r}(t_2+u)\mathrm{d}u} \lambda_0(t_2+s) f(t_2+s, X^{t_2,x}_{t_2+s})\mathrm{d}s \right) \\ &- \mathrm{E}\left(\int_0^{\tau_1} \mathrm{e}^{-\int_0^s \tilde{r}(t_1+u)\mathrm{d}u} \lambda_0(t_1+s) f(t_1+s, X^{t_1,x}_{t_1+s})\mathrm{d}s \right). \end{aligned} \tag{3.3.7}$$

Also, if $t \mapsto \tilde{r}(t)$ is increasing then

$$\begin{aligned}
&u(t_1,x) - u(t_2,x) \\
&\quad \leq \mathrm{E}\left(P \cdot 0 + \int_0^{\tau_1} \mathrm{e}^{-\int_0^s \tilde{r}(t_2+u)\mathrm{d}u} \lambda_0(t_2+s) f(t_2+s, X_s^x)\mathrm{d}s\right) \\
&\qquad\quad - \mathrm{E}\left(\int_t^{\tau_1} \mathrm{e}^{-\int_0^s \tilde{r}(t_1+u)\mathrm{d}u} \lambda_0(t_1+s) f(t_1+s, X_s^x)\mathrm{d}s\right) \\
&\quad \leq \mathrm{E}\left(\int_0^{\tau_1} \mathrm{e}^{-\int_0^s \tilde{r}(t_1+u)\mathrm{d}u} \Big(\lambda_0(t_2+s) f(t_2+s, X_s^x) - \lambda_0(t_1+s) f(t_1+s, X_s^x)\Big)\mathrm{d}s\right).
\end{aligned} \tag{3.3.8}$$

We see from (3.2.5) that $f(t+s, X_s) = X_s \beta(t+s)$. If $t \mapsto \lambda_0(t)\beta(t)$ is decreasing then $t \mapsto u(t,x)$ is increasing.

(ii) Fix $t_2 > t_1$ and pick $\tau_* = \tau_*(t_2, x) = \tau_2$ as the optimal time for $u(t_2, x)$. Since τ_2 is sub-optimal for $u(t,x)$ we have

$$\begin{aligned}
&u(t_1,x) - u(t_2,x) \\
&\quad \geq \mathrm{E}\left(\int_0^{\tau_2} \mathrm{e}^{-\int_0^s \tilde{r}(t_1+u)\mathrm{d}u} \left(\tilde{r}(t_1+s)P - \lambda_0(t_1+s) f(t_1+s, X_{t_1+s}^{t_1,x})\mathrm{d}s\right)\right) \\
&\qquad\quad - \mathrm{E}\left(\int_0^{\tau_2} \mathrm{e}^{-\int_0^s \tilde{r}(t_2+u)\mathrm{d}u} \left(\tilde{r}(t_2+s)P - \lambda_0(t_2+s) f(t_2+s, X_{t_2+s}^{t_2,x})\mathrm{d}s\right)\right) \\
&\quad \geq \mathrm{E}\left(P\left(\mathrm{e}^{-\int_0^{\tau_2} \tilde{r}(t_2+u)\mathrm{d}u} - \mathrm{e}^{-\int_0^{\tau_2} \tilde{r}(t_1+u)\mathrm{d}u}\right)\right) \\
&\qquad\quad + \mathrm{E}\left(\int_0^{\tau_2} \mathrm{e}^{-\int_0^s \tilde{r}(t_2+u)\mathrm{d}u} \lambda_0(t_2+s) f(t_2+s, X_{t_2+s}^{t_2,x})\mathrm{d}s\right) \\
&\qquad\quad - \mathrm{E}\left(\int_0^{\tau_2} \mathrm{e}^{-\int_0^s \tilde{r}(t_1+u)\mathrm{d}u} \lambda_0(t_1+s) f(t_1+s, X_{t_1+s}^{t_1,x})\mathrm{d}s\right).
\end{aligned} \tag{3.3.9}$$

If $t \mapsto \tilde{r}(t)$ is decreasing then

$$\begin{aligned}
&u(t_1,x) - u(t_2,x) \geq \mathrm{E}(P \cdot 0) \\
&\quad + \mathrm{E}\left(\int_0^{\tau_2} \mathrm{e}^{-\int_0^s \tilde{r}(t_1+u)\mathrm{d}u} \Big(\lambda_0(t_2+s) f(t_2+s, X_s^x) - \lambda_0(t_1+s) f(t_1+s, X_s^x)\Big)\mathrm{d}s\right).
\end{aligned} \tag{3.3.10}$$

Again, if $t \mapsto \lambda_0(t)\beta(t)$ is increasing then $t \mapsto u(t,x)$ is decreasing. □

The proposition above has a clear economic interpretation which is explained in detail in Section 3.6.2. In the next corollary, we provide simple sufficient conditions for the monotonicity of $t \mapsto u(t,x)$, in terms of conditions on the model parameters.

Corollary 3.3.3. *The map $t \mapsto u(t,x)$ is increasing whenever $\frac{\lambda_0'(t)}{\lambda_0(t)} \leq \frac{1}{\gamma+\delta}$ and $t \mapsto u(t,x)$ is decreasing whenever $\frac{\lambda_0'(t)}{\lambda_0(t)} \geq \frac{1}{\gamma+\delta}$.*

Proof. This corollary is proved using Proposition 3.3.2. (i) $t \mapsto \lambda_0(t)\beta(t)$ is decreasing if and only if

$$\lambda_0'(t)\beta(t) + \beta'(t)\lambda_0(t) \leq 0 \iff \frac{\lambda_0'(t)}{\lambda_0(t)} \leq -\frac{\beta'(t)}{\beta(t)}. \tag{3.3.11}$$

From Assumption 3.2.1 we have that

$$\beta(t) = h_0 \left(\int_t^{t+\gamma} \mathrm{e}^{-\int_t^s \tilde{r}(u)\mathrm{d}u} \mathrm{d}s + \int_{t+\gamma}^{\infty} \mathrm{e}^{-\int_t^s \tilde{r}(u)\mathrm{d}u} \mathrm{e}^{-\int_{t+\gamma}^s \delta \mathrm{d}u} \mathrm{d}s \right). \tag{3.3.12}$$

Given that $\mathrm{e}^{-\int_t^s \tilde{r}(u)\mathrm{d}u} \leq 1$ then

$$\beta(t) \leq h_0 \left(\int_t^{t+\gamma} 1 \mathrm{d}s + \int_{t+\gamma}^{\infty} \mathrm{e}^{-\int_{t+\gamma}^s \delta \mathrm{d}u} \mathrm{d}s \right) = h_0 \left(\gamma + \frac{1}{\delta} \right). \tag{3.3.13}$$

Thus, we have that

$$\frac{h_0}{\beta(t)} \geq \frac{1}{\gamma + \frac{1}{\delta}}. \tag{3.3.14}$$

Also,

$$\begin{aligned} \beta'(t) = h_0 &\left(\mathrm{e}^{-\int_t^{t+\gamma} \tilde{r}(u)\mathrm{d}u} - \mathrm{e}^{\int_t^t \tilde{r}(u)\mathrm{d}u} + \mathrm{e}^{\int_t^{\infty} \tilde{r}(u)\mathrm{d}u} \mathrm{e}^{-\delta(\infty - t - s_0)} \right) \\ &- h_0 \left(\mathrm{e}^{-\int_t^{t+\gamma} \tilde{r}(u)\mathrm{d}u} \mathrm{e}^{-\delta(t+s_0-t-s_0)} \right) \\ = -h_0. \end{aligned} \tag{3.3.15}$$

Using (3.3.15), (3.3.11) can further be written as

$$\frac{\lambda_0'(t)}{\lambda_0(t)} \leq \frac{h_0}{\beta(t)}. \tag{3.3.16}$$

Thus, (3.3.14) and (3.3.16) imply the first claim.

(ii) On the other hand, $t \mapsto \lambda_0(t)\beta(t)$ is increasing if and only if

$$\lambda_0'(t)\beta(t) + \beta'(t)\lambda_0(t) \geq 0 \iff \frac{\lambda_0'(t)}{\lambda_0(t)} \geq -\frac{\beta'(t)}{\beta(t)}. \tag{3.3.17}$$

We repeat the computation steps in (i) and derive

$$\beta(t) \geq h_0 \left(\gamma + \frac{1}{\delta} \right) \implies \frac{h_0}{\beta(t)} \leq \frac{1}{\gamma + \frac{1}{\delta}}. \tag{3.3.18}$$

Then (3.3.17) holds if

$$\frac{\lambda_0'(t)}{\lambda_0(t)} \geq \frac{h_0}{\beta(t)}. \tag{3.3.19}$$

Hence combining (3.3.18) and (3.3.19), it is sufficient to have that $\frac{\lambda_0'(t)}{\lambda_0(t)} \geq \frac{1}{\gamma+\delta}$. □

From the arguments above, we have sufficiently many conditions to show that the boundary is time dependent.

3.3.3 Continuity of the value function

The proof of the value function's continuity establishes the existence of the optimal boundary. Thus, we proceed by proving that $(t,x) \mapsto u(t,x)$ is continuous on $\mathbb{R}^2_+$ in the subsequent arguments.

Proposition 3.3.4. *The map $x \mapsto u(t,x)$ is decreasing.*

Proof. Let $t \in [0,t)$ and fix $y \geq x$ for all $x, y \in \mathbb{R}$ then

$$
\begin{aligned}
&u(t,y) - u(t,x) \\
&\quad = \sup_{\tau} \mathrm{E}\left(\int_0^{\tau} \mathrm{e}^{-\int_0^s \tilde{r}(t+u)\mathrm{d}u} \left(\tilde{r}(t+s)P - \lambda_0(t+s) f(t+s, X^{t,y}_{t+s}) \, \mathrm{d}s \right) \right) \\
&\qquad - \sup_{\theta} \mathrm{E}\left(\int_0^{\theta} \mathrm{e}^{-\int_0^s \tilde{r}(t+u)\mathrm{d}u} \left(\tilde{r}(t+s)P - \lambda_0(t+s) f(t+s, X^{t,x}_{t+s}) \, \mathrm{d}s \right) \right) \\
&\quad \leq \sup_{\tau} \mathrm{E}\left(\int_0^{\tau} \mathrm{e}^{-\int_0^s \tilde{r}(t+u)\mathrm{d}u} \left(\lambda_0(t+s) f(t+s, X^{t,y}_{t+s}) - \lambda_0(t+s) f(t+s, X^{t,x}_{t+s}) \, \mathrm{d}s \right) \right) \\
&\quad = \sup_{\tau} \mathrm{E}\left(\int_0^{\tau} \mathrm{e}^{-\int_0^s \tilde{r}(t+u)\mathrm{d}u} \lambda_0(t+s)\beta(t+s) \left(-X^{t,y}_{t+s} + X^{t,x}_{t+s} \mathrm{d}s \right) \, \mathrm{d}s \right) \\
&\quad = \sup_{\tau} \mathrm{E}\left(\int_0^{\tau} \mathrm{e}^{-\int_0^s \tilde{r}(t+u)\mathrm{d}u} \lambda_0(t+s)\beta(t+s) \left(-y + x \right) e^{\left(\int_t^{t+s} \sigma \mathrm{d}B_u + \int_t^{t+s} \left(\mu - \frac{\sigma^2}{2} \right) \mathrm{d}u \right)} \right) \\
&\quad \leq 0. \qquad (3.3.20)
\end{aligned}
$$

Hence $x \to u(t,x)$ is decreasing. □

Proposition 3.3.5. *The map $(t,x) \mapsto u(t,x)$ is continuous on $\mathbb{R}^2_+$.*

Proof. Let us denote $H(t,x) := \tilde{r}(t)P - \lambda_0(t) f(t,x) = \tilde{r}(t)P - \lambda_0(t)\beta(t)x$ and substitute it into (3.3.5) to yield

$$
u(t,x) = \sup_{\tau} \mathrm{E}\left(\int_0^{\tau} \mathrm{e}^{-\int_0^s \tilde{r}(t+u)\mathrm{d}u} H(t+s, X^x_s) \mathrm{d}s \right). \qquad (3.3.21)
$$

Take $t_2 > t_1 \in \mathbb{R}$ and let $\tau_1 = \tau^*(t_1, x_1)$ be optimal for $u(t_1, x_1)$. Then

$$\begin{aligned}
&u(t_1,x_1) - u(t_2,x_2) \\
&\leq \mathrm{E}\left(\int_0^{\tau_1} \mathrm{e}^{-\int_0^s \tilde{r}(t_1+u)\mathrm{d}u} H(t_1+s, X_s^{x_1})\mathrm{d}s - \int_0^{\tau_1} \mathrm{e}^{-\int_0^s \tilde{r}(t_2+u)\mathrm{d}u} H(t_2+s, X_s^{x_2})\mathrm{d}s\right) \\
&= \mathrm{E}\left(\int_0^{\tau_1} \mathrm{e}^{-\int_0^s \tilde{r}(t_1+u)\mathrm{d}u} \left(H(t_1+s, X_s^{x_1}) - H(t_2+s, X_s^{x_2})\right)\mathrm{d}s\right) \\
&\qquad + \mathrm{E}\left(\int_0^{\tau_1} \left(\mathrm{e}^{-\int_0^s \tilde{r}(t_1+u)\mathrm{d}u} - \mathrm{e}^{-\int_0^s \tilde{r}(t_2+u)\mathrm{d}u}\right) H(t_2+s, X_s^{x_2})\mathrm{d}s\right). \qquad (3.3.22)
\end{aligned}$$

We establish that

$$\begin{aligned}
H(t_1+s, X_s^{x_1}) &- H(t_2+s, X_s^{x_2}) \\
&= P\left(\tilde{r}(t_1+s) - \tilde{r}(t_2+s)\right) + \lambda_0(t_2+s)\beta(t_2+s)X_s^{x_2} \\
&\qquad - \lambda_0(t_1+s)\beta(t_1+s)X_s^{x_1} \\
&= P\left(\tilde{r}(t_1+s) - \tilde{r}(t_2+s)\right) \\
&\qquad + \left(\lambda_0(t_2+s)\beta(t_2+s) - \lambda_0(t_1+s)\beta(t_1+s)\right)X_s^{x_2} \\
&\qquad + \lambda_0(t_1+s)\beta(t_1+s)(X_s^{x_2} - X_s^{x_1}) \\
&= P\left(\tilde{r}(t_1+s) - \tilde{r}(t_2+s)\right) \\
&\qquad + \left(\lambda_0(t_2+s)\beta(t_2+s) - \lambda_0(t_1+s)\beta(t_1+s)\right)X_s^{x_2} \\
&\qquad + \lambda_0(t_1+s)\beta(t_1+s)(x_2 - x_1)X_s^1 \qquad (3.3.23)
\end{aligned}$$

where $X_s^1 = 1\exp\left(\sigma B_t + \left(\mu - \frac{\sigma^2}{2}\right)t\right)$. We substitute (3.3.23) into (3.3.22) along with the property $\mathrm{E}(a-b) \leq \mathrm{E}(|a-b|)$ for $a, b \in \mathbb{R}$ to obtain

$$\begin{aligned}
&u(t_1,x_1) - u(t_2,x_2) \\
&\leq \mathrm{E}\left(\int_0^{\tau_1} \mathrm{e}^{-\int_0^s \tilde{r}(t_1+u)\mathrm{d}u} P\Big|\left(\tilde{r}(t_1+s) - \tilde{r}(t_2+s)\right)\Big|\mathrm{d}s\right) \\
&\qquad + \mathrm{E}\left(\int_0^{\tau_1} \mathrm{e}^{-\int_0^s \tilde{r}(t_1+u)\mathrm{d}u} X_s^{x_2}\Big|\lambda_0(t_2+s)\beta(t_2+s) - \lambda_0(t_1+s)\beta(t_1+s)\Big|\mathrm{d}s\right) \\
&\qquad + \mathrm{E}\left(\int_0^{\tau_1} \mathrm{e}^{-\int_0^s \tilde{r}(t_1+u)\mathrm{d}u} \lambda_0(t_1+s)\beta(t_1+s)\Big|x_2 - x_1\Big|X_s^1\mathrm{d}s\right) \\
&\qquad + \mathrm{E}\left(\int_0^{\tau_1} \Big|\mathrm{e}^{-\int_0^s \tilde{r}(t_1+u)\mathrm{d}u} - \mathrm{e}^{-\int_0^s \tilde{r}(t_2+u)\mathrm{d}u}\Big| \cdot \Big|H(t_2+s, X_s^{x_2})\Big|\mathrm{d}s\right). \qquad (3.3.24)
\end{aligned}$$

All the integrals above are bounded from above and by replacing τ_1 with $+\infty$ we have

that

$$\begin{aligned}
&u(t_1,x_1)-u(t_2,x_2)\\
&\le \mathrm{E}\left(\int_0^\infty \mathrm{e}^{-\int_0^s \tilde r(t_1+u)\mathrm{d}u} P\Big|\left(\tilde r(t_1+s)-\tilde r(t_2+s)\right)\Big|\mathrm{d}s\right)\\
&\qquad+\mathrm{E}\left(\int_0^\infty \mathrm{e}^{-\int_0^s \tilde r(t_1+u)\mathrm{d}u} X_s^{x_2}\Big|\lambda_0(t_2+s)\beta(t_2+s)-\lambda_0(t_1+s)\beta(t_1+s)\Big|\mathrm{d}s\right)\\
&\qquad+\mathrm{E}\left(\int_0^\infty \mathrm{e}^{-\int_0^s \tilde r(t_1+u)\mathrm{d}u} \lambda_0(t_1+s)\beta(t_1+s)\Big|x_2-x_1\Big|X_s^1\mathrm{d}s\right)\\
&\qquad+\mathrm{E}\left(\int_0^\infty \Big|\mathrm{e}^{-\int_0^s \tilde r(t_1+u)\mathrm{d}u}-\mathrm{e}^{-\int_0^s \tilde r(t_2+u)\mathrm{d}u}\Big|\cdot\Big|H(t_2+s,X_s^{x_2})\Big|\mathrm{d}s\right). \qquad (3.3.25)
\end{aligned}$$

Letting $|x_2-x_1|\downarrow 0$ and $|t_2-t_1|\downarrow 0$ then we see that, by dominated convergence,

$$\limsup_{(t_1,x_1)\to(t_2,x_2)} \left(u(t_1,x_1)-u(t_2,x_2)\right)\le 0. \qquad (3.3.26)$$

Next, we fix $t_1>t_2\in\mathbb{R}$ and choose $\tau_2=\tau^*(t_2,x_2)$ as optimal for $u(t_2,x_2)$. It follows that

$$\begin{aligned}
&u(t_1,x_1)-u(t_2,x_2)\\
&\ge \mathrm{E}\left(\int_0^{\tau_2} \mathrm{e}^{-\int_0^s \tilde r(t_1+u)\mathrm{d}u} H(t_1+s,X_s^{x_1})\mathrm{d}s-\int_0^{\tau_2} \mathrm{e}^{-\int_0^s \tilde r(t_2+u)\mathrm{d}u} H(t_2+s,X_s^{x_2})\mathrm{d}s\right)\\
&=\mathrm{E}\left(\int_0^{\tau_2} \mathrm{e}^{-\int_0^s \tilde r(t_2+u)\mathrm{d}u}\left(H(t_2+s,X_s^{x_2})-H(t_1+s,X_s^{x_1})\right)\mathrm{d}s\right)\\
&\qquad+\mathrm{E}\left(\int_0^{\tau_2}\left(\mathrm{e}^{-\int_0^s \tilde r(t_2+u)\mathrm{d}u}-\mathrm{e}^{-\int_0^s \tilde r(t_1+u)\mathrm{d}u}\right)H(t_1+s,X_s^{x_1})\mathrm{d}s\right). \qquad (3.3.27)
\end{aligned}$$

We see that

$$\begin{aligned}
&H(t_2+s,X_s^{x_2})-H(t_1+s,X_s^{x_1})\\
&\qquad=P\left(\tilde r(t_2+s)-\tilde r(t_1+s)\right)\\
&\qquad\qquad+\left(\lambda_0(t_1+s)\beta(t_1+s)-\lambda_0(t_2+s)\beta(t_2+s)\right)X_s^{x_1}\\
&\qquad\qquad+\lambda_0(t_2+s)\beta(t_2+s)(x_1-x_2)X_s^1 \qquad (3.3.28)
\end{aligned}$$

Recall that $t_1>t_2$ along with the property $-\mathrm{E}(a-b)\ge-\mathrm{E}(|a-b|)$ for $a,b\in\mathbb{R}$. We

then substitute (3.3.28) into (3.3.27) to derive

$$\begin{aligned}
&u(t_1,x_1)-u(t_2,x_2)\\
&\geq \mathrm{E}\left(\int_0^{\tau_2} \mathrm{e}^{-\int_0^s \tilde{r}(t_2+u)\mathrm{d}u} P\Big|\tilde{r}(t_2+s)-\tilde{r}(t_1+s)\Big|\mathrm{d}s\right)\\
&\qquad+\mathrm{E}\left(\int_0^{\tau_2} \mathrm{e}^{-\int_0^s \tilde{r}(t_2+u)\mathrm{d}u} X_s^{x_1}\Big|\lambda_0(t_1+s)\beta(t_1+s)-\lambda_0(t_2+s)\beta(t_2+s)\Big|\mathrm{d}s\right)\\
&\qquad+\mathrm{E}\left(\int_0^{\tau_2} \mathrm{e}^{-\int_0^s \tilde{r}(t_2+u)\mathrm{d}u} \lambda_0(t_2+s)\beta(t_2+s)\Big|x_1-x_2\Big|X_s^1\mathrm{d}s\right)\\
&\qquad+\mathrm{E}\left(\int_0^{\tau_2} \Big|\mathrm{e}^{-\int_0^s \tilde{r}(t_2+u)\mathrm{d}u}-\mathrm{e}^{-\int_0^s \tilde{r}(t_1+u)\mathrm{d}u}\Big|\cdot\left(H(t_1+s,X_s^{x_1})\right)\mathrm{d}s\right). \qquad (3.3.29)
\end{aligned}$$

Again letting $|x_1-x_2|\downarrow 0$ and $|t_1-t_2|\downarrow 0$ we see that

$$\liminf_{(t_1,x_1)\to(t_2,x_2)} (u(t_1,x_1)-u(t_2,x_2))\geq 0. \qquad (3.3.30)$$

This and (3.3.26) prove that $(t,x)\mapsto u(t,x)$ is continuous on $\mathbb{R}^2$. □

Note that the arguments above are particularly useful and provide sufficient conditions to prove the existence of an optimal boundary.

3.4 Existence of an optimal boundary

The aim of this section is to prove the existence of the optimal stopping boundary given that

$$C:=\{(t,x)\in\mathbb{R}\times\mathbb{R}\colon u(t,x)>0\},\quad S:=\{(t,x)\in\mathbb{R}\times\mathbb{R}\colon u(t,x)=0\}. \qquad (3.4.1)$$

The subsequent arguments show that there is a non empty stopping set that has a time dependent boundary and a collection of points above or below the boundary depending on the time monotonic nature of the value function.

Lemma 3.4.1. *From Proposition 3.3.4, $x\mapsto u(t,x)$ is decreasing. Moreover, recalling Proposition 3.3.2,*

(i) *If $t\mapsto u(t,x)$ is decreasing then $(t,x)\in S \implies (t',x)\in S\ \forall\ t'\geq t$.*

(ii) *If $t\mapsto u(t,x)$ is increasing then $(t,x)\in S \implies (t',x)\in S\ \forall\ t'\leq t$.*

Proof. (i)The map $x\mapsto u(t,x)$ is decreasing then $\forall\ x'\geq x$, $u(t,x)\geq u(t,x')$. We know that $u(t,x)\geq 0\ \forall\ x$ and $u(t,x)=0$ in S. Then if $(t,x)\in S$

$$0=u(t,x)\geq u(t,x')\geq 0\implies u(t,x')=0. \qquad (3.4.2)$$

Also, when the map $t \mapsto u(t,x)$ is decreasing then $\forall\ t' \geq t$, $u(t,x) \geq u(t',x)$. Again, $u(t',x) \geq 0\ \forall\ t$ and $u(t,x) = 0$ in S. Thus, if $(t,x) \in S$

$$0 = u(t,x) \geq u(t',x) \geq 0 \Longrightarrow u(t',x) = 0. \tag{3.4.3}$$

Analogous arguments allow us to prove (ii). □

Recall from (3.3.5) that

$$u(t,x) = \sup_{\tau} \mathrm{E}\left(\int_0^{\tau} \mathrm{e}^{-\int_0^s \tilde{r}(t+u)\mathrm{d}u} H(t+s, X_s^x) ds\right). \tag{3.4.4}$$

where

$$H(t,x) := \tilde{r}(s)P - \lambda_0(s) f(s, X_s). \tag{3.4.5}$$

Proposition 3.4.2. *$H \in C(\mathbb{R}_+^2)$ and $\mathcal{R} := \{(t,x) : H(t,x) > 0\} \subseteq C$.*

Proof. The fact that $H \in C(\mathbb{R}_+^2)$ follows from the continuity of $\tilde{r}(t), \lambda_0(t)$ and $f(t,x)$. Fix $(t,x) \in \mathcal{R}$ and take $\tau_{\mathcal{R}} := \inf\{s \geq 0 : (t+s, X_s^x) \notin \mathcal{R}\}$. Then

$$u(t,x) \geq \mathrm{E}\left(\int_0^{\tau_{\mathcal{R}}} \mathrm{e}^{-\int_0^s \tilde{r}(t+u)\mathrm{d}u} H(t+s, X_s^x) ds\right) > 0. \tag{3.4.6}$$

This implies that $(t,x) \in \{u > 0\} = C$, hence $\mathcal{R} \subseteq C$ since (t,x) was arbitrary. □

Corollary 3.4.3. *From Proposition 3.4.2, $S \subseteq \mathcal{R}^c := \{(t,x) : H(t,x) \leq 0\}$.*

Theorem 3.4.4. *The stopping set is not empty, that is $S \neq \emptyset$.*

Proof. By contradiction assume that $S = \emptyset$ then $\tau_* = \infty$ and $\forall\ (t,x) \in \mathbb{R}_+^2$,

$$u(t,x) = \mathrm{E}\left(\int_0^{\infty} \mathrm{e}^{-\int_0^s \tilde{r}(t+u)\mathrm{d}u} \left(\tilde{r}(t+s)P - \lambda_0(t+s) f(t+s, X_s^x)\mathrm{d}s\right)\right). \tag{3.4.7}$$

Since $\mathrm{E}(X_s^x) = x e^{\mu s}$ then

$$\begin{aligned} u(t,x) &= \int_0^{\infty} \mathrm{e}^{-\int_0^s \tilde{r}(t+u)\mathrm{d}u} \tilde{r}(t+s) P \mathrm{d}s - x \int_0^{\infty} \mathrm{e}^{-\int_0^s (\tilde{r}(t+u)-\mu)\mathrm{d}u} \lambda_0(t+s)\beta(t+s)\mathrm{d}s \\ &= \left(1 - \mathrm{e}^{-\int_0^s \tilde{r}(t+u)\mathrm{d}u}\right) P - x \int_0^{\infty} \mathrm{e}^{-\int_0^s (\tilde{r}(t+u)-\mu)\mathrm{d}u} \lambda_0(t+s)\beta(t+s)\mathrm{d}s \\ &=: \alpha(t,x). \end{aligned} \tag{3.4.8}$$

Thus $\lim_{x\uparrow\infty} \alpha(t,x) = -\infty$ and this is a contradiction because $u(t,x) \geq 0\ \forall\ x$. □

The facts just proved above establishes the existence of a boundary such that the continuation set (C) and the stopping set (S) are given by (3.4.1). With reference to (3.2.25), let us recall that

$$\begin{cases} (\partial_t + L - \tilde{r}(t))\, v(t,x) = 0, & \text{in } C, \\ (\partial_t + L - \tilde{r}(t))\, v(t,x) = H(t,x), & \text{in } S \backslash \partial C. \end{cases} \tag{3.4.9}$$

Also, thanks to Lemma 3.4.1 and Theorem 3.4.4, we define

$$b(t) := \sup\{x \in \mathbb{R}_+ : u(t,x) > 0\} = \sup\{x \in \mathbb{R}_+ : (t,x) \in C\}. \tag{3.4.10}$$

Now, let us show if the optimal boundary in (3.4.10) is a decreasing or increasing function based on the conditions Corollary 3.3.3.

Corollary 3.4.5. (i) *If $t \mapsto u(t,x)$ is decreasing, then the optimal boundary $t \mapsto b(t)$ is decreasing.*

(ii) *If $t \mapsto u(t,x)$ is increasing, then the optimal boundary $t \mapsto b(t)$ is increasing.*

Proof. (i) By contradiction assume that $\exists\ t_0 < t_1$ such that $b(t_1) > b(t_0)$. From the definition of $b(t)$ in (3.4.10), $(t_1, b(t_0)) \in C$ whereas $(t_0, b(t_0)) \in S$. This contradicts Corollary 3.4.3. The proof above for case (i) admits analogous arguments which can be used to prove case (ii). □

Proposition 3.4.6. (i) *If the boundary is decreasing, then it is right continuous.*

(ii) *If the boundary is increasing, then it is left continuous.*

Proof. We will prove the first statement in (i) as the second statement in (ii) follows along the same lines. Let us pick $t_0 : b(t_0) < +\infty$. Consider a decreasing sequence $(t_n)_{n\in\mathbb{N}}$ such that $t_n \downarrow t_0$ as $n \to \infty$. The limit exists since $b(.)$ is monotonic. Then $(t_n, b(t_n)) \to (t_0, b(t_0^+))$ as $n \to \infty$ where $b(t_0^+) := \lim_{n\to\infty} b(t_n)$. Since $(t_n, b(t_n)) \in S$ for all n and S is closed, then it must be that $(t_0, b(t_0^+)) \in S$ and hence $b(t_0^+) \geq b(t_0)$ by definition of $b(t)$. Since $b(.)$ is decreasing and $t_n > t_0$ then $b(t_n) \leq b(t_0)$. Take the limit as $n \to \infty$, so that $b(t_0^+) \leq b(t_0)$. Hence $b(t_0^+) = b(t_0)$ and $b(\cdot)$ is right continuous. □

Next we show that the optimal boundary in (3.4.10) is continuous.

Proposition 3.4.7. *If the boundary $t \mapsto b(t)$ is monotonic then it is continuous on $\mathbb{R}_+$.*

Proof. This method of proof was developed from [31, 32, 33]. We only prove full argument when the boundary is decreasing because the same result for an increasing boundary can be proven by the same methods. Assume that there exists t_0 such that a discontinuity of $b(.)$ occurs. That is, $b(t_0^+) < b(t_0)$ where $b(t_0^+)$ denotes the right limit of the boundary at t_0. Consider an interval $[\underline{x}, \overline{x}]$ such that $b(t_0^+) < \underline{x} < \overline{x} < b(t_0)$. By monotonicity of $b(\cdot)$, we have that $[0, t_0) \times [\underline{x}, \overline{x}] \subset C$. Take $t_n \in [0, t_0)$ and denote E_n as the rectangle domain with vertices $(t_n, \underline{x}), (t_0, \underline{x}), (t_0, \overline{x}), (t_n, \overline{x})$. From (3.4.9), we see that for all $(t, x) \in C$

$$(\partial_t + L - \tilde{r}(t))\, u(t,x) + \tilde{r}(t)P - \lambda_0(t) f(t,x) = 0 \tag{3.4.11}$$

holds. Pick an arbitrary non-negative function ψ that is continuously differentiable infinitely many times and with compact support in the set $[\underline{x}, \overline{x}]$, i.e. $\psi \in C_c^\infty([\underline{x}, \overline{x}])$ such that $\psi \geq 0$, and $\int_{\underline{x}}^{\overline{x}} \psi(y)\mathrm{d}y = 1$. Since (3.4.11) holds in $[0, t_0) \times [\underline{x}, \overline{x}]$, then for any $t_n < t_0$ we have

$$0 = \int_{\underline{x}}^{\overline{x}} \left[(\partial_t + L - \tilde{r}(t_n))\, u(t_n, y) + \tilde{r}(t_n)P - \lambda_0(t_n) f(t_n, y)\right] \psi(y)\mathrm{d}y. \tag{3.4.12}$$

Recollect that $t \mapsto u(t,x)$ is decreasing then $\partial_t u(t,x) \leq 0$ such that (3.4.12) becomes

$$0 \leq \int_{\underline{x}}^{\overline{x}} \left[(L - \tilde{r}(t))\, u(t, y) + \tilde{r}(t)P - \lambda_0(t) f(t, y)\right] \psi(y)\mathrm{d}y. \tag{3.4.13}$$

Apply integration by parts to the inequality (3.4.13) and recall that the function $\psi(y)$ has compact support then

$$\begin{aligned} 0 \leq & \int_{\underline{x}}^{\overline{x}} u(t_n, y)\, (L^*\psi)\, (y)\mathrm{d}y \\ & + \int_{\underline{x}}^{\overline{x}} \left[-\tilde{r}(t_n) u(t_n, y) + \tilde{r}(t_n)P - \lambda_0(t_n) f(t_n, y)\right] \psi(y)\mathrm{d}y \end{aligned} \tag{3.4.14}$$

where the adjoint operator in (3.4.13) is given by

$$(L^*\psi)\, (y) = \mu \frac{\mathrm{d}}{\mathrm{d}y}(y \cdot \psi(y)) + \frac{1}{2}\sigma^2 \frac{\mathrm{d}^2}{\mathrm{d}y^2}\left(y^2 \cdot \psi(y)\right). \tag{3.4.15}$$

We take the limit $t_n \to t_0$ as $n \to \infty$ so that

$$\begin{aligned}
0 \leq \lim_{n\to\infty} &\int_{\underline{x}}^{\overline{x}} u(t_n, y)\left(L^*\psi\right)(y)\mathrm{d}y \\
&+ \int_{\underline{x}}^{\overline{x}} \left[-\tilde{r}(t_n)u(t_n, y) + \tilde{r}(t_n)P - \lambda_0(t_n)f(t_n, y)\right]\psi(y)\mathrm{d}y \\
= &\int_{\underline{x}}^{\overline{x}} u(t_0, y)\left(L^*\psi\right)(y)\mathrm{d}y \\
&+ \int_{\underline{x}}^{\overline{x}} \left[-\tilde{r}(t_0)u(t_0, y) + \tilde{r}(t_0)P - \lambda_0(t_0)f(t_0, y)\right]\psi(y)\mathrm{d}y. \qquad (3.4.16)
\end{aligned}$$

Recall that $u(t_0, y) = 0$ for all $y \in [\underline{x}, \overline{x}]$ because it is $(t_0, y) \in S$, then (3.4.16) becomes

$$0 \leq \int_{\underline{x}}^{\overline{x}} \left[\tilde{r}(t_0)P - \lambda_0(t_0)f(t_0, y)\right]\psi(y)\mathrm{d}y = \int_{\underline{x}}^{\overline{x}} H(t_0, x_0)\psi(y)\mathrm{d}y. \qquad (3.4.17)$$

Also from Proposition 3.4.2, $H(t,x) := \tilde{r}(t)P - \lambda_0(t)f(t,x), \mathcal{R} := \{(t,x) : H(t,x) > 0\} \subset C$ and $S \subseteq \mathcal{R}^c := \{(t,x) : H(t,x) \leq 0\}$. Hence

$$0 \leq \int_{\underline{x}}^{\overline{x}} H(t_0, y)\psi(y)\mathrm{d}y \leq 0. \qquad (3.4.18)$$

(3.4.18) implies $H(t_0, y) = 0$ for all $y \in [\underline{x}, \overline{x}]$, which is impossible because $H_y(t_0, y) < 0$. This is a contradiction and hence the proof. □

Combining the arguments above establishes the existence of the optimal stopping boundary.

3.5 Regularity of the value function

In this section, we show that the value function is sufficiently regular. The optimal stopping time is given by

$$\tau^*_{t,x} = \inf\{s \in \mathbb{R}_+ : X^x_s \geq b(t+s)\} = \inf\{s \in \mathbb{R}_+ : (t+s, X^x_s) \in S\} \qquad (3.5.1)$$

for all $(t,x) \in \mathbb{R}^2_+$. Then $\tau^*_{t,x} = 0$ for any $(t,x) \in \partial C$. The argument of proof on the regularity of the value function is guided by information from [34, §5] and [107, Ch VI]. Thus from [34, 107], it is shown that for any sequence $(t_n, x_n)_{n\geq 1}$ which converges to $(t_0, x_0) \in \partial C$ (that is $x = b(t_0)$) as $n \to \infty$ then we obtain

$$\lim_{n\to\infty} \tau^*_{t_n,x_n} = 0 \quad \text{(P-a.s.)} \qquad (3.5.2)$$

Lemma 3.5.1. *For all* $(t,x) \in \mathbb{R}^2_+ \backslash \partial C$ *we have*

$$\partial_x v(t,x) = \mathrm{E}\left[\mathrm{e}^{-\int_t^{t+\tau^*} \tilde{r}(u)\mathrm{d}u} \beta_1(t+\tau^*_{t,x}) X^1_{\tau^*_{t,x}}\right] \tag{3.5.3}$$

where $X^1_{\tau^*_{t,x}} = \frac{\mathrm{d}}{\mathrm{d}x} X_{\tau^*_{t,x}} = e^{(\mu - \frac{\sigma^2}{2})\tau^*} e^{\sigma B_{\tau^*}}$.

Proof. We know that the classical solution to $v(t,x)$ is given by

$$\partial_t v(t,x) + Lv(t,x) = \tilde{r}(t) v(t,x) \quad \text{in} \quad \partial C. \tag{3.5.4}$$

Then $\partial_x v(t,x)$ and $\partial_t v(t,x)$ exist and are continuous in C. Also, $v(t,x) = g(t,x) = \beta_1(t)x - P$ in S implies that $\partial_x v(t,x) = \beta_1(t)$ and $\partial_t v(t,x) = \beta_1'(t)x$ for all $(t,x) \in S \backslash \partial C$. It remains to show that (3.5.3) holds for all $(t,x) \in \partial C$. Fix $(t,x) \in \partial C$ and take $\epsilon > 0$. Let $\tau^* = \tau^*_{t,x}$ be the optimal stopping time for our problem but sub-optimal for our problem with value $v(t, x+\epsilon)$. Then we have that

$$\begin{aligned}
&v(t,x+\epsilon) - v(t,x) \\
&\quad \geq \mathrm{E}\left[\mathrm{e}^{-\int_t^{t+\tau^*} \tilde{r}(u)\mathrm{d}u} \left(\beta_1(t+\tau^*)(x+\epsilon) X^1_{\tau^*} - P - \beta_1(t+\tau^*) x X^1_{\tau^*} + P\right)\right] \\
&\quad = \mathrm{E}\left[\mathrm{e}^{-\int_t^{t+\tau^*} \tilde{r}(u)\mathrm{d}u} \beta_1(t+\tau^*) \epsilon X^1_{\tau^*}\right].
\end{aligned} \tag{3.5.5}$$

Multiply (3.5.5) by $\frac{1}{\epsilon}$ and take $\lim_{\epsilon \to 0}$ to derive

$$\partial_x v(t,x) = \lim_{\epsilon \to 0} \frac{v(t,x+\epsilon) - v(t,x)}{\epsilon} \geq \mathrm{E}\left[\mathrm{e}^{-\int_t^{t+\tau^*} \tilde{r}(u)\mathrm{d}u} \beta_1(t+\tau^*) X^1_{\tau^*}\right]. \tag{3.5.6}$$

Using the same argument, we also have that

$$\begin{aligned}
&v(t,x) - v(t,x-\epsilon) \\
&\quad \leq \mathrm{E}\left[\mathrm{e}^{-\int_t^{t+\tau^*} \tilde{r}(u)\mathrm{d}u} \left(\beta_1(t+\tau^*) x X^1_{\tau^*} - P - \beta_1(t+\tau^*)(x-\epsilon) X^1_{\tau^*} + P\right)\right] \\
&\quad = \mathrm{E}\left[\mathrm{e}^{-\int_t^{t+\tau^*} \tilde{r}(u)\mathrm{d}u} \beta_1(t+\tau^*) \epsilon X^1_{\tau^*}\right].
\end{aligned} \tag{3.5.7}$$

Also,

$$\partial_x v(t,x) = \lim_{\epsilon \to 0} \frac{v(t,x) - v(t,x-\epsilon)}{\epsilon} \leq \mathrm{E}\left[\mathrm{e}^{-\int_t^{t+\tau^*} \tilde{r}(u)\mathrm{d}u} \beta_1(t+\tau^*) X^1_{\tau^*}\right]. \tag{3.5.8}$$

Combining (3.5.6) and (3.5.8) we obtain

$$\partial_x v(t,x) = \mathrm{E}\left[\mathrm{e}^{-\int_t^{t+\tau^*} \tilde{r}(u)\mathrm{d}u} \beta_1(t+\tau^*) X^1_{\tau^*}\right]. \tag{3.5.9}$$

□

Lemma 3.5.2. *For all* $(t,x) \in \mathbb{R}^2_+ \backslash \partial C$ *we have*

$$\partial_t v(t,x) = \mathrm{E}\left[\mathrm{e}^{-\int_t^{t+\tau^*} \tilde{r}(u)\mathrm{d}u}\, \partial_t \beta_1(t+\tau^*)\, X_{\tau^*}\right]. \tag{3.5.10}$$

Proof. Let $(t,x) \in C$ and $\epsilon > 0$. Pick $\tau^* = \tau^*_{t,x}$ as the optimal for $v(t,x)$, so that

$$\begin{aligned} v(t+\epsilon,x) - v(t,x) \geq & \mathrm{E}\left[\mathrm{e}^{-\int_{t+\epsilon}^{t+\epsilon+\tau^*} \tilde{r}(u)\mathrm{d}u} (\beta_1(t+\epsilon+\tau^*)X_{\tau^*} - P)\right] \\ & - \mathrm{E}\left[\mathrm{e}^{-\int_t^{t+\tau^*} \tilde{r}(u)\mathrm{d}u} (\beta_1(t+\tau^*)X_{\tau^*} - P)\right]. \end{aligned} \tag{3.5.11}$$

Multiply (3.5.11) by $\frac{1}{\epsilon}$ and take $\lim_{\epsilon\to 0}$.

$$\begin{aligned} \partial_t v(t,x) &\geq \mathrm{E}\left[\mathrm{e}^{-\int_t^{t+\tau^*} \tilde{r}(u)\mathrm{d}u} \left(\lim_{\epsilon\to 0}\left(\frac{\beta_1(t+\epsilon+\tau^*) - \beta_1(t+\tau^*)}{\epsilon}\right) X_{\tau^*}\right)\right] \\ &= \mathrm{E}_x\left[\mathrm{e}^{-\int_t^{t+\tau^*} \tilde{r}(u)\mathrm{d}u}\, \partial_t \beta_1(t+\tau^*)\, X_{\tau^*}\right]. \end{aligned} \tag{3.5.12}$$

By the same argument,

$$\begin{aligned} v(t,x) - v(t-\epsilon,x) \leq & \mathrm{E}\left[\mathrm{e}^{-\int_t^{t+\tau^*} \tilde{r}(u)\mathrm{d}u} (\beta_1(t+\tau^*)X_{\tau^*} - P)\right] \\ & - \mathrm{E}\left[\mathrm{e}^{-\int_{t-\epsilon}^{t-\epsilon+\tau^*} \tilde{r}(u)\mathrm{d}u} (\beta_1(t-\epsilon+\tau^*)X_{\tau^*} - P)\right]. \end{aligned} \tag{3.5.13}$$

Multiply (3.5.13) by $\frac{1}{\epsilon}$ and take $\lim_{\epsilon\to 0}$ to derive

$$\begin{aligned} \partial_t v(t,x) &\leq \mathrm{E}\left[\mathrm{e}^{-\int_t^{t+\tau^*} \tilde{r}(u)\mathrm{d}u} \left(\lim_{\epsilon\to 0}\left(\frac{\beta_1(t+\tau^*) - \beta_1(t-\epsilon+\tau^*)}{\epsilon}\right) X_{\tau^*}\right)\right] \\ &= \mathrm{E}\left[\mathrm{e}^{-\int_t^{t+\tau^*} \tilde{r}(u)\mathrm{d}u}\, \partial_t \beta_1(t+\tau^*)\, X_{\tau^*}\right]. \end{aligned} \tag{3.5.14}$$

Combine (3.5.12) and (3.5.14) we get

$$\partial_t v(t,x) = \mathrm{E}\left[\mathrm{e}^{-\int_t^{t+\tau^*} \tilde{r}(u)\mathrm{d}u}\, \partial_t \beta_1(t+\tau^*)\, X_{\tau^*}\right]. \tag{3.5.15}$$

□

Theorem 3.5.3. *We have* $v \in C^1(\mathbb{R}^2_+)$.

Proof. We know that $\partial_x v(t,x)$ and $\partial_t v(t,x)$ exist and are continuous in C. It remains to prove that $\partial_x v(t,x)$ and $\partial_t v(t,x)$ are continuous across the boundary ∂C which is done in two steps below.

Step 1. (Continuity of $\partial_x v(t,x)$). Fix $(t_0,x_0)\in\partial C$ and for any sequence $(t_n,x_n)_{n\geq 1}\subseteq C$ converging to (t_0,x_0) as $n\to\infty$, we use Lemma 3.5.1, (3.5.2) and dominated convergence to derive

$$\lim_{n\to\infty}\partial_x v(t_n,x_n)=\mathrm{E}\left[\lim_{n\to\infty}\mathrm{e}^{-\int_{t_n}^{t_n+\tau^*_{t_n,x_n}}\tilde{r}(u)\mathrm{d}u}\beta_1(t_n+\tau^*_{t_n,x_n})X^1_{\tau^*_{t_n,x_n}}\right]=\beta_1(t_0). \tag{3.5.16}$$

Step 2. (Continuity of $\partial_t v(t,x)$). Using Lemma 3.5.2, we replace (t,x) with (t_n,x_n) where $(t_n,x_n)_{n\geq 1}\subseteq C$ converges to $(t_0,x_0)\in\partial C$ as $n\to\infty$ and using (3.5.2) we derive,

$$\partial_t v(t_0,x_0)=\partial_t\beta_1(t_0)x \tag{3.5.17}$$

□

Next we show that $\partial_{xx}v$ is not continuous across the boundary ∂C

Corollary 3.5.4. *We have $\partial_{xx}v$ continuous on $\mathbb{R}^2_+\backslash\partial C$. Moreover for any $(t_0,x_0)\in\partial C$ and any sequence $(t_n,x_n)\subseteq C$ converging to (t_0,x_0) as $n\to\infty$, we have*

$$\lim_{n\to\infty}\partial_{xx}v(t_n,x_n)=\left[\frac{2}{\sigma^2x_0}\left(\tilde{r}(t_0)(x_0\beta_1(t_0)-P)-\beta_1'(t_0)x_0-\beta_1(t_0)\mu x_0\right)\right] \tag{3.5.18}$$

Proof. We know that $v(t,x)=\beta_1 x-P$ in S and $\partial_{xx}v$ is continuous on $\mathbb{R}^2_+\backslash\partial C$. From (3.2.25) we have that

$$\partial_t v(t,x)+\partial_x v(t,x)\mu x+\partial_{xx}v(t,x)\frac{\sigma^2x^2}{2}=\tilde{r}(t)v(t,x). \tag{3.5.19}$$

We rearrange (3.5.19) to derive

$$\partial_{xx}v(t,x)=\frac{2}{\sigma^2x_0}\left[\tilde{r}(t)v(t,x)-\partial_t v(t,x)-\partial_x v(t,x)\mu x\right]. \tag{3.5.20}$$

Replace (t,x) by (t_n,x_n) in (3.5.20) and take the limit as $n\to\infty$. Also, using Theorem 3.5.3, it follows that

$$\begin{aligned}
&\lim_{n\to\infty}\partial_{xx}v(t_n,x_n)\\
&\quad=\lim_{n\to\infty}\left[\frac{2}{\sigma^2x_n}\left[\tilde{r}(t_n)v(t_n,x_n)-\partial_t v(t_n,x_n)-\partial_x v(t_n,x_n)\mu x_n\right]\right]\\
&\quad=\frac{2}{\sigma^2x_0}\left[\tilde{r}(t_0)v(t_0,x_0)-\partial_t v(t_0,x_0)-\partial_x v(t_0,x_0)\mu x_0\right]\\
&\quad=\frac{2}{\sigma^2x_0}\left[\tilde{r}(t_0)(x_0\beta_1(t_0)-P)-\beta_1'(t_0)x_0-\beta_1(t_0)\mu x_0\right].
\end{aligned} \tag{3.5.21}$$

Then

$$\begin{aligned}\partial_{xx}v(t_0,x_0) &= \frac{2}{\sigma^2 x_0}\left[\tilde{r}(t_0)\left(\beta_1(t_0)x_0 - P\right) - \beta_1'(t_0)x_0 - \beta_1(t_0)\mu x_0\right] \\ &= \frac{2}{\sigma^2 x_0}\left[\beta_1(t_0)x_0\left(\tilde{r}(t_0)-\mu\right) - \beta_1'(t_0)x_0 - \tilde{r}(t_0)P\right] \end{aligned} \tag{3.5.22}$$

where $\beta_1'(t_0) = -\beta_1(t_0)\lambda_0(t_0) + \left(\tilde{r}(t_0)-\mu\right)\beta_1(t_0)$. As such

$$\begin{aligned}&\partial_{xx}v(t_0,x_0) \\ &\quad= \frac{2}{\sigma^2 x_0}\left[\tilde{r}(t_0)\left(\beta_1(t_0)x_0 - P\right) - \beta_1'(t_0)x_0 - \beta_1(t_0)\mu x_0\right] \\ &\quad= \frac{2}{\sigma^2 x_0}\left[\beta_1(t_0)x_0\left(\tilde{r}(t_0)-\mu\right) - \beta_1(t_0)x_0\left(\tilde{r}(t_0)-\mu\right) + \beta(t_0)\lambda_0(t_0)x_0 - \tilde{r}(t_0)P\right] \\ &\quad= \frac{2}{\sigma^2 x_0}\left[\beta(t_0)\lambda_0(t_0)x_0 - \tilde{r}(t_0)P\right]. \end{aligned} \tag{3.5.23}$$

In that case,

$$\partial_{xx}v(t_0,x_0) = -\frac{2}{\sigma^2 x_0}H\left(t_0,x_0\right). \tag{3.5.24}$$

Recall $R := \{(t,x) : H(t,x) > 0\} \subset C$ and $S \subseteq R^c := \{(t,x) : H(t,x) \leq 0\} \subset C$. In S, $\partial_{xx}v(t_0,x_0) = -\frac{2}{\sigma^2 x_0}H\left(t_0,x_0\right) \leq 0$ hence $\partial_{xx}v$ is not continuous at ∂C if $H(t,x) < 0$. □

Proposition 3.5.5. *We have* $\sup_{t>0} b(t) < +\infty$.

Proof. We give a full proof in the case in which $t \mapsto b(t)$ is non-increasing. The other case can be treated analogously. Recall that $u(t,x) = v(t,x) - g(t,x)$ such that

$$u(t,x) = \sup_{\tau} \mathrm{E}\left[\int_0^{\tau} \mathrm{e}^{-\int_0^s \tilde{r}(t+u)\mathrm{d}u} H(t+s, X_s^x)\mathrm{d}s\right]. \tag{3.5.25}$$

Assume to reach a contradiction, that there exists $t_0 > 0$ such that $b(t_0) = +\infty$ for some t_0. Fix $t' < t_0$ and since b is non-increasing, $b(t) = \infty$, for $t \in [t', t_0]$. Given a starting point (t', x) then

$$\tau^* := \tau^*_{t',x} \geq t_0 - t' \quad , \quad \mathrm{P} - a.s. \tag{3.5.26}$$

where $\tau^*_{t',x} = \inf\{s \geq 0 : u(t'+s, X^x_s) = 0\} = \inf\{s \geq 0 : (t'+s, X^x_s) \in S\}$. Next,

$$\begin{aligned} 0 &\leq u(t',x) \\ &= \mathrm{E}\left[\int_0^{\tau^*_{t',x}} \mathrm{e}^{-\int_0^s \tilde{r}(t'+u)\mathrm{d}u} H(t'+s, X^x_s)\mathrm{d}s\right] \\ &= \mathrm{E}\left[\int_0^{t_0-t'_s} \mathrm{e}^{-\int_0^s \tilde{r}(t+u)\mathrm{d}u} H(t'+s, X^x_s)\mathrm{d}s\right] \\ &\qquad + \mathrm{E}\left[\int_{t_0-t'}^{\tau^*} \mathrm{e}^{-\int_0^s \tilde{r}(t'+u)\mathrm{d}u} H(t'+s, X^x_s)\mathrm{d}s\right]. \end{aligned} \tag{3.5.27}$$

Recall the set $\mathcal{R}$ from Theorem 3.5.3 and that $H(t,x) = 0$ is equivalent to $\tilde{r}(t)P - \lambda_0(t)\beta(t)x = 0$, hence to $x = \ell(t)$ where $\ell(t) = \frac{\tilde{r}(t)P}{\lambda_0(t)\beta(t)}$ then (3.5.27) is further continued as follows.

$$\begin{aligned} 0 \leq& \mathrm{E}\left[\int_0^{t_0-t'_s} \mathrm{e}^{-\int_0^s \tilde{r}(t'+u)\mathrm{d}u} H(t'+s, X^x_s)\mathrm{d}s\right] \\ &\qquad + \mathrm{E}\left[\int_{t_0-t'}^{\tau^*} \mathrm{e}^{-\int_0^s \tilde{r}(t'+u)\mathrm{d}u} H(t'+s, X^x_s)\mathbb{1}_{\{X^x_s \leq \ell(t'+s)\}}\mathrm{d}s\right] \\ \leq& \mathrm{E}\left[\int_0^{t_0-t'_s} \mathrm{e}^{-\int_0^s \tilde{r}(t'+u)\mathrm{d}u} \left(\tilde{r}(t'+s)P - \lambda_0(t'+s)\beta(t'+s)X^x_s\right)\mathrm{d}s\right] \\ &\qquad + \mathrm{E}\left[\int_{t_0-t'}^{\tau^*} \mathrm{e}^{-\int_0^s \tilde{r}(t'+u)\mathrm{d}u} \left(\tilde{r}(t'+s)P\right)\mathbb{1}_{\{X^x_s \leq \ell(t'+s)\}}\mathrm{d}s\right], \end{aligned} \tag{3.5.28}$$

using that $H(t'+s, X^x_s) \leq \tilde{r}(t'+s)P$. Let $x \to \infty$ then $0 \leq u(t',x) \leq -\infty$ which is a contradiction. □

3.5.1 Characterisation of the free boundary and of the value function

We will find a non-linear integral equation that characterizes uniquely the free-boundary and the value function. We use the regularity of the value function to derive an integral equation for the optimal boundary. First we need a technical lemma.

Lemma 3.5.6. *We have*

$$\lim_{T\uparrow\infty} \mathrm{E}_x\left[\mathrm{e}^{-\int_0^T \tilde{r}(t+u)\mathrm{d}u} v(T, X_{T-t})\right] = 0 \tag{3.5.29}$$

for all $x \in \mathcal{R}_+$.

Proof. With reference to (3.2.19) and (3.2.11), we see that

$$\begin{aligned} v(t,x) &= \sup_{\tau} \mathrm{E}\big[\mathrm{e}^{-\int_0^\tau \tilde{r}(t+u)\mathrm{d}u} g(t+\tau, X_\tau)\big] \\ &= \sup_{\tau} \mathrm{E}\big[\mathrm{e}^{-\int_0^\tau \tilde{r}(t+u)\mathrm{d}u} (\beta_1(t+\tau)X_\tau - P)\big]. \end{aligned} \tag{3.5.30}$$

Accordingly, when $\tau = 0$, we have $v(t,x) \geqslant \beta_1(t)x - P$. Also $t \mapsto \beta_1(t)$ is decreasing, so

$$\begin{aligned} v(t,x) &\leq \sup_{\tau \geq 0} \mathrm{E}\big[\mathrm{e}^{-\int_0^\tau \tilde{r}(t+u)\mathrm{d}u} (\beta_1(t+\tau)X_\tau)\big] \\ &\leq \sup_{\tau \geq 0} \mathrm{E}\big[\mathrm{e}^{-\int_0^\tau \tilde{r}(t+u)\mathrm{d}u} (\beta_1(t)X_\tau)\big]. \end{aligned} \tag{3.5.31}$$

The process $u \mapsto \mathrm{e}^{-\int_t^{t+\tau} \tilde{r}(u)\mathrm{d}u} X_{t+u}$ is a positive supermartingale, so using Assumption 3.2.2 and from Doob's optimal sampling theorem we obtain

$$\mathrm{E}\big[\mathrm{e}^{-\int_t^{t+\tau} \tilde{r}(u)\mathrm{d}u} X_{t+u}\big] \leq x. \tag{3.5.32}$$

From (3.5.31) and (3.5.32)

$$v(t,x) \leq \beta_1(t)x. \tag{3.5.33}$$

Then

$$\beta_1(t)x - P \leq v(t,x) \leq \beta_1(t)x. \tag{3.5.34}$$

Using (3.5.34) we conclude that

$$|v(t,x)| \leq P + \beta_1(t)x. \tag{3.5.35}$$

Based on this, we get

$$\begin{aligned} \mathrm{E}\big[\mathrm{e}^{-\int_0^{T-t} \tilde{r}(t+u)\mathrm{d}u} v(T, X_{T-t})\big] &\leq \mathrm{E}\big[\mathrm{e}^{-\int_0^{T-t} \tilde{r}(t+u)\mathrm{d}u} (P + \beta_1(T)X_{T-t})\big] \\ &\leq \mathrm{E}\big[\mathrm{e}^{-\int_0^{T-t} \tilde{r}(t+u)\mathrm{d}u} P\big] \\ &\quad + \mathrm{E}\big[\mathrm{e}^{-\int_0^{T-t} \tilde{r}(t+u)\mathrm{d}u} (\beta_1(T)X_{T-t})\big]. \end{aligned} \tag{3.5.36}$$

We see that

$$\mathrm{e}^{-\int_0^{T-t} \tilde{r}(t+u)\mathrm{d}u} P \to 0 \tag{3.5.37}$$

as $T \to \infty$ and using Assumption 3.2.2,

$$\mathrm{e}^{-\int_0^{T-t} \tilde{r}(t+u)\mathrm{d}u} X_{T-t} \to 0 \tag{3.5.38}$$

as $T \to \infty$. Hence,

$$\lim_{T\uparrow\infty} \mathrm{E}_x\left[\mathrm{e}^{-\int_0^T \tilde{r}(t+u)\mathrm{d}u} v(T, X_{T-t})\right] = 0, \tag{3.5.39}$$

and the lemma is proved. □

This helps to prove the next theorem.

Theorem 3.5.7. *If the optimal boundary is monotonic then, for all $(t,x) \in \mathbb{R}^2_+$, the value function is represented by*

$$v(t,x) \equiv -\mathrm{E}\left[\int_0^\infty \mathrm{e}^{\int_0^s \tilde{r}(t+u)\mathrm{d}u} H(t+s, X_s) \mathbb{1}_{\{(t+s,X_s)\in S\}} \mathrm{d}s\right] \tag{3.5.40}$$

and the optimal boundary $t \to b(t)$ is the unique continuous solution of the following nonlinear integral equation: for all $t > 0$

$$g(t, b(t)) \equiv -\mathrm{E}\left[\int_0^\infty \mathrm{e}^{\int_0^s \tilde{r}(t+u)\mathrm{d}u} H(t+s, X_s^{b(t)}) \mathbb{1}_{\{X_s^{b(t)} \geq b(t+s)\}} \mathrm{d}s\right]. \tag{3.5.41}$$

Proof. Here we only show how to obtain (3.5.40) then substitute $x = b(t)$ into (3.5.40) and using $v(t, b(t)) = g(t, b(t))$ we obtain (3.5.41). The proof of uniqueness is standard [107, Ch. VII §25.2, page 386] so we omit it. Thanks to Theorem 3.5.3 we have $v \in C^1(\mathbb{R}^2_+)$ and thanks to Corollary 3.5.4 we have $\partial_{xx} v$ continuous on $(\mathbb{R}^2_+)\backslash\partial C$. Then, we can find a mollifying sequence $(v_n)_{n\geq 0} \subseteq C^\infty(\mathbb{R}^2_+)$ for v such that

$$(v_n, \partial_x v_n, \partial_t v_n) \to (v, \partial_x v, \partial_t v) \tag{3.5.42}$$

as $n \to \infty$, uniformly on any compact sets , and

$$\lim_{n\to\infty} \partial_{xx} v_n(t,x) = \partial v(t,x) \text{ for all } (t,x) \notin \partial C \tag{3.5.43}$$

Let $(K_m)_{m\geq 0}$ be a sequence of compact sets converging to $\mathbb{R}^2_+$ and define

$$\tau_m := \inf\{s > 0 : (t+s, X_s^x) \notin K_m\} \wedge (T-t). \tag{3.5.44}$$

Then an application of *Itô formula* gives

$$\begin{aligned} v_n(t,x) = \mathrm{E}\left[\mathrm{e}^{\int_0^{\tau_m} \tilde{r}(t+u)\mathrm{d}u} v_n(t+\tau_m, X_{\tau_m}^x)\right] \\ - \mathrm{E}\left[\int_0^{\tau_m} \mathrm{e}^{\int_0^s \tilde{r}(t+u)\mathrm{d}u} \left(\partial_t v_n + L v_n - \tilde{r} v_n\right)(t+s, X_s) \mathbb{1}_{\{(t+s,X_s)\in S\}} \mathrm{d}s\right]. \end{aligned} \tag{3.5.45}$$

Let $n \to \infty$ and use (3.5.42) and (3.4.9), upon noticing that $(t+s, X_s)$ lies in a compact set for $s \leq \tau_m$ and that its law is absolutely continuous with respect to Lebesgue measure on $\mathbb{R}_+ \times \mathbb{R}_+$. The latter implies $\mathrm{P}\left[(t+s, X_s^x) \in \partial C\right] = 0$ for all $s \in [0, \infty)$ and enables the use of (3.5.43). Recall that v, v_x, v_t and v_{xx} are locally bounded. Then dominated convergence and (3.5.45) yield

$$\begin{aligned} v(t,x) &= \lim_{n\to\infty} v_n(t,x) \\ &= \mathrm{E}\left[\mathrm{e}^{\int_0^{\tau_m} \tilde{r}(t+u)\mathrm{d}u} v(t+\tau_m, X^x_{\tau_m})\right] \\ &\qquad - \mathrm{E}\left[\int_0^{\tau_m} \mathrm{e}^{\int_0^s \tilde{r}(t+u)\mathrm{d}u} H(t+s, X_s) \mathbb{1}_{\{(t+s,X_s)\in S\}} \mathrm{d}s\right]. \end{aligned} \tag{3.5.46}$$

Recall that $(t+s, X_s) \in S \iff X_s \geq b(t+s)$ then,

$$\begin{aligned} v(t,x) &= \mathrm{E}\left[\mathrm{e}^{\int_0^{\tau_m} \tilde{r}(t+u)\mathrm{d}u} v(t+\tau_m, X^x_{\tau_m})\right] \\ &\qquad - \mathrm{E}\left[\int_0^{\tau_m} \mathrm{e}^{\int_0^s \tilde{r}(t+u)\mathrm{d}u} H(t+s, X_s) \mathbb{1}_{\{X^{t,x}_{t+s} \geq b(t+s)\}} \mathrm{d}s\right]. \end{aligned} \tag{3.5.47}$$

We take $m \to \infty$ and, noticing that $\tau_m \to (T-t)$, we obtain

$$\begin{aligned} v(t,x) &= \mathrm{E}\left[\mathrm{e}^{\int_0^{T-t} \tilde{r}(t+u)\mathrm{d}u} v(T, X^x_{T-t})\right] \\ &\qquad - \mathrm{E}\left[\int_0^{T-t} \mathrm{e}^{\int_0^s \tilde{r}(t+u)\mathrm{d}u} H(t+s, X_s) \mathbb{1}_{\{X^{t,x}_{t+s} \geq b(t+s)\}} \mathrm{d}s\right]. \end{aligned} \tag{3.5.48}$$

Using Corollary 3.5.6 and letting $T \mapsto \infty$ we finally have

$$v(t,x) = -\mathrm{E}\left[\int_0^{\infty} \mathrm{e}^{\int_0^s \tilde{r}(t+u)\mathrm{d}u} H(t+s, X_s) \mathbb{1}_{\{(t+s,X_s)\in S\}} \mathrm{d}s\right]. \tag{3.5.49}$$

At time t, $v(t,x) = g(t,x)$ and the integral equation is obtained by setting $(t,x) = (t, b(t))$ such that

$$v(t, b(t)) = g(t, b(t)) = -\mathrm{E}\left[\int_0^{\infty} \mathrm{e}^{\int_0^s \tilde{r}(t+u)\mathrm{d}u} H(t+s, X_s) \mathbb{1}_{\{X^{t,b(t)}_s \geq b(t+s)\}} \mathrm{d}s\right]. \tag{3.5.50}$$

□

3.6 Numerical computation

In this section we show the algorithm for the numerical solution to the boundary function and give some economic interpretation of the results.

3.6.1 Boundary equation

Based on obvious complications, it is difficult solve (3.5.50) analytically but can be dealt with numerically. We use the Picard scheme to numerically solve (3.5.50). The steps are illustrated as follows. At the outset, applying Fubini to (3.5.50) gives rise to

$$\begin{aligned} g(t,b(t)) &= -\int_0^\infty \mathrm{e}^{\int_0^s \tilde{r}(t+u)\mathrm{d}u}\mathrm{E}\left[H(t+s,X_s)\mathbb{1}_{\{X_s^{t,b(t)}\geq b(t+s)\}}\right]\mathrm{d}s \\ &= -\int_0^\infty \mathrm{e}^{\int_0^s \tilde{r}(t+u)\mathrm{d}u}\left(\int_{b(t+s)}^\infty H(t+s,y)p(t+s,y,t,b(t))\mathrm{d}y\right)\mathrm{d}s \end{aligned} \tag{3.6.1}$$

where $p(t+s,y,t,b(t)) = \partial P(X_{t+s}^{t,b(t)} \leq y)$ is the transition density of the geometric Brownian motion. Set $\Pi := \{0 := t_0 < t_1 < \cdots < t_n := T\}$ be an equispaced partition of $[0,T]$ for some large T with mesh $h = 1/n$. The algorithm is initialised by letting $b^{(0)}(t_j) := 1$ for all $j = 0,1,\ldots,n$. Then set $b^{(k-1)}(t_j)$ as the derived boundary values after the k-th iteration. Next, the (k)-th iteration for all $j = 0,1,\ldots,n$ using

$$\begin{aligned} &g(t_j,b^{(k)}(t_j)) \\ &= -\int_0^T \mathrm{e}^{\int_0^s \tilde{r}(t_j+u)\mathrm{d}u}\left(\int_{b^{(k-1)}(t_j+s)}^\infty H(t_j+s,y)p(t_j+s,y,t_j,b^{(k-1)}(t_j))\mathrm{d}y\right)\mathrm{d}s. \end{aligned} \tag{3.6.2}$$

It is obvious that

$$p(t+s,y,t,b(t)) = \frac{1}{y\sigma\sqrt{2\pi s}}\exp\left(-\frac{\left(\ln(y)-\ln(b(t))-\left(\mu-\frac{\sigma^2}{2}\right)s\right)^2}{2\sigma^2 s}\right). \tag{3.6.3}$$

Substitute (3.6.3) and (3.4.5) into (3.6.2) to derive

$$g(t_j,b^{(k)}(t_j)) = -\int_0^T I\left(t_j+s,b^{(k-1)}(t_j+s),t_j,b^{(k-1)}(t_j)\right)\mathrm{d}s \tag{3.6.4}$$

where

$$\begin{aligned} &I\left(t_j+s,b^{(k-1)}(t_j+s),t_j,b^{(k-1)}(t_j)\right) \\ &\quad := \mathrm{e}^{\int_0^s \tilde{r}(t_j+u)\mathrm{d}u}\tilde{r}(t_j+s)P\left(1-\Phi\left(\xi^{(k-1)}(t_j+s)\right)\right) \\ &\qquad + \mathrm{e}^{\int_0^s \tilde{r}(t_j+u)\mathrm{d}u}\lambda_0(t_j+s)\beta(t_j+s)b^{(k-1)}(t_j)\mathrm{e}^{\mu s}P\left(1-\Phi\left(\zeta^{(k-1)}(t_j+s)\right)\right) \end{aligned} \tag{3.6.5}$$

In particular, Φ is the cumulative density of a standard normal distribution,

$$\xi^{(k-1)}(t_j+s) := \frac{\ln\left(\frac{b^{(k-1)}(t_j+s)}{b^{(k-1)}(t_j)}\right)-\left(\mu-\frac{\sigma^2}{2}\right)s}{\sigma\sqrt{s}} \tag{3.6.6}$$

and

$$\zeta^{(k-1)}(t_j+s) \coloneqq \frac{\ln\left(\frac{b^{(k-1)}(t_j+s)}{b^{(k-1)}(t_j)}\right) - \left(\mu - \frac{\sigma^2}{2}\right)s - \sigma^2 s}{\sigma\sqrt{s}}. \tag{3.6.7}$$

The outer integral with respect to ds is computed by standard quadrature method. Thus, (3.6.4) becomes

$$g(t_j, b^{(k)}(t_j)) = -h\sum_{m=0}^{n-T-j} I\left(t_j + mh + \tfrac{h}{2}, b^{(k-1)}(t_j + mh + \tfrac{h}{2}), t_j, b^{(k-1)}(t_j)\right). \tag{3.6.8}$$

Given the gain function as in (3.2.13), (3.6.2) can further be expressed as

$$\begin{aligned} &b^{(k)}(t_j) \\ &= \frac{1}{\beta_1(t_j)}\left[P - \int_0^T \vartheta(t_j, s)\left(\int_{b^{(k-1)}(t_j+s)}^{\infty} H(t_j+s, y)p(t_j+s, y, t_j, b^{(k-1)}(t_j))dy\right)\right]\mathrm{d}s \end{aligned} \tag{3.6.9}$$

where $\vartheta(t_j, s) \coloneqq \mathrm{e}^{\int_0^s \tilde{r}(t_j+u)\mathrm{d}u}$. Hence,

$$\begin{aligned} &b^{(k)}(t_j) \\ &= \frac{1}{\beta_1(t_j)}\left[P - h\sum_{m=0}^{n-T-j} I\left(t_j + mh + \tfrac{h}{2}, b^{(k-1)}(t_j + mh + \tfrac{h}{2}), t_j, b^{(k-1)}(t_j)\right)\right]. \end{aligned} \tag{3.6.10}$$

The algorithm stops when the tolerance condition

$$\max_{j=0,1,\ldots,n} |b^{(k)}(t_j) - b^{(k-1)}(t_j)| < \epsilon \tag{3.6.11}$$

is fulfilled for some $\epsilon > 0$. The Python codes for this algorithm are in Appendix A.2.

3.6.2 Economic interpretation of the assumptions

An insight into the assumptions and conditions that determines the shape of the optimal boundary is provided as follows.

- The benefit schedule $\beta(t)$ in (3.2.6) is function motivated by the declining unemployment compensation system. The time dependent parameters that influence the increase or decrease of the benefit schedule are the inflation rate $r(t)$ and the employment rate $\lambda_1(t)$. According to [10, 92, 82], $r(t)$ and $\lambda_1(t)$ are directly related which means an increase in inflation rate $r(t)$ pushes employment rate $\lambda_1(t)$

and a decrease in inflation rate $r(t)$ leads to a fall employment rate $\lambda_1(t)$. It is interesting to note that a surge in $r(t)$ and $\lambda_1(t)$ leads to a decline in the benefit schedule and a fall in $r(t)$ and $\lambda_1(t)$ causes a rise in the benefit schedule. This is because when inflation and employment rates are high individuals in the UI scheme receive benefits for relatively shorter amounts of time leading to smaller benefits. In the same way a fall in inflation and employment rate results in unemployed worker in the UI scheme earning more because the benefit is received for a longer period of time.

- In Assumption 3.2.2, we see that $r(t) + \lambda_0(t) \geq \mu$. In real life application, the wage growth rate is rather small and may possibly exceed the inflation rate $r(t)$, but even if it does, then it is hardly likely economically greater than the combined inflation-unemployment rate $r(t) + \lambda_0(t)$.
- The assumptions from Proposition 3.3.2 have clear economic appeals.

  (i) On one hand, an increase in the mapping $t \mapsto \tilde{r}(t)$ and decrease in the mapping $t \mapsto \lambda_0(t)\beta(t)$ demands that $t \mapsto r(t)$ and $t \mapsto \lambda_0(t)$ are increasing. In reality when inflation rises, prices of goods and services also rise. The available wage purchases fewer amounts of goods and services over time which leads to the demand for higher wages by workers. The rise in wage increment claims coupled with the fall in the purchase of goods and services causes a reduction in the returns on economic activities. Companies then publish lesser number of vacancies and may even lay off some workers. In due course, unemployment rate increases but at a relatively slow rate [83]. In Section 2.6.4, we see that as unemployment rate increases, the value function increases which reflects the efficiency of the insurance policy against the risk of unemployment because the benefit received when unemployment occurs is paid relatively early and for a longer period. An increase in the value function over time also leads to an increase in the mapping $t \mapsto u(t, x)$ defined in (3.3.5). In Corollary 3.4.5, the increase in $t \mapsto u(t, x)$ results in an increasing optimal boundary $t \mapsto b(t)$. This has an economic appeal because a larger rate of unemployment means a higher risk of losing the job. However before unemployment begun to rise, wages were increased to compensate for the increasing inflation rate. Thus, even though the optimal boundary is increasing, the wage is increasing fast enough in order to expedites joining

the the insurance scheme.

(ii) On the other hand, the increase in the mapping $t \mapsto \lambda_0(t)\beta(t)$ and the decrease in the mapping $t \mapsto \tilde{r}(t)$ requires that $r(t)$ and $\lambda_0(t)$ are decreasing and increasing respectively. A rise in unemployment rate coupled with a declines in inflation rate and employment rate usually happens during uncertainty shock periods such as the great financial recession in 2002 [10, 128, 92]. The macroeconomic effects of uncertainty shocks on the unemployment rate is intensified through falls in aggregate demand. Firms put out fewer job vacancies as a result of the decline in aggregate demand which amplifies the increase in unemployment rate. Consequently, household income falls more because individuals searching for jobs are unable to find jobs. This results in a further fall in aggregate demand, which amplifies the influence of uncertainty shocks. Prices of goods and services are decreased to meet the decline in aggregate demand and eventually inflation falls [25, 82]. Using similar arguments in (i), the rise in unemployment and the fall in inflation and employment suggest a decline in the value function and the mapping $t \mapsto u(t,x)$. This invariably leads to a decaying the optimal boundary based on Corollary 3.4.5. The economic rationale for the decreasing optimal boundary is that the wage of the worker is relatively low so a decreasing optimal threshold is required to accelerate the joining of the UI scheme.

- Furthermore, sufficient conditions were derived in Corollary 3.3.3 to support Proposition 3.3.2. Thus, we substitute $\gamma = 34.7$ and $\delta = 0.0094$ from the French UI system (see [76, p. 8]) into the sufficient conditions to derive the following results.

  (i) For $t \mapsto u(t,x)$ to increase

  $$\frac{\lambda_0'(t)}{\lambda_0(t)} < \frac{1}{\gamma+\delta} \implies \lambda_0(t) < \lambda_0(0) + \mathrm{e}^{\frac{t}{34.7094}}. \tag{3.6.12}$$

  (ii) Alternatively for $t \mapsto u(t,x)$ to decrease

  $$\frac{\lambda_0'(t)}{\lambda_0(t)} \geq \frac{1}{\gamma+\delta} \implies \lambda_0(t) \geq \lambda_0(0) + \mathrm{e}^{\frac{t}{34.7094}}. \tag{3.6.13}$$

Next we derive functions that will be used to verify the assumptions and conditions above.

3.6.3 Model parameters for numerical illustration

In order to exercise the stopping rule (3.2.22) the individual involved needs to be able to compute the optimal threshold expressed in (3.6.1), for which the knowledge is required about $\beta(t)$ and $\beta_1(t)$ (defined in (3.2.6) and (3.2.11) respectively). In addition, information on the parameters $r(t)$, $\lambda_0(t)$, $\lambda_1(t)$, h_0, γ, δ, μ and σ is essential along with Assumptions 3.2.2 and 3.2.1. Specifically:

- The loss-of-job rate $\lambda_0(t)$, re-employment rate $\lambda_1(t)$ and inflation rate $r(t)$ can be extracted from using publicly available data from the Office for National Statistics (ONS) [135, 134]. Detailed analysis and modelling of this data will be done in the next chapter (Chapter 4). In the meantime, for simplicity we use the automated trend-line exponential equations from Excel.
- Furthermore, the wage growth rate μ, a simple approach is just to set $\mu = 0.004$ as done in Section 2.5. Recall that it may be possible that the individual's wage growth rate μ is, to some extent must not exceed the inflation rate $r(t)$ as seen in Assumption 3.2.2. Practically, this would often mean that the actual growth rate μ is kept at the lowest possible level.
- Similarly, the volatility σ^2 can be estimated by using the suitable value in Section 2.5.
- To be specific, the French UI system back in the 1990s (see [76, p. 8]) gives rise to choosing the following numerical values in (2.2.3): $h_0 = 0.574$, $s_0 = 8\,(52/12) \doteq 34.7$ (weeks) and $\delta = -(3/52)\ln(1 - 0.15) \doteq 0.0094 = 0.94\%$ (per week).
- Finally, given that $\beta(t)$ and $\beta_1(t)$ should be available through the insurance policy's terms and conditions are derived from the above parameters, they can be calculated or estimated. We calculated them in for this numerical illustration

In summary, certain estimation procedures are executed along with the on-line observation of the wage dynamics (X_t). Given the parameters in the section above, where all equations under consideration can be seen as special cases, it is clear that the numerical solution to (3.5.41) takes different forms. More details showing numerical solutions given specific model parameters are provided in the next subsection.

3.6.4 Numerical examples

The monetary unit used is the euro and set the premium $P = 9\,000.00$ (euro). The numerically illustrate is done for two cases according to Proposition (3.3.2) where, (i) $t \mapsto u(t,x)$ and $t \mapsto b(t)$ are increasing and (ii) $t \mapsto u(t,x)$ and $t \mapsto b(t)$ are decreasing.

Example 3.6.1. First of all for (i), set the inflation rate equation as

$$r(t) = 0.0252\mathrm{e}^{0.0012t}, \tag{3.6.14}$$

the loss-of-job rate $\lambda_0(t)$ equation as

$$\lambda_0(t) = 0.0596\mathrm{e}^{0.0004t}, \tag{3.6.15}$$

and the re-employment rate $\lambda_1(t)$ equation as

$$\lambda_1(t) = 0.7076\mathrm{e}^{0.0007t}. \tag{3.6.16}$$

The corresponding results using the equations shown above are displayed in Fig. 9. The wage dynamics are not very visible in the plots of the optimal boundary in Fig. 9(a) and Fig. 10(a) because the initial wage is relatively low. In order to show the lines in details, we insert a subplot that zooms the wage process. When $X_0 = 346$, the wage process never hits the optimal boundary within the time interval. The optimal time of entry in this case when $X_0 = 60\,000$ is

$$\tau^* = 75. \tag{3.6.17}$$

At $\tau_* = 75$, the wage is given by

$$b(\tau^*) = 88\,601.49757 \approx 88\,601 \text{ (euro)} \tag{3.6.18}$$

Also using (3.2.25), we obtain the value of this contract at the time of entry is

$$v(\tau^*, b(\tau^*)) = (\beta_1(\tau^*) \times b[\tau^*]) - P = 299.5549 \approx 300 \text{ (euro)}. \tag{3.6.19}$$

The computed benefit schedule is shown in Fig. 11 to highlight that it is declining.

Example 3.6.2. For (ii), set the inflation rate equation as

$$r(t) = 0.0909\mathrm{e}^{-0.009t}, \tag{3.6.20}$$

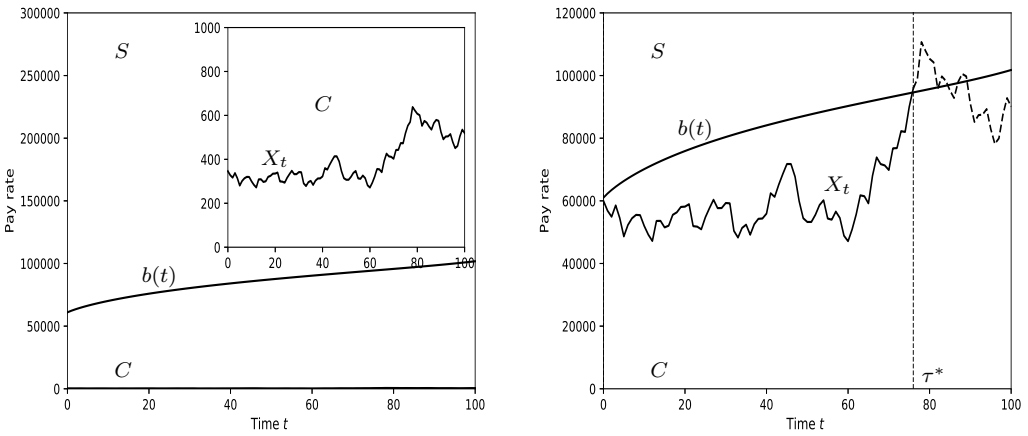

(a) Optimal boundary with $X_0 = 346$ (b) Optimal boundary with $X_0 = 60\,000$

FIGURE 9: Numerical values of the parameters used are $\mu = 0.0004$, $P = 9\,000$ and $\sigma = 0.04$. In particular, (a) is a plot which contains subplot that zooms the entry time of a sample path a wage process (geometric Brownian motion) X starting at $X_0 = 346$. The geometric Brownian motion does not hits the optimal boundary. (b) A plot of a sample path a wage process (geometric Brownian motion) X starting at $X_0 = 60\,000$. The geometric Brownian motion hits the optimal boundary at $\tau^* = 75$. The boundary divides the state space into the continuation region C and the stopping region S.

the loss-of-job rate $\lambda_0(t)$ equation as

$$\lambda_0(t) = 0.0878\mathrm{e}^{0.0009t}, \tag{3.6.21}$$

and the re-employment rate $\lambda_1(t)$ equation as

$$\lambda_1(t) = 0.7245\mathrm{e}^{-0.05t}. \tag{3.6.22}$$

The corresponding results using the equations shown above are displayed in Fig. 10. The optimal time of entry in this case is

$$\tau^* = 62. \tag{3.6.23}$$

At $\tau_* = 62$, the wage is given by

$$b(\tau^*) = 287.3488 \approx 287 \text{ (euro)} \tag{3.6.24}$$

Also using (3.2.25), we obtain the value of this contract at the time of entry is

$$v(\tau^*, b(\tau^*)) = (\beta_1(\tau^*) \times b[\tau^*]) - P = 417.5570 \approx 418 \text{ (euro)}. \tag{3.6.25}$$

Also the computed benefit schedule is shown in Fig. 11 to demonstrate that it is in-

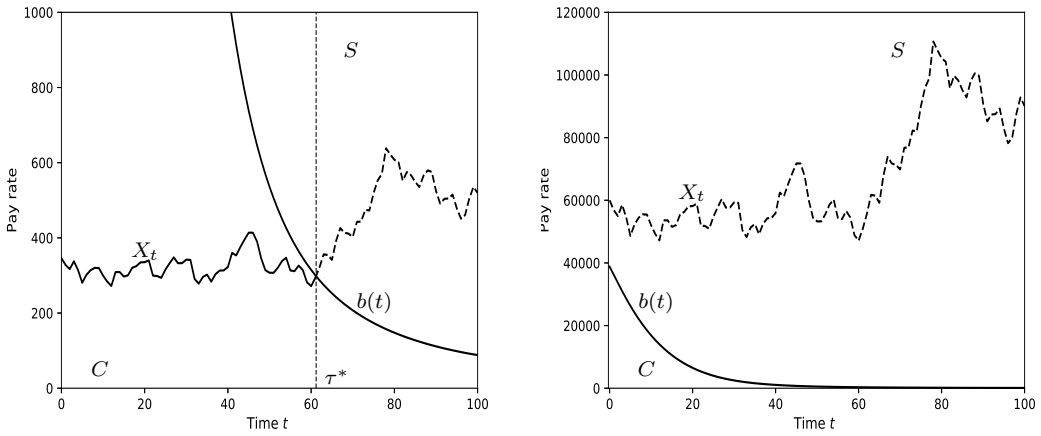

(a) Optimal boundary with $X_0 = 346$

(b) Optimal boundary with $X_0 = 60\,000$

FIGURE 10: Numerical values of the parameters used are $\mu = 0.0004$, $P = 9\,000$ and $\sigma = 0.04$. In particular, (a) is a plot that zooms the entry time of a sample path a wage process (geometric Brownian motion) X starting at $X_0 = 346$. The geometric Brownian motion hits the optimal boundary at $\tau^* = 62$. (b) A plot of a sample path a wage process (geometric Brownian motion) X starting at $X_0 = 60\,000$. The geometric Brownian motion does not need to hit the optimal boundary because it starts in the stopping region thus $\tau^* = 0$. The boundary divides the state space into the continuation region C and the stopping region S.

creasing.

3.6.5 Economic interpretation of results

A monotonic decline or increment of the optimal boundary is as a result of the changes in the various rates. First and foremost, from Sections 2.6.4 and 3.6.2 we see that for (i), a bigger rate of unemployment means a higher risk of losing the job. Nonetheless, before unemployment begun to rise, wages were increased to compensate for the increase in inflation rates. Thus, even though the optimal boundary is increasing, the wage is increasing fast enough in order to expedite joining the insurance scheme. For (ii), a

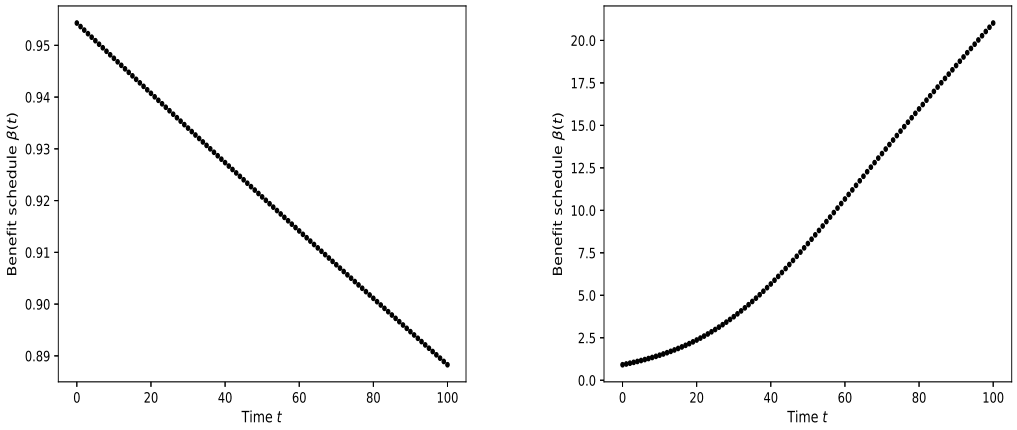

(a) Benefit schedule when $t \to b(t)$ is increasing (b) Benefit schedule when $t \to b(t)$ decreasing

FIGURE 11: Numerical values of the parameters used are $s_0 = 34.7$ and $\delta = 0.0094$. In particular, (a) is the trajectory of the benefit schedule in (3.2.6) for Example 3.6.1. (b) The trajectory of the benefit schedule in (3.2.6) for Example 3.6.2.

rise in unemployment rate leads to a decaying optimal boundary because the wage of the worker is relatively low so a decreasing optimal threshold is required to accelerate the joining of the UI scheme. These results are reflected in the numerical examples (Example 3.6.1 and Example 3.6.2) for the time-dependent case.

It is important to note that in Fig. 9, even though the wage drops back below the boundary after the optimal time, the wage values are relatively very high. Since the financial crisis, uncertainty has been a concept that has kept most businesses on their toes. High income earners such as CEOs have responded by buying unemployment insurance to mitigate the costs of a potential unemployment. Thus, even though the optimal boundary is increasing, the level of uncertainty from a high income earner's point of view is a good basis to make the individual choose to enter the UI scheme for unemployment coverage over a fall in wage. Thus, a high income earners is satisfied to have purchased the scheme before the wage dropped further.

The unemployment rate is set as an increasing function for both examples based on the assumptions but its values over time are relatively higher values in Example 3.6.2 than in Example 3.6.1. When the same wage dynamics ($X_0 = 346$) is used to find the optimal entry time in both examples, we observe that in Example 3.6.1 (see Fig. 9(a)), the optimal entry time may occur at a further time outside the time interval. This value

is bigger that the optimal entry time in Example 3.6.1 which is 62 with initial wage $X_0 = 346$. When the initial value of the wage dynamics is increased ($X_0 = 60\,000$) the optimal entry time in Example 3.6.2 is 75 and the optimal entry time in Example 3.6.1 is 0. Even tough more sensitivity analysis may be to be conducted, based on this we can say that a rise in the unemployment rate means the individual are more likely to enter the UI scheme earlier.

Furthermore, as explained in Section 3.6.2, the benefit schedule $\beta(t)$ in (3.2.6) falls when $r(t)$ and $\lambda_1(t)$ are increasing. This is illustrated in Fig. 11. When inflation and employment rates are high, individuals in the UI scheme receive benefits for relatively shorter amounts of time which leads to smaller benefits because they find jobs faster. In the same way a fall in inflation and employment rate results in unemployed worker in the UI scheme earning more because the benefit is received for a longer period of time.

The value of the UI scheme is also affected by the time varying rates. Lower values of the lose-of-job rates results along with increasing inflation and employment rates produces lower values of the UI scheme. This is because the value function is computed using the benefit schedule and the wage of the individual. On the other hand, a higher values of the unemployment rate coupled with decaying inflation and employment rates higher values of the UI scheme.

Most workers would like to have some financial security when they loose their jobs and this can be done using UI schemes. This study is a good starting point to aid individuals decide when to purchase the UI scheme given that they know the rate of inflation, unemployment and reemployment in their respective living environments.

To emphasis, an interesting point is the inclusion of publicly available rate performance; specifically for unemployment and employment rates in the UI model to make it realistic. It is essential to examine the data to set more accurate assumptions as well as modify our UI model if necessary. Thus, in the subsequent chapter (Chapter 4) we explore, analyse and model the UK labour force data.

Chapter 4

Analysis and Modelling of the Labour Force Data

Our UI scheme can be made more realistic by incorporating labour force data. In this chapter the labour force data from the Office for National Statistics (ONS) in the United Kingdom is used. A brief overview of the data is given to understand the levels, rates and flow of the labour market. Due to the assumption that the time until the current employment ends, τ_0, and the unemployment spell of duration, τ_1, had exponential distribution in Chapter 2 and Chapter 3 which guarantees a Markovian nature of the corresponding transitions, multi-state models are then used to investigate the movement in the labour market. We also determine the distribution that best fits the data to serve as a guide to a possible modification of the UI model in Chapter 2 and Chapter 3.

4.1 Labour force data

The data for the parameterisation of the holding time τ_0 and τ_1 in our UI scheme models is derived from the Office for National Statistics (ONS) in the United Kingdom (UK) [135, 134]. The labour force data is collected by conducting labour force surveys (LFS) that gather information from respondents (0.2% of the population living in the UK), with the intent of extrapolating the results to reflect the status of the larger

population. Only respondents who meet the basic criterion, that is, are between the working age of 16 to 64 are only considered for the LFS. The labour force data most importantly provides in-depth insights regarding the change in economic situation of each respondent over time on a quarterly basis. This is key to enable modelling the flow of the labour market in this study.

The labour force data used in this study has been collected 73 consecutive times between October 2001 to December 2019 on a quartely basis with variables that represent information on the labour market. These variables are classified into employment (E), unemployment (U) and inactivity (I). The first category which is employment (E) comprises records on individuals in the labour force who are actively working. Next, is unemployment (U) which refers to jobless individuals who are actively looking for work. Finally, the economically inactive category represents individuals who are within the labour market however, not in search of, available or willing to work. Note that, the data estimates do not detail the effect of certain external factors such as early retirement, disability, mortality and immigration.

The data consistently captures details and insight into the levels, rates, inflows and outflows of the employment, unemployment and inactive states in the UK labour force. The data is inspected using descriptive statistics and data visualisation to check the quality and to give a general overview of the data to understand it better.

4.1.1 Descriptive statistics

In Table 4.1 details of all variables under consideration and their corresponding numerical attributes (minimum, 25th percentile, median, mean, maximum) are provided. Looking at the values in Table 4.1, we see that unemployment related variables give the lowest values, the inactivity related variables have the second lowest values and the employment related variables have the highest values for the numerical attributes. The mean net flow values for unemployment and inactivity are negative which means that on average more individuals exit unemployment and inactivity than enter. On the other hand, the mean net flow values in employment shows that on average more individuals enter employment than leave on average. However, the percentage change denoted by $\%\Delta$ between the minimum and maximum number of individuals throughout the observed time period shows that $\%\Delta U > \%\Delta E > \%\Delta I$. The computations are as follows $\%\Delta E = \frac{(31637095-27323941)\times 100}{27323941} = 15.79\%, \%\Delta U = \frac{(2661505-1256547)\times 100}{1256547} = 111.81\%$

and $\%\Delta I = \frac{(9487165-8477559)\times 100}{8477559} = 11.91\%$. Note that even though inactivity and unemployment have different values, they are sometimes collectively known as unemployment which is the sum of all inactivity and unemployment values depending on the application. In that case, when we consider an adjusted version of unemployment which is all unemployed individuals plus inactive individuals, we have that $\%\Delta U = \frac{(12121619-9734107)\times 100}{9734107} = 24.53\%$ and thus $\%\Delta U > \%\Delta E$.

4.1.2 Visualisation of the data

Next, we focus on data visualisation by exploring the levels and rates of employment, unemployment and inactivity as well as the inflows and outflows.

Levels of employed, unemployed and inactive individuals

We begin by observing the levels or number of employed, unemployed and inactive individuals. This is illustrated in Fig. 12. The first observation is that the levels of unemployment and inactivity have similar trends over the given time. We also see the development of unemployment and inactivity in the UK between 2001 and 2019 is characterised by the upswing period from 2001 through to 2012 and the downswing period from 2013 to 2019. The variation in the trajectory seems to be relatively higher and fluctuates more in the inactivity levels than the unemployment levels. We also observe that there was a steady increase from the early 2000's to 2007 in employment, unemployment and inactivity. In 2008 through to 2012, there was an abrupt rise in unemployment and inactivity due to people being laid off during the UK financial recession [10, 128, 92]. Consequently there was a swift fall in the number of employed individuals from 2008 to 2010. Following this fall was a steady slow rise mainly due to increment in the number of working immigrants with the permit to work in UK and young UK citizens coming of age to enter the labour market. The downswing from 2012 to 2019 in inactivity and unemployment levels is also known as the recovery period. This is when the economy stabilised after the uncertainty shock wave (2008 financial recession) hit [71, 114].

In this chapter, there are four rates of measurement; the transition rates, the probability rates, the percentage rates of change and the rates which show the proportion of the individuals in each state to the total labour force. Further details on these rates are provided as the computations unfold. Based on the information available in the data,

Variable Name	Minimum	Q1	Median	Mean	Q3	Maximum
Still in employment	26375458	27360394	27738572	28113045	28990491	30535621
Employment to Unemployment	252421	317974	344452	354245	387600	551005
Employment to Inactivity	448657	512763	539276	537225	565523	629774
Employment Gross Inflow	830616	859127	884104	891470	916915	1102218
Employment Gross Outflow	742360	859127	884104	891470	916915	1102218
Employment Net Flow	-271603	33323	109071	93448	162006	298479
Still in unemployment	580794	762557	868285	1019410	1381740	1750252
Unemployment to Employment	374809	432176	461977	475316	514720	607930
Unemployment to Inactivity	244446	280004	310827	325110	364907	445481
Unemployment Gross Inflow	445481	688748	743680	780480	908141	1034164
Unemployment Gross Outflow	635285	715911	766785	800427	892153	1001448
Unemployment Net Flow	-154103	-57222	-25801	-19946	6287	207280
Still in inactivity	7529392	7847554	7957874	7973301	8090436	8459134
Inactivity to Employment	368638	480975	512350	509601	546995	627106
Inactivity to Unemployment	315528	366897	418546	426235	483159	563155
Inactivity Gross Inflow	755716	829029	864144	862335	892165	1027671
Inactivity Gross Outflow	788711	902656	942634	935837	974423	1054284
Inactivity Net Flow	-203555	-109593	-86400	-73502	-22262	64323
Total labour level	37647261	39108168	40409452	39957991	40836553	41371202
Total employment level	27323941	28331085	28717529	29114982	29967006	31637095
Total unemployment level	1256547	1457096	1639274	1815145	2298712	2661505
Total inactivity level	8477559	8874713	9017104	9020853	9145256	9145256
Date	12/2001	06/2006	12/2010	11/2010	06/2015	12/2019

TABLE 4.1: Descriptive statistics of the data.

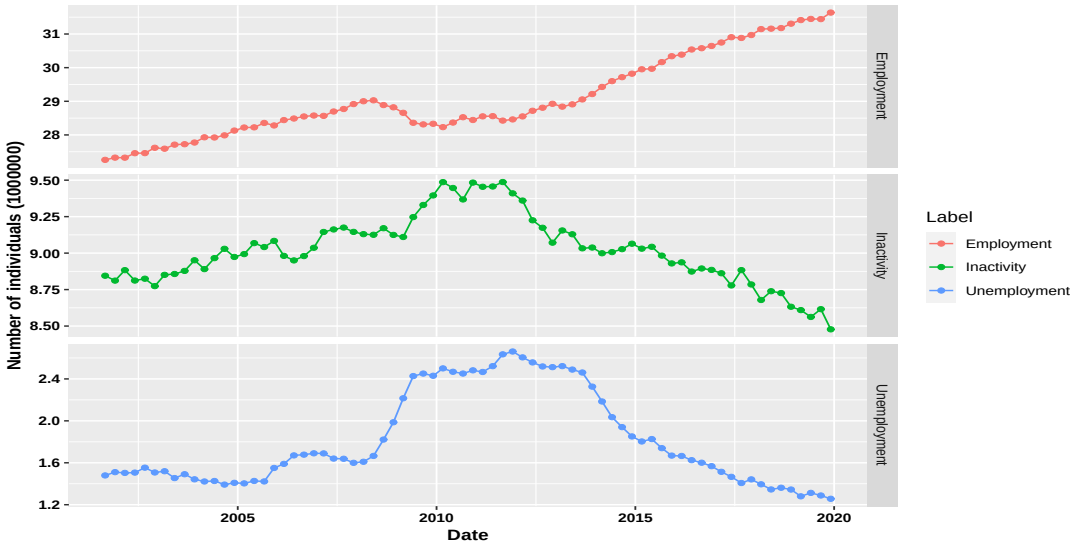

FIGURE 12: Plots of quarterly number of individuals in the UK who are employed (E), unemployed (U) and inactive (I) states from September 2001 to December 2019.

we explore the rates (proportions) in Fig. 13 and percentage rate of change in Fig. 14 of employment, unemployment and inactivity in the subsequent sections to know how fast levels have risen or declined over the period.

The employment, unemployment and inactivity rates

The rates for each state is computed as the corresponding levels for each state divided by the total number of individuals in the labour market [134]. A preview of the employment, unemployment and inactivity rates is displayed in Fig. 13. We see a swift rise in unemployment and inactivity rate during the financial recession period between 2008 to 2012. Specifically, the unemployment rate grew from approximately 5.3% to 8.7%, the rate of inactivity rose from about 22.7% to 23.8%, whilst the employment rate increase dropped from around 73% to 70%. Outside the financial recession period, we see a steady fall in the unemployment and inactivity rates and a steady rise in employment rate.

The employment, unemployment and inactivity percentage rate of change

The percentage rate of change, also known as percentage change denoted by $\%\Delta$, is derived by dividing the difference of the number of individuals in each state by the

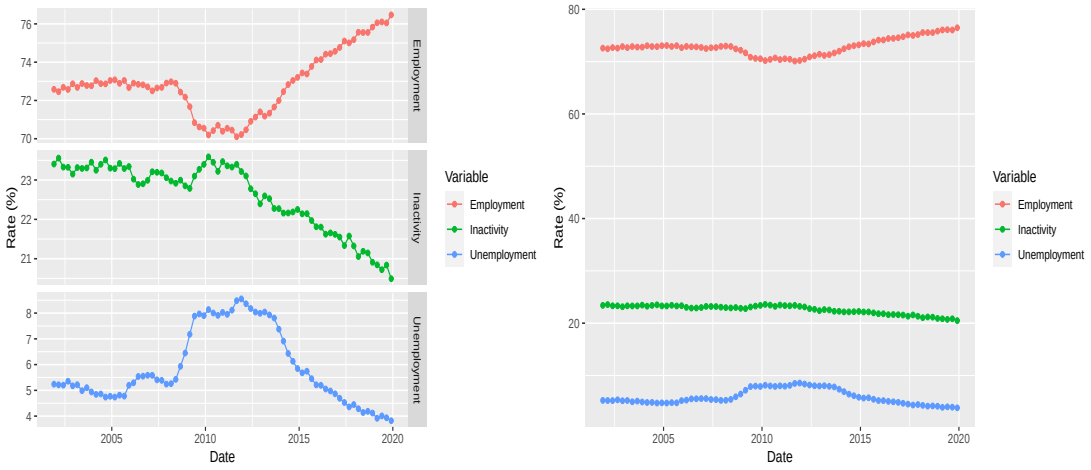

FIGURE 13: Plots of quarterly rates of employment (E), unemployment (U) and inactivity (I) from September 2001 to December 2019.

previous value. That is the percentage rates of change for employment, unemployment and inactivity at any quarterly date points denoted by t are given by $\%\Delta E(t) = \frac{E(t)-E(t-1)}{E(t-1)} \times 100\%, \%\Delta U(t) = \frac{U(t)-U(t-1)}{U(t-1)} \times 100\%$ and $\%\Delta I(t) = \frac{I(t)-I(t-1)}{I(t-1)} \times 100\%$ respectively. In Fig. 14, we observe that the $\%\Delta$ for unemployment fluctuates the most. This means the change in unemployment is the highest be it an increment or a decrement. Again, notice that $\%\Delta$ in employment are mostly equal to or above zero but within 2008 to 2012 we observe some falls below zero. This is due to financial recession. The $\%\Delta$ of inactivity mostly fluctuates between $+1$ and -1. During the recession period we also see an increment in $\%\Delta$ for unemployment and inactivity.

The employment, unemployment and inactivity inflows and outflows

Let us also note that the quarterly stock of individuals in employed (E), unemployed (U) and inactive (I) is obtained by accumulating the corresponding flow categories. Gross flows (inflows or outflows) are the total number of people moving from one state to another, for instance from employment (E) to unemployment (U), or inactivity (I), and the total number of people who move in the opposite direction (see Fig. 15 and Fig. 16). In total, there are nine different flow categories for the three economic activity groupings, with an additional two which are individuals entering or leaving working age. The net flows (inflows or outflows) are the differences between the total number of people in each of the three economic activity categories at two different time

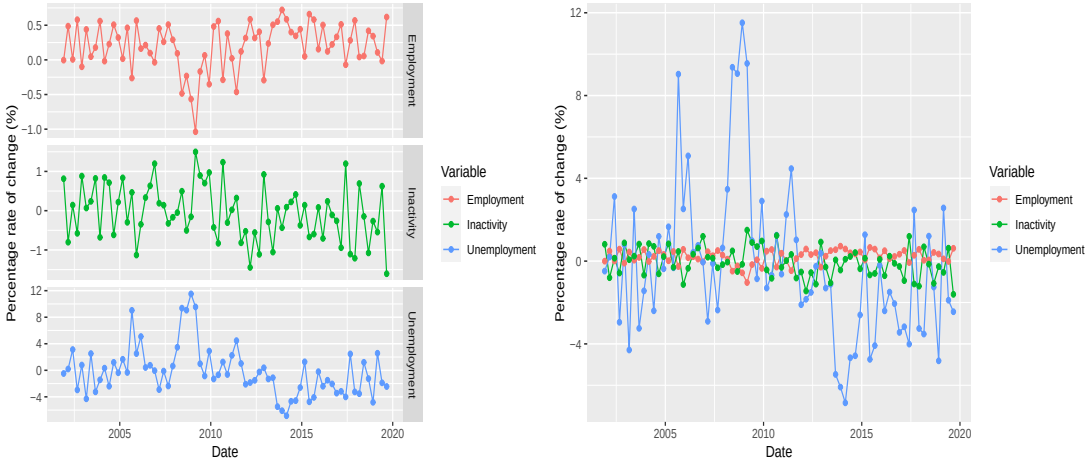

FIGURE 14: Plots of the quarterly percentage rate of change for employment (E), unemployment (U) and inactivity (I) from September 2001 to December 2019.

points (see Fig. 17).

Figure 15 indicates that holistically, the movement of individuals from the inactivity state is more than the flow of people from the employment state. Consequently, less number of people transfer from the unemployment state than the inactivity and employment state. Specifically, from 2001 to 2007 most people transitioned from the inactivity state at an average of 894347, the employment outflow at an average of 893350, and the unemployment outflow at an average of 730327. From 2008 to 2013, more individuals moved out of the inactivity state at an average of 965546 compared to the employment outflow at an average of 938508. The average unemployment outflow between 2008 to 2013 is 903467. Between 2013 and 2019, 857388 averagely got out of employment which is less than the average number of individuals that got out of inactivity (953698).

The mean gross outflow from unemployment from 2013 to 2019 is 795961. Figure 16 shows that outside the recession period (2008 to 2013), gross inflow for employment is less than gross inflow for inactivity. Also, the gross inflow for inactivity is less than the gross inflow of employment. The calculated averages for the gross inflows during the recession period demonstrates that $983756 > 928423 > 965546$ which are values of the employment, unemployment and inactivity gross inflows receptively.

Furthermore, the number of individuals who are employed is given by the summation of those who stay employed (EE), move from unemployment to employment (UE), and

transfer from inactivity to employment (IE) per quarters (see Fig. 18).The number of unemployed people per quarter is given by adding up those who move from employment to unemployment (EU), those who remain unemployed (UU) and those who transition from inactivity to unemployment (IU) (see Fig. 19). Finally, the sum of individuals that transfer from employment to inactivity (EI), change from unemployment to inactivity (UI), and those who keep on in inactive (II) gives the total number of inactive folks (see Fig. 21).

Figure 20 shows the quarterly number of individuals that transition from employment to employment (EE), employment to unemployment (EU), employment to inactivity (EI), unemployment to unemployment (UU), unemployment to employment (UE), unemployment to inactivity (UI), inactivity to inactivity (II), inactivity to employment (IE) and inactivity to unemployment (IU). Most individuals stay employed, followed by individuals that stay inactive, then lastly those that remain unemployed. Based on all the raised arguments and findings, it can be seen why the inactivity rate falls more steadily in Fig. 13 compared to the employment and unemployment rates.

(a) Gross outflows

(b) Gross outflows (split up)

FIGURE 15: Graphs illustrating the quarterly gross outflows from 2001 to 2019 into each state. In (a) the resulting three plots share the same x and y axis and in (b) the resulting three plots split up into three different y axes while the x axis remains in-tact.

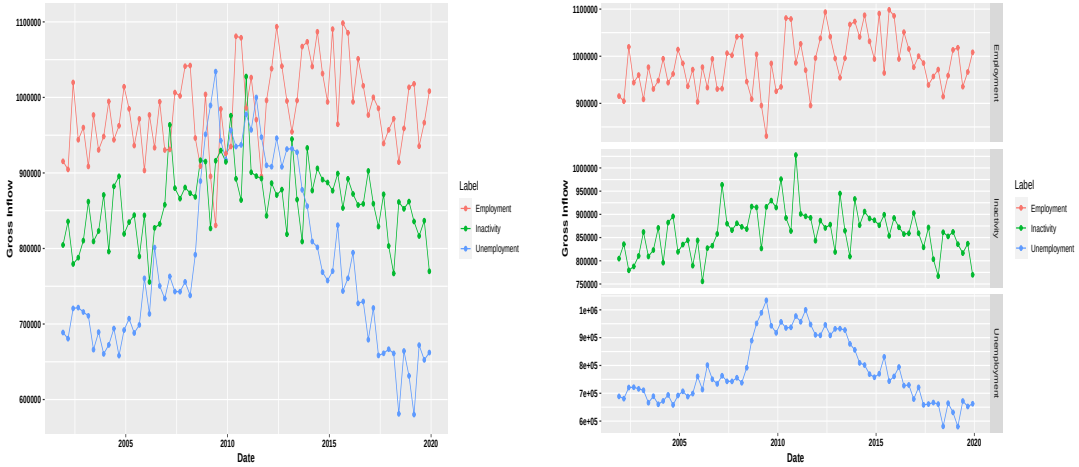

(a) Gross inflows

(b) Gross inflows (split up)

FIGURE 16: Graphs illustrating the quarterly gross inflows from 2001 to 2019 into each state. In (a) the resulting three plots share the same x and y axis and in (b) the resulting three plots split up into three different y axes while the x axis remains in-tact.

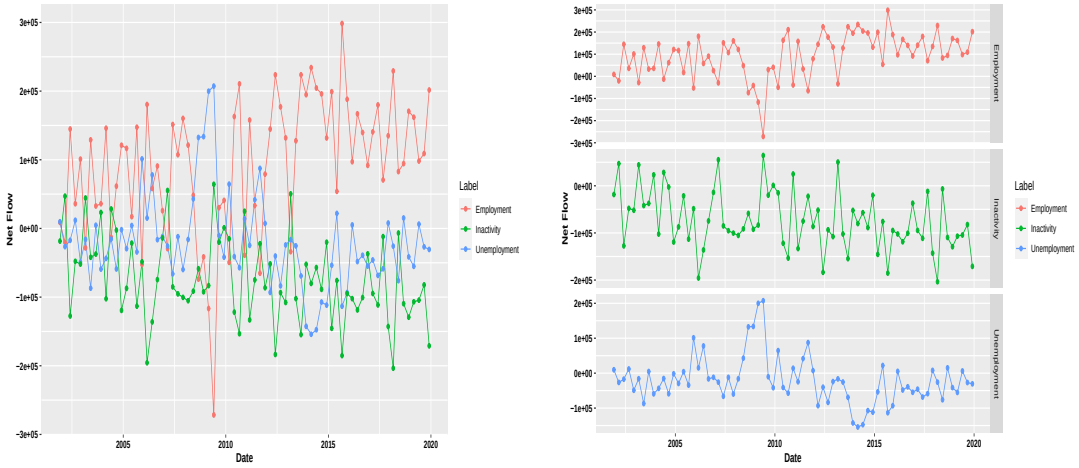

(a) Net flows

(b) Net flows (split up)

FIGURE 17: Graphs illustrating the quarterly net flows from 2001 to 2019 for each state. Specifically, in (a) the resulting three plots share the same x and y axis and (b) the resulting three plots split up into three different y axes while the x axis remains in-tact.

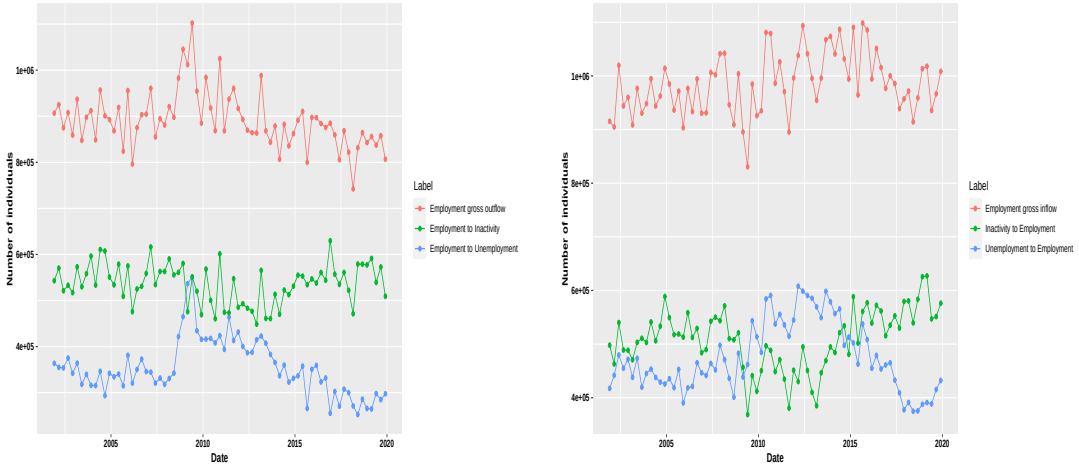

(a) Employment gross outflow (b) Employment gross inflow

FIGURE 18: Graphs illustrating quarterly observations from 2001 to 2019 for (a) employment gross outflows to inactivity and unemployment; and (b) employment gross inflows from unemployment and inactivity.

(a) Unemployment gross outflow (b) Uneployment gross inflow

FIGURE 19: Graphs illustrating observations per quarter from 2001 to 2019 for (a) unemployment gross outflows to inactivity and employment; and (b) unemployment gross inflow from employment and inactivity.

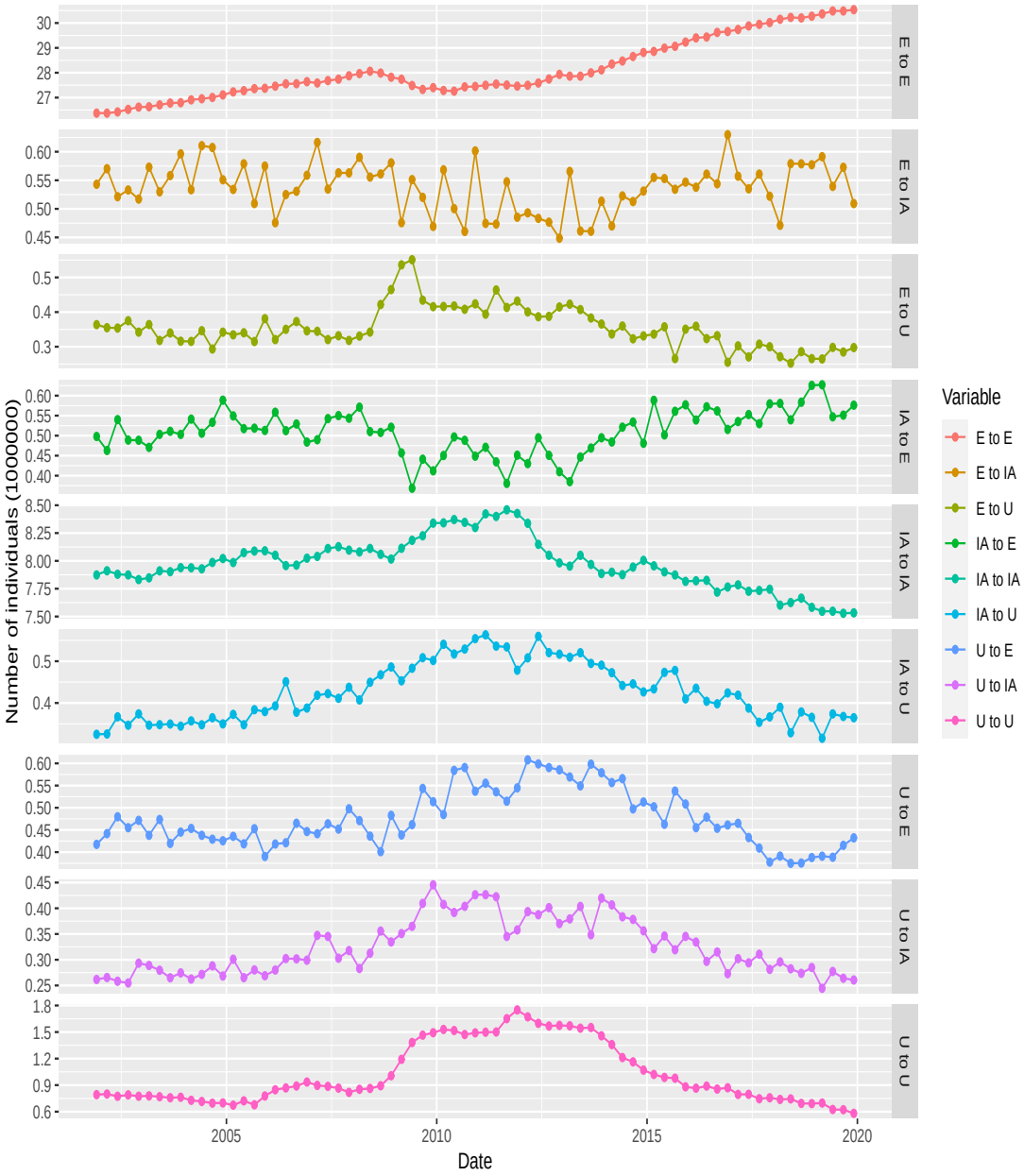

FIGURE 20: Graphs illustrating quarterly observations from 2001 to 2019 for individuals that transition from employment to employment (EE), employment to unemployment (EU), employment to inactivity (E_IA), unemployment to unemployment (UU), unemployment to employment (UE), unemployment to inactivity (U_IA), inactivity to inactivity ($_IA_IA$), inactivity to employment ($_IAE$) and inactivity to unemployment ($_IAU$).

(a) Inactivity gross outflow

(b) Inactivity gross inflow

FIGURE 21: Graphs illustrating observations from 2001 to 2019 for each quarter on (a) inactivity gross outflows to unemployment and employment; and (b) inactivity gross inflow from employment and unemployment.

4.1.3 The Covid-19 shock wave hit on the labour force

The economic stability after the financial recession from 2008 to 2012 had a positive impact on the labour market. This was evident as unemployment and inactivity began to fall whilst employment started to rise until February 2020 when the world economy was hit by the Covid-19 pandemic. Given the gravity of the impact, a worldwide recession started taking place from early March 2020. As the Covid-19 shock wave hit, there has been an increase in unemployment insurance claims, a growth in the unemployment rate and momentous reduction in the employment rate.

Based on official information from the ONS virtual platform [134], the UK labour force data has been published until February 2020 (at the time of writing this thesis). Due to this we do not have access to official data for the crucial months of the Covid-19 epidemic (March to July 2020). However, provisional predictions from the ONS show that the UK labour market is at risk following the Covid-19 pandemic and forecasts that in the short term about at least 20% of the workers will lose their jobs or become inactive [11]. The prediction indicates that the number of unemployed individuals will increase from 1.34 million to over 6 million (i.e., a 4.66 million increment) by the end of May 2020. This takes the effective current unemployment rate to around 20%, which

is more than five times the most recent officially published rate of 3.9%. It can be said that the Covid-19 pandemic has led and will further lead to a sharp spike in the number of individuals in unemployment and inactivity and an abrupt drop in the number of employed individuals. These estimates might turn out to be harsher as the lockdown continues.

To summarise, all the aforementioned descriptions and features of employment, unemployment and inactivity are to enable us understand and interpret the changes in the level of the labour market needed to compute the unemployment and reemployment rates to formulate more realistic UI scheme models.

4.2 Multistate Markov modelling

In Chapter 2, for simplicity we assumed that the time until the current employment ends, τ_0, and the unemployment spell of duration, τ_1, had exponential distribution (with parameters λ_0 and λ_1, respectively). As mentioned in the Introduction, this guarantees a Markovian nature of the corresponding transitions.

Possible transitions in the state space of our insurance model are shown in Fig. 22, where symbols E and U encode the states of being employed and unemployed, respectively. Note that all transitions occur in a Markovian fashion; that is, the holding times are exponentially distributed (with parameters λ_0 if in state E, or λ_1 if in states U). The parameters λ_0 or λ_1 are called the unemployment transition rate and the reemployment transition rate and are constant in Chapter 2. In Chapter 3, λ_0 and λ_1 are time-varying.

Multistate Markov models are a useful way of estimating probability rates and rates of transition between states. Thus, in the subsequent sections, we give a brief overview of Markov chains and fit Markov models to the data.

4.2.1 Brief overview of Markov models

Markov models have been used in several disciplines to explain life course dynamics [2, 86, 41, 19]. With this modelling approach the population under study in this thesis is divided into compartments representing states, together with certain assumptions for individuals to move from one compartment to another. This section is a compilation of information from [3, 13, 69, 95, 126, 68, 108, 14, 15].

The Markov property

Denote an individual's employment journey by a continuous-time Markov jump process (MJP) $Y_t, t \geq 0$ with finitely many states on a probability space $(\Omega, (\mathcal{F}_t)_{t\geq 0}, \mathrm{P})$. Here, Ω is the sample space, $(\mathcal{F}_t)_{t\geq 0}$ is the filtration (interpreted as all information about the process up to and including time t) associated to the process and P is the probability measure. Let S denote the state space of the process. The process Y is said to have Markov property if

$$\mathrm{P}\left(Y_t = j \mid \mathcal{F}_s\right) = \mathrm{P}\left(Y_t = j \mid Y_s\right) \tag{4.2.1}$$

for all $i \in S$ and $t \geq s \geq 0$. More specifically, for any state $i_1, i_2, \ldots, i_k, i, j$ in S and all times $0 \leq s_0 < s_1 < \cdots < s_k < s < t$,

$$\mathrm{P}\left(Y_t = j | Y_{s_0} = i_0, Y_{s_1} = i_1, \ldots, Y_{s_k} = i_k, Y_s = i\right) = \mathrm{P}\left(Y_t = j | Y_s = i\right). \tag{4.2.2}$$

The transition probability

The transition probability for a continuous-time Markov jump process for $i, j \in S$ and $0 \leq s \leq t$,

$$p_{ij}(s,t) := \mathrm{P}(Y_t = j \,|\, Y_s = i) \tag{4.2.3}$$

We assume that the state space is finite, $|S| = \ell < \infty$ then the transition matrix is written as

$$\mathbf{P}(s,t) := (p_{ij}(s,t))_{i,j=1}^{\ell} \tag{4.2.4}$$

Note that $0 \leq p_{ij}\,(s,t) \leq 1$ for all $i, j \in S$ and $\sum_j p_{ij}\,(s,t) = 1$ for all $i \in S$. Also, if the state i is absorbing, then $p_{ij}(s,t) = 0$ for all $j \neq i$ and $p_{ii}(s,t) = 1$, for all $s \leq t$.

The Chapman–Kolmogorov equation

The Markov property implies that for any u, such that $s \leq u \leq t$, then the transition probability $p_{ij}(s,t)$ can be expressed as

$$p_{ij}(s,t) = \sum_{k\in S} p_{ik}(s,u) p_{kj}(u,t) \tag{4.2.5}$$

for all $i, j \in S$. This is known as the Chapman–Kolmogorov equation. Equation (4.2.5) can also be written in matrix form,

$$\mathbf{P}(s,t) = \mathbf{P}(s,u)\,\mathbf{P}(u,t) \tag{4.2.6}$$

for all $s \leq u \leq t$.

The transition intensity

The convenient infinitesimal characterisation of the transition probabilities is as follows: for all $t \geq 0$ and $i, j \in S$, as $h \downarrow 0$ we have

$$p_{ij}(t, t+h) = \lambda_{ij}(t)\, h + o(h) \qquad (i \neq j), \tag{4.2.7}$$

$$p_{ii}(t, t+h) = 1 + \lambda_{ii}(t)\, h + o(h). \tag{4.2.8}$$

Clearly, $\lambda_{ij} \geq 0$ for $i \neq j$ and $\lambda_{ii} < 0$. Moreover, by summing up the relations (4.2.7) and (4.2.8) over $j \in S$, it follows that, for any $i \in S$ and for all $t \geq 0$,

$$\sum_{j \in S} \lambda_{ij}(t) = 0. \tag{4.2.9}$$

Here, $\lambda_{ij}(t)$ is called the transition rate or transition intensity from i to j at time t. In particular,

$$\lambda_i(t) := |\lambda_{ii}(t)| = \sum_{j \neq i} \lambda_{ij}(t) > 0. \tag{4.2.10}$$

Let $\mathbf{\Lambda}(t)$ denote the transition rate matrix, also known as the generator matrix, defined as

$$\mathbf{\Lambda}(t) := (\lambda_{ij}(t))_{i,j=1}^{\ell}. \tag{4.2.11}$$

The sum of all elements in each row of (4.2.11) is zero due to (4.2.9).

If the Markov model is *time-homogenous* then the transition probabilities depend only on the time shift, $p_{ij}(s, t) = p_{ij}(t - s)$, and the transition rates do not depend on time, $\lambda_{ij}(t) \equiv \lambda_{ij} = \text{const}$. In this case, it is sufficient to consider the transition probabilities

$$p_{ij}(t) := \mathrm{P}(Y_t = j \,|\, Y_0 = i). \tag{4.2.12}$$

The transition probability matrix and the generator matrix are reduced to

$$\mathbf{P}(t) = (p_{ij}(t))_{i,j=1}^{\ell}, \qquad \mathbf{\Lambda} = (\lambda_{ij})_{i,j=1}^{\ell}. \tag{4.2.13}$$

The Kolmogorov differential equations

For $i \neq j$, consider the transition probability $p_{ij}(s, t+h)$, with $h \downarrow 0$. Using the Chapman–Kolmogorov equation in (4.2.5) and the asymptotic expansion for $p_{ij}(t, t+h)$,

we obtain

$$p_{ij}(s,t+h) = \sum_{k\in S} p_{ik}(s,t)\, p_{kj}(t,t+h) \tag{4.2.14}$$

$$= \sum_{k\neq j} p_{ik}(s,t)\,\big(\lambda_{kj}(t)\,h + o(h)\big) + p_{ij}(s,t)\,\big(1+\lambda_{jj}(t)\,h + o(h)\big). \tag{4.2.15}$$

Hence,

$$\frac{p_{ij}(s,t+h) - p_{ij}(s,t)}{h} = \sum_{k\in S} p_{ik}(s,t)\,\lambda_{kj}(t) + o(h). \tag{4.2.16}$$

Upon taking the limit as $h \downarrow 0$, this yields

$$\frac{\partial p_{ij}(s,t)}{\partial t} = \sum_{k\in S} p_{ik}(s,t)\,\lambda_{kj}(t), \tag{4.2.17}$$

or, in matrix form,

$$\frac{\partial \mathbf{P}(s,t)}{\partial t} = \mathbf{P}(s,t)\boldsymbol{\Lambda}(t). \tag{4.2.18}$$

This is called the *forward Kolmogorov equations*. The initial conditions are

$$p_{i,j}(s,t)|_{t=s} = \delta_{ij} := \begin{cases} 0, & i \neq j, \\ 1, & i = j, \end{cases} \tag{4.2.19}$$

that is,

$$\mathbf{P}(s,s) = \mathbf{I} \ \text{ (identity matrix)}. \tag{4.2.20}$$

Similarly, by using the Chapman–Kolmogorov equation in (4.2.5) on the interval $[s-h,t]$, we get the *backward Kolmogorov equations*

$$\frac{\partial p_{ij}(s,t)}{\partial s} = -\sum_{k\in S} \lambda_{ik}(s) p_{kj}(s,t), \tag{4.2.21}$$

or, in matrix form,

$$\frac{\partial \mathbf{P}(s,t)}{\partial s} = -\boldsymbol{\Lambda}(s)\mathbf{P}(s,t). \tag{4.2.22}$$

The corresponding "terminal" conditions are

$$p_{i,j}(s,t)|_{s=t} = \delta_{ij} := \begin{cases} 0, & i \neq j, \\ 1, & i = j, \end{cases} \tag{4.2.23}$$

that is,

$$\mathbf{P}(t,t) = \mathbf{I}. \tag{4.2.24}$$

In the time-homogeneous case, the Kolmogorov differential equations are reduced to

$$\frac{\partial p_{ij}(t)}{\partial t} = \sum_{k\in S} p_{ik}(t)\,\lambda_{kj}, \qquad \frac{\partial p_{ij}(t)}{\partial t} = \sum_{k\in S} \lambda_{ik} p_{kj}(t), \tag{4.2.25}$$

or in matrix form

$$\frac{\partial \mathbf{P}(t)}{\partial t} = \mathbf{P}(t)\mathbf{\Lambda}, \qquad \frac{\partial \mathbf{P}(t)}{\partial t} = \mathbf{\Lambda}\mathbf{P}(t). \tag{4.2.26}$$

The Kolmogorov forward equations and the Kolmogorov backward equations are collectively called the Kolmogorov differential equations (KDE).

Pathwise description of the Markov model

Define the *residual holding time* R_t as the (random) amount of time between $t \geq 0$ and the next jump, which is characterised by the property

$$\{R_t > w,\, Y_t = i\} = \{Y_u = i \text{ for all } u \in [t, t+w]\}. \tag{4.2.27}$$

The distribution of R_t (assuming that $Y_t = i$) is given by

$$\mathrm{P}(R_t > w \,|\, Y_t = i) = \exp\left(-\int_t^{t+w} \lambda_i(u)\,\mathrm{d}u\right). \tag{4.2.28}$$

Recall that $\lambda_i(u) = \sum_{j\neq i} \lambda_{ij}(u)$. In particular, the conditional density of R_t (given $Y_t = i$) is

$$-\frac{\mathrm{d}\,\mathrm{P}(R_t > w \,|\, Y_t = i)}{\mathrm{d}w} = \lambda_i(t+w)\exp\left(-\int_t^{t+w} \lambda_i(u)\,\mathrm{d}u\right). \tag{4.2.29}$$

To show this, note that, by the Markov property,

$$\begin{aligned}
\mathrm{P}(R_t > w+h \,|\, Y_t = i) &= \mathrm{P}(R_t > w+h \,|\, \underbrace{Y_t = i,\, R_t > w}_{\text{amounts to } Y_{t+w} = i}) \cdot \mathrm{P}(R_t > w \,|\, Y_t = i) \\
&= \mathrm{P}(R_{t+w} > h \,|\, Y_{t+w} = i) \cdot \mathrm{P}(R_t > w \,|\, Y_t = i) \\
&= \big(1 - \lambda_i(t+w)\,h + o(h)\big) \cdot \mathrm{P}(R_t > w \,|\, Y_t = i),
\end{aligned} \tag{4.2.30}$$

and it follows that the function $y(w) = \mathrm{P}(R_t > w \,|\, Y_t = i)$ satisfies the differential equation

$$y'(w) = -\lambda_i(s+w)\,y(w), \qquad y(0) = 1, \tag{4.2.31}$$

which solves to (4.2.28). It is also possible to characterise the distribution of the jump destination from state i held at time s the process jumps at time $t + R_t$ to a new state j with probability proportional to the transition rate $\lambda_{ij}(t + R_t)$. To see this, consider the probability

$$\begin{aligned}
&\mathrm{P}(Y_{t+w+h} = j, w < R_t \leq w + h \,|\, Y_t = i) \\
&\qquad = \mathrm{P}(Y_{t+w+h} = j, R_t > w \,|\, Y_t = i) \\
&\qquad = \mathrm{P}(Y_{t+w+h} = j \,|\, Y_t = i, R_t > w) \cdot \mathrm{P}(R_t > w \,|\, Y_t = i) \\
&\qquad = \mathrm{P}(Y_{t+w+h} = j \,|\, Y_{t+w} = i) \cdot \mathrm{P}(R_t > w \,|\, Y_t = i) \\
&\qquad = (\lambda_{ij}(t + w)\, h + o(h)) \cdot \exp\left(- \int_t^{t+w} \lambda_i(u)\, \mathrm{d}u \right). \qquad (4.2.32)
\end{aligned}$$

Hence, dividing by h and taking the limit as $h \downarrow 0$, the joint probability distribution/density of Y_{t+R_t} and R_t is, conditionally on $Y_t = i$, is given by

$$\lambda_{ij}(t + w) \cdot \exp\left(- \int_t^{t+w} \lambda_i(u)\, \mathrm{d}u \right) = \frac{\lambda_{ij}(t + w)}{\lambda_i(t + w)} \cdot \lambda_i(t + w) \exp\left(- \int_t^{t+w} \lambda_i(u)\, \mathrm{d}u \right). \qquad (4.2.33)$$

The second factor here is the density of R_t, whereas the first factor is

$$\mathrm{P}(Y_{t+R_t} = j \,|\, Y_t = i) = \frac{\lambda_{ij}(t + w)}{\lambda_i(t + w)}. \qquad (4.2.34)$$

Moreover, formula (4.2.33) implies that Y_{t+R_t} is independent of R_t. When the Markov model is time-homogeneous, $\lambda_{ij}(t) \equiv \lambda_{ij}$, $\lambda_i(t) \equiv \lambda_i$ such that

$$\mathrm{P}(Y_{R_0} = j \,|\, Y_0 = i) = \frac{\lambda_{ij}}{\lambda_i}. \qquad (4.2.35)$$

Maximum likelihood estimation

Consider the time-homogeneous case to estimate the transition rate λ_{ij}. Set $T_0, T_1 < \cdots < T_n$ as the consecutive jump time such that $T_0 = R_{i_0}, T_1 = T_0 + R_{i_0}, \ldots, T_n = T_{n-1} + R_{i_{n-1}}$. This means that the process starts in state i_0, stays for time T_0 and jumps to state i_0, where it stays for T_1 and so on. Then, $(T_0 = t_0 = 0, Y_{t_0} = i_0), (T_1 = t_1, Y_{t_1} = i_1), \ldots, (T_n = t_n, Y_{t_n} = i_n)$ denotes the observations at successive times $t_0 < t_1 < t_2 < \cdots < t_n$ between states $S = i_0, i_1, \ldots, i_n$. The likelihood function is given by

$$\begin{aligned}
L(\{\lambda_{ij}\} \,|\, \{(t_k, i_k)\}) &= \prod_{k=1}^{n} \lambda_{i_{k-1}, i_k}\, \mathrm{e}^{-\lambda_i (t_k - t_{k-1})} \\
&= \prod_{i \in S} \mathrm{e}^{-\lambda_i v_i} \prod_{j \neq i} (\lambda_{ij})^{n_{ij}}, \qquad (4.2.36)
\end{aligned}$$

where n_{ij} is the total number of observed jumps from i to j and v_i is the total time spent in state i. Recall from (4.2.13) that $\mathbf{\Lambda} = \{\lambda_{ij}\}$. We take the logarithm of (4.2.36) to derive

$$\log L(\mathbf{\Lambda}) = \sum_{i \in S} \sum_{j \neq i} \left[\log(\lambda_{ij}) n_{ij} - \lambda_{ij} v_i\right]. \tag{4.2.37}$$

Taking the partial derivative of (4.2.37) with respect to λ_{ij} and equating it to 0 we get

$$\frac{\partial \log L(\mathbf{\Lambda})}{\partial \lambda_{ij}} = 0 \iff \sum_{i \in S} \sum_{j \neq i} \left[\frac{n_{ij}}{\lambda_{ij}} - v_i\right]. \tag{4.2.38}$$

Thus, maximising (4.2.36) leads to the maximum likelihood estimator (MLE)

$$\widehat{\lambda}_{ij} = \frac{n_{ij}}{v_i}. \tag{4.2.39}$$

Solving the Kolmogorov differential equations

The transition probabilities can be derived through the transition intensities by solving the KDE. Solving the KDE in (4.2.18) and (4.2.22) can be challenging when the transition rates are time dependent. However, there are some techniques that can been used to solve the KDE and fit time inhomogeneous Markov models [103]. One approach is the to consider the generator matrix as a piecewise function as shown in [29]. Another approach is to transform the time-dependent intensity matrix into the smooth parametric form. This transformation requires choosing from a class of functions that fits the shape and nature of the intensity. Some mathematical functions used to model the time-dependent transition rates using the smooth parametric approach are the Weibull function of time model [106], the Gompertz–Makeham model for human mortality [57, 87] and the Sigmoid model [100]. The next method is the nonparametric approach. In this approach, the shape of the transition intensity is determined from the data rather than making any specific assumptions about the shape of the transition intensities. Some non-parametric techniques to estimate the transition rates are weighted smoothing approach [66] and spline representation approach [39]. Notwithstanding time-varying transition rate models are often solved numerically which is explained in [103].

In the subsequent section, we consider the time-homogeneous Markov process where the transition rates do not depend on time ($\lambda_{ij}(t) = \lambda_{ij}$). The formal solution of KDE in (4.2.26) is

$$\mathbf{P}(t) = \exp\{t\mathbf{\Lambda}\}, \qquad t \geq 0. \tag{4.2.40}$$

One approach to numerically evaluate the matrix exponential in (4.2.40) is the Matrix Decomposition method. In this method, the transition intensity matrix can be decomposed as

$$\mathbf{\Lambda} = \mathbf{\Phi Q \Phi}^{-1} \tag{4.2.41}$$

where $\mathbf{Q}$ is a diagonal matrix that contains the eigenvalues of $\mathbf{\Lambda}$ ($\{q_1, \cdots, q_\ell\}$) and $\mathbf{\Phi}$ is a matrix that contains the i^{th} eigenvector of $\mathbf{\Lambda}$ in the i^{th} column. Substitute (4.2.41) into (4.2.40) to obtain

$$\mathbf{P}(t) = \mathbf{\Phi} \cdot \exp(t\mathbf{Q}) \cdot \mathbf{\Phi}^{-1} = \mathbf{\Phi} \cdot \operatorname{diag}\left(\mathrm{e}^{q_1 t}, \ldots, \mathrm{e}^{q_\ell t}\right) \cdot \mathbf{\Phi}^{-1}. \tag{4.2.42}$$

In the next sections, we study the two-state, four-state, five-state and lake models for the labour force market.

4.3 Two-state model

We first investigate the simplest two-state model with constant transition rates as displayed in Fig. 22. An individual may be in the employed state E or the unemployed state U.

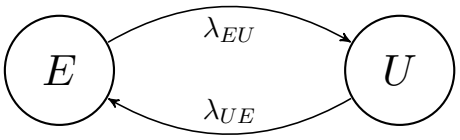

FIGURE 22: Graphical representation of the transitions between possible states of the labour market, labelled employment (E) and unemployment (U). This diagram also shows the arrows from each state to the other states that signify transition rate λ_{ij} for $i, j \in \{E, U\}$.

Transition from E to U and U to E occur at rate λ_{EU} and λ_{UE} respectively. Relating this to Chapter 2, $\lambda_0 = \lambda_{EU}$ and $\lambda_1 = \lambda_{UE}$. Consequently, the generator matrix or transition rate matrix $\mathbf{\Lambda}$ in Kolmogorov's equation (see (4.2.18) and (4.2.22)) is

$$\Lambda = \begin{bmatrix} -\lambda_{EU} & \lambda_{EU} \\ \lambda_{UE} & -\lambda_{UE} \end{bmatrix}. \tag{4.3.1}$$

The data is collected up to time t. Thus, using (4.3.1), we find the transition probabilities $p_{ij}(0,t) = p_{ij}(t) = \mathrm{P}(Y(t) = j | Y(0) = i)$ for each $i, j \in \{E, U\}$ for continuous-time Markov chain.

4.3.1 Finding the probability matrix with the transition matrix for the two-state model

In this section, three approaches are used to find the probability matrix using the generator matrix for the two-state model (Fig. 22).

The backward equation approach

The first approach is the backward equation approach. We know that

$$p_{EE}(t) + p_{EU}(t) = p_{UE}(t) + p_{UU}(t) = 1 \tag{4.3.2}$$

for all $t \geq 0$, and so it is sufficient to solve just $p_{EE}(t)$ and $p_{UE}(t)$. Recall that the backward equation is given by

$$\mathbf{P}'(t) = \mathbf{\Lambda}\mathbf{P}(t) \tag{4.3.3}$$

where $\mathbf{P}(t) = \{p_{ij}(t)\}$ and where $\mathbf{P}'(t) = \frac{\mathrm{d}\mathbf{P}(t)}{\mathrm{d}t}$. This yields the equations

$$p'_{EE}(t) = \lambda_{EU}\left[p_{UE}(t) - p_{EE}(t)\right] \tag{4.3.4}$$

$$p'_{UE}(t) = \lambda_{UE}\left[p_{EE}(t) - p_{UE}(t)\right]. \tag{4.3.5}$$

We obtain

$$\lambda_{UE}p'_{EE}(t) + \lambda_{EU}p'_{UE}(t) = 0 \implies \lambda_{UE}p_{EE}(t) + \lambda_{EU}p_{UE}(t) = c \tag{4.3.6}$$

where c is an arbitrary constant. On account of Fig. 22, $\mathbf{P}(0) = \mathbf{I}$, so we get

$$\lambda_{EU}p_{EE}(0) + \lambda_{UE}p_{UE}(0) = c \iff \lambda_{EU} = c. \tag{4.3.7}$$

Thus,

$$\lambda_{UE}p_{EE}(t) + \lambda_{EU}p_{UE}(t) = \lambda_{UE} \implies \lambda_{EU}p_{UE}(t) = \lambda_{UE} - \lambda_{UE}p_{EE}(t). \tag{4.3.8}$$

Substituting (4.3.8) into the differential equation (4.3.4), we have that

$$p'_{EE}(t) = \lambda_{UE} - \lambda_{UE}p_{EE}(t) - \lambda_{EU}p_{EE}(t) = \lambda_{UE} - (\lambda_{UE} + \lambda_{EU})p_{EE}(t) \tag{4.3.9}$$

Solving (4.3.9) yields

$$p_{EE}(t) = ce^{-(\lambda_{EU}+\lambda_{UE})t} + \frac{\lambda_{UE}}{\lambda_{EU}+\lambda_{UE}}. \tag{4.3.10}$$

With $\mathbf{P}(0) = \mathbf{I}$, we obtain

$$p_{EE}(t) = \frac{\lambda_{UE}}{\lambda_{EU}+\lambda_{UE}} + \frac{\lambda_{EU}}{\lambda_{EU}+\lambda_{UE}}e^{-(\lambda_{EU}+\lambda_{UE})t}. \tag{4.3.11}$$

Using (4.3.2),

$$p_{EU}(t) = 1 - p_{EE}(t) = \frac{\lambda_{EU}}{\lambda_{EU}+\lambda_{UE}} - \frac{\lambda_{EU}}{\lambda_{EU}+\lambda_{UE}}e^{-(\lambda_{EU}+\lambda_{UE})t}. \tag{4.3.12}$$

We also have that from (4.3.8)

$$\begin{aligned} p_{UE}(t) &= \frac{\lambda_{UE}}{\lambda_{EU}} - \frac{\lambda_{UE}}{\lambda_{EU}}\left(\frac{\lambda_{UE}}{\lambda_{EU}+\lambda_{UE}} + \frac{\lambda_{EU}}{\lambda_{EU}+\lambda_{UE}}e^{-(\lambda_{EU}+\lambda_{UE})t}\right) \\ &= \frac{\lambda_{UE}}{\lambda_{EU}+\lambda_{UE}} - \frac{\lambda_{UE}}{\lambda_{EU}+\lambda_{UE}}e^{-(\lambda_{EU}+\lambda_{UE})t}. \end{aligned} \tag{4.3.13}$$

Similarly, using (4.3.2) we see that

$$p_{UU}(t) = 1 - p_{UE}(t) = \frac{\lambda_{EU}}{\lambda_{EU}+\lambda_{UE}} + \frac{\lambda_{UE}}{\lambda_{EU}+\lambda_{UE}}e^{-(\lambda_{EU}+\lambda_{UE})t}. \tag{4.3.14}$$

The forward equation approach

An alternative approach which is the forward equation approach is to solve

$$\mathbf{P}'(t) = \mathbf{P}(t)\mathbf{\Lambda}. \tag{4.3.15}$$

Now we derive the following equations

$$p'_{EE}(t) = -p_{EE}(t)\lambda_{EU} + p_{EU}(t)\lambda_{UE} \tag{4.3.16}$$

$$p'_{UE}(t) = -p_{UE}(t)\lambda_{EU} + p_{UU}(t)\lambda_{UE} \tag{4.3.17}$$

$$p'_{EU}(t) = -p_{EU}(t)\lambda_{UE} + p_{EE}(t)\lambda_{EU} \tag{4.3.18}$$

$$p'_{UU}(t) = -p_{UU}(t)\lambda_{UE} + p_{UE}(t)\lambda_{EU}. \tag{4.3.19}$$

The equations can further be written as

$$p'_{EE}(t) = -p_{EE}(t)\lambda_{EU} + \lambda_{UE}(1 - p_{EE}(t)) = \lambda_{UE} - (\lambda_{EU}+\lambda_{UE})p_{EE}(t) \tag{4.3.20}$$

$$p'_{UE}(t) = -p_{UE}(t)\lambda_{EU} + \lambda_{UE}(1 - p_{UE}(t)) = \lambda_{UE} - (\lambda_{EU}+\lambda_{UE})p_{UE}(t) \tag{4.3.21}$$

$$p'_{EU}(t) = -p_{EU}(t)\lambda_{UE} + \lambda_{EU}(1 - p_{EU}(t)) = \lambda_{EU} - (\lambda_{EU}+\lambda_{UE})p_{EU}(t) \tag{4.3.22}$$

$$p'_{UU}(t) = -p_{UU}(t)\lambda_{UE} + \lambda_{EU}(1 - p_{UU}(t)) = \lambda_{EU} - (\lambda_{EU}+\lambda_{UE})p_{UU}(t). \tag{4.3.23}$$

Solving (4.3.20), (4.3.21), (4.3.22) and (4.3.23) yields

$$p_{EE}(t) = c_1 \mathrm{e}^{-(\lambda_{EU}+\lambda_{UE})t} + \frac{\lambda_{UE}}{\lambda_{EU}+\lambda_{UE}} \quad p_{EU}(t) = c_3 \mathrm{e}^{-(\lambda_{EU}+\lambda_{UE})t} + \frac{\lambda_{EU}}{\lambda_{EU}+\lambda_{UE}} \tag{4.3.24}$$

$$p_{UE}(t) = c_2 \mathrm{e}^{-(\lambda_{EU}+\lambda_{UE})t} + \frac{\lambda_{UE}}{\lambda_{EU}+\lambda_{UE}} \quad p_{UU}(t) = c_4 \mathrm{e}^{-(\lambda_{EU}+\lambda_{UE})t} + \frac{\lambda_{EU}}{\lambda_{EU}+\lambda_{UE}} \tag{4.3.25}$$

When $\mathbf{P}(0) = \mathbf{I}$, we obtain the same results in (4.3.11), (4.3.12), (4.3.13) and (4.3.14).

The matrix decomposition approach

A more straightforward approach to finding the transition probabilities is to compute the matrix exponential in (4.2.40). The eigenvalues of the generator matrix $\mathbf{\Lambda}$ in (4.3.1) is 0 and $-(\lambda_{EU}+\lambda_{UE})$ and the corresponding eigenvectors are $(1,1)^\intercal$ and $\left(\frac{\lambda_{EU}}{\lambda_{UE}}, 1\right)^\intercal$. Let $\mathbf{Q}$ be a diagonal matrix consisting of the eigenvalues of $\mathbf{\Lambda}$ such that

$$\mathbf{Q} = \begin{bmatrix} 0 & 0 \\ 0 & -(\lambda_{EU}+\lambda_{UE}) \end{bmatrix}. \tag{4.3.26}$$

Also, set $\mathbf{\Phi}$ as a matrix of the associated eigenvectors of $\mathbf{\Lambda}$ ordered in the same order of the eigenvalues in $\mathbf{Q}$ such that

$$\mathbf{\Phi} = \begin{bmatrix} 1 & \frac{-\lambda_{EU}}{\lambda_{UE}} \\ 1 & 1 \end{bmatrix}; \quad \mathbf{\Phi}^{-1} = \begin{bmatrix} \frac{\lambda_{UE}}{\lambda_{EU}+\lambda_{UE}} & \frac{\lambda_{EU}}{\lambda_{EU}+\lambda_{UE}} \\ \frac{-\lambda_{UE}}{\lambda_{EU}+\lambda_{UE}} & \frac{\lambda_{UE}}{\lambda_{EU}+\lambda_{UE}} \end{bmatrix}. \tag{4.3.27}$$

Now, $\mathbf{\Lambda}$ can be decomposed into

$$\mathbf{\Lambda} = \mathbf{\Phi}\mathbf{Q}\mathbf{\Phi}^{-1}. \tag{4.3.28}$$

In that case, we derive

$$\mathbf{P}(t) = \mathrm{e}^{\mathbf{\Lambda}t} = \mathbf{\Phi}\mathrm{e}^{\mathbf{Q}t}\mathbf{\Phi}^{-1} = \mathbf{\Phi} \cdot \mathrm{diag}\left(\mathrm{e}^{q_1 t}, \cdots, \mathrm{e}^{q_\ell t}\right) \cdot \mathbf{\Phi}^{-1} \tag{4.3.29}$$

$$= \begin{bmatrix} \frac{\lambda_{UE}}{\lambda_{EU}+\lambda_{UE}} + \frac{\lambda_{EU}}{\lambda_{EU}+\lambda_{UE}}\mathrm{e}^{-(\lambda_{EU}+\lambda_{UE})t} & \frac{\lambda_{EU}}{\lambda_{EU}+\lambda_{UE}} - \frac{\lambda_{EU}}{\lambda_{EU}+\lambda_{UE}}\mathrm{e}^{-(\lambda_{EU}+\lambda_{UE})t} \\ \frac{\lambda_{UE}}{\lambda_{EU}+\lambda_{UE}} - \frac{\lambda_{UE}}{\lambda_{EU}+\lambda_{UE}}\mathrm{e}^{-(\lambda_{EU}+\lambda_{UE})t} & \frac{\lambda_{EU}}{\lambda_{EU}+\lambda_{UE}} + \frac{\lambda_{UE}}{\lambda_{EU}+\lambda_{UE}}\mathrm{e}^{-(\lambda_{EU}+\lambda_{UE})t} \end{bmatrix}. \tag{4.3.30}$$

Consequently, we see that all three approaches give the same result.

The long-term behaviour

Here we compute the limiting and stationary distributions. A probability distribution denoted by π is a limiting distribution if for all state i, j

$$\lim_{t\to\infty} p_{ij}(t) = \pi_j. \tag{4.3.31}$$

This is equivalent to

$$\lim_{t\to\infty} \mathbf{P}(t) = \Pi \tag{4.3.32}$$

where Π is a matrix with rows equal to π. Also π is a stationary distribution if

$$\pi\mathbf{P}(t) = \pi \tag{4.3.33}$$

for $t \geq 0$. That is

$$\pi_j = \sum_i \pi_i p_{ij}(t) \tag{4.3.34}$$

for all states j. Thus, when we take the limit of 4.3.29 as $t \to \infty$ we have that

$$\lim_{t\to\infty} \mathbf{P}(t) = \Pi = \frac{1}{\lambda_{EU} + \lambda_{UE}} \begin{bmatrix} \lambda_{UE} & \lambda_{EU} \\ \lambda_{UE} & \lambda_{EU} \end{bmatrix}. \tag{4.3.35}$$

We observe that $\mathbf{P}(t)$ converges to the distribution

$$\Pi = \left[\frac{\lambda_{UE}}{\lambda_{EU}+\lambda_{UE}}, \frac{\lambda_{EU}}{\lambda_{EU}+\lambda_{UE}}\right] \tag{4.3.36}$$

which is the unique stationary distribution. That is to say, in the long run, the chain will be in the employment (E) state with a probability of $\frac{\lambda_{UE}}{\lambda_{EU}+\lambda_{UE}}$.

4.3.2 Two-state model fitting

The labour force state transition (LST) models can be used as decision models because they can be used to simulate labour market' transitions across various states over time. In this section, we show how to estimate the generator matrix and probability matrix of a continuous-time Markov model using our discrete time data (quarterly observations). We further use the derived results to run (t-step) simulations and compare the simulated values with the actual data.

Estimating the generator matrix and the probability matrix from the data using diagonal adjustment (DA)

From Section 4.2.1, let $\widehat{\mathbf{\Lambda}} = (\widehat{\lambda}_{ij})_{i,j\in S}$ denote the maximum likelihood estimator (MLE) of $\mathbf{\Lambda}$ where

$$\widehat{\lambda}_{ij} = \frac{n_{ij}}{v_i} \tag{4.3.37}$$

where n_{ij} is the total number of observed jumps from i to j and v_i is the total time spent in state i. The complicated aspect is that our data is collected at quarterly time intervals so v_i is unknown. Thus, we estimate $\mathbf{\Lambda}$ using the maximum likelihood estimator for the transition probability. For a time-homogeneous process, the likelihood function at m (quarterly) time points is given by

$$L(\mathbf{P}) = \prod_{i\in S}\prod_{j\in S} p_{ij}^{n_{ij}(m)} \tag{4.3.38}$$

Taking the logarithm of (4.3.38) we derive

$$\log L(\mathbf{P}) = \sum_{i\in S}\sum_{j\in S} p_{ij}^{n_{ij}(m)}. \tag{4.3.39}$$

The likelihood function in (4.3.38) is similar to the likelihood function for n dependent multinomial distribution [115, 111]. Thus the maximum likelihood estimator for the transition probability also known as the relative probability rate in (4.2.3) is given by

$$\widehat{p}_{ij}(m) = \frac{n_{ij}(m)}{n_i(m)}. \tag{4.3.40}$$

where $n_{ij}(m)$ is the total number of observed jumps from i to j before m and $n_i(m) = \sum_j n_{ij}(m)$. Let $\widehat{P} = (\widehat{p}_{ij})_{i,j\in S}$ denote the relative probability matrix. Next, we use the diagonal adjustment (DA) method to compute the generator matrix for our data analysis. In this approach, we find the probability rates for each quarter by using (4.3.40) and (4.2.40) to obtain

$$\widehat{\mathbf{\Lambda}} = \log \widehat{\mathbf{P}} = \mathbf{\Psi}\cdot\log(\mathbf{D})\cdot\mathbf{\Psi}^{-1} = \mathbf{\Psi}\cdot \text{ diag } (\log(d_1),\ldots,\log(d_\ell))\cdot\mathbf{\Psi}^{-1} \tag{4.3.41}$$

where $\mathbf{D}$ is the diagonal matrix that contains the eigenvalues of $\widehat{\mathbf{P}}$ ($\{d_1,\ldots,d_\ell\}$) and $\mathbf{\Psi}$ is a matrix that contains the i^{th} eigenvector of $\widehat{\mathbf{P}}$ in the i^{th} column. To ensure that the row of the matrix $\widehat{\mathbf{\Lambda}}$ sums up to zero, all negative diagonal elements in each row are replaced with zero and the diagonal elements are re-calculated as the negative

sum of the non-diagonal elements [108, 69]. To summarise, let $\tilde{\lambda}$ denote the transition rate derived from the DA method such that $\tilde{\mathbf{\Lambda}} = [\tilde{\lambda}_{ij}]_{i,j \in S}$. Then the procedure for computation is

$$\tilde{\lambda}_{ij} = \begin{cases} 0 & \text{if } (i \neq j) \text{ and } \widehat{\lambda}_{ij} < 0 \\ \widehat{\lambda}_{ij} & \text{otherwise} \end{cases} \tag{4.3.42}$$

followed by

$$\tilde{\lambda}_{ij} = -\sum_{j=1, j \neq i}^{\ell} \widehat{\lambda}_{ij} \quad \text{for } i = 1, 2, \ldots, \ell. \tag{4.3.43}$$

Two-state model fitting

The model fitting is done using four different scenarios based on the time intervals of the data at hand. The first scenario is the entire time interval which is the total number of quarterly time steps in the data. The entire time interval is then split into 3 according to the impact of the UK financial recession. The divisions are pre-recession, recession and the post-recession which are the periods before, during and after the financial recession respectively. Details of each scenario, the time intervals and the number of observation is shown in Table 4.2.

Scenario	Time interval	Number of observations
Entire	September 2001 – December 2019	73
Pre-recession	September 2001 – December 2007	25
Recession	January 2008 – December 2012	20
Post-recession	January 2013 – December 2019	28

TABLE 4.2: The scenarios, their corresponding time intervals and number of observation for the data analysis.

The parameter for the simulation of the model are derived from the labour force data in [134, 135]. These values are shown in Table 4.3. Note that values for unemployment is the sum of all unemployed and inactive individuals in the data.

Parameters	Entire	Pre-recession	Recession	Post-recession
N	37647261	37647261	39740790	40517859
E	27325028	27325028	29001072	28840555
U	10322233	10322233	10739718	11677304
E to E	26375755	26375755	27965849	27861367
E to U	906629	906629	920845	988327
U to E	915392	915392	1042197	954431
U to U	9252629	9252629	9623060	10412045

TABLE 4.3: Parameter for t-step simulations of the models derived from the labour force data.

Let $\mathbf{O}$ denote a matrix which contains transition frequencies (levels) from the first to the last day of the quarter under consideration (see Table 4.2).

Entire data scenario for the two-state model

Using the values in Table 4.3, the transition frequencies for the entire data scenario of the two-state model from from September 2001 to December 2001 is given by

$$\mathbf{O}_{\text{entire}} = \begin{bmatrix} 26375755 & 906629 \\ 915392 & 9252628 \end{bmatrix}. \tag{4.3.44}$$

The matrix of relative transition probabilities is given by

$$\widehat{\mathbf{P}}_{\text{entire}} = \begin{bmatrix} \frac{26375755}{26375755+906629} & \frac{906629}{26375755+906629} \\ \frac{915392}{915392+9252628} & \frac{9252628}{915392+9252628} \end{bmatrix} = \begin{bmatrix} 0.96676870 & 0.0332313 \\ 0.09002657 & 0.9099734 \end{bmatrix}. \tag{4.3.45}$$

Next, we compute relative transition rates using $\widehat{\mathbf{\Lambda}}_{\text{entire}} = \log \widehat{\mathbf{P}}_{\text{entire}}$ in (4.3.41). We have that

$$\mathbf{D}_{\text{entire}} = \begin{bmatrix} 1.00 & 0.00 \\ 0.00 & 0.88 \end{bmatrix}, \ \mathbf{\Psi}_{\text{entire}} = \begin{bmatrix} 0.71 & -0.35 \\ 0.71 & 0.94 \end{bmatrix} \text{ and } \mathbf{\Psi}^{-1}_{\text{entire}} = \begin{bmatrix} 1.03 & 0.38 \\ -0.78 & 0.78 \end{bmatrix}. \tag{4.3.46}$$

Then

$$\begin{aligned}\widehat{\mathbf{\Lambda}}_{\text{entire}} &= \mathbf{\Psi}_{\text{entire}} \cdot \log(\mathbf{D}_{\text{entire}}) \cdot \mathbf{\Psi}_{\text{entire}}^{-1} \\ &= \begin{bmatrix} 0.71 & -0.35 \\ 0.71 & 0.94 \end{bmatrix} \cdot \begin{bmatrix} 0.00 & 0.00 \\ 0.00 & -0.13 \end{bmatrix} \cdot \begin{bmatrix} 1.03 & 0.38 \\ -0.78 & 0.78 \end{bmatrix} \\ &= \begin{bmatrix} -0.03546486 & 0.03546486 \\ 0.09607750 & -0.09607750 \end{bmatrix}. \end{aligned} \tag{4.3.47}$$

We then replace all negative diagonal elements in each row with zero and re-calculate the diagonal elements as the negative sum of the non-diagonal elements in (4.3.47). Thus, the computed transition matrix using the DA approach is given by

$$\mathbf{\Lambda}_{\text{entire}} = \begin{bmatrix} -0.03546486 & 0.03546486 \\ 0.09607750 & -0.09607750 \end{bmatrix}. \tag{4.3.48}$$

We further compute the probability matrix using (4.3.48). Then from Section 4.3.1 we have that

$$\mathbf{Q}_{\text{entire}} = \begin{bmatrix} -0.13 & 0.00 \\ 0.00 & 0.00 \end{bmatrix}, \mathbf{\Phi}_{\text{entire}} = \begin{bmatrix} -0.35 & 0.71 \\ 0.94 & 0.71 \end{bmatrix}, \mathbf{\Phi}_{\text{entire}}^{-1} = \begin{bmatrix} -0.78 & 0.78 \\ 1.03 & 0.38 \end{bmatrix}. \tag{4.3.49}$$

Subsequently

$$\begin{aligned}\mathbf{P}_{\text{entire}} &= \mathbf{\Phi}_{\text{entire}} \cdot \exp(\mathbf{Q}_{\text{entire}}) \cdot \mathbf{\Phi}_{\text{entire}}^{-1} \\ &= \begin{bmatrix} -0.35 & 0.71 \\ 0.94 & 0.71 \end{bmatrix} \cdot \begin{bmatrix} 0.88 & 0.00 \\ 0.00 & 1.00 \end{bmatrix} \cdot \begin{bmatrix} -0.78 & 0.78 \\ 1.03 & 0.38 \end{bmatrix} \\ &= \begin{bmatrix} 0.96676870 & 0.0332313 \\ 0.09002657 & 0.9099734 \end{bmatrix}. \end{aligned} \tag{4.3.50}$$

Note that (4.3.50) is equal to (4.3.45) which is as expected. The unique stationary distribution for the entire data scenario is computed as

$$\begin{bmatrix} 0.7303921, 0.2696079 \end{bmatrix}. \tag{4.3.51}$$

The DA approach explained in Subsection 4.3.2 and demonstrated in Subsection 4.3.2 can be computed using R (see [108, p.2]). Thus, for subsequent computations, we will display only the results from R to minimise repetition of steps. The codes used to compute the entire data scenario is shown in Appendix A.3 as an example.

Next, we use the probability matrix along with initial conditions from the data to run simulations and compare the simulated values to our data.

For the entire data scenario of the two-state model, we use (4.3.50) and the initial states given by

$$\left[\frac{E}{N}, \frac{U}{N}\right] = \left[\frac{27325028}{37647261}, \frac{10322233}{37647261}\right] \approx \left[0.73, 0.27\right] \tag{4.3.52}$$

to obtain the simulated values. The simulated values and actual data of employment and unemployment rates and levels for the entire data scenario of the two-state model are shown in Fig. 23. The outcomes for the two-state model will be discussed after considering all the scenarios.

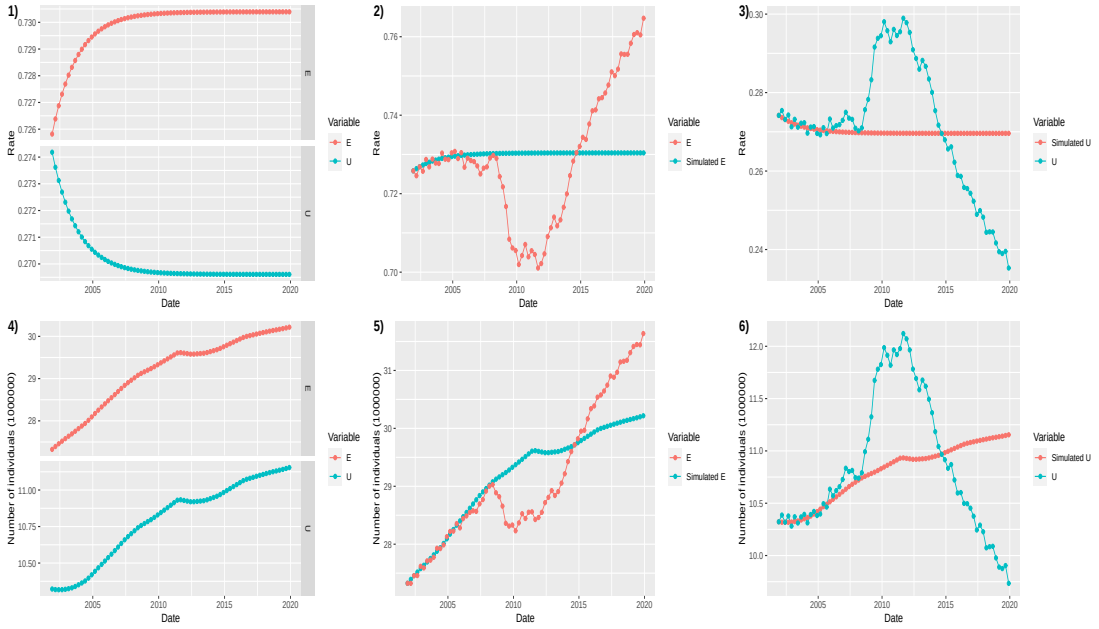

FIGURE 23: Graphs showing the t-step simulated values and actual data of employment and unemployment rates and levels for the entire data scenario of the two-state model. Plot 1) shows the simulated values for employment and unemployment rate only. Plot 4) shows employment and unemployment levels only. Plot 2) illustrates simulated and actual for employment rates. Plot 5) illustrates simulated and actual for employment levels. Plot 3) displays simulated and actual for unemployment rates. Plot 6) displays simulated and actual for unemployment levels.

Pre-recession data scenario for the two-state model

The parameters for the pre-recession data scenario are the same as the parameters used in the entire data scenario (4.3.2). Thus, the generator matrix and probability matrix in (4.3.48) and (4.3.50) respectively are the same. The only difference is the time interval (see Table 4.2). Using (4.3.50) and the initial states in (4.3.52), we run simulations and show the results in Fig. 24.

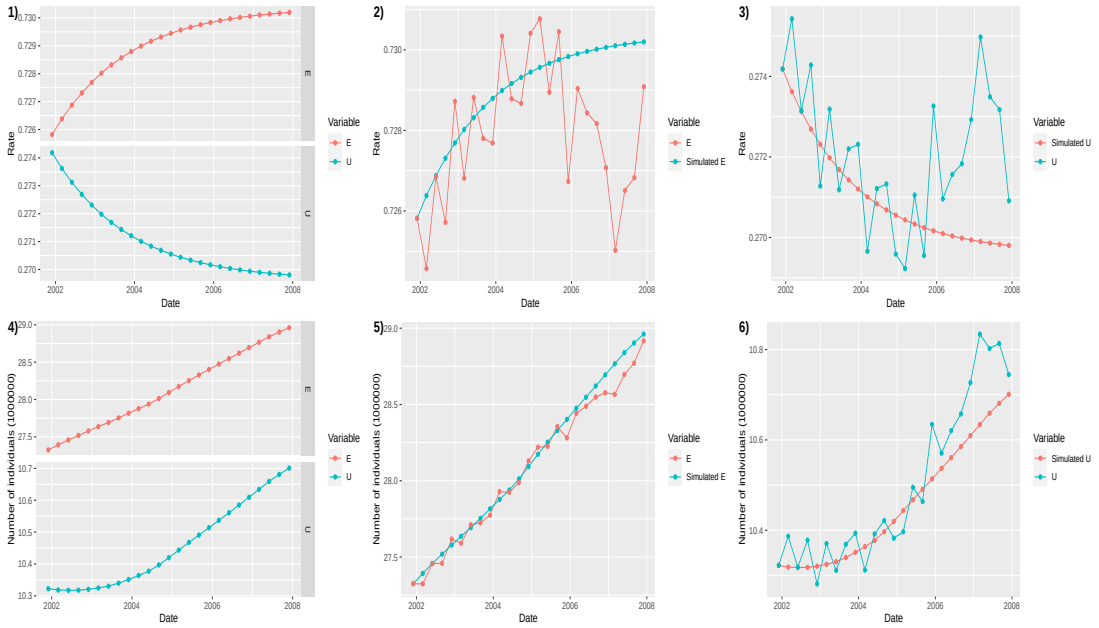

FIGURE 24: Graphs showing the t-step simulated values and actual data of employment and unemployment rates and levels of the pre-recession data scenario. Plot 1) shows the simulated values for employment and unemployment rate only. Plot 4) shows employment and unemployment levels only. Plot 2) illustrates simulated and actual for employment rates. Plot 5) illustrates simulated and actual for employment levels. Plot 3) displays simulated and actual for unemployment rates. Plot 6) displays simulated and actual for unemployment levels.

Recession data scenario for the two-state model

The transition frequencies for the recession data scenario of the two-state model from January 2008 to March 2008 is written as

$$\mathbf{O}_{\text{recession}} = \begin{bmatrix} 27965849 & 920845 \\ 1042197 & 9623060 \end{bmatrix}. \tag{4.3.53}$$

Again, we use the DA technique explained in Section 4.3.2 and demonstrated in Section 4.3.2. The DA approach can also be easily computed in R (see [108, p.2]). The matrix of estimated transition probabilities is given by

$$\widehat{\mathbf{P}}_{\text{recession}} = \begin{bmatrix} \frac{27965849}{27965849+920845} & \frac{920845}{27965849+920845} \\ \frac{1042197}{1042197+9623060} & \frac{9623060}{1042197+9623060} \end{bmatrix} = \begin{bmatrix} 0.96812217 & 0.03187783 \\ 0.09771888 & 0.90228112 \end{bmatrix}. \tag{4.3.54}$$

The computed transition matrix using the DA approach in R is given by

$$\mathbf{\Lambda}_{\text{recession}} = \begin{bmatrix} -0.03414 & 0.03414 \\ 0.10470 & -0.10470 \end{bmatrix}. \tag{4.3.55}$$

Consequently

$$\mathbf{P}_{\text{recession}} = \begin{bmatrix} 0.96812218 & 0.03187783 \\ 0.09771888 & 0.90228112 \end{bmatrix}. \tag{4.3.56}$$

The unique stationary distribution for the recession data scenario is given by

$$\begin{bmatrix} 0.7540229, 0.2459771 \end{bmatrix}. \tag{4.3.57}$$

Again using (4.3.50) and the initial states given by

$$\begin{bmatrix} \frac{E}{N}, \frac{U}{N} \end{bmatrix} = \begin{bmatrix} \frac{29001072}{39740790}, \frac{10739718}{39740790} \end{bmatrix} \approx \begin{bmatrix} 0.73, 0.27 \end{bmatrix}, \tag{4.3.58}$$

we run t-step simulations and display the results in Fig. 25.

Post-recession data scenario for the two-state model

The transition frequencies for the post-recession data scenario of the two-state model from January 2013 to March 2013 is written as

$$\mathbf{O}_{\text{post-recession}} = \begin{bmatrix} 27861367 & 988327 \\ 954431 & 10412045 \end{bmatrix}. \tag{4.3.59}$$

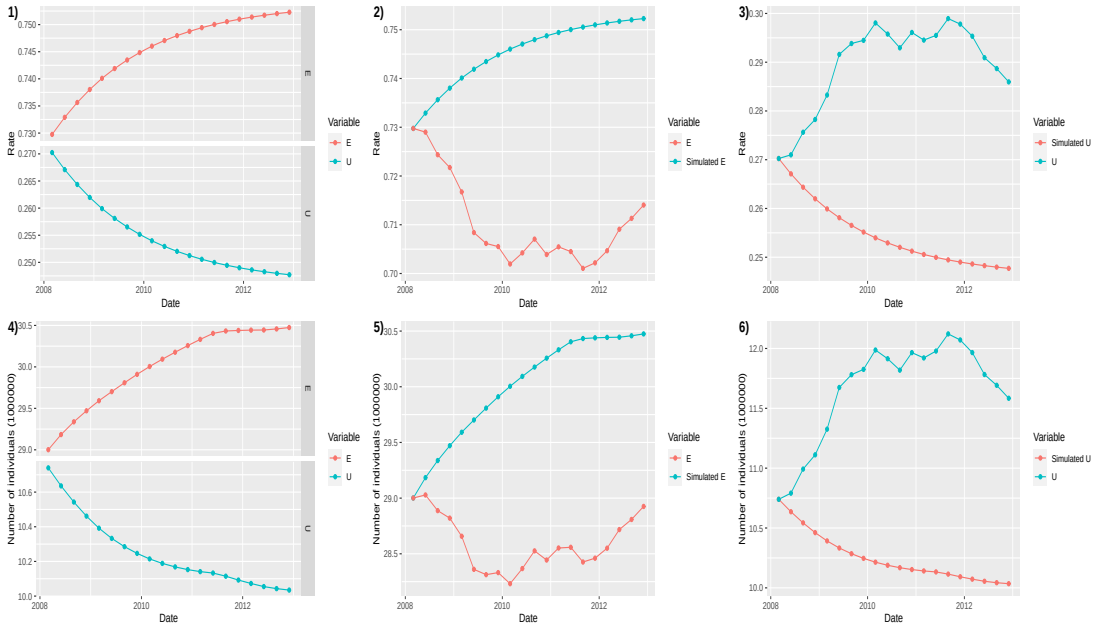

FIGURE 25: Graphs showing the t-step simulated values and actual data of employment and unemployment rates and levels for the recession data scenario of the two-state model. Plot 1) shows the simulated values for employment and unemployment rate only. Plot 4) shows employment and unemployment levels only. Plot 2) illustrates simulated and actual for employment rates. Plot 5) illustrates simulated and actual for employment levels. Plot 3) displays simulated and actual for unemployment rates. Plot 6) displays simulated and actual for unemployment levels.

The matrix of estimated transition probabilities is given by

$$\widehat{\mathbf{P}}_{\text{post-recession}} = \begin{bmatrix} \frac{27861367}{27861367+988327} & \frac{988327}{27861367+988327} \\ \frac{954431}{954431+10412045} & \frac{10412045}{954431+10412045} \end{bmatrix} = \begin{bmatrix} 0.96574220 & 0.0342578 \\ 0.08396895 & 0.9160311 \end{bmatrix}. \tag{4.3.60}$$

The computed transition matrix using the DA approach in R is given by

$$\mathbf{\Lambda}_{\text{post-recession}} = \begin{bmatrix} -0.03646 & 0.03646 \\ 0.08936 & -0.08936 \end{bmatrix}. \tag{4.3.61}$$

Consequently

$$\mathbf{P}_{\text{post-recession}} = \begin{bmatrix} 0.96574220 & 0.0342578 \\ 0.08396895 & 0.9160311 \end{bmatrix}. \tag{4.3.62}$$

The unique stationary distribution for the post-recession data scenario is given by

$$\left[0.7102365, 0.2897635\right]. \tag{4.3.63}$$

The t-step simulation is done using (4.3.50) and the initial states given by

$$\left[\frac{E}{N}, \frac{U}{N}\right] = \left[\frac{28840555}{40517859}, \frac{11677304}{40517859}\right] \approx \left[0.71, 0.29\right]. \tag{4.3.64}$$

The results of are shown in Fig. 26.

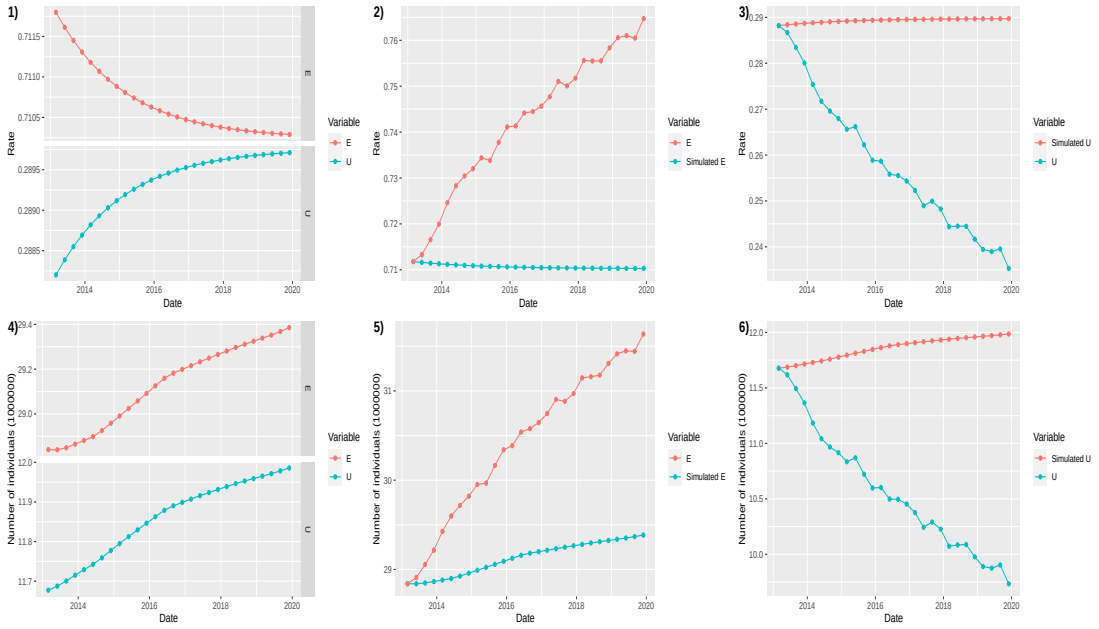

FIGURE 26: Graphs showing the t-step simulated values and actual data of employment and unemployment rates and levels for the post-recession data scenario of the two-state model. Plot 1) shows the simulated values for employment and unemployment rate only. Plot 4) shows employment and unemployment levels only. Plot 2) illustrates simulated and actual for employment rates. Plot 5) illustrates simulated and actual for employment levels. Plot 3) displays simulated and actual for unemployment rates. Plot 6) displays simulated and actual for unemployment levels.

The root mean square error and coefficient of determination for the two-state model.

After deriving the simulations, we use the root mean square error (RMSE) as a measure to check the error between the simulated values in relation to the observed data. RMSE

is a measure of accuracy used to compare the difference between the simulated values and the actual data [67, §2]. The RMSE formula given that the simulated values are denoted by $\widehat{y}_t$ and y_t represents the observed data at time t over a period of T is given by

$$RMSE = \sqrt{\frac{\sum_{t=1}^{T}(\widehat{y}_t - y_t)^2}{T}}. \tag{4.3.65}$$

We support the absolute fit measure, RMSE, with the relative fit measure, coefficient of determination (R^2). The coefficient of determination (R^2) measures the proportion of the variance in the simulated values that are predictable from the actual data [40, Ch.I]. The formula for R^2 is given by

$$R^2 = 1 - \frac{\sum_{t=1}^{T}(y - \widehat{y}_t)^2}{\sum_{t=1}^{T}(y_t - \bar{y})^2} \tag{4.3.66}$$

where $\bar{y} = \frac{1}{T}\sum_{t=1}^{T} y_t$. The RMSE and R^2 values for the two-state model for the four scenarios are displayed in Table 4.4 and Table 4.5 respectively.

Parameters	Entire	Pre-recession	Recession	Post-recession
Employment rate	0.01637554	0.001924639	0.0377082	0.03482574
Unemployment rate	0.01637554	0.001924639	0.0377082	0.03482574
Employment level	0.6678523	0.07532717	1.52287	1.434191
Unemployment level	0.6678523	0.07532717	1.52287	1.434191

TABLE 4.4: RMSE values to assess the performance of the two-state model for the four scenarios in Table 4.2.

Parameters	Entire	Pre-recession	Recession	Post-recession
Employment rate	0.002514518	0.1737243	0.6878303	0.932229
Unemployment rate	0.002514518	0.1737243	0.6878303	0.932229
Employment level	0.7064425	0.987504	0.1662591	0.9816291
Unemployment level	0.02166971	0.9217928	0.7860486	0.9778135

TABLE 4.5: R^2 values to assess the performance of the two-state model for the four scenarios in Table 4.2.

Discussions for the two-state model fitting

In Fig. 23 for the entire data scenario of the two-state model, we see that the simulated values for rates and levels are close to the actual data from 2001 to 2008. After this period, in Fig. 23 plot 2) and plot 5) we observe that the simulated values for employment rates and levels are above the corresponding actual values for employment rates and levels from 2008 to 2014. To add on, from 2015 to 2020 in Fig. 23 plot 2) and plot 5) we see that the simulated values for employment rates and levels fall below the corresponding actual values for employment rates and levels. Also in Fig. 23 plot 3) and plot 5), the simulated values for unemployment rates and levels are less than the corresponding actual values for unemployment rates and levels within the period 2008 to 2014. Furthermore, Fig. 23 plot 3) and plot 5) show that the simulated values for unemployment rates and levels are greater than the corresponding actual values for unemployment rates and levels within the period 2015 to 2020. All the outlined observed characteristics support the reason why the RMSE values in Table 4.4 are low. Thus, the difference in the simulated and actual values cancel out each other as both take different forms of direction at a given point and switch to the opposite direction. At the same time, we can say that the model is able to predict the values better from 2008 to 2014. As a result, we split the entire data scenario into 3 time points to help interpret the results better.

The closeness between the simulated values and the actual data in plot 2), plot 3), plot 5) and plot 6) for Fig. 24, Fig. 25 and Fig. 26 are ranked as pre-recession<post-recession<recession for the two-state model. This ranking also reflects in RMSE values in Table 4.4. From Table 4.4, it can be seen that the pre-recession period has the smallest RMSE values for employment rate, unemployment rate, employment level, and unemployment level compared to that of the entire, recession and post-recession periods. This indicates that the simulated values during the pre-recession period best fits the rates and level of employment and unemployment in the actual data set for the UK. The derived R^2 values in Table 4.5 illustrate acceptable values and shows that the rates and levels of employment and unemployment in the actual data are explained by the simulated values.

It is important to note that the two state model best predicts employment and unemployment rates and levels during the precession period when the economy is very stable. During the recession period, employment and unemployment rates and levels

become more unpredictable due to the instability in the economy. This is demonstrated in Fig. 25. After the recession period, the economy begins to recover from the recession shock. As a result the employment and unemployment rates and levels are somewhat unpredictable (not as unpredictable as the recession period) and this reflects in Fig. 26.

On the whole, the two-state model is not a very good fit but can be used to predict employment and unemployment rates and levels. Also, the two-state model is relatively simple and does not account for external interventions such as mortality, birth and immigration. To explore this further, we therefore include external interventions in the two-state model to form the four and five state models detailed in the subsequent sections.

4.4 Four-state model

The statistical framework for the next multi-state model is shown in Fig. 27. The inclusion of external entry and mortality allows four states for each quarterly transitions. The four-states are employed (E), unemployed (U), new entry denoted by B and mortality/exit state is denoted by D. To explain further, state B contains individuals that do not meet certain labour force criteria such as age and immigrants without working permits willing to work. Once the criteria limitations no longer hold, individuals transit from state B to either state E, U or D. Individuals may also move from state E to state U and vise versa, or may die.

Similar to Section 4.3, the transition from one compartment to another is described by rates. The transition rates between E and U are denoted by λ_{EU} and λ_{UE}. Set $\bar{N} = E + U + B$ as the total population and $N = E + U$ as the total labour force. We assume that all new external entries into state E and U from state B are denoted by β_E and β_U respectively. The exit rates from state E and U to state D are represented by μ_E and μ_U respectively. Thus, state D is an absorbing state.

The generator matrix or transition rate matrix $\mathbf{\Lambda}$ is given by

$$\mathbf{\Lambda} = \begin{bmatrix} -(\beta_E + \beta_U) & \beta_E & \beta_U & 0 \\ 0 & -(\lambda_{EU} + \mu_E) & \lambda_{EU} & \mu_E \\ 0 & \lambda_{UE} & -(\lambda_{UE} + \mu_U) & \mu_U \\ 0 & 0 & 0 & 0 \end{bmatrix}. \tag{4.4.1}$$

We use the matrix exponential approach to find the probability matrix. We find the

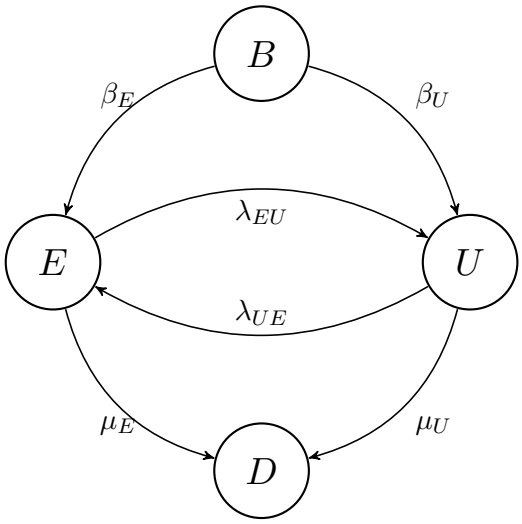

FIGURE 27: Graphical representation of the transition rates between employment (E), unemployment (U), entry (B) and exit (D) states. All new external entries into state E and U from state B are denoted by β_E and β_U respectively. The exit rates from state E and U are represented by μ_E and μ_U respectively.

eigenvalues q such that for some non zero vector $\boldsymbol{\phi}$,

$$\boldsymbol{\Lambda}\boldsymbol{\phi} = q\boldsymbol{\phi}. \tag{4.4.2}$$

Rewrite (4.4.2) to derive

$$(\boldsymbol{\Lambda} - \mathbf{I}q)\,\boldsymbol{\phi} = \begin{bmatrix} -(q+\beta_E+\beta_U) & \beta_E & \beta_U & 0 \\ 0 & -(q+\lambda_{EU}+\mu_E) & \lambda_{EU} & \mu_E \\ 0 & \lambda_{UE} & -(q+\lambda_{UE}+\mu_U) & \mu_U \\ 0 & 0 & 0 & -q \end{bmatrix} \boldsymbol{\phi} = \mathbf{0} \tag{4.4.3}$$

where $\mathbf{I}$ is the identity matrix and $\mathbf{0}$ is the zero vector. Note that (4.4.3) is true for some non-zero vector $\boldsymbol{\phi}$ if an only if

$$|\boldsymbol{\Lambda} - \mathbf{I}q| = \mathbf{0} \tag{4.4.4}$$

where $|\cdot|$ is the determinant. We have that

$$|\mathbf{\Lambda} - \mathbf{I}q| = \begin{vmatrix} -(q+\beta_E+\beta_U) & \beta_E & \beta_U & 0 \\ 0 & -(q+\lambda_{EU}+\mu_E) & \lambda_{EU} & \mu_E \\ 0 & \lambda_{UE} & -(q+\lambda_{UE}+\mu_U) & \mu_U \\ 0 & 0 & 0 & -q \end{vmatrix} = \mathbf{0}. \quad (4.4.5)$$

The determinant of an upper triangular matrix is the product of its diagonal elements. From (4.4.5) we get

$$-q\left(-(q+\beta_E+\beta_U)\right)\left(-(q+\lambda_{EU}+\mu_E)\right)\left(-(q+\lambda_{UE}+\mu_U)\right) = 0 \quad (4.4.6)$$

We solve for q in (4.4.6) to obtain the eigenvalues of the generator matrix $\mathbf{\Lambda}$ in (4.4.1). The eigenvalues are

$$q_1 = 0 \quad (4.4.7)$$

$$q_2 = \frac{1}{2}\left(-\nu - \lambda_{UE} - \lambda_{EU} - \mu_E - \mu_U\right) \quad (4.4.8)$$

$$q_3 = \frac{1}{2}\left(\nu - \lambda_{UE} - \lambda_{EU} - \mu_E - \mu_U\right) \quad (4.4.9)$$

$$q_4 = -\beta_E - \beta_U \quad (4.4.10)$$

where $\nu = \sqrt{\left(\lambda_{EU}+\lambda_{UE}+\mu_E+\mu_U\right)^2 - 4\left(\lambda_{UE}\mu_E + \lambda_{EU}\mu_U + \mu_E\mu_U\right)}$. The corresponding eigenvectors are those $\boldsymbol{\phi}$ such that $(\mathbf{\Lambda} - \mathbf{I}q)\,\boldsymbol{\phi} = \mathbf{0}$ for some eigenvalue q. Using (4.4.3), we write $\boldsymbol{\phi} = (\varphi_1, \varphi_2, \varphi_3, \varphi_4)^\intercal$ and $\mathbf{0} = (0,0,0,0)^\intercal$ such that

$$(\mathbf{\Lambda} - \mathbf{I}q)\,\boldsymbol{\phi} = \begin{bmatrix} -(q+\beta_E+\beta_U) & \beta_E & \beta_U & 0 \\ 0 & -(q+\lambda_{EU}+\mu_E) & \lambda_{EU} & \mu_E \\ 0 & \lambda_{UE} & -(q+\lambda_{UE}+\mu_U) & \mu_U \\ 0 & 0 & 0 & -q \end{bmatrix} \cdot \begin{bmatrix} \varphi_1 \\ \varphi_2 \\ \varphi_3 \\ \varphi_4 \end{bmatrix} = \begin{bmatrix} 0 \\ 0 \\ 0 \\ 0 \end{bmatrix}. \quad (4.4.11)$$

To find the eigenvectors, we substitute each of the eigenvalues of the generator matrix ((4.4.7), (4.4.8), (4.4.9), (4.4.10)) into (4.4.11) and solve the system that is obtained. First, substitute the eigenvalue $q_1 = 0$ in (4.4.7) into the matrix (4.4.11) and solve the

system

$$(\mathbf{\Lambda} - \mathbf{I}(0))\,\boldsymbol{\phi} = \begin{bmatrix} -(\beta_E + \beta_U) & \beta_E & \beta_U & 0 \\ 0 & -(\lambda_{EU} + \mu_E) & \lambda_{EU} & \mu_E \\ 0 & \lambda_{UE} & -(\lambda_{UE} + \mu_U) & \mu_U \\ 0 & 0 & 0 & 0 \end{bmatrix} \cdot \begin{bmatrix} \varphi_1 \\ \varphi_2 \\ \varphi_3 \\ \varphi_4 \end{bmatrix} = \begin{bmatrix} 0 \\ 0 \\ 0 \\ 0 \end{bmatrix}. \tag{4.4.12}$$

We then multiply both sides of the equation by an invertible matrix denoted by $\mathbf{A}$ such that the derived coefficient matrix is in reduced echelon form. We then perform the matrix multiplication for

$$\mathbf{A}\,(\mathbf{\Lambda} - \mathbf{I}(0))\,\boldsymbol{\phi} = \mathbf{A0} \tag{4.4.13}$$

where

$$\mathbf{A} = \begin{bmatrix} \frac{1}{-(\beta_E+\beta_U)} & \frac{-\beta_E\lambda_{UE}-\beta_U\lambda_{UE}-\beta_E\mu_U}{(\beta_E+\beta_U)(\lambda_{UE}\mu_E+\lambda_{EU}\mu_U+\mu_E\mu_U)} & \frac{-\beta_E\lambda_{EU}-\beta_U\lambda_{EU}-\beta_U\mu_E}{(\beta_E+\beta_U)(\lambda_{UE}\mu_E+\lambda_{EU}\mu_U+\mu_E\mu_U)} & 0 \\ 0 & \frac{-\lambda_{UE}-\mu_U}{\lambda_{UE}\mu_E+\lambda_{EU}\mu_U+\mu_E\mu_U} & -\frac{\lambda_{EU}}{\lambda_{UE}\mu_E+\lambda_{EU}\mu_U+\mu_E\mu_U} & 0 \\ 0 & -\frac{\lambda_{UE}}{\lambda_{UE}\mu_E+\lambda_{EU}\mu_U+\mu_E\mu_U} & \frac{-\lambda_{EU}-\mu_E}{\lambda_{UE}\mu_E+\lambda_{EU}\mu_U+\mu_E\mu_U} & 0 \\ 0 & 0 & 0 & 1 \end{bmatrix}. \tag{4.4.14}$$

The matrix multiplication of (4.4.13) yields

$$\begin{bmatrix} 1 & 0 & 0 & -1 \\ 0 & 1 & 0 & -1 \\ 0 & 0 & 1 & -1 \\ 0 & 0 & 0 & 0 \end{bmatrix} \cdot \begin{bmatrix} \varphi_1 \\ \varphi_2 \\ \varphi_3 \\ \varphi_4 \end{bmatrix} = \begin{bmatrix} 0 \\ 0 \\ 0 \\ 0 \end{bmatrix}. \tag{4.4.15}$$

Equation (4.4.15) as a sytem of scalar equation is given by

$$\begin{cases} \varphi_1 - \varphi_4 = 0 \\ \varphi_2 - \varphi_4 = 0 \\ \varphi_3 - \varphi_4 = 0 \end{cases} \implies \begin{cases} \varphi_1 = \varphi_4 \\ \varphi_2 = \varphi_4 \\ \varphi_3 = \varphi_4 \end{cases} \tag{4.4.16}$$

We then use (4.4.16) to determine the entries of $\boldsymbol{\phi}$ in terms of φ_4. Accordingly,

$$\boldsymbol{\phi} = \begin{bmatrix} \varphi_1 \\ \varphi_2 \\ \varphi_3 \\ \varphi_4 \end{bmatrix} = \begin{bmatrix} \varphi_4 \\ \varphi_4 \\ \varphi_4 \\ \varphi_4 \end{bmatrix}. \tag{4.4.17}$$

Setting $\varphi_4 = 1$ in $\begin{pmatrix}\varphi_4 & \varphi_4 & \varphi_4 & \varphi_4\end{pmatrix}^\intercal$, we have that $\begin{pmatrix}1 & 1 & 1 & 1\end{pmatrix}^\intercal$ is an eigenvector of the generator matrix in (4.4.1) associated with the eigenvalue $q_1 = 0$. We repeat this procedure for the other eigenvalues in (4.4.8), (4.4.9) and (4.4.10). Consequently, the eigenvalues of the generator matrix are given as

$$\boldsymbol{\phi}_1 = \begin{pmatrix}1, 1, 1, 1\end{pmatrix}^\intercal, \tag{4.4.18}$$

$$\boldsymbol{\phi}_2 = \begin{pmatrix}\frac{(-\beta_E\lambda_{UE}-2\beta_U\lambda_{UE}+\beta_E\lambda_{EU}+\beta_E\mu_E-\beta_E\mu_U+\beta_E\nu)}{(\lambda_{UE}(-2\beta_E-2\beta_U+\lambda_{UE}+\lambda_{EU}+\mu_E+\mu_U+\nu+2\mu_B))}, -\frac{-\lambda_{UE}+\lambda_{EU}+\mu_E-\mu_U+\nu}{2\lambda_{UE}}, 1, 0\end{pmatrix}^\intercal, \tag{4.4.19}$$

$$\boldsymbol{\phi}_3 = \begin{pmatrix}\frac{(-\beta_E\lambda_{UE}-2\beta_U\lambda_{UE}+\beta_E\lambda_{EU}+\beta_E\mu_E-\beta_E\mu_U-\beta_E\nu)}{(\lambda_{UE}(-2\beta_E-2\beta_U+\lambda_{UE}+\lambda_{EU}+\mu_E+\mu_U-\nu+2\mu_B))}, -\frac{-\lambda_{UE}+\lambda_{EU}+\mu_E-\mu_U-\nu}{2\lambda_{UE}}, 1, 0\end{pmatrix}^\intercal, \tag{4.4.20}$$

$$\boldsymbol{\phi}_4 = \begin{pmatrix}1, 0, 0, 0\end{pmatrix}^\intercal \tag{4.4.21}$$

Let $\mathbf{Q}$ be a diagonal matrix consisting of the eigenvalues of $\boldsymbol{\Lambda}$ such that

$$\mathbf{Q} = \begin{bmatrix} q_1 & 0 & 0 & 0 \\ 0 & q_2 & 0 & 0 \\ 0 & 0 & q_3 & 0 \\ 0 & 0 & 0 & q_4 \end{bmatrix}. \tag{4.4.22}$$

Using (4.4.18), (4.4.19),(4.4.20) and (4.4.21),

$$\boldsymbol{\Phi} = \begin{bmatrix}\boldsymbol{\phi}_1 & \boldsymbol{\phi}_2 & \boldsymbol{\phi}_3 & \boldsymbol{\phi}_4\end{bmatrix}. \tag{4.4.23}$$

In that case, we derive

$$\mathbf{P}(t) = \mathrm{e}^{\boldsymbol{\Lambda} t} = \boldsymbol{\Phi}\mathrm{e}^{\mathbf{Q}t}\boldsymbol{\Phi}^{-1} = \boldsymbol{\Phi} \cdot \text{ diag } \begin{pmatrix}\mathrm{e}^{\phi_1 t}, \cdots, \mathrm{e}^{\phi_\ell t}\end{pmatrix} \cdot \boldsymbol{\Phi}^{-1}. \tag{4.4.24}$$

Next we fit the four-state model in Fig. 27 to our data using similar arguments from Section 4.3.2.

4.4.1 Four-state model fitting

The parameters for the t-step simulation of the four-state model in Fig. 27 are seen in Table 4.3 with additional entries for state B and D in Table 4.6. There is no publicly available data on entry and exit rates and levels to and from UK labour force so we use the number of individuals in UK birth and mortality register from [85, 24, 105]. These parameters came from only first time point and may not be appropriate but will do for now.

Parameters	Entire	Pre-recession	Recession	Post-recession
$\bar{N}$	70347261	70347261	77230790	79227859
B	32700000	32700000	37490000	38710000
D	12600200	12600200	12116000	11939300
B to B	9343128	9343128	12317254	13079917
B to E	12701680	12701680	14077937	14091229
B to U	4798154	4798154	5213361	5705423
B to D	5857037	5857037	5881448	5833432
E to D	4894303	4894303	4549701	4346148
U to D	1848859	1848859	1684852	1759719

TABLE 4.6: Parameter for computations and t-step simulations.

Entire data scenario for the four-state model

The transition frequencies for the entire data scenario of the four-state model from September 2001 to December 2001 is written as

$$\mathbf{O}_{\text{entire}} = \begin{bmatrix} 9343129 & 12701680 & 4798154 & 5857037 \\ 0 & 26375755 & 906629 & 4894303 \\ 0 & 915392 & 9252628 & 1848859 \\ 0 & 0 & 0 & 0 \end{bmatrix}. \tag{4.4.25}$$

The matrix of relative transition probabilities is given by

$$\begin{aligned} \widehat{\mathbf{P}}_{\text{entire}} &= \begin{bmatrix} \frac{9343129}{32700000} & \frac{12701680}{32700000} & \frac{4798154}{32700000} & \frac{5857037}{32700000} \\ 0 & \frac{26375755}{32176687} & \frac{906629}{32176687} & \frac{4894303}{32176687} \\ 0 & \frac{915392}{12016879} & \frac{9252628}{12016879} & \frac{1848859}{12016879} \\ 0 & 0 & 0 & 1 \end{bmatrix} \\ &= \begin{bmatrix} 0.2857226 & 0.38843058 & 0.14673254 & 0.1791143 \\ 0 & 0.81971631 & 0.02817658 & 0.1521071 \\ 0 & 0.07617552 & 0.76996931 & 0.1538552 \\ 0 & 0 & 0 & 1 \end{bmatrix}. \end{aligned} \tag{4.4.26}$$

Following this, we compute relative transition rates using $\widehat{\mathbf{\Lambda}}_{\text{entire}} = \log \widehat{\mathbf{P}}_{\text{entire}}$ in (4.3.41). We have that

$$\mathbf{D}_{\text{entire}} = \begin{bmatrix} 1.00 & 0.00 & 0.00 & 0.00 \\ 0.00 & 0.85 & 0.00 & 0.00 \\ 0.00 & 0.00 & 0.74 & 0.00 \\ 0.00 & 0.00 & 0.00 & 0.29 \end{bmatrix} \text{ then } \log(\mathbf{D}_{\text{entire}}) = \begin{bmatrix} 0.00 & 0.00 & 0.00 & 0.00 \\ 0.00 & -0.17 & 0.00 & 0.00 \\ 0.00 & 0.00 & -0.30 & 0.00 \\ 0.00 & 0.00 & 0.00 & -1.25 \end{bmatrix}. \tag{4.4.27}$$

Also,

$$\mathbf{\Psi}_{\text{entire}} = \begin{bmatrix} 0.50 & 0.56 & 0.01 & 1.00 \\ 0.50 & 0.59 & -0.34 & 0.00 \\ 0.50 & 0.58 & 0.94 & 0.00 \\ 0.50 & 0.00 & 0.00 & 0.00 \end{bmatrix} \text{ and } \mathbf{\Psi}^{-1}_{\text{entire}} = \begin{bmatrix} 0.00 & 0.00 & 0.00 & 2.00 \\ 0.00 & 1.25 & 0.45 & -1.70 \\ 0.00 & -0.77 & 0.78 & -0.01 \\ 1.00 & -0.69 & -0.26 & -0.05 \end{bmatrix}. \tag{4.4.28}$$

Consequently,

$$\widehat{\mathbf{\Lambda}}_{\text{entire}} = \mathbf{\Psi}_{\text{entire}} \cdot \log(\mathbf{D}_{\text{entire}}) \cdot \mathbf{\Psi}^{-1}_{\text{entire}} = \begin{bmatrix} -1.2527 & 0.75120 & 0.2846 & 0.2169 \\ 0 & -0.20050 & 0.0355 & 0.1650 \\ 0 & 0.09598 & -0.2631 & 0.1672 \\ 0 & 0 & 0 & 0 \end{bmatrix}. \tag{4.4.29}$$

We repeat the steps for the DA approach using (4.4.29) which are to replace all negative diagonal elements in each row with zero and re-calculate the diagonal elements as the negative sum of the non-diagonal elements. Thus, the computed transition matrix using the DA approach is given by

$$\mathbf{\Lambda}_{\text{entire}} = \begin{bmatrix} -1.2527 & 0.75120 & 0.2846 & 0.2169 \\ 0 & -0.20050 & 0.0355 & 0.1650 \\ 0 & 0.09598 & -0.2631 & 0.1672 \\ 0 & 0 & 0 & 0 \end{bmatrix}. \tag{4.4.30}$$

We then compute the probability matrix using (4.4.30). From Section 4.3.1 we have that

$$\mathbf{Q}_{\text{entire}} = \begin{bmatrix} -1.25 & 0.00 & 0.00 & 0.00 \\ 0.00 & -0.30 & 0.00 & 0.00 \\ 0.00 & 0.00 & -0.17 & 0.00 \\ 0.00 & 0.00 & 0.00 & 0.00 \end{bmatrix} \text{ and } \exp(\mathbf{Q}_{\text{entire}}) = \begin{bmatrix} 0.29 & 0.00 & 0.00 & 0.00 \\ 0.00 & 0.74 & 0.00 & 0.00 \\ 0.00 & 0.00 & 0.85 & 0.00 \\ 0.00 & 0.00 & 0.00 & 1.00 \end{bmatrix}. \tag{4.4.31}$$

In addition,

$$\mathbf{\Phi}_{\text{entire}} = \begin{bmatrix} 1.00 & 0.01 & 0.56 & 0.50 \\ 0.00 & -0.34 & 0.59 & 0.50 \\ 0.00 & 0.94 & 0.58 & 0.50 \\ 0.00 & 0.00 & 0.00 & 0.50 \end{bmatrix} \text{ and } \mathbf{\Phi}^{-1}_{\text{entire}} = \begin{bmatrix} 1.00 & -0.69 & -0.26 & -0.05 \\ 0.00 & -0.77 & 0.78 & -0.01 \\ 0.00 & 1.25 & 0.45 & -1.70 \\ 0.00 & 0.00 & 0.00 & 2.00 \end{bmatrix}. \tag{4.4.32}$$

Subsequently,

$$\mathbf{P}_{\text{entire}} = \mathbf{\Phi}_{\text{entire}} \cdot \exp(\mathbf{Q}_{\text{entire}}) \cdot \mathbf{\Phi}^{-1}_{\text{entire}} = \begin{bmatrix} 0.2857 & 0.3884 & 0.1467 & 0.1791 \\ 0 & 0.8197 & 0.0282 & 0.1521 \\ 0 & 0.0762 & 0.7700 & 0.1538 \\ 0 & 0 & 0 & 1 \end{bmatrix}. \tag{4.4.33}$$

We observe that (4.4.33) is equal to (4.4.26) which is as expected. To iterate, the DA approach explained in Section 4.3.2 and demonstrated in Section 4.4.1 can be computed in R (see [108, p.2] and Appendix A.3). From this point we use the probability matrix along with initial conditions from the data to run simulations and compare the simulated values to our data.

For the entire data scenario of the four-state model, we use (4.4.33) and the initial states given by

$$\left[\tfrac{B}{N}, \tfrac{E}{N}, \tfrac{U}{N}, D\right] = \left[\tfrac{32700000}{70347261}, \tfrac{27325028}{70347261}, \tfrac{10322233}{70347261}, 0\right] \approx \left[0.46, 0.39, 0.15, 0\right] \tag{4.4.34}$$

to simulate t-step values and compare them to the actual value. The outcome of our simulation is shown in Fig. 28. The results for the four-state model will be discussed after considering all the scenarios.

Pre-recession data scenario for the four-state model

The parameters for the pre-recession data scenario are the same as the parameters used in the entire data scenario. Thus, the generator matrix and probability matrix

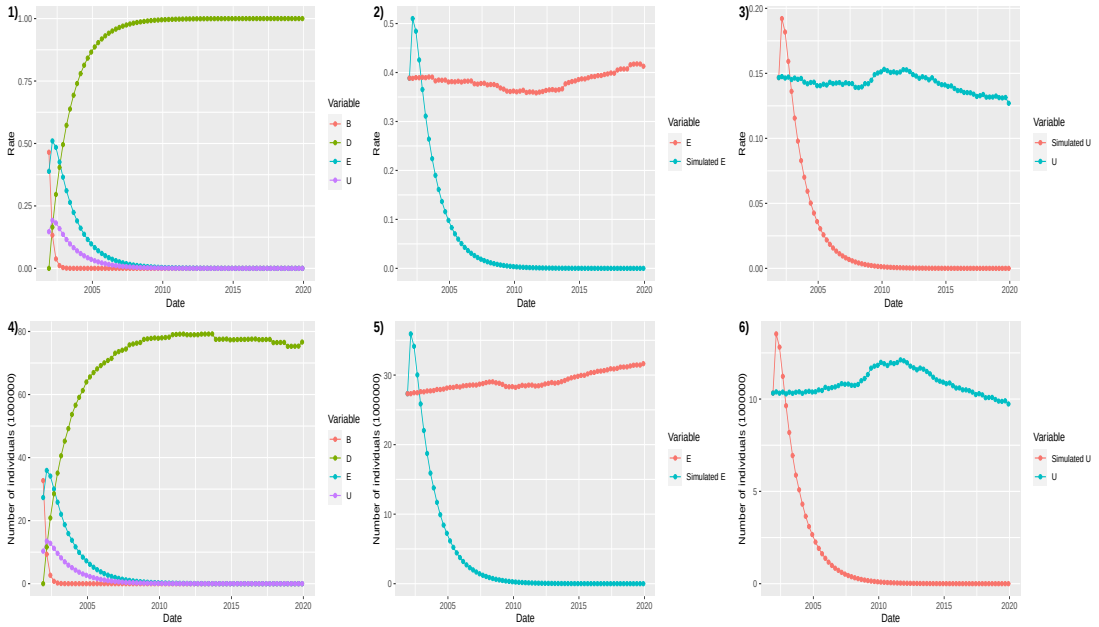

FIGURE 28: Graphs showing the t-step simulated values and actual data of employment and unemployment rates and levels for the entire data scenario of the four-state model. Plot 1) shows the simulated values for employment, unemployment, entry and exit rates only. Plot 4) shows employment, unemployment, entry and exit levels only. Plot 2) illustrates simulated and actual for employment rates. Plot 5) illustrates simulated and actual for employment levels. Plot 3) displays simulated and actual for unemployment rates. Plot 6) displays simulated and actual for unemployment levels.

in (4.4.30) and (4.4.33) respectively are the same. The only difference is the time interval (see Table 4.2). Using (4.4.33) and the initial states in (4.4.34), we derive t-step simulated values. The results are shown in Fig. 29.

Recession data scenario for the four-state model

The transition frequency matrix in this case for the time interval January 2008 to March 2008 is given as

$$\mathbf{O}_{\text{recession}} = \begin{bmatrix} 12317254 & 14077937 & 5213361 & 5881448 \\ 0 & 27965849 & 920845 & 4549701 \\ 0 & 1042197 & 9623060 & 1684852 \\ 0 & 0 & 0 & 0 \end{bmatrix}. \tag{4.4.35}$$

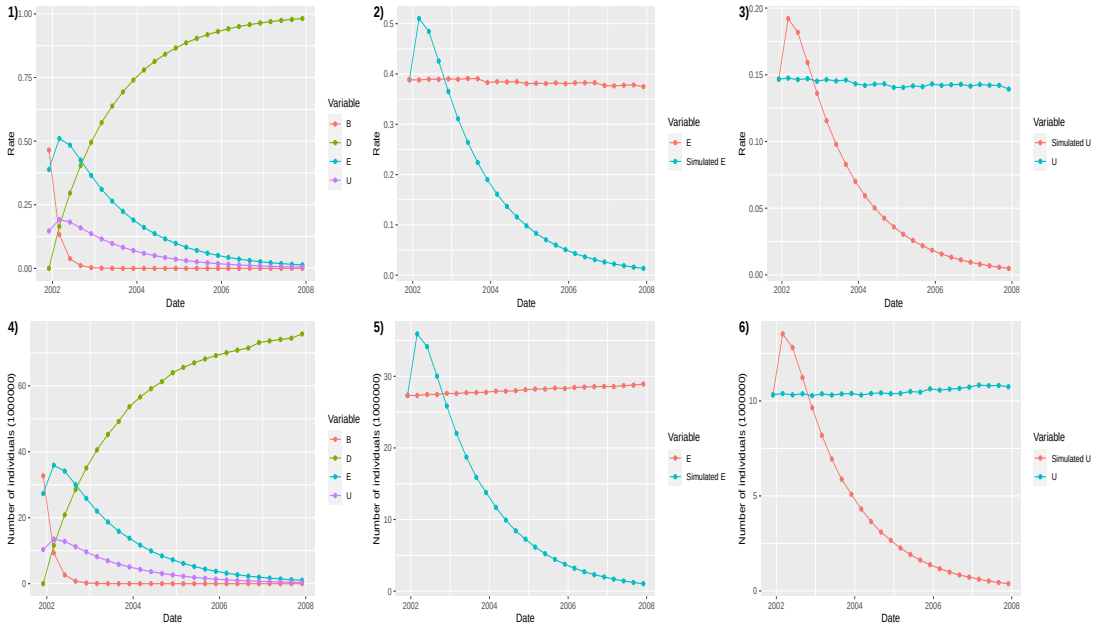

FIGURE 29: Graphs showing the t-step simulated values and actual data of employment and unemployment rates and levels for the pre-recession data scenario of the four-state model. Plot 1) shows the simulated values for employment, unemployment, entry and exit rates only. Plot 4) shows employment, unemployment, entry and exit levels only. Plot 2) illustrates simulated and actual for employment rates. Plot 5) illustrates simulated and actual for employment levels. Plot 3) displays simulated and actual for unemployment rates. Plot 6) displays simulated and actual for unemployment levels.

The matrix of relative transition probabilities is given by

$$\begin{aligned}\widehat{\mathbf{P}}_{\text{recession}} &= \begin{bmatrix} \frac{12317254}{37490000} & \frac{14077937}{37490000} & \frac{5213361}{37490000} & \frac{5881448}{37490000} \\ 0 & \frac{27965849}{33436395} & \frac{920845}{33436395} & \frac{4549701}{33436395} \\ 0 & \frac{1042197}{12350109} & \frac{9623060}{12350109} & \frac{1684852}{12350109} \\ 0 & 0 & 0 & 1 \end{bmatrix} \\ &= \begin{bmatrix} 0.3285477 & 0.37551179 & 0.1390600 & 0.1568804 \\ 0 & 0.83638948 & 0.0275402 & 0.1360703 \\ 0 & 0.08438768 & 0.7791883 & 0.1364241 \\ 0 & 0 & 0 & 1 \end{bmatrix}. \end{aligned} \tag{4.4.36}$$

Using the DA approach explained in Section 4.3.2 and demonstrated in Section 4.4.1. The computed transition matrix using the DA approach in R is given by

$$\mathbf{\Lambda}_{\text{recession}} = \begin{bmatrix} -1.113 & 0.6762 & 0.25300 & 0.1838 \\ 0 & -0.1804 & 0.03415 & 0.1463 \\ 0 & 0.1046 & -0.25130 & 0.1467 \\ 0 & 0 & 0 & 0 \end{bmatrix}. \tag{4.4.37}$$

Subsequently

$$\mathbf{P}_{\text{recession}} = \begin{bmatrix} 0.3285477 & 0.37551179 & 0.1390600 & 0.1568804 \\ 0 & 0.83638948 & 0.0275402 & 0.1360703 \\ 0 & 0.08438768 & 0.7791883 & 0.1364241 \\ 0 & 0 & 0 & 1 \end{bmatrix}. \tag{4.4.38}$$

Using (4.4.38) and the initial states given by

$$\left[\tfrac{B}{N}, \tfrac{E}{N}, \tfrac{U}{N}, D\right] = \left[\tfrac{37490000}{77230790}, \tfrac{29001072}{77230790}, \tfrac{10739718}{77230790}, 0\right] \approx \left[0.48, 0.38, 0.14, 0\right], \tag{4.4.39}$$

we simulate t-step values and compare them to the actual value. The outcome of our simulation is shown in Fig. 30.

Post-recession data scenario for the four-state model

The transition frequency matrix in this case for the time interval January 2013 to March 2013 is given as

$$\mathbf{O}_{\text{post-recession}} = \begin{bmatrix} 13079917 & 14091229 & 5705423 & 5833432 \\ 0 & 27861367 & 988327 & 4346148 \\ 0 & 954431 & 10412045 & 1759719 \\ 0 & 0 & 0 & 0 \end{bmatrix}. \tag{4.4.40}$$

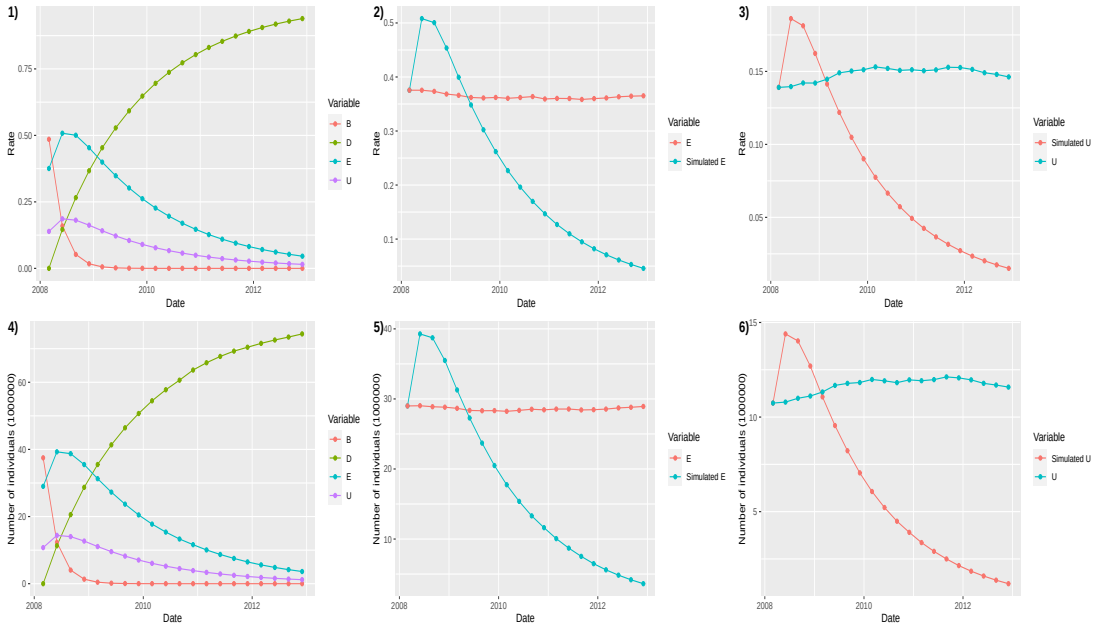

FIGURE 30: Graphs showing the t-step simulated values and actual data of employment and unemployment rates and levels for the recession data scenario of the four-state model. Plot 1) shows the simulated values for employment, unemployment, entry and exit rates only. Plot 4) shows employment, unemployment, entry and exit levels only. Plot 2) illustrates simulated and actual for employment rates. Plot 5) illustrates simulated and actual for employment levels. Plot 3) displays simulated and actual for unemployment rates. Plot 6) displays simulated and actual for unemployment levels.

The matrix of relative transition probabilities is given by

$$\begin{aligned}\widehat{\mathbf{P}}_{\text{recession}} &= \begin{bmatrix} \frac{13079917}{38710001} & \frac{14091229}{38710001} & \frac{5705423}{38710001} & \frac{5833432}{38710001} \\ 0 & \frac{27861367}{33195842} & \frac{988327}{33195842} & \frac{4346148}{33195842} \\ 0 & \frac{954431}{13126195} & \frac{10412045}{13126195} & \frac{1759719}{13126195} \\ 0 & 0 & 0 & 1 \end{bmatrix} \\ &= \begin{bmatrix} 0.3285477 & 0.37551179 & 0.1390600 & 0.1568804 \\ 0 & 0.83638948 & 0.0275402 & 0.1360703 \\ 0 & 0.08438768 & 0.7791883 & 0.1364241 \\ 0 & 0 & 0 & 1 \end{bmatrix}. \end{aligned} \tag{4.4.41}$$

To reiterate, we apply the DA approach explained in Section 4.3.2 and demonstrated in Section 4.4.1. The computed transition matrix using the DA approach in R is given

by

$$\mathbf{\Lambda}_{\text{post-recession}} = \begin{bmatrix} -1.085 & 0.6475 & 0.26260 & 0.1749 \\ 0 & -0.1768 & 0.03652 & 0.1403 \\ 0 & 0.0892 & -0.23330 & 0.1441 \\ 0 & 0 & 0 & 0 \end{bmatrix}. \tag{4.4.42}$$

Then

$$\mathbf{P}_{\text{post-recession}} = \begin{bmatrix} 0.337895 & 0.36402037 & 0.14738886 & 0.1506957 \\ 0 & 0.83930292 & 0.02977261 & 0.1309245 \\ 0 & 0.07271193 & 0.79322644 & 0.1340616 \\ 0 & 0 & 0 & 1 \end{bmatrix}. \tag{4.4.43}$$

By using (4.4.43) and the initial states given by

$$\left[\frac{B}{N}, \frac{E}{N}, \frac{U}{N}, D\right] = \left[\frac{38710000}{79227859}, \frac{28840555}{79227859}, \frac{11677304}{79227859}, 0\right] \approx \left[0.49, 0.36, 0.15, 0\right], \tag{4.4.44}$$

we simulate t-step values and compare them to the actual value. The results of our simulation is shown in Fig. 31.

The root mean square error and coefficient of determination for the four-state model.

The RMSE and R^2 values for the four-state model are displayed in Table 4.7 and Table 4.8 respectively.

Parameters	Entire	Pre-recession	Recession	Post-recession
Employment rate	0.3457144	0.3457144	0.2028004	0.2815643
Unemployment rate	0.1285666	0.1285666	0.09088482	0.089691
Employment level	27.43777	27.43777	20.41562	24.58125
Unemployment level	10.22532	10.22532	8.84823	8.074786

TABLE 4.7: RMSE values to assess the performance of the four-state model for the four scenarios in Table 4.2.

Discussions for the four-state model fitting

The four state model is an extension of the two-state model to which further includes the entry and exit factors. In plot 1) and plot 5) of Fig. 28, Fig. 29, Fig. 30 and Fig. 31

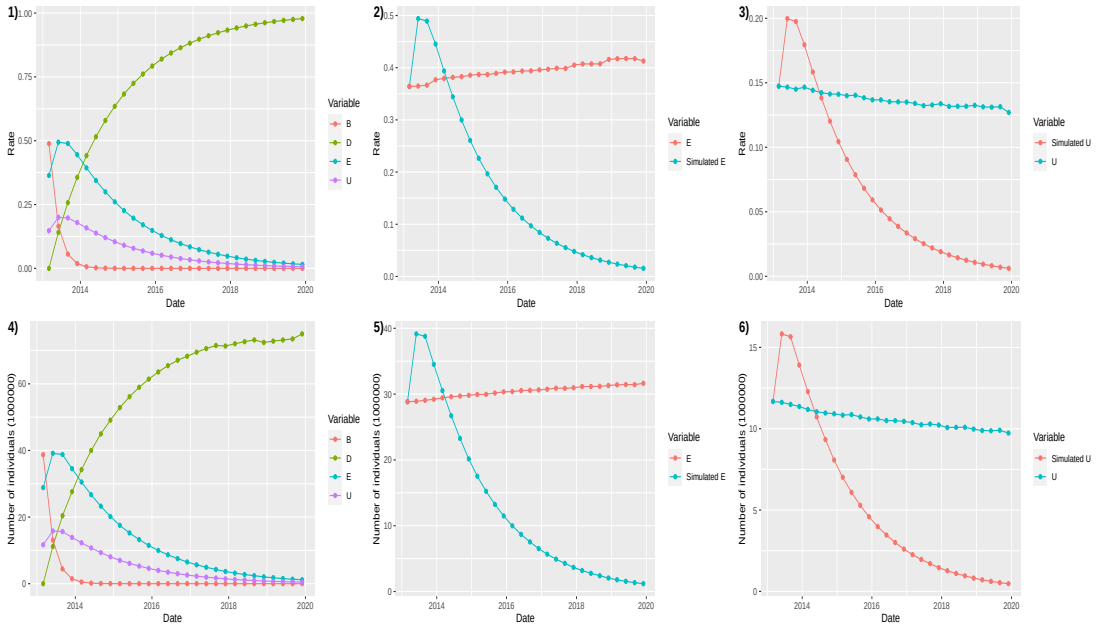

FIGURE 31: Graphs showing the t-step simulated values and actual data of employment and unemployment rates and levels for the post-recession data scenario of the four-state model. Plot 1) shows the simulated values for employment, unemployment, entry and exit rates only. Plot 4) shows employment, unemployment, entry and exit levels only. Plot 2) illustrates simulated and actual for employment rates. Plot 5) illustrates simulated and actual for employment levels. Plot 3) displays simulated and actual for unemployment rates. Plot 6) displays simulated and actual for unemployment levels.

the entry rates and levels fall whilst exit rates and levels increase. This is attributed to the fact that in the four-state model individuals transition from state E and state U to state D which is an absorbing state and individuals leave state B to state E and state U. The employment and unemployment rates and levels increase to attain a maximum and fall thereafter because individuals move in and out of state E and state U. The simulated values for employment rates and levels are predominantly higher than the simulated values for unemployment rates and levels.

To add on, the trend of the simulated values and actual values for unemployment rates and levels in plot 3) and plot 6) of Fig. 28, Fig. 29, Fig. 30 and Fig. 31 are similar. The similarity in plot 3) and plot 6) for all four scenarios reflects in the RMSE values in Table 4.7. That is for all four scenarios, the RMSE values for unemployment rates are approximately equal to 0.1 and the RMSE values for unemployment levels are also

Parameters	Entire	Pre-recession	Recession	Post-recession
Employment rate	0.0210185	0.0210185	0.5209847	0.8569706
Unemployment rate	0.05186431	0.05186431	0.5532286	0.9239236
Employment level	0.3295091	0.3295091	0.09641019	0.9281154
Unemployment level	0.1107471	0.1107471	0.6631474	0.9154006

TABLE 4.8: R^2 values to assess the performance of the four-state model for the four scenarios in Table 4.2.

relatively close to each other. In the same way, the pattern of the simulated values and actual values for employment rates and levels in plot 2) and plot 5) of Fig. 28, Fig. 29, Fig. 30 and Fig. 31 are also alike. Again, for all four scenarios, the RMSE values for employment rates and levels are relatively close to each other.

From Table 4.7, the simulated employment rates and levels using the four-state model during the recession period best predicts or fits the actual data as compared to the other periods. This is because during the recession phase, employment rates and levels are decreasing in the real world and when using the five-state model. During the post-recession period, unemployment rates and levels decrease as the economy would have started taking a stable shape. Hence enabling better prediction of the rates and levels of unemployment as compared to employment rates and levels which increase [10, 92, 71].

To support the argument raised above, from Table 4.8 it can be seen that the R^2 values for the post-recession period has the highest values. Supporting the initial assertion that the rate and level of movement for unemployment largely follows the movement of factors during the post-recession period. In addition, the R^2 values for the recession are also high.

We further extend the four-state model in Section 4.4 to include the inactive I state which results in a five-state model.

4.5 Five-state model

In this section, the inactive I state is added to the model. The transition rates from I to E and U are λ_{IE} and λ_{IU} respectively. Entry rates into I from B, E and U are denoted

by β_I, λ_{EI} and λ_{UI}. The exit rate from I is denoted by μ_I. Also let $\bar{N} = E+I+U+B$ be the total population and $N = E + I + U$ represent the total labour force. The transitions diagram related to this model is shown in Fig. 32.

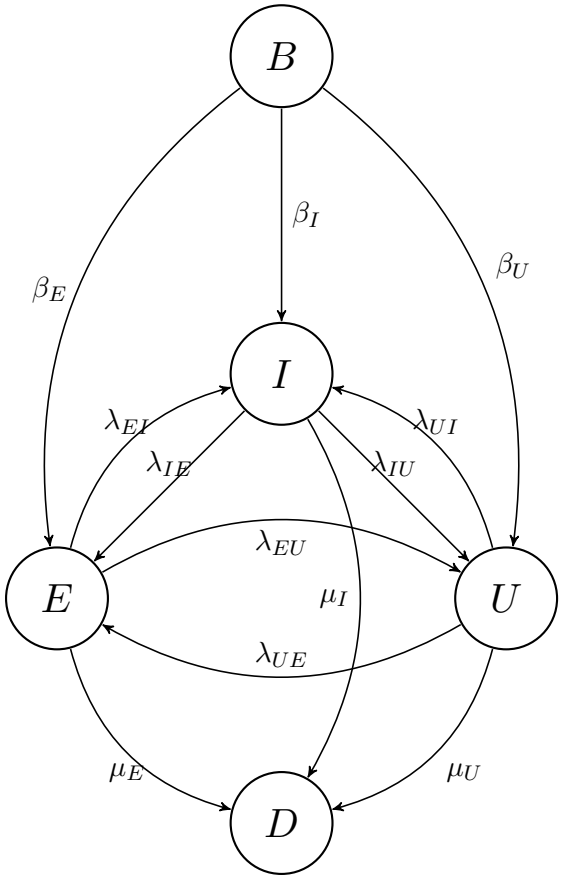

FIGURE 32: Graphical representation of the transition rates between employment (E), unemployment (U), inactivity (U), entry (B) and exit (D) states. Here, individuals enter state B at rate β_B. All new external entries into the other respective states from state B is denoted by β_E, β_U and β_I. Also, the exit rate from the states are represented by μ_E, μ_U, μ_I and μ_B.

The generator matrix or transition rate matrix $\mathbf{\Lambda}$ for Fig. 32 is given by

$$\mathbf{\Lambda} = \begin{bmatrix} \kappa & \beta_E & \beta_U & \beta_I & 0 \\ 0 & -(\lambda_{EU} + \lambda_{EI} + \mu_E) & \lambda_{EU} & \lambda_{EI} & \mu_E \\ 0 & \lambda_{UE} & -(\lambda_{UE} + \lambda_{UI} + \mu_U) & \lambda_{UI} & \mu_U \\ 0 & \lambda_{IE} & \lambda_{IU} & -(\lambda_{IE} + \lambda_{IU} + \mu_I) & \mu_I \\ 0 & 0 & 0 & 0 & 0 \end{bmatrix} \tag{4.5.1}$$

where $\kappa = -(\beta_E + \beta_U + \beta_I)$. We apply the matrix exponential approach to find the probability matrix as shown in the two-state model (4.3.1) and the four-state (model Section 4.4). The five-state model has more parameters and as such the eigenvalues and eigenvectors of the generator matrix in (4.5.1) are lengthy. These can be computed using the programming language Python. We then proceed by fitting the five-state model to the data.

4.5.1 Five-state model fitting

Again t-step simulations are run and compared to the actual data. The parameters for the simulation and computations in this subsection are in Table 4.3, Table 4.6 and Table 4.9.

Entire data scenario for the five-state model

The transition frequencies for the entire data scenario for the five-state model from September 2001 to December 2001 is given by

$$\mathbf{O}_{\text{entire}} = \begin{bmatrix} 9343129 & 12701680 & 702261 & 4095894 & 5857037 \\ 0 & 26375755 & 363624 & 543005 & 4894303 \\ 0 & 417425 & 792240 & 261623 & 270600 \\ 0 & 497967 & 325124 & 7873642 & 1578259 \\ 0 & 0 & 0 & 0 & 0 \end{bmatrix}. \tag{4.5.2}$$

Parameters	Entire	Pre-recession	Recession	Post-recession
U	1510768	1510768	1609762	2522005
I	8811465	8811465	9129956	9155299
B to U	702261	702261	781424	1232228
B to I	4095894	4095894	4431938	4473195
E to U	363624	363624	330631	422803
U to E	417425	417425	471023	569356
E to I	543005	543005	590213	565523
U to I	261623	261623	282931	379330
I to E	497967	497967	571174	385075
I to U	325124	325124	407238	509448
U to U	792240	792240	852497	1570299
I to I	7873642	7873642	8080394	7952968
U to D	270600	270600	252540	380055
I to D	1578259	1578259	1432312	1379664

TABLE 4.9: Parameter for t-step simulation and computations.

The matrix of relative transition probabilities is given by

$$\widehat{\mathbf{P}}_{\text{entire}} = \begin{bmatrix} \frac{9343129}{38710001} & \frac{12701680}{38710001} & \frac{702261}{38710001} & \frac{4095894}{38710001} & \frac{5857037}{38710001} \\ 0 & \frac{27861367}{32176687} & \frac{27861367}{32176687} & \frac{988327}{32176687} & \frac{4346148}{32176687} \\ 0 & \frac{417425}{1741888} & \frac{792240}{1741888} & \frac{261623}{1741888} & \frac{270600}{1741888} \\ 0 & \frac{497967}{10274992} & \frac{325124}{10274992} & \frac{7873642}{10274992} & \frac{1578259}{10274992} \\ 0 & 0 & 0 & 0 & 1 \end{bmatrix}$$

$$= \begin{bmatrix} 0.2857226 & 0.38843057 & 0.02147587 & 0.12525669 & 0.1791143 \\ 0 & 0.81971631 & 0.01130085 & 0.01687573 & 0.1521071 \\ 0 & 0.23963940 & 0.45481684 & 0.15019508 & 0.1553487 \\ 0 & 0.04846398 & 0.03164226 & 0.76629179 & 0.1536020 \\ 0 & 0 & 0 & 0 & 1 \end{bmatrix}. \quad (4.5.3)$$

The computed transition matrix using the DA method as shown in Section 4.3.2 and Section 4.4.1 using R is given by

$$\mathbf{\Lambda}_{\text{entire}} = \begin{bmatrix} -1.253 & 0.75110 & 0.04172 & 0.24300 & 0.2169 \\ 0 & -0.20220 & 0.01776 & 0.01948 & 0.1649 \\ 0 & 0.38130 & -0.80000 & 0.24880 & 0.1699 \\ 0 & 0.05284 & 0.05276 & -0.27230 & 0.1667 \\ 0 & 0 & 0 & 0 & 0 \end{bmatrix}. \tag{4.5.4}$$

Subsequently,

$$\mathbf{P}_{\text{entire}} = \begin{bmatrix} 0.2857226 & 0.38843057 & 0.02147587 & 0.12525669 & 0.1791143 \\ 0 & 0.81971631 & 0.01130085 & 0.01687573 & 0.1521071 \\ 0 & 0.23963940 & 0.45481684 & 0.15019508 & 0.1553487 \\ 0 & 0.04846398 & 0.03164226 & 0.76629179 & 0.1536020 \\ 0 & 0 & 0 & 0 & 1 \end{bmatrix}. \tag{4.5.5}$$

Applying (4.5.5) and the initial states given by

$$\begin{aligned} \left[\tfrac{B}{N}, \tfrac{E}{N}, \tfrac{U}{N}, \tfrac{I}{N}, D\right] &= \left[\tfrac{32700000}{70347261}, \tfrac{27325028}{70347261}, \tfrac{1510768}{70347261}, \tfrac{8811465}{70347261}, 0\right] \\ &\approx \left[0.46, 0.39, 0.02, 0.13, 0\right] \end{aligned} \tag{4.5.6}$$

we simulate t-step values and compare them to the actual value. The outcome of our simulation is shown in Fig. 33. Discussions on the five-state model will be done after considering all the scenarios.

Pre-recession data scenario for the five-state model

The parameters for the pre-recession data scenario are the same as the parameters used in the entire data scenario. Thus, the generator matrix and probability matrix in (4.5.4) and (4.5.5) respectively are the same. The only difference is the time interval (see Table 4.2). Using (4.5.5) and the initial states in (4.5.6), we derive t-step simulated values. The results are shown in Fig. 34.

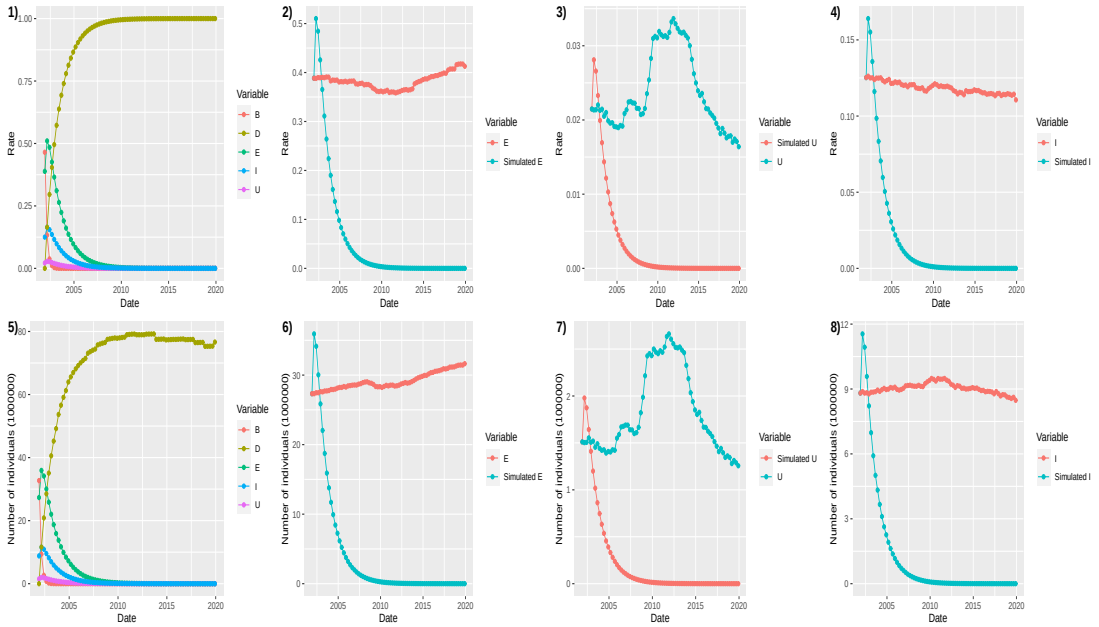

FIGURE 33: Graphs showing the t-step simulated values and actual data of employment and unemployment rates and levels for the entire data scenario for the five-state model. Plot 1) shows the simulated values for employment, unemployment, inactivity, entry and exit rates only. Plot 5) shows employment, unemployment, inactivity, entry and exit levels only. Plot 2) illustrates simulated and actual for employment rates. Plot 6) illustrates simulated and actual for employment levels. Plot 3) displays simulated and actual for unemployment rates. Plot 7) displays simulated and actual for unemployment levels. Plot 4) represents simulated and actual for inactivity rates. Plot 7) displays simulated and actual for inactivity levels.

Recession data scenario for the five-state model

The transition frequencies for the recession data scenario of the five-state model from January 2008 to March 2008 is written as

$$\mathbf{O}_{\text{recession}} = \begin{bmatrix} 12317254 & 14077937 & 781424 & 4431938 & 5881448 \\ 0 & 27965849 & 330631 & 590213 & 4549701 \\ 0 & 471023 & 852497 & 282931 & 252540 \\ 0 & 571174 & 407238 & 8080394 & 1432312 \\ 0 & 0 & 0 & 0 & 0 \end{bmatrix}. \tag{4.5.7}$$

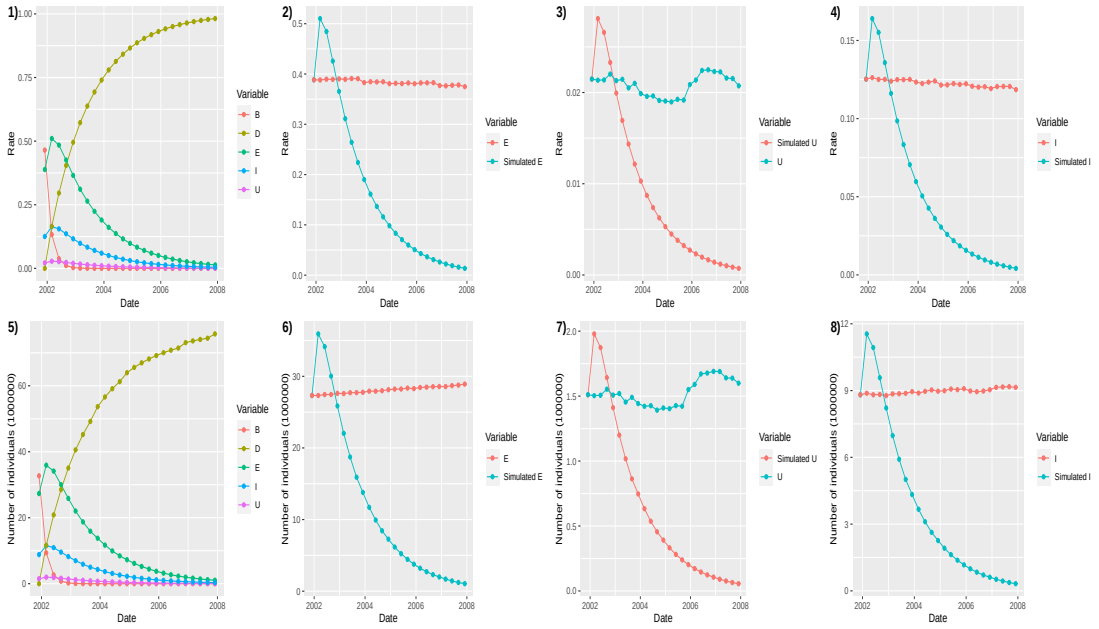

FIGURE 34: Graphs showing the t-step simulated values and actual data of employment and unemployment rates and levels for the pre-recession data scenario for the five-state model. Plot 1) shows the simulated values for employment, unemployment, inactivity, entry and exit rates only. Plot 5) shows employment, unemployment, inactivity, entry and exit levels only. Plot 2) illustrates simulated and actual for employment rates. Plot 6) illustrates simulated and actual for employment levels. Plot 3) displays simulated and actual for unemployment rates. Plot 7) displays simulated and actual for unemployment levels. Plot 4) represents simulated and actual for inactivity rates. Plot 7) displays simulated and actual for inactivity levels.

The matrix of relative transition probabilities is given by

$$\widehat{\mathbf{P}}_{\text{recession}} = \begin{bmatrix} 0.3285477 & 0.37551178 & 0.020843531 & 0.11821653 & 0.1568804 \\ 0 & 0.83638950 & 0.009888357 & 0.01765181 & 0.1360703 \\ 0 & 0.25337562 & 0.458580488 & 0.15219600 & 0.1358479 \\ 0 & 0.05444358 & 0.038817407 & 0.77021286 & 0.1365262 \\ 0 & 0 & 0 & 1 & \end{bmatrix}. \tag{4.5.8}$$

The computed generator matrix from using the DA approach in R is given by

$$\mathbf{\Lambda}_{\text{recession}} = \begin{bmatrix} -1.113 & 0.67630 & 0.03785 & 0.21520 & 0.1838 \\ 0 & -0.18180 & 0.01509 & 0.02045 & 0.1463 \\ 0 & 0.39700 & -0.79310 & 0.25030 & 0.1458 \\ 0 & 0.05727 & 0.06451 & -0.26860 & 0.1468 \\ 0 & 0 & 0 & 0 & 0 \end{bmatrix}. \tag{4.5.9}$$

Following this,

$$\mathbf{P}_{\text{recession}} = \begin{bmatrix} 0.3285477 & 0.37551178 & 0.020843531 & 0.11821653 & 0.1568804 \\ 0 & 0.83638950 & 0.009888357 & 0.01765181 & 0.1360703 \\ 0 & 0.25337562 & 0.458580488 & 0.15219600 & 0.1358479 \\ 0 & 0.05444358 & 0.038817407 & 0.77021286 & 0.1365262 \\ 0 & 0 & 0 & 1 & \end{bmatrix}. \tag{4.5.10}$$

To add on, using (4.5.5) and the initial states given by

$$\begin{aligned} \left[\tfrac{B}{N}, \tfrac{E}{N}, \tfrac{U}{N}, \tfrac{I}{N}, D\right] &= \left[\tfrac{37490000}{77230790}, \tfrac{29001072}{77230790}, \tfrac{1609762}{77230790}, \tfrac{9129956}{77230790}, 0\right] \\ &\approx \left[0.49, 0.38, 0.02, 0.12, 0\right] \end{aligned} \tag{4.5.11}$$

we simulate t-step values and compare them to the actual value. The results of our simulation is shown in Fig. 35.

Post-recession data scenario for the five-state model

The transition frequencies for the post-recession data scenario for the five-state model from January 2008 to March 2008 is written as

$$\mathbf{O}_{\text{post-recession}} = \begin{bmatrix} 13079917 & 14091229 & 1232228 & 4473195 & 5833432 \\ 0 & 27861367 & 422803 & 565523 & 4346148 \\ 0 & 569356 & 1570299 & 379330 & 380055 \\ 0 & 385075 & 509448 & 7952968 & 1379664 \\ 0 & 0 & 0 & 0 & 0 \end{bmatrix}. \tag{4.5.12}$$

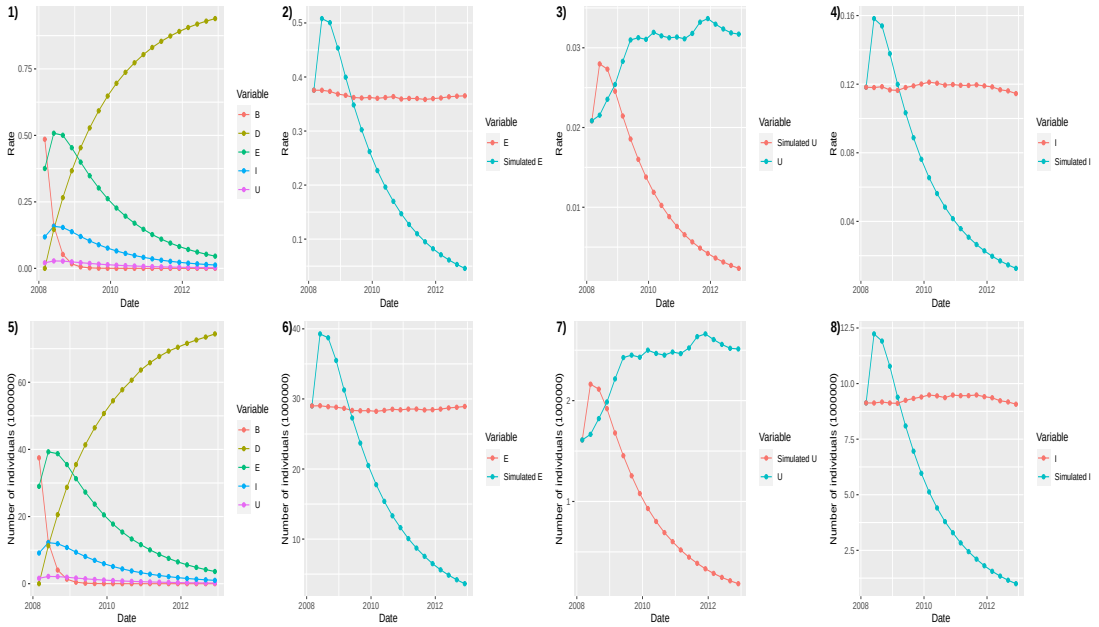

FIGURE 35: Graphs showing the t-step simulated values and actual data of employment and unemployment rates and levels for the recession data scenario for the five-state model. Plot 1) shows the simulated values for employment, unemployment, inactivity, entry and exit rates only. Plot 5) shows employment, unemployment, inactivity, entry and exit levels only. Plot 2) illustrates simulated and actual for employment rates. Plot 6) illustrates simulated and actual for employment levels. Plot 3) displays simulated and actual for unemployment rates. Plot 7) displays simulated and actual for unemployment levels. Plot 4) represents simulated and actual for inactivity rates. Plot 7) displays simulated and actual for inactivity levels.

The matrix of relative transition probabilities is given by

$$\widehat{\mathbf{P}}_{\text{post-recession}} = \begin{bmatrix} 0.337895 & 0.36402037 & 0.03183229 & 0.11555657 & 0.1506957 \\ 0 & 0.83930294 & 0.01273663 & 0.01703596 & 0.1309245 \\ 0 & 0.19639467 & 0.54166172 & 0.13084676 & 0.1310968 \\ 0 & 0.03765221 & 0.04981327 & 0.77763249 & 0.1349020 \\ 0 & 0 & 0 & 0 & 1 \end{bmatrix}. \tag{4.5.13}$$

The computed generator matrix using the DA approach in R is written as

$$\mathbf{\Lambda}_{\text{post-recession}} = \begin{bmatrix} -1.09 & 0.65 & 0.06 & 0.21 & 0.17 \\ 0.00 & -0.18 & 0.02 & 0.02 & 0.14 \\ 0.00 & 0.29 & -0.63 & 0.20 & 0.14 \\ 0.00 & 0.04 & 0.08 & -0.26 & 0.15 \\ 0.00 & 0.00 & 0.00 & 0.00 & 0.00 \end{bmatrix}. \tag{4.5.14}$$

Subsequently,

$$\mathbf{P}_{\text{post-recession}} = \begin{bmatrix} 0.337895 & 0.36402037 & 0.03183229 & 0.11555657 & 0.1506957 \\ 0 & 0.83930294 & 0.01273663 & 0.01703596 & 0.1309245 \\ 0 & 0.19639467 & 0.54166172 & 0.13084676 & 0.1310968 \\ 0 & 0.03765221 & 0.04981327 & 0.77763249 & 0.1349020 \\ 0 & 0 & 0 & 0 & 1 \end{bmatrix}. \tag{4.5.15}$$

Using (4.5.5) and the initial states given by

$$\begin{aligned} \left[\tfrac{B}{N}, \tfrac{E}{N}, \tfrac{U}{N}, \tfrac{I}{N}, D\right] &= \left[\tfrac{38710000}{79227859}, \tfrac{28840555}{79227859}, \tfrac{2522005}{79227859}, \tfrac{9155299}{79227859}, 0\right] \\ &\approx \left[0.49, 0.36, 0.03, 0.12, 0\right] \end{aligned} \tag{4.5.16}$$

we simulate t-step values and compare them to the actual value. The outcome of our simulation is shown in Fig. 36.

The root mean square error and coefficient of determination for the five-state model.

Following this, the RMSE and R^2 values for the five-state model are displayed in Table 4.10 and Table 4.11 respectively.

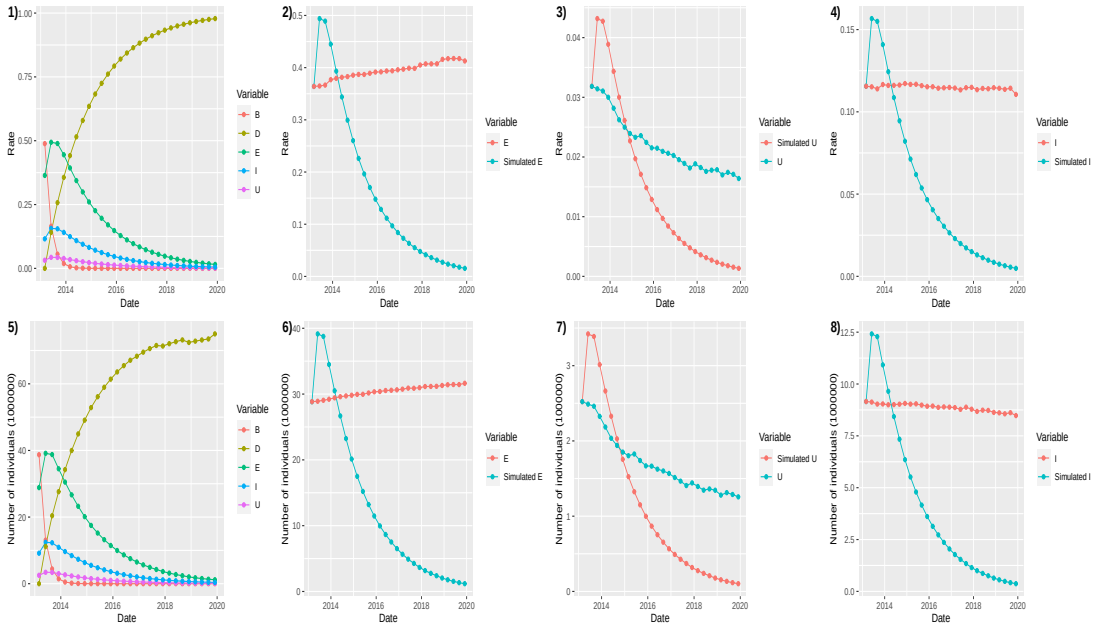

FIGURE 36: Graphs showing the t-step simulated values and actual data of employment and unemployment rates and levels for the post-recession data scenario for the five-state model. Plot 1) shows the simulated values for employment, unemployment, inactivity, entry and exit rates only. Plot 5) shows employment, unemployment, inactivity, entry and exit levels only. Plot 2) illustrates simulated and actual for employment rates. Plot 6) illustrates simulated and actual for employment levels. Plot 3) displays simulated and actual for unemployment rates. Plot 7) displays simulated and actual for unemployment levels. Plot 4) represents simulated and actual for inactivity rates. Plot 7) displays simulated and actual for inactivity levels.

Parameters	Entire	Pre-recession	Recession	Post-recession
Employment rate	0.3456961	0.3456961	0.2026961	0.2816874
Unemployment rate	0.02264684	0.02264684	0.02132988	0.01152597
Inactivity rate	0.1063957	0.1063957	0.06996408	0.07826705
Employment level	27.43686	27.43686	16.00656	21.57998
Unemployment level	1.795637	1.795637	1.684051	0.8851902
Inactivity level	8.466665	8.466665	5.524827	5.999352

TABLE 4.10: RMSE values to assess the performance of the five-state model for the four scenarios in Table 4.2.

Parameters	Entire	Pre-recession	Recession	Post-recession
Employment rate	0.0210151	0.0210151	0.5208599	0.8568977
Unemployment rate	0.060819601	0.060819601	0.7170292	0.96064738
Inactivity rate	0.5501068	0.5501068	0.001026337	0.299389
Employment level	0.3296153	0.3296153	0.09495269	0.9266801
Unemployment level	0.113106	0.113106	0.7299813	0.9573919
Inactivity level	0.08141323	0.08141323	0.2477127	0.6653022

TABLE 4.11: R^2 values to assess the performance of the five-state model for the four scenarios in Table 4.2.

Discussions for the five-state model fitting

The five-state model is an extension of the four-state model which further incorporates the inactivity state. Plot 1) and plot 5) of Fig. 33, Fig. 34, Fig. 35 and Fig. 36 illustrate that the entry rates and levels fall whilst exit rates and levels increase. This is attributed to the fact that in the five-state model individuals move from state E, state U and state I to state D which is an absorbing state and individuals transition from state B to state E, state U and state I.

We see that the simulated values for employment rates and levels are higher than the simulated values for inactivity rates, followed by the simulated values for unemployment rates and levels. However the simulated values for employment, inactivity and unemployment rates and levels have similar trends. That is, the employment, unemployment and inactivity rates and levels increase to a point and fall thereafter because individuals move in and out of state E, state U and state I.

In addition, the trend of the simulated values and actual values for employment rates and levels in plot 2) and plot 6) of Fig. 33, Fig. 34, Fig. 35 and Fig. 36 are similar. The similarity in plot 2) and plot 6) for all four scenarios reflects in the RMSE values in Table 4.10. Specifically, for all four scenarios, the RMSE values for employment rates are marginally close and the RMSE values for employment levels are also relatively close to each other. Futhermore, the pattern of the simulated values and actual values for inactivity rates and levels in plot 4) and plot 8) of Fig. 33, Fig. 34, Fig. 35 and Fig. 36 are also similar in terms of trend. Again, for all four scenarios, the RMSE values for inactivity rates and levels are relatively close to each other.

From Table 4.10, the simulated employment and inactivity rates and levels using the five-state model during the recession period best predicts or fits the actual data as compared to the other periods. This is due to the fact that during the recession phase, employment and inactivity rates and levels are predominately decreasing in the real world, and when using the four-state model. During the recession period, the economy rebounds from the impact of the recession as such unemployment rates and levels decrease [10, 92, 71]. Hence enabling better prediction of the rates and levels of unemployment as compared to employment and inactivity rates and levels using the five-state model. To support the argument raised, from Table 4.11 it can be seen that the R^2 values which display acceptable values and show that the rates and levels of employment and unemployment in the actual data are explained by the simulated values.

We see that the Markov models give more accurate predictions during shorter periods (pre-recession, recession, post-recession) as compared to longer periods (entire). In Section 4.3.2, the two-state model predicts employment and unemployment rates and levels best when the economy is stable (pre-recession). In Section 4.4.1, the four-state model predicts employment rates and levels best when the economy is unstable (recession). The four-state model predicts unemployment rates and levels best when the economy is recovering from a shock-wave (post-recession). In Section 4.5.1, the five-state model predicts employment and inactivity rates and levels best when the economy is unstable (recession). Whilst, the five-state model predicts unemployment rates and levels best when the economy is recovering from a shock-wave (recession).

To summarise, the LST (two-state, four-state, five-state) models do not fit the labour force data very well. This poor fit could be attributed to the selection of parameters. The parameters are not estimated in any optimal way, but simply using the first time point. The four-state and five-state model cannot be used to fit the labour force flow because their closed nature and incorporation of an absorbing state compels the employment, inactivity and unemployment rates and levels to fall asymptotically. Thus, in the extension of the model to a four-state and five state model, an optimal choice of parameters would inevitably improve the fit.

To make the model more realistic using the same parameters for the LST models, we explore labour force lake models in the subsequent section.

4.6 Lake model of the labour force

In this section, we develop lake models of employment and unemployment and employment, unemployment and inactivity to measure the flow of workers in the labour market. We then run simulations and compare the results with the real data.

4.6.1 Lake model of employment and unemployment

The lake model of employment and unemployment is explored in [113]. The lake model of employment and unemployment also known as the two-state lake model is used to model the dynamics between employment and unemployment. Figure 37 illustrates the pattern of how a two-state lake model works.

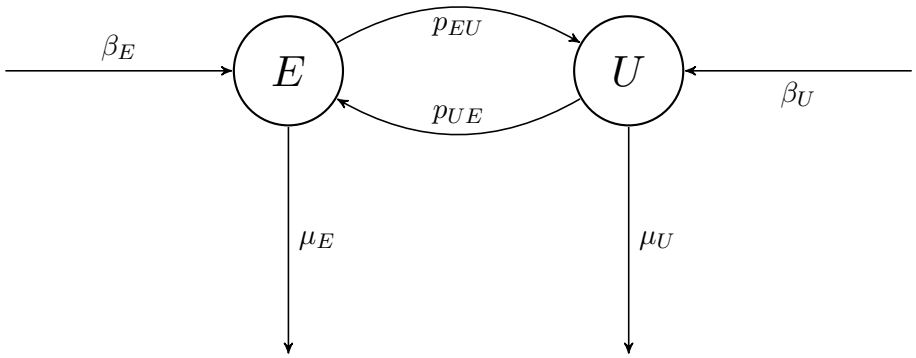

FIGURE 37: Graphical representation of the flow in the labour market for the two-state lake model. The possible states of the labour market are labelled employment (E) and unemployment (U). The probability of finding a job denoted by p_{UE} and the probability of losing a job denoted by p_{EU}. Here, individuals enter state E and state U at rates β_E and β_U respectively. The exit rates from state E and state U are μ_E and μ_U respectively.

The aggregate variables for the lake model of employment and unemployment are $E(t)$ which denotes the total number of employed individuals at time t, $U(t)$ which represents the total number of unemployed individuals at time t and $N(t) = E(t)+U(t)$ which is the total number of people in the labour force. We set $e(t) = \frac{E(t)}{N(t)}$ and $u(t) = \frac{U(t)}{N(t)}$ as the employment rate and the unemployment rate respectively.

Laws of motion for the aggregate variables

We begin by developing the laws of motion for the aggregate variables. The number of employed individuals that stay in the labour force is denoted by $(1-\mu_E)E(t)$ and the mass of employed people that stay employed is given by $(1-p_{EU})(1-\mu_E)E(t)$. Similarly, the number of jobless individuals that remain in the labour force is $(1-\mu_U)U(t)$ and $p_{UE}(1-\mu_U)U(t)$ represents the number of unemployed individuals that will find a job. Consequently, the number of employed workers at time $t+1$ is

$$E(t+1) = (1-p_{EU})(1-\mu_E)E(t) + p_{UE}(1-\mu_U)U(t) + \beta_E E(t). \tag{4.6.1}$$

In the same way the mass of jobless individuals at time $t+1$ is

$$U(t+1) = p_{EU}(1-\mu_E)E(t) + (1-p_{UE})(1-\mu_U)U(t) + \beta_U U(t). \tag{4.6.2}$$

We let

$$\mathbf{V}(t) \coloneqq \begin{bmatrix} U(t) \\ E(t) \end{bmatrix} \tag{4.6.3}$$

then the law of motion for the $\mathbf{K}$ is

$$\mathbf{V}(t+1) = \mathbf{K}\mathbf{V}(t) \tag{4.6.4}$$

where

$$\mathbf{K} \coloneqq \begin{bmatrix} (1-p_{UE})(1-\mu_U)+\beta_U & p_{EU}(1-\mu_E) \\ p_{UE}(1-\mu_U) & (1-p_{EU})(1-\mu_E)+\beta_E \end{bmatrix} \tag{4.6.5}$$

This law shows how total employment and unemployment change over time. The total number of workers is

$$N(t+1) = E(t+1) + U(t+1) = (1-\mu_E+\beta_E)E(t) + (1-\mu_U+\beta_U)U(t). \tag{4.6.6}$$

Assumption 4.6.1. In what follows, we assume that $\mu = \mu_E = \mu_U$ and $\beta = \beta_E = \beta_U$.

Using Assumption 4.6.1, (4.6.6) can be written as

$$N(t+1) = (1-\mu+\beta)N(t) = (1+\rho)N(t)$$

where $\rho = \beta - \mu$ is the growth rate of the labour force.

Laws of motion for the rates

The law of motion for the rates is derived when we divide both sides of (4.6.4) by $N(t+1)$ to obtain

$$\begin{bmatrix} U(t+1)/N(t+1) \\ E(t+1)/N(t+1) \end{bmatrix} = \frac{1}{1+\rho}\mathbf{K} \begin{bmatrix} U(t)/N(t) \\ E(t)/N(t) \end{bmatrix}. \tag{4.6.7}$$

Setting

$$\mathbf{v}(t) \coloneqq \begin{bmatrix} u(t) \\ e(t) \end{bmatrix} = \begin{bmatrix} U(t)/N(t) \\ E(t)/N(t) \end{bmatrix}, \tag{4.6.8}$$

we can write (4.6.4) as

$$\mathbf{v}(t+1) = \widehat{\mathbf{K}}\mathbf{v}(t) \tag{4.6.9}$$

where

$$\widehat{\mathbf{K}} \coloneqq \frac{1}{1+\rho}\mathbf{K}. \tag{4.6.10}$$

Note that $e(t)+u(t) = e(t+1)+u(t+1) = 1$ and the sum of the columns in $\widehat{\mathbf{K}}$ is 1. The aggregate variables $E(t)$ and $U(t)$ do not converge because the total value $N(t)$ grows at rate ρ. We modify the python codes in [113] for our computations. We use (4.6.5), (4.6.9), (4.6.10) and initial values computed from the data to simulate the dynamics of the number of employed and unemployed individuals. We then compare the simulated values with our actual data and display the results in the next section.

Model fitting for two-state lake model

After identifying the two-state lake model, we simulate the dynamics of the aggregate variables $(E(t), U(t), N(t))$ at different time steps using initial parameters from the data. The simulated values are compared with the data to assess the performance of the models. This comparison is done using RMSE, R^2 and plots.

The parameters for the simulation of the model are derived from the labour force data in [134, 135]. There is no publicly available data on entry and exit rates to and from UK labour force so we use UK birth and mortality rates from [85] and [24, 105] respectively.

The parameters for the simulation of the two-state lake model are shown in Table 4.12.

Parameters	Entire	Pre-recession	Recession	Post-recession
$N(t)$	37647261	37647261	39740790	40517859
$E(t)$	27325028	27325028	29001072	28840555
$U(t)$	10322233	10322233	10739718	11677304
$e(t)$	0.7258	0.7258	0.7298	0.7118
$u(t)$	0.2742	0.2742	0.2702	0.2882
$\widehat{p}_{EU}$	0.0332	0.0332	0.0319	0.0343
$\widehat{p}_{UE}$	0.0900	0.0900	0.0977	0.0840
β	0.01012	0.01012	0.01330	0.01368
μ	0.0098	0.0098	0.0091	0.0090

TABLE 4.12: Parameter for simulations of the lake model.

Figure 38 shows plots of simulated data and the actual data for the time intervals defined in Table 4.2. The performance of the models are further measured using RMSE and R^2. The values are shown in Table 4.13 and Table 4.14.

Parameters	Entire	Pre-recession	Recession	Post-recession
Employment	1.652355	0.6409675	12.23883	0.4514864
Unemployment	8.475462	0.3193458	13.54234	2.184255
Total labour force	2.069542	0.9540317	1.344444	2.585402

TABLE 4.13: RMSE values to assess the performance of two-state lake model for all scenarios in Table 4.2.

Parameters	Entire	Pre-recession	Recession	Post-recession
Employment	0.8336775	0.9676875	0.2041849	0.970718
Unemployment	0.03211377	0.2340382	0.7448238	0.9685013
Total labour force	0.9311835	0.9927698	0.9091902	0.9712936

TABLE 4.14: R^2 values to assess the performance of the two-state lake model for all scenarios in Table 4.2.

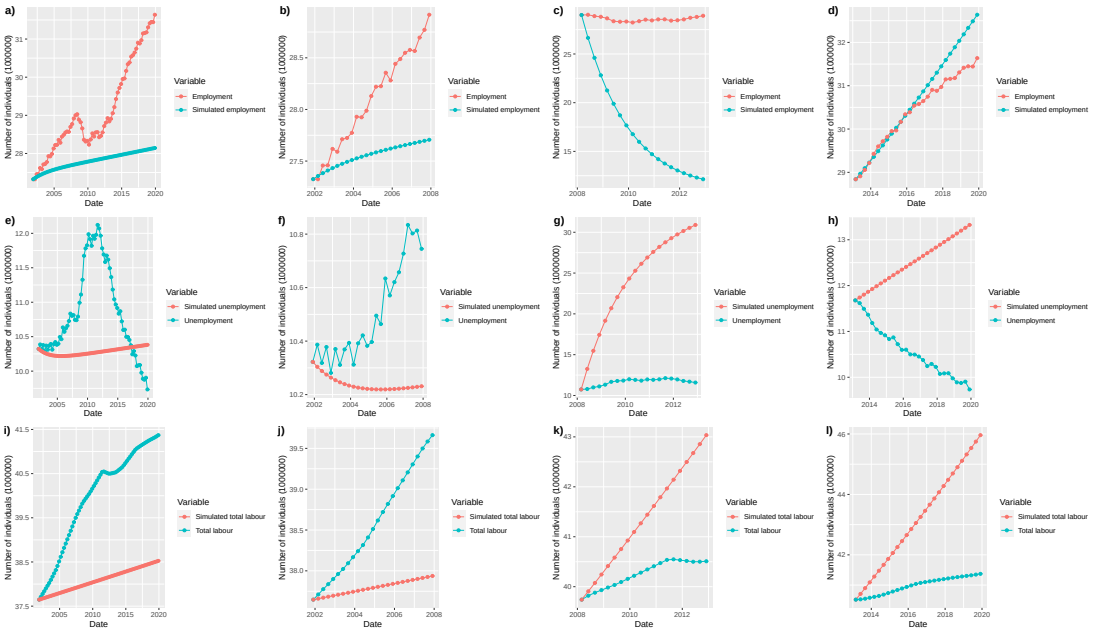

FIGURE 38: Plots of simulated data and actual data for each state using the time intervals defined in Table 4.2. Plot a) shows the simulated values and actual data for employment levels for the entire data scenario. Plot b) illustrates the simulated values and actual data for employment levels for the pre-recession data scenario. Plot c) displays the simulated values and actual data for employment levels for the recession data scenario. Plot d) shows the simulated values and actual data for employment levels for the recession data scenario. Plot e) illustrates the simulated values and actual data for unemployment levels for the entire data scenario. Plot f) illustrates the simulated values and actual data for unemployment levels for the pre-recession data scenario. Plot g) displays the simulated values and actual data for unemployment levels for the recession data scenario. Plot h) represents the simulated values and actual data for unemployment levels for the recession data scenario. Plot i) illustrates the simulated values and actual data for total labour force levels for the entire data scenario. Plot j) illustrates the simulated values and actual data for inactivity levels for the pre-recession data scenario. Plot k) displays the simulated values and actual data for total labour force levels for the recession data scenario. Plot l) represents the simulated values and actual data for total labour force levels for the recession data scenario.

Discussions for the two-state lake model

The two-state lake model is a model that shows the inflow and outflow of individuals to and from the labour market. After simulating values using the two-state lake model, some interesting findings were uncovered. From plot a), plot e) and plot i) of Fig. 38 we observe that in the initial stage (2001–2005), the simulated values are close to the actual data values in the entire data scenario. The RMSE values for the entire data scenario are high because in plot a) and plot i) of Fig. 38 we see that although the simulated employment and total labour force levels are increasing steadily, the actual data values of employment and total labour force levels increase at a much faster rate. Also from plot e) of Fig. 38 we notice that the actual unemployment levels rise above and fall below the simulated unemployment levels.

During the pre-recession period, levels of employment and total labour force increase and unemployment levels decrease [10]. In support of [10], we identify that the simulated employment and total labour force values are increasing and the simulated unemployment values are decreasing during the pre-recession period. This explains why for the pre-recession data scenario, the RMSE values in Table 4.13 shows that the two-state lake model best predicts unemployment levels followed by employment levels then total labour force levels. This observation also reflects in the plot b), plot f) and plot j) of Fig. 38.

Throughout a recession interim, employment levels fall, unemployment levels rise. Consequently, total labour force increases at a slower rate. Plot c), g) and k) of Fig. 38 shows that the simulated employment values fall faster than the actual employment values, the simulated unemployment values rise faster the actual employment values whilst the simulated total labour force values are relatively close to the actual total labour force values. This explains why the RMSE values in Table 4.13 show that the two-state lake model best predicts the total labour force data in the recession data scenario.

For the post-recession period, employment and total labour force levels rise while unemployment levels falls in an economy. We notice from plot d), plot h) and plot l) of Fig. 38 and the RMSE values in Table 4.13 that the two-state lake model best fits the actual employment data during the post-recession period.

4.6.2 Lake model of employment, unemployment and inactivity

The lake model of employment, unemployment and inactivity also known as the three-state lake model is an extension of the model in Section 4.6.1. Here we assume that the movement between the states are caused by firing, quiting or searching for a job as well as entry and exit from the labour force. In order to derive the flow dynamics shown in Fig. 39, we consider the following variables. Let $E(t), U(t)$ and $I(t)$ be the total numbers of employed, unemployed and inactive workers at time t respectively. Also, the total number of workers in the labour force at time t is represented by $N(t) = E(t) + U(t) + I(t)$. Thus, the values of the rates are given by $e(t) = \frac{E(t)}{N(t)}, u(t) = \frac{U(t)}{N(t)}$ and $i(t) = \frac{I(t)}{N(t)}$.

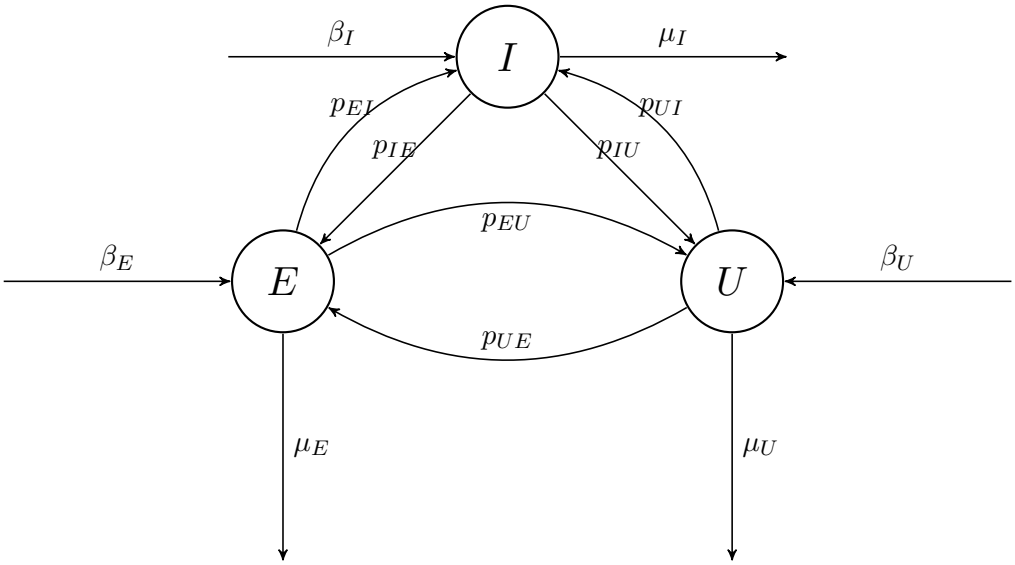

FIGURE 39: Graphical representation of the flow in the labour market as a guide to develop the lake model of employment, unemployment and inactivity. The possible states of the labour market are labelled employment (E), unemployment (U) and inactivity (I). This diagram also shows the arrows from each state to other states that signify transition probabilities p_{ij} for $i, j \in \{E, U, I\}$. The entry and exit rates to and from state E, U and I are $\beta_E, \beta_U, \beta_I$ and μ_E, μ_U, μ_Urespectively.

The rates of transition between the states are governed by the following parameters. Let p_{UE} be the job finding rate for currently unemployed workers, p_{IE} denote the job finding rate for currently inactive workers; p_{EI} signify the dismissal/quitting rate to

inactive state for currently employed workers; p_{EU} represent the dismissal/quitting rate to unemployed state for currently employed workers; p_{UI} symbolise the rate to unemployed state from inactive; p_{IU} be the rate from unemployed to inactive state. Set the parameter β as the entry rate into the labour force; and μ as the exit rate from the labour force. The mass of employed workers at time $t+1$ is given as follows,

$$\begin{aligned} E(t+1) &= (1-p_{EI})(1-\mu_E)E(t) + (1-p_{EU})(1-\mu_E)E_t + p_{UE}(1-\mu_U)U(t) \\ &\quad + p_{AE}(1-\mu_A)I(t) + \beta_E E(t) - (1-\mu_E)E(t) \qquad (4.6.11) \\ U(t+1) &= (1-p_{UE})(1-\mu_U)U(t) + (1-p_{UI})(1-\mu_U)U(t) + p_{EU}(1-\mu_E)E(t) \\ &\quad + p_{AU}(1-\mu_A)I(t) + \beta_U U(t) - (1-\mu_U)U(t) \qquad (4.6.12) \\ A(t+1) &= (1-p_{AE})(1-\mu_A)I(t) + (1-p_{EI})(1-\mu_E)E(t) + p_{EI}(1-\mu_E)E(t) \\ &\quad + p_{UI}(1-\mu_U)U(t) + \beta_A I(t) - (1-\mu_A)I(t) \qquad (4.6.13) \end{aligned}$$

The total number of workers in the labour force becomes

$$N(t+1) = (1-\mu_E+\beta_E)E(t) + (1-\mu_U-\beta_U)U(t) + (1-\mu_U+\beta_A)I(t). \quad (4.6.14)$$

If $\mu = \mu_E = \mu_I = \mu_U$ and $\beta = \beta_E = \beta_A = \beta_U$ then

$$N(t+1) = (1-\mu+\beta)N(t). \quad (4.6.15)$$

We set

$$\mathbf{V}_t \coloneqq \begin{pmatrix} I(t) \\ U(t) \\ E(t) \end{pmatrix}. \quad (4.6.16)$$

The law of motion of $\mathbf{V}$ which tells how employment, unemployment and inactivity evolve over time is given by

$$\mathbf{V}(t+1) = \mathbf{K}\mathbf{V}(t), \quad (4.6.17)$$

where

$$\mathbf{K} \coloneqq \begin{pmatrix} \Phi & p_{UI}(1-\mu_U) & p_{EI}(1-\mu_E) \\ p_{AU}(1-\mu_A) & \Psi & p_{EU}(1-\mu_E) \\ p_{AE}(1-\mu_A) & p_{UE}(1-\mu_U) & \Omega \end{pmatrix} \quad (4.6.18)$$

with $\Phi = (1-p_{AE}-p_{AU})(1-\mu_A)+\beta_I, \Psi = (1-p_{UE}-p_{UI})(1-\mu_U)+\beta_U$ and $\Omega = (1-p_{EI}-p_{EU})(1-\mu_E)+\beta_E$.

Assumption 4.6.2. Again, we assume that the $\mu = \mu_E = \mu_A = \mu_U$ and $\beta = \beta_E = \beta_A = \beta_U$.

With reference to Assumption 4.6.2, (4.6.17) becomes

$$\begin{pmatrix} \frac{I(t+1)}{N(t+1)} \\ \frac{U(t+1)}{N(t+1)} \\ \frac{E(t+1)}{N(t+1)} \end{pmatrix} = \frac{1}{1-\mu+\beta}\mathbf{K} \begin{pmatrix} \frac{I(t)}{N(t)} \\ \frac{U(t)}{N(t)} \\ \frac{E(t)}{N(t)} \end{pmatrix}. \tag{4.6.19}$$

Based of the above information, it can be said that the growth rate of the labour force is given by $\rho = \beta - \mu$ such that

$$\mathbf{v}(t) = \begin{pmatrix} i(t) \\ u(t) \\ e(t) \end{pmatrix} = \begin{pmatrix} \frac{I(t)}{N(t)} \\ \frac{U(t)}{N(t)} \\ \frac{E(t)}{N(t)} \end{pmatrix}. \tag{4.6.20}$$

Then,

$$\mathbf{v}(t+1) = \widehat{\mathbf{K}}\mathbf{v}(t) \qquad \text{where} \qquad \widehat{\mathbf{K}} := \frac{1}{1+\rho}\mathbf{K} \tag{4.6.21}$$

Model fitting for three-state lake model

Using similar arguments as in Section 4.6.1, we notice that simulate the dynamics of the aggregate variables $(E(t), U(t), I(t), N(t))$ at different time steps using initial conditions from the data. The performance of the models is accessed by comparing the simulated values with the data using RSME, the coefficient of determination (R^2) and plots. The parameters for our illustration are shown in Table 4.12 and Table 4.15.

Parameters	Entire	Pre-recession	Recession	Post-recession
$U(t)$	1510768	1510768	1609762	2522005
$I(t)$	8811465	8811465	9129956	9155299
$u(t)$	0.040130	0.040130	0.040507	0.062244
$i(t)$	0.234053	0.234053	0.229738	0.225957
$\widehat{p}_{EU}$	0.0133	0.0133	0.01145	0.01466
$\widehat{p}_{EI}$	0.0199	0.0199	0.0204	0.0196
$\widehat{p}_{UE}$	0.2837	0.2837	0.2932	0.2260
$\widehat{p}_{UI}$	0.1778	0.1778	0.1761	0.1506
$\widehat{p}_{IE}$	0.0573	0.0573	0.0631	0.0435
$\widehat{p}_{IU}$	0.0374	0.0374	0.0450	0.0576

TABLE 4.15: Parameter for simulations of the lake model.

Figure 40 shows plot of simulated data and the actual data for the time intervals defined in Table 4.2. The performance of the models are measured using the evaluation metrics RMSE and R^2 displayed in Table 4.16 and Table 4.17 respectively.

Parameters	Entire	Pre-recession	Recession	Post-recession
Employment	1.604337	0.6047017	2.526076	0.3737226
Unemployment	0.5428011	0.09969416	0.79438	1.110893
Inactivity	0.4002489	0.3053444	0.4720625	1.18122

TABLE 4.16: RMSE values to assess the performance of the models.

Parameters	Entire	Pre-recession	Recession	Post-recession
Employment	0.8169215	0.9671357	0.0524951	0.9671949
Unemployment	0.007371375	0.04316064	0.2186831	0.9028163
Inactivity	0.4984624	0.61819	0.6262669	0.9127542

TABLE 4.17: Table containing R^2 values to assess the performance of the models.

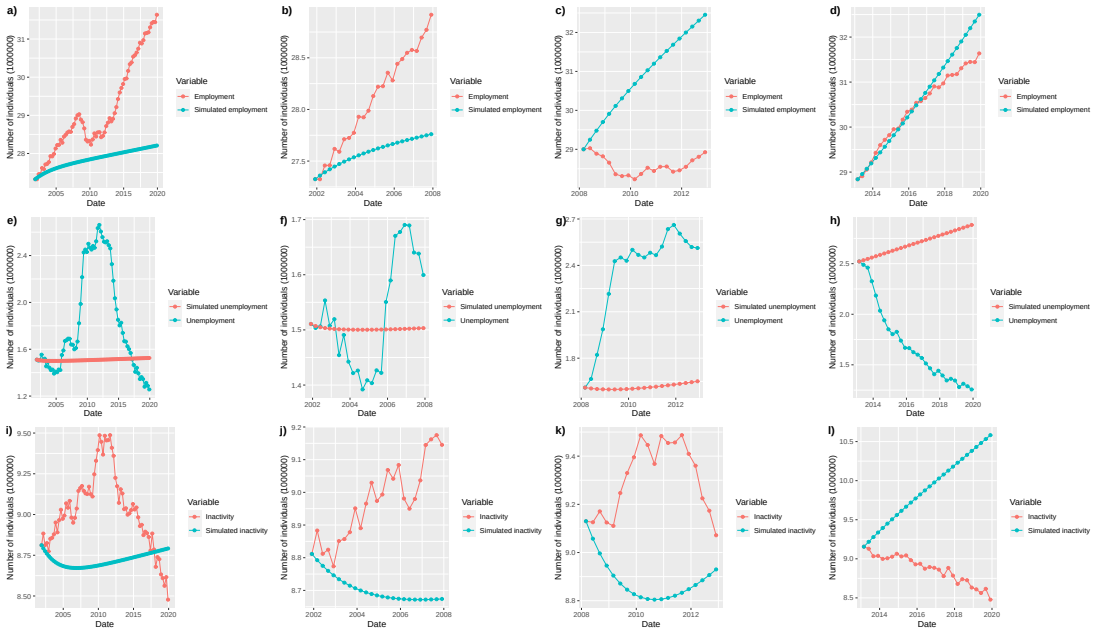

FIGURE 40: Plots of simulated data and actual data for each state using the time intervals defined in Table 4.2. Plot a) shows the simulated values and actual data for employment levels for the entire data scenario. Plot b) illustrates the simulated values and actual data for employment levels for the pre-recession data scenario. Plot c) displays the simulated values and actual data for employment levels for the recession data scenario. Plot d) shows the simulated values and actual data for employment levels for the recession data scenario. Plot e) illustrates the simulated values and actual data for unemployment levels for the entire data scenario. Plot f) illustrates the simulated values and actual data for unemployment levels for the pre-recession data scenario. Plot g) displays the simulated values and actual data for unemployment levels for the recession data scenario. Plot h) represents the simulated values and actual data for unemployment levels for the recession data scenario. Plot i) illustrates the simulated values and actual data for inactivity levels for the entire data scenario. Plot j) illustrates the simulated values and actual data for inactivity levels for the pre-recession data scenario. Plot k) displays the simulated values and actual data for inactivity levels for the recession data scenario. Plot l) represents the simulated values and actual data for inactivity levels for the recession data scenario.

Discussion for the three-state lake model

In plot a), plot e) and plot i) of Fig. 40 we notice that in the early stages (2001–2005), the simulated values are close to the actual data values in the entire data scenario. Although the RMSE values in Table 4.16 for the entire data scenairio are relatively small because from plot e) and plot i) of Fig. 40, the actual unemployment and inactivity levels rise above and fall below the simulated unemployment and inactivity levels. The RMSE values for employment leves in the entire data scenario are high because plot a) of Fig. 40 reveals that although the simulated employment and total labour force levels are increasing steadily, the actual data values of employment and total labour force levels increase at a much faster rate.

During the pre-recession and post recession period, levels of employment increase. The three-state lake model best fits the employment levels during the pre-recession period and post-recession period because the simulated employment values are rising.

The three-state lake model best predicts unemployment levels during the recession period because the actual values and simulated values of unemployment levels are increasing simultaneously. The actual unemployment data trend is similar to the actual inactivity data trend. However, the simulated values for unemployment and inactivity vary as shown in Fig. 40. As a result, the three-state lake model best forecasts inactivity levels in the pre-recession phase.

The above observations and discussions in Section 4.6.1 reveal that the two-state lake model predicts labour force flow more accurately during the short time intervals than relatively long ones (entire data scenario). The results of the two-state lake model is similar to that of the three-state lake model. Adding a new state to the model did not completely revise the results for the estimation. Thus, the performance of these two methods was found to be relatively accurate when uncertain circumstances do not occur.

An interesting discovery is that the exponential distribution assumption for the parameterisation of the unemployment rate and employment rate in the formulation of our UI scheme is reasonable. However, to construct more realistic UI schemes, we have to check if other distributions can predict labour force rates better. This brings us to the the next section which is identifying distributions that fits the labour force data.

4.7 Identifying distributions that fit the labour force data

In this section we identify distributions that best fit the employment, unemployment, inactivity and adjusted unemployment (which is the sum of unemployment and inactivity) rates. Even though inactivity and unemployment have different values, they are sometimes collectively known as unemployment (which is the sum of all inactivity and unemployment values) depending on the application. To make the understanding clearer, we call this adjusted unemployment denoted by $\bar{U}$ that is $\bar{U} = U + I$. We show how to identify the distributions using the programming languages Minitab and R.

4.7.1 Identifying the distribution that best fits the data using Minitab

Minitab is a statistical software can be used to analyze, visualize, predict patterns and discover relationships between variables in a given dataset [94]. In Minitab, distribution tests are performed to determine if the data follows 14 probability distributions. A detailed explanation of this test is found in [53, 110]. We use two measure, Anderson–Darling test statistic (AD) and the p-value, produced by the test as a guide to select the distribution that best fits the data.

The AD statistic computes the deviation between a fitted line using the candidate distribution and a nonparametric step function using the data. To determine the p-value, the null hypothesis (H_0) and the alternative hypothesis (H_1) for these hypothesis tests are

- H_0: The data follows the candidate distribution.
- H_1: The data does not follow the candidate distribution.

The p-value measures the evidence against the null hypothesis (H_0) calculated from the AD statistic. A small p-value means that we reject the null hypothesis but since we want to determine the probability distribution that our data follows, distributions with high p-values are suitable options.

The results from Minitab are displayed in Table A.1. The first line of Table A.1 shows that normal distribution is not the best candidate, because the p-value is less than 0.05. Also, since we would like to identify the data without transformation, we skip the Box–Cox transformation distribution. We then see that the distributions with p-values higher than 0.005 are Weibull, smallest extreme value and largest extreme value distributions for all the rates. However, we use R to further select suitable candidates

because in Minitab, the computed p-values are < 0.010 which does not necessarily mean they are greater that 0.005.

4.7.2 Identifying the distribution that best fits the data using R

In R, the *fitdistrplus* package has a descdist function which is used to derive possible distribution functions. This function produces descriptive statistics and Cullen and Frey skewness-kurtosis plots [36] for each rate which are displayed in Table 4.18 and Figure 41 respectively to help make a choice among a set of parametric distributions.

Descriptive statistics

The descriptive statistics are minimum, maximum, median, mean, standard deviation, skewness and kurtosis values for the rates. From Table 4.18 the minimum, maximum, median and mean values show that employment > inactivity > unmployment. When we consider only employment and adjusted unemployment rates, the values of the minimum, maximum , median and mean in Table 4.18 show that employment > unemployment. Skewness is a measure of symmetry or the lack of symmetry. A nonzero

Statistics	Rates			
	Employment	Unemployment	Inactivity	Unemployment $(U + I)$
Minimum	0.7010535	0.0382003	0.2049145	0.2431148
Maximum	0.764713	0.08551785	0.2358759	0.3187915
Median	0.7282966	0.05354392	0.2297377	0.2840911
Mean	0.728509	0.05884596	0.2259994	0.2848453
Standard deviation	0.01645045	0.01428072	0.008599666	0.01974254
Skewness	0.3096558	0.5951262	-0.8635381	-0.1561019
Kurtosis	2.562624	1.933245	2.50764	2.46628

TABLE 4.18: Descriptive statistics from the *fitdistrplus* package in R for employment, unemployment, inactivity and adjusted unemployment (which is the sum of unemployment and inactivity) rates.

skewness shows a lack of symmetry, negative skew shows longer or fatter tail on the

left side and while positive skew illustrates a longer or fatter tail on the right of the distribution. Thus all the rates exhibit lack of skewness. It turns out that employment and unemployment rates have longer or fatter tails on the right. On the other hand inactivity rates and adjusted unemployment rates are skewed to the left. The kurtosis value is used to quantify whether the data are heavy-tailed or light-tailed relative to a normal distribution. Zero kurtosis is implies the normal distribution, negative values of kurtosis indicate that a distribution is flat and has thin tails, of lacks outliers. Positive values of kurtosis indicate that a distribution is peaked and has heavy tails or outliers. Consequently, all the rates are peaked and have heavy tails.

Cullen and Frey skewness-kurtosis plots

Skewness-kurtosis plots proposed by [30, 36] serve as guide to select the distribution that best fits to data from the options; normal, uniform, logistic, exponential, gamma, Weibull and log-normal distributions. The skewness-kurtosis Cullen and Frey plots for the rates are shown in Fig. 41. The single blue point labelled observation is used to represent the distribution of the data. Notice that in all the plots in Fig. 41 the observations fall in the grey section of labeled beta distribution. Looking at the plots we can select candidate distributions for the data at first glance but we can not decide the best option. Thus we run some further analysis using goodness-of-fit plots and criteria to make our choice more robust.

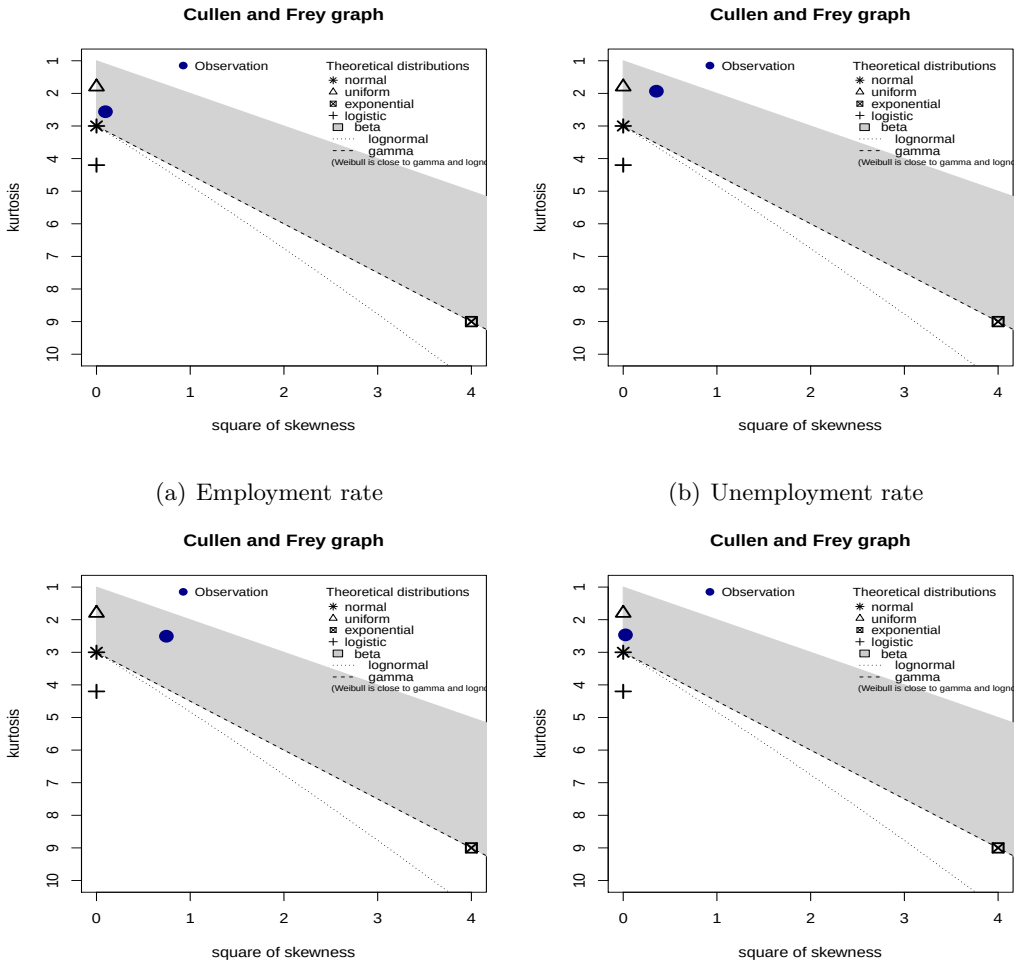

(a) Employment rate

(b) Unemployment rate

(c) Inactivity rate

(d) Unemployment ($U + I$) rate

FIGURE 41: Graphs illustrating the Cullen and Frey plots for employment, unemployment, inactivity and adjusted unemployment (unemployment plus inactivity) rates.

Goodness-of-fit plot and criteria

In this subsection, we use the denscomp, cdfcomp, qqcomp and ppcomp functions from the *fitdist* package in R to produce goodness-of-fit plots and criteria. The plots comprise of density plots, cumulated density function (CDF) plots, Q–Q plots and P–P plots. The density plots show the histograms of the empirical distribution of the rates along with the fitted distributions for comparison. The CDF plots illustrate the CDF representations for the empirical distribution of the rates and the fitted distributions.

The Q–Q plots are scatter plots that show the empirical quantiles on the y–axis against the theoretical quantiles on the x–axis. If both sets of quantiles are the same in terms of distribution, the points form a seemingly straight line. The P–P plots compare the empirical cumulative distribution functions of the data on the y–axis with the fitted distribution functions on the x–axis. The point pattern on the P–P plots are linear through the origin and has unit slope.

We further use the goodness-of-fit criteria which are Akaike information criteria (AIC) and Bayesian information criteria (BIC) for model selection. The AIC and BIC are penalised-likelihood criteria used to estimate the quality of statistical models relative to other models for a given set of data to help select the best model. Details of AIC and BIC computations are shown in [22, Ch. II] and [89, Ch. XI]. The lower the AIC and BIC value, the better the fit of the model. With this in mind we examine the plots, AIC and BIC values for our data.

Firstly, the plots and criteria for employment rates are shown in Fig. 42 and Table 4.19 respectively. In Fig. 42, the histogram of the empirical distribution of the employment rate is skewed to the right, has a peak and heavy tails which confirms the skewness and kurtosis values in Table 4.18. We also see that in all the plots in Fig. 42 that the exponential and uniform distributions do not fit the data very well. From Table 4.19, we see that the normal and log-normal distributions have the lowest AIC and BIC values for the employment rate. This is confirmed in the Cullen and Frey graph for employment rates (Fig. 41) where the observation point is relatively close to the normal distribution point and the log-normal distribution line. According to the AIC and BIC values in Table 4.18, the distributions with the lowest values are ranked as follows: Weibull > gamma > logistic > beta > normal > log-normal. Thus, the log-normal distribution highlighted in blue in Table 4.18 is the best fit amongst the candidate distributions under consideration for employment rates.

Secondly, we repeat the goodness-of-fit plots and criteria for unemployment rates and show the results in Fig. 43 and Table 4.20 respectively. The histogram in Fig. 43 is skewed to the right, peaked and heavy tailed as indicated in Table 4.18. Also from Fig. 43 we observe that the exponential and uniform distributions are not the best fits in all the plots. The ranking of the lowest AIC and BIC values in Table 4.20 is logistic > Weibull > normal > beta > gamma > log-normal. Consequently, the AIC and BIC value highlighted in blue in Table 4.20 which represents log-normal distribution

is the best fit for unemployment rates.

Thirdly, using similar techniques we display the goodness-of-fit plots and criteria for inactivity rates in Fig. 44 and Table 4.21 respectively. The histogram in Fig. 44 confirms the skewness and kurtosis values in Table 4.18 because the histogram is skewed to the left and peaked. Furthermore, all the inactivity rate plots in Fig. 44 establish the fact that the exponential and uniform distributions are the worst fits among the distribution options under consideration. The lowest AIC and BIC values in Table 4.21 tell us that logistic > log-normal > gamma > beta > normal > Weibull. Subsequently, the best fit for inactivity rates is Weibull distribution.

Finally, Fig. 45 and Table 4.22 contain the goodness-of-fit plots and criteria for adjusted unemployment rates. The skewness and kurtosis values in Table 4.18 affirm the shape of the histogram in Fig. 45 which is skewed to the left and peaked. In addition, all the adjusted unemployment rate plots in Fig. 45 show that the exponential and uniform distributions are the worst fits among the distribution options under consideration. The smallest AIC and BIC values in Table 4.22 show that logistic > Weibull > gamma > log-normal > beta > normal. The best fit for inactivity rates is normal distribution.

In summary, with the exception of exponential and normal distribution, it is difficult to notice the best fit from the distributions in Fig. 42, Fig. 43, Fig. 44 and Fig. 45 because the distributions are close to each other. The AIC and BIC values in Table 4.19, Table 4.20, Table 4.21 and Table 4.22 are used to select the best distributions for the rates. These are Weibull for inactivity rates, normal distribution for adjusted unemployment (U+I) rates and log-normal distribution for employment and unemployment rates. This information is a good serves as a guide to select the best distribution candidate to make the UI scheme model more realistic.

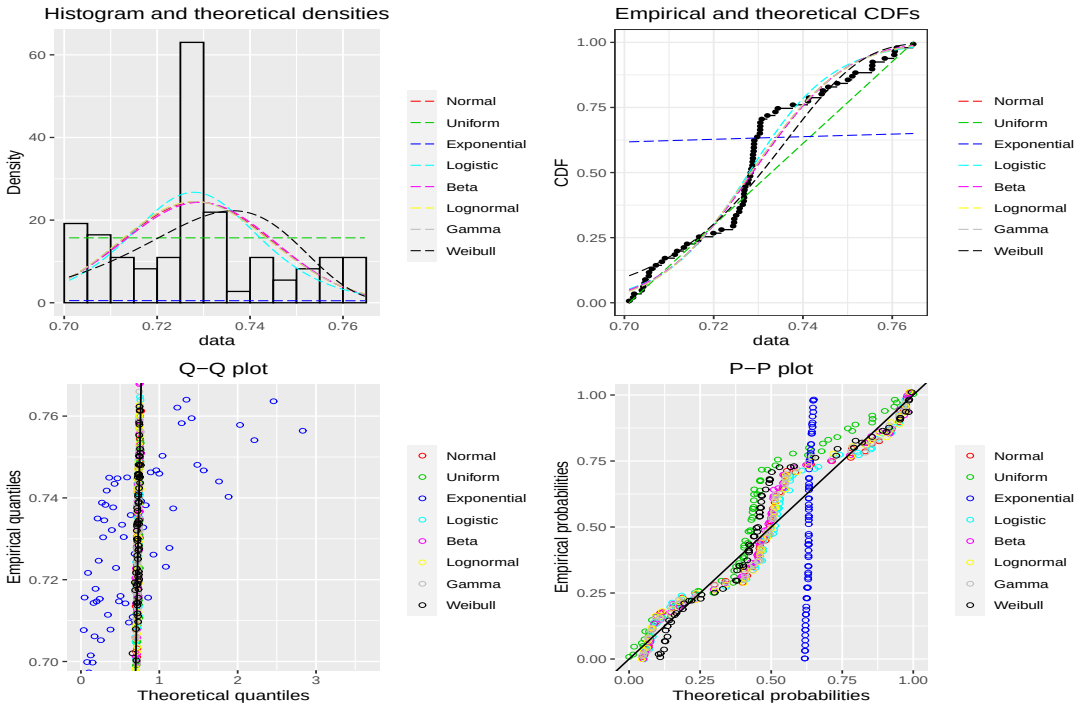

FIGURE 42: Plots of histogram, empirical and theoretical CDF, Q–Q plot and P–P plot for employment rates with fitted distributions.

Distribution	Akaike information criteria (AIC)	Bayesian information criteria (BIC)
Normal	-389.5226	-384.9417
Exponential	101.7537	104.0442
Logistic	-387.3464	-382.7655
Beta	-388.9440	-384.3631
Log-normal	-389.9826	-385.4016
Gamma	-385.4016	-385.2581
Weibull	-376.2044	-371.6235

TABLE 4.19: Goodness-of-fit criteria for employment rates for normal, exponential, logistic, beta, log-normal, gamma and Weibull distributions.

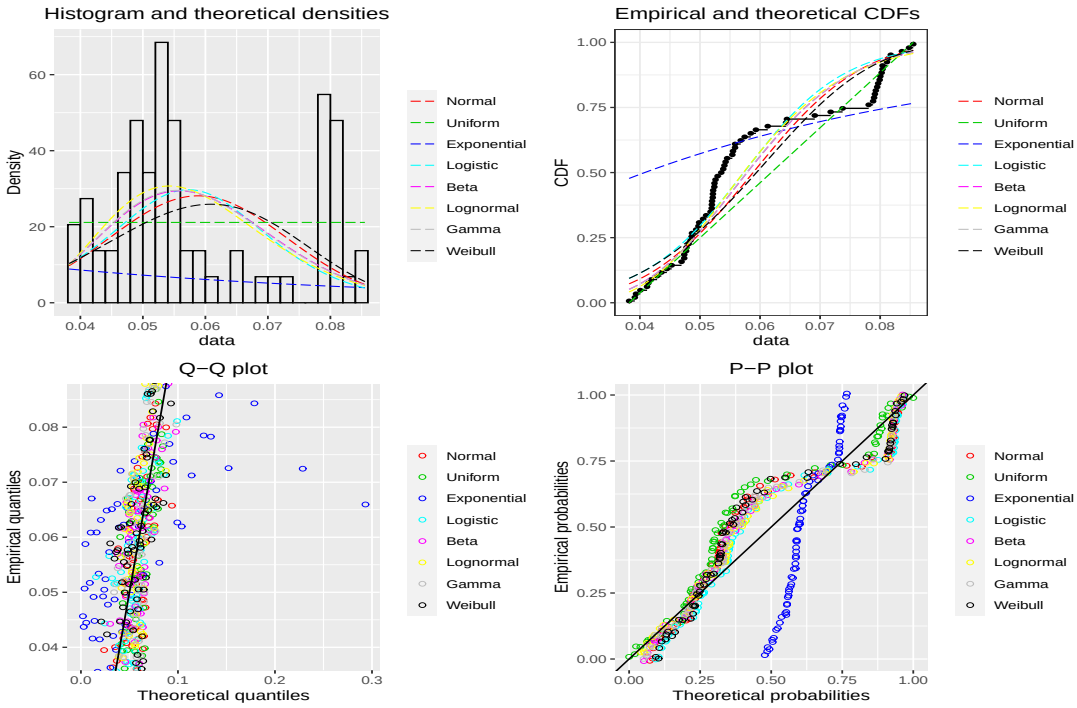

FIGURE 43: Plots of histogram, empirical and theoretical CDF, Q–Q plot and P–P plot for unemployment rates with fitted distributions.

Distribution	Akaike information criteria (AIC)	Bayesian information criteria (BIC)
Normal	-410.1732	-405.5923
Exponential	-265.5935	-263.3030
Logistic	-405.0523	-400.4714
Beta	-416.5849	-412.0040
Log-normal	-419.0182	-414.4372
Gamma	-416.8396	-412.2587
Weibull	-407.2079	-402.6270

TABLE 4.20: Goodness-of-fit criteria for unemployment rates for normal, exponential, logistic, beta, log-normal, gamma and Weibull distributions.

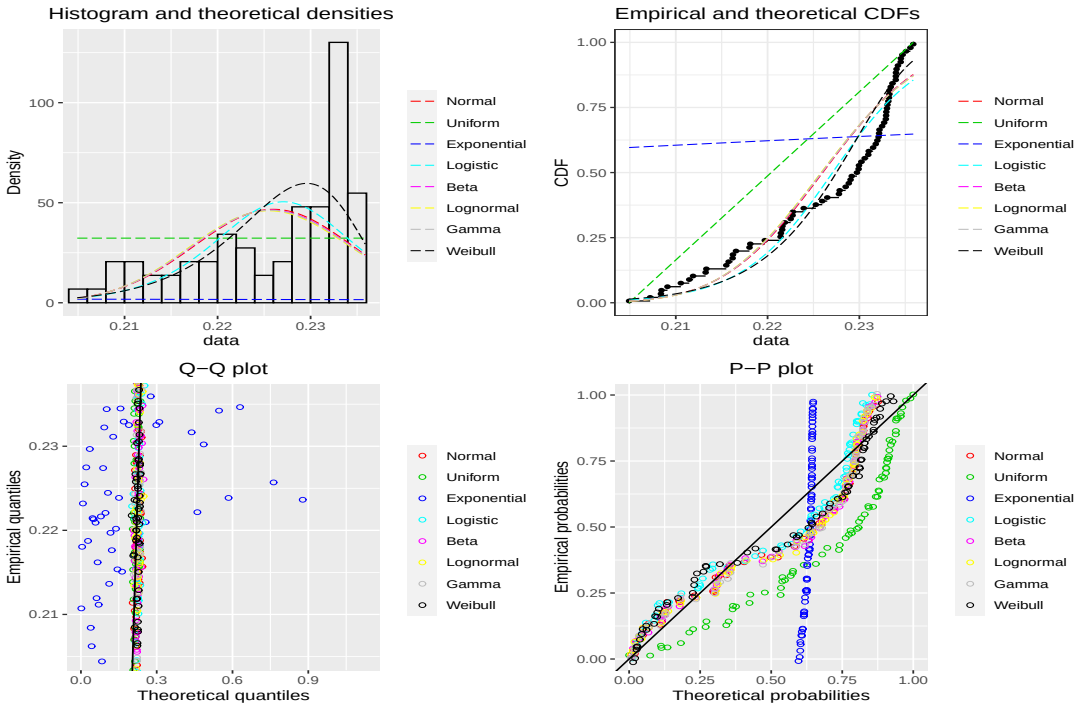

FIGURE 44: Plots of histogram, empirical and theoretical CDF, Q–Q plot and P–P plot for inactivity rates with fitted distributions.

Distribution	Akaike information criteria (AIC)	Bayesian information criteria (BIC)
Normal	-484.2225	-479.6416
Exponential	-69.13457	-66.84411
Logistic	-481.28854	-476.7075
Beta	-483.1153	-478.5344
Log-normal	-481.8174	-477.2365
Gamma	-482.6401	-478.0592
Weibull	-501.8136	-497.2326

TABLE 4.21: Goodness-of-fit criteria for inactivity rates for normal, exponential, logistic, beta, log-normal, gamma and Weibull distributions.

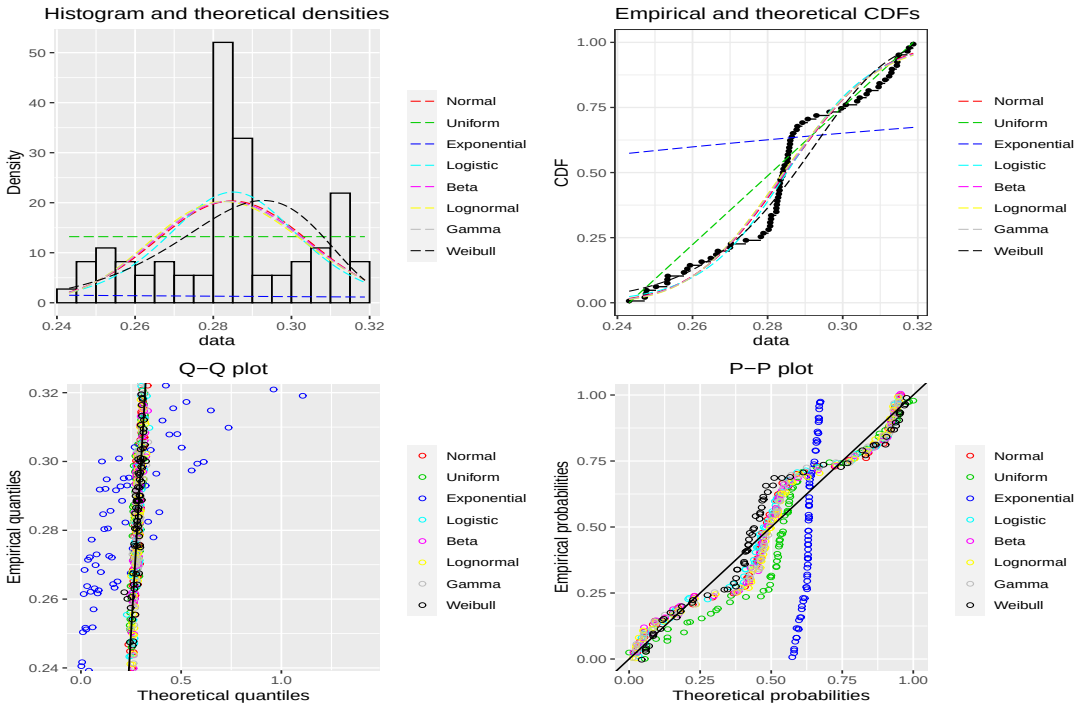

FIGURE 45: Plots of histogram, empirical and theoretical CDF, Q–Q plot and P–P plot for adjusted unemployment $(U + I)$ rates with fitted distributions.

Distribution	Akaike information criteria (AIC)	Bayesian information criteria (BIC)
Normal	-362.8889	-358.3080
Exponential	-35.34811	-33.05765
Logistic	-360.2077	-355.6267
Beta	-362.5699	-357.9890
Log-normal	-361.7767	-357.1958
Gamma	-362.2420	-357.6611
Weibull	-360.8905	-356.3096

TABLE 4.22: Goodness-of-fit criteria for adjusted unemployment $(U + I)$ rates for normal, exponential, logistic, beta, log-normal, gamma and Weibull distributions.

Chapter 5

Summary and Concluding remarks

The aim of this thesis is to develop models unemployment insurance schemes to cushion the financial and morale blow of loss of job but also to encourage the unemployed to seek new jobs more proactively due to the continuous reduction of benefit payments. Our focus has been to determine the optimal entry time for an individual to enter the unemployment insurance schemes. In this final chapter we summarise our results and mention some future directions.

5.1 Summary of results

In Chapter 2, we set up and solved a simple optimal stopping problem in a stylized UI model. The model and its solution are useful by illustrating approaches to optimal strategy of an individual seeking to get insured. By including consumption in the model, we have also demonstrated how a fair premium can be calculated, which makes our UI model usable also from the insurer's perspective. An explicit closed-form solution of the corresponding optimal stopping problem was possible due to some simplifying assumptions — in particular, exponential distribution of time τ_0 to loss of job and constant inflation rate r. The analysis also strongly relied on the simplest model for the wage process (X_t), that is, geometric Brownian motion with constant drift μ and volatility σ^2.

In Chapter 3, the risk-free rate, unemployment rate and employment rate in the

simple model in Chapter 2 are made time-dependent, which caused complications to the model. We found the optimal stopping rule that maximises the expected payoff for an unemployed individual under the UI scheme. We formulated the stopping problem based on the assumption that risk-free rate, unemployment rate and reemployment rate are time-dependent. We also proved that the optimal stopping time for our problem is the first time the wage process exceeds a time-dependent optimal boundary $b(t)$, which is non-negative, continuous, either non-decreasing or non-increasing and bounded. Prior to this, we proved the continuity of the value function. We found the regularity for the value function and we derived an integral equation that uniquely characterises the optimal boundary. We numerically solved the integral equation and provide plots of the optimal boundary. Finally, we interpreted and discussed our results economically.

In Chapter 4, we gave a brief overview of the dataset using descriptive statistics and visualization. Following this, we used the (LST) models to investigate the movement between employment, unemployment and inactivity. We further explored the two-state and three-state lake models for the labour force. The performance and accuracy of the LST and lake modelling techniques are obtained by comparing our simulations to the actual data. The results of our findings are discussed. Additionally, we fitted distributions to data in order to choose the best candidate probability distribution for future work suggestions.

5.2 Future directions

Let us indicate a few directions of making our UI model more realistic. Firstly, indefinite term of UI insurance could be replaced by a finite expiration term for the benefit schedule (akin to American call option with finite horizon), which would lead to a harder (time-dependent) optimal stopping problem (cf. [107, §25.2]).

After fitting distributions to the real labour force data in Chapter 4, the model can be modified. Note, however, that fitting a different distribution for τ_0 and τ_0 will invalidate the expression (2.2.10) for the expected net present value $\mathrm{eNPV}(x;\tau)$ and, therefore, will change the gain function in the optimal stopping problem (2.2.14), making it more difficult to solve. In addition, since the labour force data can considered as time series data, some time series analysis can also be done and the results incorporated in the UI scheme.

The implicit assumption of passive waiting for a new job during the unemployment spell may not be realistic, or at least not desirable as individuals would rather be expected to seek jobs more pro-actively. Thus, it may be interesting to combine our UI model with job-seeking models such as in [17].

The inclusion of utility terms in the optimal setting is novel in this context, and illuminates significant changes in the individual's behaviour when driven by utility considerations. In particular, the value of the optimal stopping problem (2.7.6) is an increasing function of the preference coefficient κ (see Proposition 2.7.1). This result is intuitively appealing, as it conforms with the usual impact of utility function (under the Expected Utility Theory), allowing one to convert extra satisfaction into extra premium. This is confirmed by our analysis of suboptimal solutions in Section 2.6.3 (see Fig. 7). It would also be interesting to study the optimal stopping problem (2.7.6) in more detail.

The results from Section 2.7.4 indicates that the individual is happy to pay more than before to protect themselves from the perceived risk of significant losses. That is to say, an additional amount of satisfaction is convertible into an extra premium. However, choosing another mode of paying premium may also well change the threshold. Consequently, one direction that can be studied is to change the premium to depend on the wage and exhibit other modes of payment such a monthly or quarterly.

A portfolio of sustainable insurance products could be developed to offer competitive benefits based on the possible states of the policyholder (such as 'unemployed/employed', 'dead', 'education', 'marriage', etc.). It would be interesting to analyse optimal strategies of switching between employment and unemployment from the point of view of the regulator and/or insurer. This can be used as a guide explore optimal pricing of insurance schemes and to optimise reserving.

Appendix A

Appendix

A.1 Definitions

In this section, we have some definitions that have been references in Chapter 1.

Stopping times

Definition A.1.1. A random variable $\tau : \Omega \to [0, \infty]$ is called a stopping time if $\{\tau \leq t\} \in \mathcal{F}$ for all $t \geq 0$ and $\mathrm{P}(\tau < \infty) = 1$.

Fubini's theorem

Fubini's theorem, also known as Tonelli's theorem, shows a link between a multiple integral and a repeated one.

Theorem A.1.1. *If $f : \mathbb{R}^2 \to \mathbb{R}$ is an integrable function (i.e. $\iint |f(x, y)| \mathrm{d}x\mathrm{d}y < \infty$) on the rectangular region $[a, b] \times [c, d]$, then the equality*

$$\int_a^b \int_c^d f(x, y) \mathrm{d}y\mathrm{d}x = \int_c^d \int_a^b f(x, y) \mathrm{d}x\mathrm{d}y \tag{A.1.1}$$

applies. [51, 63]

Lebesgue's dominated convergence theorem

Theorem A.1.2. *Suppose that $\{f_n\}$ is a sequence of measurable functions, such that $f_n \to f$ point-wise almost everywhere as $n \to \infty$, and that $|f_n| \leq g$ for all n, where g*

is integrable. Then f is integrable, and

$$\int f \mathrm{d}\mu = \lim_{n\to\infty} \int f_n \mathrm{d}\mu \tag{A.1.2}$$

[21, 63].

A.2 Python codes for time-dependent case

The python codes used to to solve the time-dependent case are presented below.

```
import matplotlib.pyplot as plt
from scipy import interpolate
from mpmath import *
from matplotlib.figure import Figure
from matplotlib.backends.backend_agg import FigureCanvasAgg as
    FigureCanvas
import pandas as pd
from mpl_toolkits import mplot3d
from mpl_toolkits.mplot3d import Axes3D
from matplotlib import cm
from matplotlib.ticker import LinearLocator, FormatStrFormatter
import mpl_toolkits.mplot3d as plt3d
from  IPython.display  import  *
import numpy as np
import sympy as sp
from scipy.special import gammainc
import time
from datetime import timedelta
sp.init_printing(use_unicode=False, wrap_line=False)
from scipy.special import erf, erfc
from numpy import sin
from scipy.integrate import quad
from mpl_toolkits.axes_grid1.inset_locator import zoomed_inset_axes

#Symbols and parameters
bt = sp.Symbol('b_t')
bts = sp.Symbol('b_(t+s)')
s = sp.Symbol('s')
t = sp.Symbol('t')
y = sp.Symbol('y')
u = sp.Symbol('u')
```

```
mu = sp.Symbol('mu')
sigma = sp.Symbol('sigma')
gamma = sp.Symbol('gamma')
delta = sp.Symbol('delta')
P = 9000
mu = 0.0004
sigma = 0.002
gamma =34.7
delta = 0.0094
h0 = 0.7
P = 9000

############################################################
#Functions for computation

#Inflation rate
def r(t):
  a = 0.0252*sp.exp(0.0012*t)    #Exponential
  return a
#Reemployment rate
def lambda1(t):
  a = 0.7076*sp.exp(0.0007*t)   #Exponential
  return a
#Inflation rate + Reemployment rate
def tilde_r1(t):
  a = r(t)+lambda1(t)
  return a
#Benefit schedule
def expint_r1(s,t):
  a = sp.exp(-(sp.integrate(tilde_r1(u), (u, t, s))))
  return a
def beta_a1(t):
  a = lambda t: quad(expint_r1a, t, t+gamma, args=(t,))
  return a
def expdelta_r(s,t):
  a = sp.exp(-(sp.integrate(delta, (u, t+gamma, s))))
  return a
def expintdelta_r(s,t):
  a = expint_r1(s,t)*expdelta_r(s,t)
  return a
def beta_b1(t):
```

```
  a = lambda t: quad(expintdelta_ra, t+gamma, inf, args=(t,))
  return a
def beta(t):
  a = h0*(beta_b1(t)[0]+beta_a1(t)[0])
  return a
#Unemployment Rate
  def lambda0(t):
  a = 0.0596*sp.exp(-0.0004*t) #Exponential
  return a
#Inflation rate + Reemployment rate
def tilde_r(t):
  a = r(t)+lambda0(t)
  return a
def expint_r(s,t):
  a = sp.exp(-(sp.integrate(tilde_r(u), (u, t, s))))
  return a
def expintmu_r(s,t):
  mu = 0.0004
  a = sp.exp(-(sp.integrate(tilde_r(u)- mu, (u, t, s))))
  return a
def lambda0_beta(t):
  a = lambda0b(t)*beta(t)
  return a
def expintmulam_r(s,t):
  mu = 0.0004
  a = expintmu_ra(s,t)*lambda0_beta(s)
  return a
def beta1(t):
  a = lambda t: quad(expintmulam_r, t, inf, args=(t,))[0]
  return a

def I_int_1(s,bt,bts):
  lnbt = sp.log(bts/bt)
  g = (mu - ((sigma**2)/2))*s
  d = sigma*sp.sqrt(2*s)
  a = 0.5 - (0.5 * (sp.erf((lnbt-g)/d)))
  return a
def I_1(s,t,bt,bts):
  a = expint_r(s,t)*tilde_r(t+s)*P*I_int_1(s,bt,bts)
  return a
def I_int_2(s,bt,bts):
```

```
  lnbt = sp.log(bts/bt)
  g = (mu - ((sigma**2)/2))*s
  w = (sigma**2)*s
  d = sigma*sp.sqrt(2*s)
  a = 0.5 - (0.5 * (sp.erf((lnbt-g-w)/d)))
  return a
def I_2_a(s,t,bt,bts):
  a = expint_r(s,t)*bt*sp.exp(mu*s)*I_int_2(s,bt,bts)
  return a
def I_2(s,t,bt,bts):
  a = I_2b(s,t,bt,bts)*lambda0_beta(t+s)
  return a
def I_total(s,t,bt,bts):
  a = I_1b(s,t,bt,bts) + I_2(s,t,bt,bts)
  return a

############################################################
#Boundary function algorithm
# Parameters
T = 100# final time
t = 0     #0.001  # initial time
h = 1  # time step
Pi = np.arange(start=t, stop=T, step=h)  # Pi = t:h:T # time grid
b_0 = np.ones(len(Pi)) # b_0 = zeros(1,length(Pi)); % initialising the
    starting boundary
b_1 = np.ones(len(Pi))  # b_1 = zeros(1,length(Pi)); % defining the next
    -step boundary
b_2 = np.ones(len(Pi))
eps = 1e-1  #1e-6 % fixed-point tolerance
j = 1.  # initialising the number of iterations
S = np.arange(start=(t+h/2), stop=(T+h/2), step=h)  # S = t+h/2:h:1-h/2;
     % vector of middle points
Y = np.arange(start=0, stop=T, step=h)  # Y = -1:h:1; % space grid
# Computing the first iteration of the fixed-point algorithm
B_0 = np.ones(len(S))
error = []
for k in np.arange(len(Pi)-1,-1,-1):
  P = 9000
  t_k = Pi[k]
  b_1[k] = (1/beta1(t_k))*(P-np.sum(I_total(S[k:],t_k,b_0[t_k],B_0[k:]))
    )
```

```
print(b_1)
err = np.max(np.abs(b_1- b_0))# error related to first iteration
print(err)
error.append(err)
plt.plot(np.arange(len(b_1)),(b_1))

while err > eps:
  b_2 = np.abs(b_0)
  b_0 = np.abs(b_1)
  b_1 = np.abs(b_2)
  j = j+1
  inter = interpolate.interpolatedunivariatespline(pi, b_0)
  b_0 = inter(s)
  for k in np.arange(len(pi)-1,-1,-1):
    p = 9000
    t_k = pi[k]
    b_1[k] = (1/beta1(t_k))*(p-np.sum(i_total(s[k:],t_k,b_0[t_k],b_0[k
    :])))
  err = np.max(np.abs(b_1 - b_0))# error related to first iteration
  error.append(err)
print(error)
print(j)
j = str(j)
print('number of iterations is ' + j + '.')

# Beta plot
plt.figure()
ax = plt.axes()
timer = np.arange(len(Pi))
plt.plot(timer,beta(Pi),'k*')
ax.set_facecolor("white")
plt.xlabel('Time $t$',fontdict={'fontsize': 11, 'fontweight': 'medium'})
plt.ylabel(r'Benefit schedule $\beta(t)$',fontdict={'fontsize': 11, '
    fontweight': 'medium'})
plt.show()

##Simulation of a Brownian motion and computation of the optimal
    stopping time
random.seed(60)
mu = mu
sigma = sigma
```

```
N = 50*T #number of steps within each simulation
deltat = T/N #time step
X = np.zeros(len(Pi))  # % initialising the Brownian motion path
X[0] = 346 # starting point
for i in np.arange(1,len(Pi)):
  t_i = Pi[i]  # corresponding time
  X[i] = X[i-1]*(np.exp((mu-(sigma**2)/2)*deltat +sigma*np.sqrt(deltat)*
    np.random.normal(0,1)))
  index = np.where(X>=b_1)[0][0]  #  index of optimal stopping time
print(index)
tau = Pi[index]  # % optimal stopping time
print(tau)

#Optimal boundary plot
plt.figure()
ax = plt.axes()
ax.set_ylim((0, 300000))
ax.set_xlim((0, T-1))
ax.set_facecolor("white")
ax.fill_between(Pi, -0.5, b_1, color="lightblue", alpha=0.5)
plt.plot(Pi,b_1, color='black', linewidth=1.5)
plt.plot(Pi,X, color='black',linewidth=1.5) # % plotting the Brownian
    bridge path
plt.xlabel('Time $t$ ',fontdict={'fontsize': 11, 'fontweight': 'medium'
    })
plt.ylabel('Pay rate',fontdict={'fontsize': 11, 'fontweight': 'medium'})
plt.text(8,280000, r'$\mathcal{S}$', fontsize=20)
sub_axes = plt.axes([.43, .4, .45, .45])
sub_axes.set_ylim((0, 1000)) #Limit
sub_axes.set_xlim((0, T-1))
sub_axes.set_facecolor("white")
sub_axes.fill_between(Pi, -0.5, b_1, color="lightblue", alpha=0.5)
sub_axes.plot(Pi,b_1, color='black', linewidth=1.5)
sub_axes.plot(Pi,X, color='black',linewidth=1.5) # % plotting the
    Brownian bridge path
sub_axes.text(8, 100, r'$\mathcal{C}$', fontsize=20)
plt.show()
```

Listing A.1: Python codes

A.3 R codes for Markov model fitting

The R codes for model fitting using the DA approach is as follows.

```
library(tidyr)
library(xtable)
library(ggplot2)
library(tidyverse)
library(ctmcd)
library(expm)
library("markovchain")
library(matlib)
States <- c("E","U") #Labels
byRow <- TRUE
tm_abs <- matrix(data = c( 26375755, 906629,915392, 9252628), nrow = 2,
byrow = byRow, dimnames = list(States, States))    #Matrix
tm_rel <- rbind((tm_abs/rowSums(tm_abs))) # Relative probability
ev1 <- eigen(tm_rel)
L1 <- ev1$values   #Eigenvalues of relative probability
V1 <- ev1$vectors  #Eigenvectors of relative probability
inv(V1)          #Inverse of Eigenvectors of relative probability
xtable(diag(L1)) #Diagonal of Eigenvalues of relative probability
xtable(logm(diag(L1))) #Log of diagonal of Eigenvalues
Q <- V1 %*% logm(diag(L1)) %*% inv(V1) #Log of relative probability
logm(tm_rel) #Log of relative probability
gmem <- gm(tm=tm_rel,te=1,method="DA") #DA result for transition matrix
A <- gmem$par
ev <- eigen(A)
L <- ev$values #Eigenvalues of transition matrix
V <- ev$vectors #Eigenvectors of transition matrix
P = V %*% expm(diag(L)) %*% inv(V) #Probability matrix
mc <- new("markovchain", states = c("E", "U"),
transitionMatrix = P,
name = "Labour")
steadyStates(mc) #steady state
```

Listing A.2: R codes

A.4 Identifying the distributions fits the labour force data

This section contains plots referenced in Section 4.7.

Distribution	Employment rate		Unemployment rate		Inactivity rate		Unemployment $(U + I)$	
	AD	P	AD	P	AD	P	AD	P
Normal	1.532	< 0.005	3.851	< 0.005	3.547	< 0.005	1.483	< 0.005
Box-Cox transformation	1.432	< 0.005	1.722	< 0.005	3.050	< 0.005	1.499	< 0.005
Lognormal	1.494	< 0.005	2.597	< 0.005	3.691	< 0.005	1.548	< 0.005
3-parameter lognormal	1.465	*	1.568	*	3.588	*	29.190	*
Exponential	32.061	< 0.003	20.138	< 0.003	31.137	< 0.003	29.190	< 0.003
2-parameter exponential	5.295	< 0.010	3.424	< 0.010	11.898	< 0.005	9.187	< 0.010
Weibull	2.635	< 0.010	3.962	< 0.010	2.841	< 0.010	1.880	< 0.010
3-parameter Weibull	1.611	< 0.005	1.705	< 0.005	2.728	< 0.005	1.525	< 0.005
Smallest extreme value	2.762	< 0.010	5.114	< 0.010	2.728	< 0.010	2.106	< 0.010
Largest extreme value	1.772	< 0.010	2.207	< 0.010	4.492	< 0.010	2.344	< 0.010
Gamma	1.521	< 0.005	3.028	< 0.005	3.682	< 0.005	1.534	< 0.005
3-parameter gamma	1.897	*	1.745	*	8.077	*	1.643	*
Logistic	1.455	< 0.005	3.568	< 0.005	3.235	< 0.005	1.457	< 0.005
Loglogistic	1.434	< 0.005	2.490	< 0.005	3.345	< 0.005	1.479	< 0.005
3-parameter Loglogistic	1.424	*	1.397	*	3.235	*	1.561	*

TABLE A.1: Summary of results from Minitab on 14 distributions used to fit the data for employment, unemployment and inactivity rates and adjusted unemployment (sum of unemployment and inactivity) rates.

References

[1] Acemoglu, D. and Shimer, R. Productivity gains from unemployment insurance. *European Economic Review*, **44** (2000), 1195–1224. (doi:10.1016/S0014-2921(00)00035-0)

[2] Alarid-Escudero, F., Krijkamp, E. M., Enns, E.A., Hunink, M.G., Pechlivanoglou, P. and Jalal, H. Cohort state-transition models in R: From conceptualization to implementation. Preprint, 2020. (arXiv:2001.07824)

[3] Andersen, P.K., Borgan, Ø., Gill, R.D., and Keiding, N. *Statistical Models Based on Counting Processes*. Springer-Verlag, New York, 1993. (doi:10.1007/978-1-4612-4348-9)

[4] Anquandah, J.S. and Bogachev, L.V. Optimal stopping and utility in a simple model of unemployment insurance. *Risks*, **7**(3) (2019), Paper 94, 1–41. (doi: 10.3390%2Frisks7030094). Reprinted in: S. Federico, G. Ferrari and L. Regis (eds.), *Applications of Stochastic Optimal Control to Economics and Finance*, pp. 1–41, MDPI, Base, 2020.

[5] Arrow, K.J., Blackwell, D., and Girshick, M.A. Bayes and minimax solutions of sequential decision problems. *Econometrica*, **17** (1949), 213–244. (doi:10.2307/1905525)

[6] Asenjo, A. and Pignatti, C. Unemployment insurance schemes around the world evidence and policy options. *International Labour Organization* , Research Department Working Paper No. 49, October 2019. (https://www.ilo.org/wcmsp5/groups/public/—dgreports/—inst/documents/publication/wcms_723778.pdf)

[7] Baily, M.N. Some aspects of optimal unemployment insurance. *Journal of Public Economics*, **10** (1978), 379–402. (doi:10.1016/0047-2727(78)90053-1)

[8] Basso A., Nardon M. and Pianca P. A two-step simulation procedure to analyze the exercise features of American options. *Decisions in Economics and Finance*, **27**(1) (2004), 35–56. (doi:10.1007/s10203-004-0045-2)

[9] Bather, J. Bayes procedures for deciding the sign of a normal mean. *Mathematical Proceedings of the Cambridge Philosophical Society*, **54** (1962), 599–620. (doi:10.1017/S0305004100040640)

[10] Bell, D.N.F. and Blanchflower, D.G. UK unemployment in the great recession. *National Institute Economic Review*, **214** (2010), R3–R25. (doi:10.1177/0027950110389755)

[11] Bell, D.N.F. and Blanchflower, D.G. US and UK labour market before and during the Covid-19 crash. *National Institute Economic Review*, **252** (2020), R52–R69. (doi:10.1017/nie.2020.14)

[12] Bellman, R. On the theory of dynamic programming. *Proceedings of the National Academy of Sciences of the United States of America*, **38**(8) (1952), 716–719. (doi:10.1073/pnas.38.8.716)

[13] Bielecki, T.R. and Rutkowski, M. *Credit Risk: Modeling, Valuation and Hedging*. Springer–Verlag, New York, 2004. (doi:10.1007/978-3-662-04821-4)

[14] Bladt, M. and SØrensen, M. Statistical inference for discretely observed Markov jump processes. *Journal of the Royal Statistical Society: Series B (Statistical Methodology)*, **67**(3) (2005), 395–410. (doi:10.1111/j.1467-9868.2005.00508.x)

[15] Bladt, M. and SØrensen, M. Efficient estimation of transition rates between credit ratings from observations at discrete time points. *Quantitative Finance*, **9**(2) (2009), 147–160. (doi:10.1080/14697680802624948)

[16] Borch, K. The utility concept applied to the theory of insurance. *ASTIN Bulletin*, **1** (1961), 245–255. (doi:10.1017/S0515036100009685)

[17] Boshuizen, F.A. and Gouweleeuw, J.M. A continuous-time job search model: general renewal processes. *Communications in Statistics. Stochastic Models*, **11** (1995), 349–369. (doi:10.1080/15326349508807349)

[18] Boyarchenko, S.I. and Levendorskii, S.Z. *Irreversible Decisions under Uncertainty*. Springer-Verlag, Berlin, 2007. (doi.org/10.1007/978-3-540-73746-9)

[19] Brauer, F., van den Driessche, P. and Wu, J. *Mathematical Epidemiology*. Lecture Notes in Mathematics, **1945**. Springer-Verlag, Berlin, 2008. (doi.org/10.1007/978-3-540-78911-6)

[20] Breakwell, J. and Chernoff, H. Sequential tests for the mean of a normal distribution II (Large t) *Annals of Mathematical Statistics*, **35**(1) (1964), 162–173. (doi:10.1214/aoms/1177703738)

[21] Browder, A. *Mathematical Analysis*. Undergraduate Texts in Mathematics. Springer-Verlag, New York, 1996. (doi:10.1007/978-1-4612-0715-3)

[22] Burnham, K.P. and Anderson, D.R. *Model Selection and Multimodel Inference*. Springer–Verlag, New York, 2002. (doi:10.1007/b97636)

[23] Carr, P., Jarrow, R. and Myneni, R. Alternative characterization of American put options. *Mathematical Finance*, **2**(2) (1992), 87–106. (doi:10.1111/j.1467-9965.1992.tb00040.x)

[24] Caul, S. Deaths registered in England and Wales, *Office for National Statistics*, United Kingdom, (2020). (https://www.ons.gov.uk/peoplepopulationandcommunity/birthsdeathsandmarriages/deaths/datasets/monthlyfiguresondeathsregisteredbyareaofusualresidence)

[25] Chappie, S. Phillips and the inflation-unemployment trade-off. *New Zealand Economic Papers*, **30**(2) (1996), 219–228. (doi:10.1080/00779959609544258)

[26] Chen, X., Li, X. and Yi, F. Optimal stopping investment with non-smooth utility over an infinite time horizon. *Journal of Industrial and Management Optimization*, **15** (2019), 81–96. (doi:10.3934/jimo.2018033)

[27] Choi, K.J. and Shim, G. Disutility, optimal retirement, and portfolio selection. *Mathematical Finance*, **16** (2006), 443–467. (doi:10.1111/j.1467-9965.2006.00278.x)

[28] Chow, Y.S., Robbins, H. and Siegmund, D. *Great Expectations: The Theory of Optimal Stopping*. Houghton Mifflin, Boston, MA, 1971.

[29] Cook, R.J., Zeng, L. and Lee, K.-A. A multi-state model for bivariate interval-censored failure time data. *Biometrics*, **64** (2008), 1100–1109. (doi:10.1111/j.1541-0420.2007.00978.x)

[30] Cullen, A.C., Frey, H.C. and Frey, C.H. *Probabilistic Techniques in Exposure Assessment: A Handbook for Dealing with Variability and Uncertainty in Models*

and Inputs. Springer-Verlag, New York, 1999.

[31] De Angelis, T. A note on the continuity of free-boundaries in finite-horizon optimal stopping problems for one-dimensional diffusions. *SIAM Journal on Control and Optimization*, **53**(1) (2015), 167–184. (doi:10.1137/130920472)

[32] De Angelis, T. and Ekström, E. The dividend problem with a finite horizon. *Annals of Applied Probability*, **27**(6) (2017), 3525–3546. (doi:10.1214/17-aap1286)

[33] De Angelis, T. and Milazzo, A. Optimal stopping for the exponential of a Brownian bridge. *Journal of Applied Probability*, **57**(1) (2020), 361–384. (doi:10.1017/jpr.2019.98)

[34] De Angelis, T. and Peskir, G. Global C^1 regularity of the value function in optimal stopping problems. *Annals of Applied Probability*, Future papers, (2020). (https://www.e-publications.org/ims/submission/AAP/user/submissionFile/39139?confirm=a5b47f7f)

[35] De Angelis, T. and Stabile, G. On the free boundary of an annuity purchase. *Finance and Stochastics*, **23** (2019), 97–137. (doi: 10.1007/s00780-018-00379-8)

[36] Delignette-Muller, M.L. and Dutang, C. fitdistrplus: An R package for fitting distributions. *Journal of Statistical Software*, **64**(4) (2015), 33–58. (doi:10.18637/jss.v064.i04)

[37] De Saporta, B., Dufour F., Zhang H. and Elegbede, C. Optimal stopping for the predictive maintenance of a structure subject to corrosion. *Proceedings of the Institution of Mechanical Engineers, Part O: Journal of Risk and Reliability*, **226**(2) (2011), 169–181. (doi:10.1177/1748006x11413681)

[38] Dhami, S. *The Foundations of Behavioral Economic Analysis*. Oxford University Press, Oxford, 2016.

[39] Dierckx, P. *Curve and Surface Fitting with Splines*. Clarendon Press, Oxford, 1993.

[40] Draper, N.R. and Smith, H. *Applied Regression Analysis*, 3rd ed. Wiley Series in Probability and Statistics. John Wiley & Sons, Oxford, 1998. (doi10.1002/9781118625590)

[41] Dunn, S., Constantinides, A. and Moghe, P.V. *Numerical Methods in Biomedical Engineering*. Elsevier, Amsterdam, 2006. (doi:/10.1016%2Fb978-0-12-186031-8.x5000-6)

[42] Durrett, R. *Essentials of Stochastic Processes*, 1st ed. Springer Texts in Statistics. Springer-Verlag, New York, 1999.

[43] Durrett, R. *Probability: Theory and Examples*, 4th ed. Cambridge University Press, 2010. (doi:10.1017/CBO9780511779398)

[44] Dvoretzky, A., Kiefer, J. and Wolfowitz, J. Sequential decision problems for processes with continuous time parameter problems of estimation. *Annals of Mathematical Statistics*, **24**(3) (1953), 403–415. (doi:10.1214/aoms/1177728980)

[45] Dynkin, E.B. The optimum choice of the instant for stopping a Markov process. *Soviet Mathematics Doklady.* , **4** (1963), 627–629.

[46] Ekström, E. and Lu, B. Optimal selling of an asset under incomplete information. *International Journal of Stochastic Analysis*, **2011** (2011), Article ID 543590, 1–17. (doi:10.1155/2011/543590)

[47] Engelbert, H.J. On optimal stopping rules for Markov processes with continuous time article data. *Theory of Probability and Its Applications*, **19**(2) 1974, 278–296. (doi:10.1137/1119034)

[48] Estevão, M. and Sá, F. The 35-hour workweek in France: Straightjacket or welfare improvement? *Economic Policy*, **23** (2008), 417–463. (doi:10.1002/9781444306835.ch1)

[49] Etheridge, A. *A Course in Financial Calculus*. Cambridge University Press, Cambridge, 2002. (doi:10.1017/CBO9780511810107)

[50] Fakeev A.G. Optimal stopping rules for stochastic processes with continuous parameter. *Theory of Probability and Its Applications*, **15**(2) (1969), 324–331. (doi:10.1137/1115039)

[51] Finney R.L. and Thomas, G.B. *Calculus and Analytic Geometry*, 8th ed. Addison-Wesley Longman, New York, 1992. (doi:10.1007/978-0-201-53174-9)

[52] Fredriksson, P. and Holmlund, B. Optimal unemployment insurance design: Time limits, monitoring, or workfare? *International Tax and Public Finance*, **13** (2006), 565–585. (doi:10.1007/s10797-006-6249-3)

[53] Frost, J. How to identify the distribution of your data. *Statistics by Jim*, (online), 2020. (https://statisticsbyjim.com/hypothesis-testing/identify-distribution-data/)

[54] Furman, J. The economic case for strengthening unemployment insurance. Remarks at Center for American Progress, Washington DC, July 16, 2016. (https://obamawhitehouse.archives.gov/sites/default/files/page/files/20160711_furman_uireform_cea.pdf)

[55] Gerrard, R., Højgaard, B. and Vigna, E. Choosing the optimal annuitization time post-retirement. *Quantitative Finance*, **12** (2012), 1143–1159. (doi:10.1080/14697680903358248)

[56] GoCompare.com. Unemployment protection insurance (search & comparison web site) (online). (https://www.gocompare.com/unemployment-protection)

[57] Gompertz, B. On the nature of the function expressive of the law of human mortality. *Philosophical Transactions of the Royal Society of London*, **115** (1825), 513–583. (https://www.jstor.org/stable/107756?seq=1metadata_info_tab_contents)

[58] Grigelionis, B.I. and Shiryaev, A.N. On Stefan's problem and optimal stopping rules for Markov processes. *Theory of Probability and Its Applications*, **11** (1966), 541–558. (doi:10.1137/1111060)

[59] Gubian, A., Jugnot, S., Lerais, F. and Passeron, V. Les effets de la RTT sur l'emploi: des estimations *ex ante* aux évaluations *ex post* (French). [The effects of the shorter working week on employment: from *ex-ante* simulations to *ex-post* evaluations.] *Économie et Statistique*, **376–377** (2004), 25–54. (ISSN: 0336-1454)

[60] Hairault, J.-O., Langot, F., Ménard, S. and Sopraseuth, T. Optimal unemployment insurance in a life cycle model. *Society for Economic Dynamics Meeting Papers*, Paper 422 (2007), 25 pp. (https://economicdynamics.org/meetpapers/2007/paper_422.pdf)

[61] Henderson, V. and Hobson, D. An explicit solution for an optimal stopping/optimal control problem which models an asset sale. *Annals of Applied Probability*, **18** (2008), 1681–1705. (doi:10.1214/07-AAP511)

[62] Hempel, F. et al. Coordination of social security, training modules. *International Labour Organization*, **37** (2010), 1–114. (https://www.ilo.org/wcmsp5/groups/public/—europe/—ro-geneva/—sro-budapest/documents/publication/wcms_168752.pdf)

[63] Hernández-Lerma, O. and Lasserre J.B. Fatou's lemma and Lebesgue's convergence theorem for measures. *Journal of Applied Mathematics and Stochastic Ana-*

lysis, **13**(2) (2000), 137–146. (doi:10.1155/s1048953300000150)

[64] Holmlund, B. Unemployment insurance in theory and practice. *Scandinavian Journal of Economics*, **100** (1998), 113–141. (doi:10.1111/1467-9442.00093)

[65] Hopenhayn, H.A. and Nicolini, J.P. Optimal unemployment insurance. *Journal of Political Economy*, **105** (1997), 412–438. (doi:10.1086/262078)

[66] Hubbard, R.A., Inoue, L.Y.T. and Fann, J.R. Modeling nonhomogeneous markov processes via time transformation. *Biometrics*, **64**(3) (2007), 843–850. (doi:10.1111/j.1541-0420.2007.00932.x)

[67] Hyndman, R.J. and Koehler, A.B. Another look at measures of forecast accuracy. *Biometrics*, **22** (2006), 679–688. (doi:10.1016/j.ijforecast.2006.03.001)

[68] Israel, R.B., Rosenthal, J.S. and Wei, J.Z. Finding generators for Markov chains via empirical transition matrices, with applications to credit ratings. *Mathematical Finance*, **11**(2) (2001), 245–265. (doi:10.1111/1467-9965.00114)

[69] Inamura, Y. Estimating continuous time transition matrices from discretely observed data. *Bank of Japan Working Paper Series*, No. 06-E07, April 2006. (https://www.boj.or.jp/en/research/wps_rev/wps_2006/data/wp06e07.pdf)

[70] Jang, B., Park, S. and Rhee, Y. Optimal retirement with unemployment risks. *Journal of Banking and Finance*, **37** (2013), 3585–3604. (doi:10.1016/j.jbankfin.2013.05.017)

[71] Jenkins, J. and Chandler, M. Labour market gross flows data from the Labour Force Survey. *Economic and Labour Market Review*, **4**, (2010), 25–30. (doi:10.1057//elmr.2010.22)

[72] Jensen, U. An optimal stopping problem in risk theory. *Scandinavian Actuarial Journal* **2** (1997), 149–159. (doi:10.1080/03461238.1997.10413984)

[73] Kaas, R., Goovaerts, M., Dhaene, J. and Denuit, M. *Modern Actuarial Risk Theory using R*, 2nd ed. Springer-Verlag, Berlin, 2008. (doi:10.1007/978-3-540-70998-5)

[74] Karatzas, I. and Shreve, S. *Methods of Mathematical Finance*. Springer-Verlag, New York, 1998. (doi:10.1007/978-1-4939-6845-9)

[75] Karpowicz, A. and Szajowski, K. Double optimal stopping of a risk process. *Stochastics* **79** (2007), 155–167. (doi:10.1080/17442500601084204)

[76] Kerr, K.B. Unemployment compensation systems and reforms in selected OECD countries. Background paper BP-415E, Parliamentary Research Branch (Canada). Library of Parliament, Ottawa, 1996, 22 pp. (http://publications.gc.ca/collections/Collection-R/LoPBdP/BP-e/bp415-e.pdf)

[77] Kolsrud, J., Landais, C., Nilsson, P. and Spinnewijn, J. The optimal timing of unemployment benefits: Theory and evidence from Sweden. *American Economic Review*, **108** (2018), 985–1033. (doi:10.1257/aer.20160816)

[78] Kugler, A.D. *Strengthening reemployment in the unemployment insurance system.* Brookings Institution, Oxford, 2015.

[79] Landais, C., Nekoei, A., Nilsson, P., Seim, D. and Spinnewijn, J. Risk-based selection in unemployment insurance: Evidence and implications. Institute for Fiscal Studies, IFS Working Paper W17/22 (2017), 69 pp. (doi:10.1920/wp.ifs.2017.W1722)

[80] Landais, C. and Spinnewijn, J. The value of unemployment insurance. Preprint, London School of Ecnomics and Political Science, 2018, 86 pp. (http://econ.lse.ac.uk/staff/clandais/cgi-bin/Articles/valueUI.pdf)

[81] Lawrence, S. ILO comparable annual employment and unemployment estimates. *Bulletin of Labour Statistics*, (3) (1999), XII-XII.

[82] Leduc, S. and Liu, Z. Uncertainty shocks are aggregate demand shocks. *Federal Reserve Bank of San Francisco, Working Paper Series*, Working Paper 2012-10 (2015), 33 pp. (doi:10.24148/wp2012-10)

[83] Lehmann, E. A search model of unemployment and inflation. *Scandinavian Journal of Economics*, **114** (2011), 245–266. (doi:10.1111/j.1467-9442.2011.01670.x)

[84] Lindley, D.V. Dynamic programming and decision theory. *Journal of the Royal Statistical Society, Series C (Applied Statistics)*, **10** (1961), 39–51. (doi:10.2307/2985407)

[85] Littleboy, K. Births in England and Wales: summary tables. *Office for National Statistics*, 2020. (https://www.ons.gov.uk/peoplepopulationandcommunity/birthsdeathsandmarriages/livebirths/bulletins/birthsummarytablesenglandandwales/2018)

[86] Macdonald, A.S., Richards, S.J. and Currie, I.D. *Modelling Mortality with Actuarial Applications*. Cambridge University Press, 2018. (doi.org/10.1017%2F9781107051386)

[87] Makeham, W.M. On the law of mortality and the construction of annuity tables. *The Assurance Magazine and Journal of the Institute of Actuaries*, **8**(6) (1860), 301–310. (doi:10.1017/S204616580000126X)

[88] McCall, J.J. Economics of information and job search. *Quarterly Journal of Economics*, **84** (2015), 113–126. (doi:10.2307/1879403)

[89] McElreath, R. *Statistical Rethinking: A Bayesian Course with Examples in R and Stan*. Chapman and Hall/CRC, New York, 2018. (doi:10.1201/9781315372495)

[90] Merton, R.C. Lifetime portfolio selection under uncertainty: The continuous-time case. *The Review of Economics and Statistics*, **51** (1969), 247–257. (doi:10.2307/1926560)

[91] Merton, R.C. Optimum consumption and portfolio rules in a continuous-time model. *Journal of Economic Theory*, **3** (1971), 373–413. (doi:10.1016/0022-0531(71)90038-X)

[92] Millard, S. The great recession and the UK labour market. *SSRN Electronic Journal*, Bank of England, working paper No. 566, November 2015 (https://doi.org/10.2139%2Fssrn.2694471)

[93] Ministry of Health, Labour and Welfare, Japan. *Expert Meeting on Building Social Safety Nets for Employment–Strategies in Asia*. International Labour Organization (ILO), February 2011. (https://www.social-protection.org/gimi/RessourcePDF.action?id=23303)

[94] Minitab.com. Minitab statistical software (online). (http://www.minitab.com/en-us/products/minitab/)

[95] Moler, C. and Van Loan, C. Nineteen dubious ways to compute the exponential of a matrix, twenty-five years later. *SIAM Review*, **45** (2003), 3–49. (doi:10.1137/S00361445024180)

[96] Muciek, B.K. Optimal stopping of a risk process: Model with interest rates. *Journal of Applied Probability*, **39** (2002), 261–270. (doi:10.1239/jap/1025131424)

[97] Mucci, A.G. Existence and explicit determination of optimal stopping times. *Stochastic Processes and their Applications*, **8** (1978), 33–58. (doi:10.1016/0304-

4149(78)90066-2)

[98] Nazir, F., Cheema, M.A., Zafar, M.I. and Batool, Z. Socio-economic impacts of unemployment in urban Faisalabad, Pakistan. *Journal of Social Sciences*, **18** (2009), 183–188.

[99] von Neumann, J. and Morgenstern, O. *Theory of Games and Economic Behavior*, 3rd ed. Princeton University Press, Princeton, NJ, 1953.

[100] Nusselder, W.J. Successful aging: measuring the years lived with functional loss. *Journal of Epidemiology & Community Health*, **60** (2006), 448–455. (doi:10.1136/jech.2005.041558)

[101] Office for National Statistics (Great Britain). Full report: moving between un employment and employment, *Office for National Statistics*, 2013. (https://www.bl.uk/collection-items/full-report-moving-between-unemployment-and-employment)

[102] Office for National Statistics. Full report: moving between unemployment and employment,*The National Archives*, United Kingdom, (2013). (https://webarchive.nationalarchives.gov.uk/20150907153300/http://www.ons.gov.uk/ons/rel/lmac/moving-between-unemployment-and-employment/2013/rpt-–moving-between-unemployment-and-employment.html)

[103] Ogurtsova, E. *Estimating transition rates for multistate models from panel data and repeated cross-sections*. PhD thesis, University of Groningen, 2014. (doi:10.978-94-6259-405-0)

[104] Øksendal, B. *Stochastic Differential Equations: An Introduction with Applications*, 6th ed. Universitext. Springer-Verlag, Berlin, 2003. (doi:10.1007/978-3-642-14394-6)

[105] Owen-Williams, R. Quarterly mortality, England. *Office for National Statistics*, United Kingdom, 2020. (https://www.ons.gov.uk/peoplepopulationandcommunity/birthsdeathsandmarriages/deaths/datasets/quarterlymortalityreportsanalysis)

[106] Pérez-Ocón, R., Ruiz-Castro, J. E. and Gamá-Pérez, M. L. A piecewise Markov process for analysing survival from breast cancer in different risk groups. *Statistics in Medicine*, **20** (2001), 109–122. (doi:10.1002/1097-0258(20010115)20:1%3C109::AID-SIM615%3E3.0.CO;2-N)

[107] Peskir, G. and Shiryaev, A. *Optimal Stopping and Free-Boundary Problems*. Lectures in Mathematics, ETH Zürich. Birkhäuser, Basel, 2006. (doi:10.1007/978-3-7643-7390-0)

[108] Pfeuffer, M. ctmcd: An R Package for estimating the parameters of a continuous-time Markov chain from discrete-time data. *The R Journal*, **9**(2) (2017), 127–141. (doi:10.32614/rj-2017-038)

[109] Pham, H. *Continuous-time Stochastic Control and Optimization with Financial Applications*. Stochastic Modelling and Applied Probability, **61**. Springer-Verlag, Berlin, 2009. (doi:10.1007/978-3-540-89500-8)

[110] Pochampally, K.K. and Gupta, S.M. *Reliability Analysis with Minitab*. CRC Press, Boca Raton, FL, 2016. (doi:10.1201/b19630)

[111] Rao, C.R. Maximum likelihood estimation for the multinomial distribution. *Sankhya: The Indian Journal of Statistics*, **18** (1957), 139–148. (www.jstor.org/stable/25048341)

[112] Rebollo-Sanz, Y.F. and García-Pérez, J.I. Are unemployment benefits harmful to the stability of working careers? The case of Spain. *SERIEs*, **6** (2015), 1–41. (doi:10.1007/s13209-014-0120-z)

[113] Sargent, T.J. and Stachurski, J. A lake model of employment and unemployment (online). *Quantitative Economics with Python*, 2020. (https://python.quantecon.org/lake_model.html)

[114] Scott, Y. Labour market flows: March 2019 (online), *Office for National Statistics*. (https://www.ons.gov.uk/employmentandlabourmarket/peopleinwork/employmentandemployeetypes/articles/labourmarketflows/march2019)

[115] Sheena, Y. Efficiency of maximum likelihood estimation for a multinomial distribution with known probability sums. Preprint, 2019. (arXiv:1906.05461)

[116] Shepp, L.A. Explicit solutions to some problems of optimal stopping. *Annals of Mathematical Statistics*, **40** (1963), 993–1010. (doi:10.1214/aoms/1177697604)

[117] Shiryaev, A.N. On optimum methods in quickest detection problems. *Theory of Probability and Its Applications*, **8** (1963), 22–46. (doi:10.1137/1108 002)

[118] Shiryaev, A.N. Two problems of sequential analysis. *Cybernetics*, **3** (1967), 63–69. (doi:10.1007/BF01078755)

[119] Shiryaev, A.N. *Optimal Stopping Rules*. Applications of Mathematics, **8**. Springer-Verlag, Berlin, 1978. (doi:10.1007/978-3-540-74010-0)

[120] Shiryaev, A.N. *Probability*, 2nd ed. Graduate Texts in Mathematics, **95**. Springer-Verlag, New York, 1996. (doi:10.1007/978-1-4757-2539-1)

[121] Shiryaev, A.N. *Essentials of Stochastic Finance: Facts, Models, Theory*. Advanced Series on Statistical Science & Applied Probability, **3**. World Scientific, Singapore, 1999. (doi:10.1142/3907)

[122] Siegmund, D.O. Some problems in the theory of optimal stopping rules. *Annals of Mathematical Statistics*, **38** (1967), 1627–1640. (doi:10.1214%2Faoms%2F1177698596)

[123] Snell, J.L. Applications of martingale system theorems. *Transactions of the American Mathematical Society.*, **72** (1952), 293–312. (doi:10.1090/S0002-9947-1952-0050209-9)

[124] Stabile, G. Optimal timing of the annuity purchase: a combined stochastic control and optimal stopping problem. *International Journal of Theoretical and Applied Finance*, **9** (2006), 151–170. (doi:10.1142/S0219024906003524)

[125] Taylor, H.M. Optimal stopping in a Markov process. *Annals of Mathematical Statistics*, **39** (1968), 1333–1344. (doi:10.1214%2Faoms%2F1177698259)

[126] Taylor, H.M. and Karlin, S. *An Introduction to Stochastic Modeling*, 3rd ed. Academic Press, San Diego, CA, 1998.

[127] Thompson, M.E. Continuous parameter optimal stopping problems. *Zeitschrift für Wahrscheinlichkeitstheorie und Verwandte Gebiete*, **19** (1971), 302–318. (doi:10.1007/BF00535835)

[128] UKCES. The labour market story: the UK following recession (online). *UKCES briefing paper*,(https://www.gov.uk/government/uploads/system/uploads/attachment_data/file/344439/The_Labour_Market_Story-_The_UK_Following_Recession.pdf)

[129] Ushakov, I.A. *Optimal Resource Allocation: With Practical Statistical Applications and Theory*. John Wiley & Sons, Hoboken, NJ, 2013. (doi:10.1002/9781118400715)

[130] Villeneuve, S. On threshold strategies and the smooth-fit principle for optimal stopping problems. *Journal of Applied Probability*, **44** (2007), 181–198. (doi:10.

1239/jap/1175267171)

[131] WageIndicator.org. Minimum wage — France (with effect from 01-01-2018 to 31-12-2018) (online). (https://wageindicator.org/salary/minimum-wage/france/)

[132] Wald, A. Sequential tests of statistical hypotheses. *Annals of Mathematical Statistics*, **16** (1945), 117–186. (doi:10.1214/aoms/1177731118)

[133] Wang, T. and Wirjanto, T.S. Risk aversion, uncertainty, unemployment insurance benefit and duration of "wait" unemployment. *Annals of Economics and Finance*, **7** (2016), 1–34. (http://aeconf.com/Articles/May2016/aef170101.pdf)

[134] Watson, B. A02 SA: Employment, unemployment and economic inactivity for people aged 16 and over and aged from 16 to 64 (seasonally adjusted), *Office for National Statistics*, United Kingdom, (2020). (https://www.ons.gov.uk/employmentandlabourmarket/peopleinwork/employmentandemployeetypes/datasets/employmentunemploymentandeconomicinactivityforpeopleaged16andoverandagedfrom16to64seasonallyadjusteda02sa)

[135] Watson, B. X02: Labour force survey flows estimates, *Office for National Statistics*, United Kingdom, (2020). (https://www.ons.gov.uk/employmentandlabourmarket/peopleinwork/employmentandemployeetypes/datasets/labourforcesurveyflowsestimatesx02)

[136] Whittle, P. Some general results in sequential analysis. *Biometrika*, **52** (1964), 123–141. (doi.org/10.1093/biomet/51.1-2.123)

[137] Wong, D. *Generalized Optimal Stopping Problems and Financial Markets*. Addison Wesley Longman, 1996. (doi:10.1201%2F9780203753729)

[138] Yeh, J. *Martingales and Stochastic Analysis*. Series on Multivariate Analysis, **1**. World Scientific, Singapore, 1995. (doi:10.1142/2948)